SOME SPECTROSCOPIC STUDIES

OF DERIVATIVES OF THE GROUP III ELEMENTS.

A Thesis submitted by

Eric Martin Johnson, B.A.,

for the Degree of

Doctor of Philosophy

at the University of Oxford

March

1971.

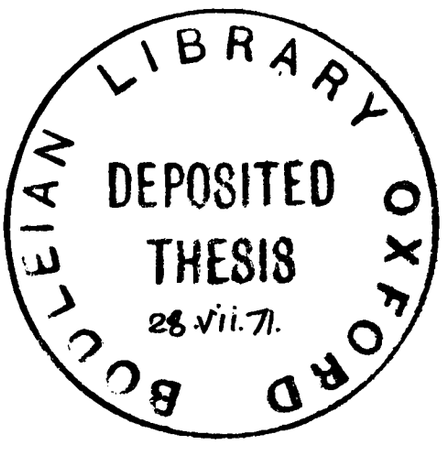

Jesus College,

Oxford.

For my parents.

I have nothing to offer but blood, sweat, toil and tears.

Winston S. Churchill

(House of Commons, May 13th, 1940)

CONTENTS

Contents i

List of Tables vii

List of Figures x

Acknowledgements xiii

SECTION I : INTRODUCTORY

Chapter 1 : Introduction 1

1.1. The Problem 1

1.2. Previous Investigations 2

(a) Trimethylboron 3

(b) Trimethylaluminium 4

(c) Trimethylgallium 7

(d) Trimethylindium 8

(e) Trimethylthallium 11

1.3. Theoretical Considerations 12

(a) Electron Deficiency 12

(b) The Bonding in Electron-Deficient Molecules 19

(c) The Factors Governing Oligomerization 23

1.4. Lines of Attack 37

Chapter 2 : The Interpretation of Vibrational Spectra 42

2.1. The Origins of Infrared and Raman Spectra 42

2.2. Molecular Vibrations : Normal Modes 45

2.3. Molecular Symmetry 46

(a) The Symmetry Elements 47

(b) The Character Table 47

(c) The Normal Modes 50

(d) The Representation of Normal Modes 53

2.4. The Selection Rules 54

(a) Infrared Activity 54

(b) Raman Activity 57

2.5. Effects of the Solid State 63

(a) Site Symmetry Approach 64

(b) Aggregate Unit Approach 67

(c) Factor Group Approach 68

SECTION II : EXPERIMENTAL

Chapter 3 : Instruments and Apparatus 71

3.1. Problems Encountered in the Study of the Group III Trimethyl Compounds 71

(a) General 71

(b) Sampling 73

(c) Spectroscopic 73

3.2. Instrumentation 74

(a) Raman Spectroscopy 74

(b) Infrared Spectroscopy 78

3.3. Special Sampling Devices 80

(a) Raman 80

(b) Infrared 92

Chapter 4 : Sample Preparation and Manipulation 95

4.1. The Vacuum Line 95

4.2. Preparation 99

(a) Trimethylboron 99

(b) Trimethylaluminium, Trimethylgallium and Trimethylindium 100

(c) Trimethylthallium 104

4.3. Purification 104

4.4. Sample Cells 105

(a) Raman Liquid Cell 105

(b) Infrared Gas Cells 108

(c) X-ray Diffraction Cell 109

Chapter 5 : Matrix-Isolation Methods 110

5.1. The Nature of the Technique 110

5.2. The Scope of the Technique 111

(a) Unstable Species 111

(b) Vibrational Analysis 112

(c) Diffusion Experiments 113

5.3. The Validity of the Technique 115

(a) The Matrix Shift 115

(b) Matrix Splittings 118

5.4. The Experimental Arrangement 120

(a) The Furnace Section 122

(b) The Cryotip Section 122

(c) The Cryotip 123

(d) Operation 125

5.5. Problems Encountered 126

5.6. Matrix-Isolation Raman Spectroscopy 128

(a) Development Work 129

(b) The Problems Encountered 133

SECTION III : RESULTS

Chapter 6 : The Vapour and Liquid Phase Spectra 135

6.1. The Presentation of Results 135

(a) The Tables 136

(b) Intensities 137

6.2. Calibration 138

(a) Raman Spectra 138

(b) Infrared Spectra 139

6.3. Trimethylboron 140

(a) Room Temperature Spectra 140

(b) Low Temperature Raman Spectrum 140

6.4. Trimethylaluminium 142

(a) Room Temperature Spectra 142

(b) High Temperature Solution Spectra 144

(c) High Temperature Vapour-Phase Spectra 146

6.5. Trimethylgallium 147

(a) Room Temperature Spectra 147

(b) Low Temperature Spectra 151

(c) Nuclear Magnetic Resonance Spectrum 151

6.6. Trimethylindium 152

(a) Room Temperature Spectra 152

(b) Low Temperature Spectra 152

6.7. Trimethylthallium 154

Chapter 7 : The Solid-State Results 157

7.1. Introductory 157

7.2. Results 158

(a) The Experiments 158

(b) The Tables 160

7.3. Trimethylboron 161

7.4. Trimethylaluminium 163

7.5. Trimethylgallium, Trimethylindium and Trimethylthallium 166

7.6. X-ray Diffraction Results for Trimethylgallium and Trimethylindium 174

Chapter 8 : The Matrix-Isolation Spectra 177

8.1. Introductory 177

8.2. Trimethylgallium 178

8.3. Trimethylaluminium 183

8.4. Trimethylboron 188

SECTION IV : DISCUSSION

Chapter 9 : Discussion 194

9.1. Monomeric Species 194

(a) The Table 194

(b) Correlations 199

(c) Calculations 207

(d) Conclusions 219

9.2. Dimeric Species 222

9.3. New Diffusion Species 226

9.4. Larger Aggregates 230

9.5. Conclusions 240

(a) The Structures 240

(b) Oligomerization Tendency 243

References 245

Summary 261

LIST OF TABLES

Chapter 1

1.1. Summary of the Reported Structures of the Group III Trimethyl Compounds 14

1.2. Summary of the Experimental Parameters for the Group III Trimethyl Compounds 15

1.3. Representative Electron Deficient Compounds 20

1.4. M $\hat{C}$ M Angles in Compounds with M_2C_2 Rings 26

1.5. M-M and Non-Bonded C-C Distances for M_2Me_6 and $(MMe_2)_n$ 28

1.6. Data Relating to M_2Me_6 Formation for the Group III Elements 29

1.7. Melting Points and Boiling Points for the Group III Trimethyl Compounds 35

Chapter 2

2.1. Character Table for the D_{3h} Point Group 49

2.2. (a) Reducible Representation for $XY_3(D_{3h})$ Species 52

(b) Number of Genuine Vibrations for $XY_3(D_{3h})$ Species 52

2.3. Predicted Spectral Features for $XY_3(D_{3h})$ Molecules 62

2.4. M-C Stretching Features for Solid Trimethylindium and Trimethylthallium 70

Chapter 3 : No Tables

Chapter 4

4.1. Fractionation Temperatures for the Purification of

the Group III Trimethyl Compounds 106

Chapter 5

5.1. Matrix Shifts for Small Molecules 117

Chapter 6

6.1. The Vibrational Spectra of the Fluid Phases of Trimethylboron 141

6.2. The Raman Spectra of the Fluid Phases of Trimethylaluminium 143

6.3. The Low-Frequency Infrared Spectra of the Fluid Phases of Trimethylaluminium 145

6.4. The Vibrational Spectra of the Fluid Phases of Trimethylgallium 150

6.5. The Vibrational Spectra of the Fluid Phases of Trimethylindium 153

6.6. The Vibrational Spectra of the Fluid Phases of Trimethylthallium 155

Chapter 7

7.1. The Infrared Spectrum of Solid Trimethylboron 162

7.2. The Raman Spectrum of Solid Trimethylaluminium 164

7.3. The Infrared Spectrum of Solid Trimethylaluminium 165

7.4. The Vibrational Spectra of Solid Trimethylgallium 167 & 168

7.5. The Vibrational Spectra of Solid Trimethylindium 169 & 170

7.6. The Vibrational Spectra of Solid Trimethylthallium 171 & 172

7.7. Unit Cell Dimensions for Solid Trimethylgallium, Trimethylindium and Trimethylthallium 176

Chapter 8

8.1. The Infrared Spectrum of Matrix-Isolated Trimethylgallium 179

8.2. The Infrared Spectrum of Matrix-Isolated Trimethylaluminium 186

8.3. The Raman Spectrum of Matrix-Isolated Trimethylaluminium in the Region 200-800 cm^{-1} 189

8.4. The Infrared Spectrum of Matrix-Isolated Trimethylboron 191

Chapter 9

9.1. Vibrational Assignments for the Group III Trimethyl Compounds 195

9.2. Frequency Comparisons for the CH_3 Symmetric Deformation and Rocking Modes of the Main Group Methyl Compounds 202

9.3. Product Rule Calculations for Trimethylboron 208

9.4. Force Constant Calculations for the Group III Trimethyl Compounds 210

9.5. Force Constant Calculations for Trimethylboron and Boron Trifluoride 215

9.6. Bond Length Calculations for the Group III Trimethyl Compounds 218

9.7. Electronegativity Differences and Force Constants for the Group III Trimethyl Compounds 221

9.8. Vibrational Frequencies for Representative Al_2Y_6 Molecules (Skeletal Modes Only) 224

9.9. Tentative Assignments for the Matrix-Isolation Diffusion Species 227

9.10. Corresponding Vibrational Modes for the MC_3 Unit with Planar and Pyramidal Configurations 229

9.11. Low Frequency Features for Solid Trimethylgallium, Trimethylindium and Trimethylthallium 238

LIST OF FIGURES

Chapter 1

1.1. The Trimethylaluminium Dimer 5

1.2. The Crystal Structure of Trimethylindium 10

1.3. The Crystal Structure of Trimethylthallium 13

1.4. Elements of the Periodic Table Capable of Electron Deficient Compound Formation 17

1.5. (a) Pictorial Representation of the Overlap of sp^3 Atomic Orbitals in Al_2Me_6 to yield a 3-centre Molecular Orbital 22

(b) Molecular Orbital Diagram for the Bridge Bonding in Trimethylaluminium Dimer 22

1.6. Melting and Boiling Points for the Group III Trimethyl Compounds 36

1.7. Summary of Research Undertaken in This Investigation 40

Chapter 2

2.1. Symmetry Elements of the D_{3h} Point Group 48

2.2. The Normal Modes of Vibration of the $XY_3(D_{3h})$ Unit 55

2.3. The M-C Stretching Modes for the MC_3 Unit in Different Site Symmetries 66

Chapter 3

3.1. The Coaxial (a) and Right-Angle (b) Viewing Techniques 77

3.2. Raman Variable Temperature Assembly for Liquid Samples 83

3.3. Raman Low Temperature Solid Sampling Assembly (Coaxial Viewing) 86

3.4. The Right-Angle Viewing Arrangement for Solid Samples 89

3.5. Raman Low Temperature Solid Sampling Assembly (Right-Angle Viewing) 90

3.6. Infrared Low Temperature Solid Sampling Assembly 94

Chapter 4

4.1. The General Purpose Vacuum Line 96

4.2. The Preparation of Trimethylaluminium, Trimethylgallium and Trimethylindium 101

4.3. Liquid Cell for Raman Spectroscopy 107

4.4. X-ray Diffraction Cell 107

Chapter 5

5.1. The Infrared Matrix-Isolation Assembly 121

5.2. The AC - 3L - 110 Cryo-Tip Flow System 124

5.3. The Raman Matrix-Isolation Assembly 132

Chapter 6

6.1. The Vapour-Phase Raman Spectrum of Trimethylaluminium 148

Chapter 7

7.1. The Vapour-Phase and Solid-Phase Infrared Spectra of Trimethylgallium in the 1200 cm^{-1} Region 159

Chapter 8

8.1. The Infrared Spectra of Vapour-Phase and Matrix-Isolated Trimethylgallium 181

8.2. The Infrared Spectrum of Matrix-Isolated Trimethylgallium Before and After Diffusion 182

8.3. The Matrix-Isolation Infrared Spectra of Trimethylaluminium Monomer and Dimer 187

8.4. The Infrared Spectra of Vapour-Phase and Matrix-Isolated Trimethylboron in the 260-380 cm^{-1} Region 193

Chapter 9

9.1. Correlation Diagram for the Monomeric Group III Compounds 200

9.2. CH_3 Symmetric Deformation Frequency vs. Electronegativity 204

9.3. CH_3 Rocking Frequency vs. Electronegativity 205

9.4. The Normal Modes of Vibration for the $X_2Y_6(D_{2h})$ Skeleton 223

9.5. Correlation Diagram for the Solid Trimethyl Compounds of the Group III Elements (M-C Stretching Region) 233

9.6. Correlation Diagram for the Solid Trimethyl Compounds of the Group III Elements (CH_3 Symmetric Deformation Region) 234

9.7. Correlation Diagram for the Solid Trimethyl Compounds of the Group III Elements (Low Frequency Region) 237

PHOTOGRAPH

The General Purpose Vacuum Line 97

ACKNOWLEDGEMENTS

I should like to acknowledge my deep debt of gratitude to my supervisor, Dr. A.J. Downs, for his continuous guidance, advice and encouragement throughout the investigation described in this thesis.

I must also express my sincere thanks to my colleagues in the "Downs' Group" for their support, both practical and spiritual. In particular, I must mention Dr. C.J. Adams not only for his clear-sighted advice but also for his unique sense of humour.

Gratitude is expressed for the technical assistance I received. I should like to thank Dr. A.G. Lee of Cambridge University and Mr. J.H. Darling for samples of trimethylthallium; Dr. J.S. Ogden and Dr. M.J. Ricks for providing access to their matrix-isolation apparatus; Mr. I.J. Tickle for the use of his low-temperature X-ray crystallographic assembly; Spex Industries Limited and Dr. D.M. Adams of Leicester University for the opportunity of using their Raman spectrometers. Finally I must acknowledge my indebtedness to Mrs. Joan Griffin for her typing of the thesis and, in particular, for her wonderfully co-operative attitude throughout its preparation.

The research described in this thesis was carried out during the tenure of a Science Research Council Studentship and I should also like to acknowledge the financial support I received from Jesus College.

SECTION I

BLOOD

Chapter 1

Introduction

1.1. The Problem

Although the trimethyl compounds of the Group III elements have all been known for many years, their structures, particularly in the condensed phases, are still, in some cases, unknown. Previous studies have been haphazard, concentrating for the most part on the elucidation of the structure of one compound in one phase, with the result that it has not been possible to assess the factors influencing the structures in a systematic way.

In the vapour phase, the structures of the trimethyl compounds of the four lighter members of Group III have been extensively studied, and, whilst the boron, gallium and indium compounds are all monomeric, the aluminium compound adopts a symmetrical, dimeric structure with bridging methyl groups. In the solid state, trimethylaluminium retains this dimeric unit, but the indium compound favours the formation of an unusual, weakly-bound tetrameric unit. Oligomerization is, therefore, a feature of common occurrence in the Group III trimethyl series, and the present investigation was undertaken with three fundamental objectives: firstly, to study, systematically, the structures adopted by all the compounds in all three phases. Secondly to produce and examine, where possible, such hitherto uncharacterized species as a monomeric trimethylaluminium molecule, and finally, to investigate the factors influencing the nature and degree of oligomerization.

Throughout the investigation the compounds have been examined using the techniques of infrared and Raman spectroscopy. In this way it has proved possible not only to correlate results from previous investigations between different phases, but also to investigate the effect of such variables as temperature and phase on degree of aggregation. By use of the matrix-isolation method it has also proved possible to investigate the effect of environment on structure at very low temperatures and to study the oligomerization processes in a novel and informative way.

In the next section of this chapter a summary of the results of previous investigations in this field is given and in the remaining sections the theoretical background to the problem and the various lines of attack employed in the investigation are discussed.

1.2. Previous Investigations

Coates and Wade[1] have selectively reviewed the literature with respect to the organometallic derivatives of the Group III elements up to 1967. Their account is concerned mainly with the inorganic aspects of the chemistry of the compounds, rather than with the olefin-addition and "aufbau" reactions which make them commercially important; these aspects have been reviewed elsewhere.[2,3] More recently the organometallic chemistry of gallium, indium and thallium[4] and of thallium alone[5] have also been reviewed.

During the course of this investigation a number of studies, using such techniques as X-ray crystallography and electron diffraction, but not vibrational spectroscopy, have been published. These studies have

confirmed, for the most part, the findings of the present investigation, and in some cases have facilitated the interpretation of the results. The following survey thus summarizes the state of knowledge relating to the structural chemistry of tri-organo compounds of the Group III elements as it is at the present time, rather than as it was at the commencement of the investigation.

At the end of this section a summary of the known structures is given in Table 1.1, and a summary of the molecular parameters in Table 1.2.

(a) Trimethylboron

The infrared spectrum in the vapour phase[6,7,8,9] and the Raman spectrum in the liquid phase[6,9] have been interpreted in terms of a monomeric molecule with a planar BC_3 skeleton and freely rotating methyl groups, assignment being facilitated in the case of the infrared spectrum by the examination of almost pure trimethylboron-b^{10}.[8] Electron diffraction studies[10,11] of the vapour and entropy calculations[9] also support this conclusion.

Both the proton[12] and ^{11}B[13,14] nuclear magnetic resonance spectra of trimethylboron have been examined, in both cases only a single, unsplit resonance being observed.

Trimethylboron, which melts at -160°C, has not previously been examined in the solid phase. The higher alkyl derivatives of boron[15] and trivinylboron[16,17] are also monomeric. Thus carbon-bridging has not been reported for simple organoboron compounds, though it is a feature of the kinetically stable polynuclear systems such as the carboranes.[18]

(b) Trimethylaluminium

The substantiation in 1941[19] of the dimeric nature of trimethylaluminium has resulted in the extensive study of the compound in all three phases by a variety of techniques.

In the vapour phase, vapour density measurements[19] have shown that trimethylaluminium is predominantly dimeric at 70°C, but that dissociation increases with rising temperature, the heat of dissociation of one mole of dimer to two moles of monomer being 20.4 k.cal.[19,20] An early electron diffraction study[21] was erroneously interpreted in terms of an ethane-like structure, the first indication of the bridged, dimeric structure being given by infrared[22] and Raman[23] investigations of the vapour and liquid phases, respectively. The spectra were consistent with a D_{2h} model (Figure 1.1, p. 5); more recent reinvestigations of the infrared[24,25,26,27] (including $Al_2(CD_3)_6$[28]) and Raman[29,30] spectra have confirmed this conclusion, but have revised and extended the original vibrational assignments.

Molecular weight studies of trimethylaluminium in benzene solution[31] confirm that the dimeric form is retained in solution. The proton magnetic resonance spectrum has been studied in cyclopentane[32,33] and toluene[34] solution and, at approximately -70°C, two signals were observed, as expected, one for the terminal and one for the bridging methyl protons. As the temperature was increased, however, the peaks broadened and ultimately coalesced, indicating that the lifetime of a methyl group in either a terminal or bridging position is short relative to the time for an n.m.r. transition. The free energy of activation for the process

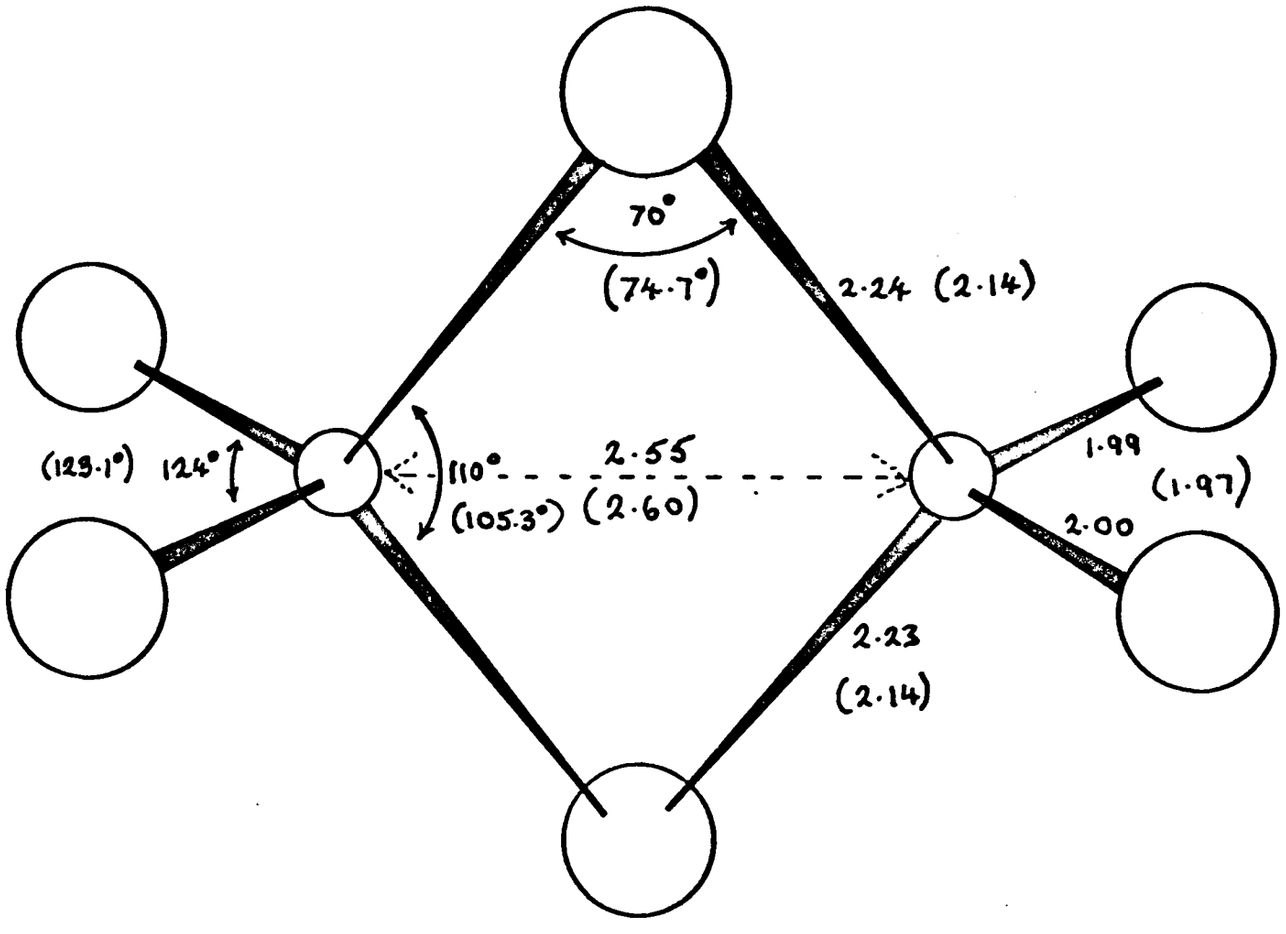

(All distances in Å)

Figure 1.1: The Trimethylaluminium Dimer[37,38]

(ΔG^{*} = 11.0 k.cals/mole)[35] is consistent with the breakage of an Al-C bond in the rate-determining step. The ^{27}Al ($I = {}^{5}/_{2}$) n.m.r. spectrum[36] has also been examined, a single resonance being observed.

Single-crystal X-ray analysis[37] has shown that the bridged, dimeric structure is retained in the solid state and has also produced the molecular dimensions given in Figure 1.1. A more recent reinvestigation[38] has altered some of the parameters; these latter results are included in parentheses in Figure 1.1. According to the reinvestigation, the plane of the terminal AlC_2 units is at an angle significantly different from 90° to the plane of the central Al_2C_2 ring, with the result that the effective point group is C_{2h} rather than D_{2h}, appropriate to the idealised geometry. This distortion is probably attributable to crystal packing effects and there is no reason to suspect any deviation from D_{2h} symmetry in the fluid phases.

A further refinement of the second X-ray analysis[39] is claimed to favour hydrogen-bridge bonds, Al-H-C-Al, in the molecule, but this view is not supported by an ^{27}Al nuclear quadrupole resonance study of the solid,[40] which favours the Al-C-Al bridged structure of Figure 1.1. The solid-state vibrational spectra have not been reported.

The structure of the monomer of trimethylaluminium, as studied at elevated temperatures by electron diffraction,[41] consists of a D_{3h} AlC_3 skeleton with freely rotating methyl groups.

Other straight-chain trialkyls of aluminium tend also to be dimeric in benzene solution,[31] dissociation becoming more facile with increasing chain length, but the branched-chain alkyls are generally monomeric,[42,43]

presumably for steric reasons. The proton n.m.r. spectra of triethyl-, tri-n-propyl-, and tri-n-butylaluminium[35,44] show, at sufficiently low temperatures, changes in the CH_2 region ascribable to the existence of two types of alkyl group. Triphenylaluminium is dimeric in benzene solution[45,46] and in the solid state[47]. Trivinylaluminium polymerizes too easily to allow study[48], but there is n.m.r. evidence[49] that the phenylethynyl group may be a better bridging group than a simple alkyl or aryl group.

(c) Trimethylgallium

Trimethylgallium has been shown to be monomeric in the vapour phase by vapour density measurements[50]. Subsequent infrared studies of the vapour[51,52,53] and Raman studies of the liquid[52,53] have not only supported this conclusion, but have also implied that the trimethylgallium molecule adopts a D_{3h} planar configuration in the fluid phases. No electron diffraction studies have been reported.

In benzene solution trimethylgallium has been shown to be monomeric by cryoscopic measurements[54] and in the proton magnetic resonance spectrum of trimethylgallium in cyclopentane solution[54] one resonance only is observed, which remains virtually unaffected by change in temperature down to -100°C.

Trimethylgallium, which melts at -19°C, has not previously been examined in the solid phase.

Triethylgallium, although reported as dimeric in solution[55,56], has now been shown to be monomeric both in benzene and cyclopentane solution[54], as it is in the vapour phase[19]. Trivinylgallium, on the

other hand, has been found to be dimeric in cyclohexane solution[57], as has the compound $Me_2Ga.C{\equiv}C.Ph$[58]. Triphenylgallium, whilst monomeric in benzene and cyclohexane solution[57], has been shown by X-ray crystallographic studies[59], to contain chains of weakly bonded trigonal molecules in which each gallium atom has fivefold coordination.

Thus, whilst aggregation has not been reported for trimethylgallium, it is by no means of rare occurrence in the chemistry of organogallium compounds.

(d) Trimethylindium

Although an early cryoscopic investigation[60] indicated that trimethylindium was tetrameric in benzene solution, more recent colligative measurements in benzene, cyclopentane and dichloromethane[54,61] and vapour density measurements[19], have shown no evidence of association. This conclusion is supported by an early electron diffraction study[62] which was not, however, able to distinguish between a planar (D_{3h}) or pyramidal (C_{3v}) model for the monomeric molecule.

The vapour-phase infrared and liquid-phase Raman spectra of trimethylindium[52] have been interpreted in terms of a monomeric, planar model for the molecule. Proton magnetic resonance studies[61] in cyclopentane, dichloromethane, benzene and toluene solutions yielded only one resonance, even at temperatures as low as -90°C, although appreciable concentration - and temperature - dependence of the chemical shift was observed in the first two solvents.

In the solid state, by contrast, a single-crystal X-ray analysis[63] has revealed an unusual type of structure with a polymeric network of

tetramer units in which each indium atom is penta-coordinated by methyl groups. Figure 1.2 (p. 10) illustrates both the tetrameric unit (a) and the penta-coordination about each atom (b).

The tetrameric unit is held together by unsymmetrical methyl bridges and the tetramers also interact, albeit more weakly, through further methyl bridges. Within each tetramer nearly trigonal Me_3In 'monomer' units can be distinguished with short ('normal') indium-carbon bond lengths. One indium-carbon bond of each 'monomer' points almost directly normal to the trigonal plane of another Me_3In unit within the tetramer, forming an unsymmetrical, linear $In\text{-}CH_3...In$ bridge. A second indium-methyl bond of each 'monomer' points approximately at the trigonal plane of an $InMe_3$ unit in an adjacent tetramer, forming a further $In\text{-}CH_3...In$ bridge. There are, therefore, five methyl groups about each indium atom, with three short ('normal') In-C bonds of 2.1 Å in the trigonal plane, and two much longer In-C bonds, one of 3.1 Å within the tetrameric unit and the other of 3.6 Å to the next tetramer; these longer bonds lie on either side of the trigonal plane, inclined at 163° to each other, thereby producing a distorted trigonal-bipyramidal environment for the indium atom.

Triethylindium and triphenylindium are both monomeric in benzene and cyclohexane solution[56], but, whilst triethylindium has not been examined in the solid state, a recent X-ray analysis of a single crystal of triphenylindium[59] has shown that it has a chain-like structure similar to that of triphenylgallium in which each metal atom is penta-coordinated by carbon atoms. More significantly, however, the In...C

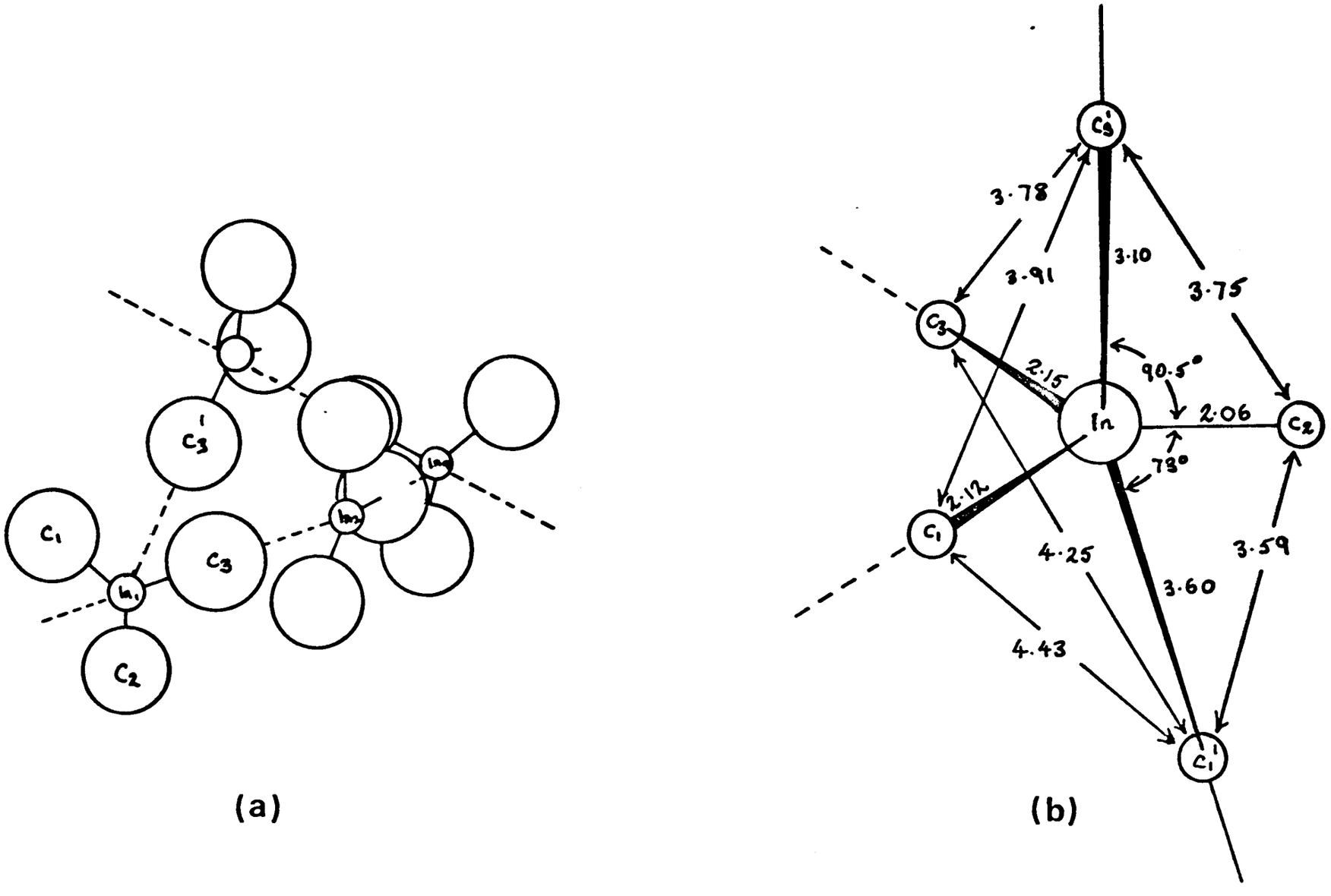

Figure 1.2: The Crystal Structure of Trimethylindium[63]

'long' distances are not only appreciably shorter than the sum of the van der Waals radii, but much more so than in the gallium compound.

Trivinylindium has not yet been reported, but $Me_2InC{\equiv}CPh$[58], like the analogous gallium compound, has been found to be dimeric in cyclohexane solution.

(e) Trimethylthallium

Trimethylthallium has been little studied, particularly in the vapour phase, for which no vapour density, electron diffraction or infra-red data have been published.

Freezing point measurements[56,64] have shown that trimethylthallium is monomeric in benzene solution. The proton magnetic resonance spectrum of trimethylthallium in (α - $^2H_3$) toluene or dichloromethane[65,66] exhibits, below -60°C, the two peaks expected from coupling of the methyl protons with the thallium nuclei. (Separate ^{203}Tl ($I = \frac{1}{2}$) and ^{205}Tl ($I = \frac{1}{2}$) resonances were not resolved, as the two isotopes have almost identical magnetic moments). As the temperature is raised, the Tl doublets collapse, indicating rapid intermolecular exchange of methyl groups. This exchange is both concentration- and solvent-dependent, showing second order kinetics with an energy of activation of approximately 6 k.cal/mole. These results have been interpreted in terms of a dimeric transition state with methyl bridges:

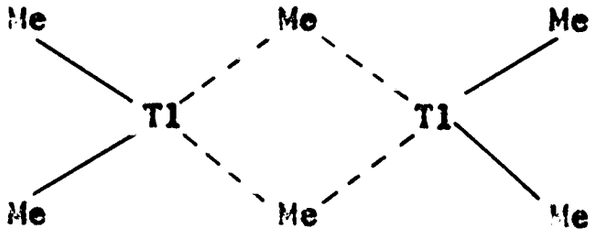

Very recently a single-crystal X-ray investigation has been published for trimethylthallium[67]. The compound is isostructural with trimethylindium, the metal atom again being at the centre of a distorted trigonal bipyramid of carbon atoms (Fig. 1.3 p. 13). Three short ('normal') bonds are equatorially disposed and two long apical bonds are inclined at 171° to each other. The differences between the inter- and intra-tetrameric long M-C bond distances are, however, much smaller in trimethylthallium (3.31 ± 0.09 Å and 3.16 ± 0.09 Å respectively) than in trimethylindium (3.59 ± 0.04 Å and 3.11 ± 0.04 Å respectively). Thus the tetrameric unit is of less significance in trimethylthallium than in trimethylindium and the crystal structure is probably better considered in terms of a polymeric aggregate.

Triethylthallium is monomeric in benzene solution[56] giving proton magnetic resonance results similar to those of the methyl compound[65]. Triphenylthallium is similarly monomeric in benzene solution[56], but, in common with trivinylthallium, it undergoes too rapid organic radical exchange for Tl-H coupling to be observed, even at -100°C[66].

Table 1.1 (p. 14) summarizes the reported structures for the Group III trimethyl compounds and Table 1.2 (p. 15) summarizes the bond data.

1.3. Theoretical Considerations

(a) Electron Deficiency

In 1916, G.N. Lewis[68] was able to rationalize the chemistry of molecular compounds with two fundamental concepts:

(i) a chemical bond consists of a shared pair of electrons

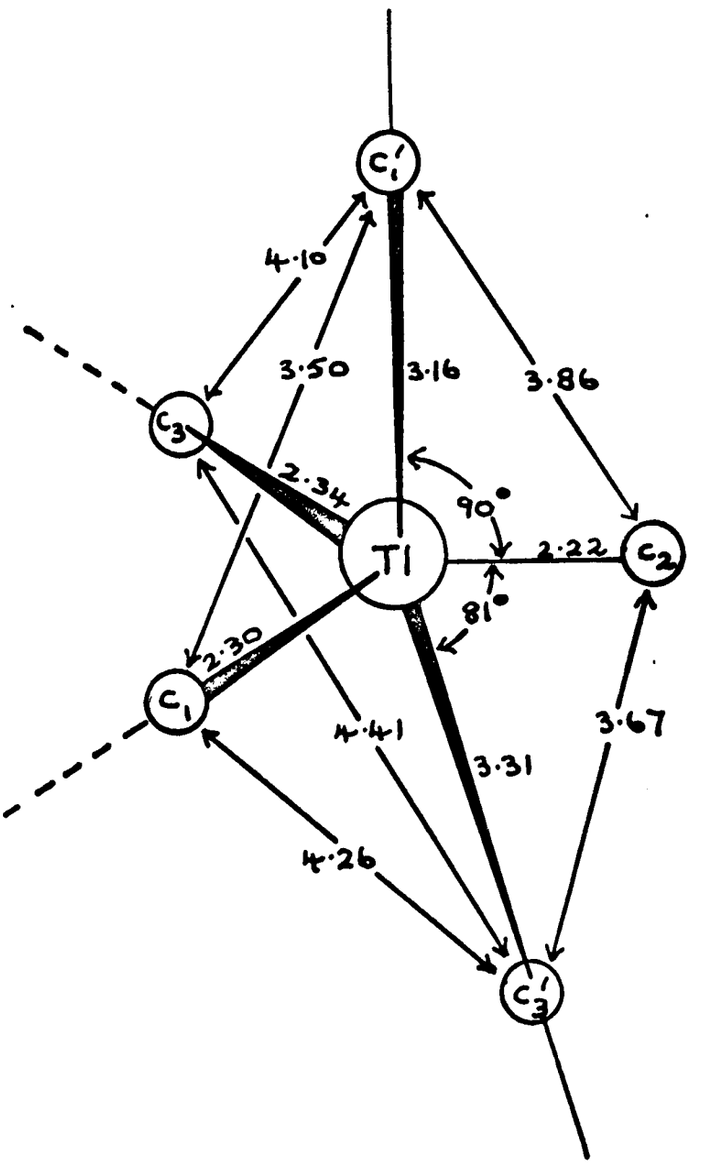

Figure 1.3: The Crystal Structure of Trimethylthallium[67]

COMPOUND	VAPOUR	LIQUID	SOLID
BMe_3	M	M	-
$AlMe_3$	M ⇌ D	D	D
$GaMe_3$	M	M	-
$InMe_3$	M	M	T
$TlMe_3$	-	M	'T'

M = monomer

D = dimer

T = tetramer

[⇌ indicates that the equilibrium lies heavily to the right]

Table 1.1 : Summary of the Reported Structures of the Group III Trimethyl Compounds.

COMPOUND	STUDY	M - C (Å)	C - E (Å)	C - $\hat{M}$ - C (°)	M - $\hat{C}$ - M (°)	Reference
BMe_3	Vapour: Elec. Diff	1.578	1.113	119.4		11
$AlMe_3$	Vapour: Elec. Diff.	1.964	1.113	111.8		41
Al_2Me_6	Solid: X-ray Diff.					
	Terminal	1.99(1.97)		124(123.1)		37
	Bridging	2.23(2.14)		110(105.3)	70(74.7)	(38)
$InMe_3$	Vapour: Elec. Diff.	2.16		-		62
$InMe_3$	Solid: X-ray Diff.	2.15		122		63
	Equatorial	2.12		117		
		2.06		119		
	Axial - intra-tet.	3.11		163		
	Axial - inter-tet.	3.59				
$TlMe_3$	Solid: X-ray Diff.	2.30		118		67
	Equatorial	2.34		110		
		2.22		131		
	Axial - intra-tet.	3.16		171		
	Axial - inter-tet.	3.31				

Table 1.2 : Summary of the Experimental Parameters for the Group III Trimethyl Compounds

(ii) each atom in a molecule achieves a noble gas electron shell by the formation of chemical bonds.

These empirical concepts not only withstood the advent of quantum mechanics[69] and the discovery of electron spin[70] in 1926, but were, in fact, given a theoretical basis by these discoveries. With the availability of physical techniques for structural investigation, these twin concepts were still found to be valid and it is probably true, even today, that the structures of the vast majority of main group moleculer compounds can be rationalised in terms of such electron-pair bonds.

The first group of compounds for which Lewis type structures could not be written, the boron hydrides, were investigated by Stock[71] in the period 1912-1933. Although in question for many years, their spatial structures were ultimately solved by X-ray crystallography[72,73], or, in the case of diborane, by infrared and Raman spectroscopy[74], proton magnetic resonance spectroscopy[75] and electron diffraction[76]. At first the boron hydrides were considered unique, but it soon became clear that such compounds were of rather common occurrence amongst the hydrogen and organometallic compounds of elements in a particular region of the periodic table. These compounds, characterized by a total number of valence electrons less than $2(n-1)$, where n is the number of atoms in the molecule, are commonly called <u>electron deficient</u>.

Electron deficient compounds are found only when an atom with more low-energy orbitals than valence electrons is combined with certain ligands. All the compounds formed by the elements of Groups IV-VII [see Fig. 1.4 (p. 17)] have sufficient valency electrons to achieve a

I	II	III	IV	V	VI	VII	VIII
Li	Be	B	C	N	O	F	Ne
Na	Mg	Al	Si	P	S	Cl	Ar
K	Ca	Ga	Ge	As	Se	Br	Kr
Rb	Sr	In	Sn	Sb	Te	I	Xe
Cs	Ba	Tl	Pb	Bi	Po	At	Rn

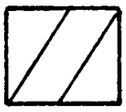

Elements forming compounds by electron loss to give noble gas electronic structures.



Elements forming compounds by electron gain or electron sharing to give noble gas electronic structures.



Elements potentially capable of forming electron deficient compounds.

Figure 1.4: Elements of the Periodic Table Capable of Electron Deficient Compound Formation.

noble gas structure by the formation of conventional electron-pair bonds, or by the gain of one or more electrons to yield anions. The heavier members of Groups I and II, on the other hand, prefer to achieve a noble gas configuration by electron loss, thereby forming large cations with a charge of one or two. For the remaining elements of Groups I and II, and for all the elements of Group III, however, ionization is energetically relatively difficult and the formation of molecular compounds is often preferable. For ligands without non-bonding valence electrons, however, simple electron-pair bond formation will then leave the central atom electronically deficient with the result that oligomerization or polymerization with electron sharing and delocalization may be energetically advantageous - yielding so-called electron-deficient compounds. Thus electron-deficient systems are formed by the elements in the region of the main periodic table left unshaded in Figure 1.4.

With the d- and f- block elements special considerations apply, with the diminished significance of the noble-gas configuration, and classical electron-deficient compounds are less commonly found. Zinc, cadmium and mercury are exceptional in having a full d-electron core, but electron deficient structures have not been reported, with the possible exception of dimethylzinc in the solid phase[77].

The nature of the ligands involved in the formation of electron-deficient compounds is less easy to delineate. Whilst hydrogen and alkyl groups are obvious examples, such species as alkenyl, alkynyl, aryl or halogen groups, in which extra electrons are present, but not

necessarily available, may or may not be considered to give rise to electron-deficient species. In the case of, for example, aluminium compounds, the structures of the alkyl, alkenyl, alkynyl, aryl and halogen compounds are analogous. Accordingly, in this study all of these compounds are considered electron-deficient. Chemically electron-deficient compounds are characterised by the extreme ease with which they react with molecules containing atoms with available electron pairs, a characteristic exhibited by all the above compounds, but not, for example, by the structurally analogous $(Me_2AlNMe_2)_2$ [78]:

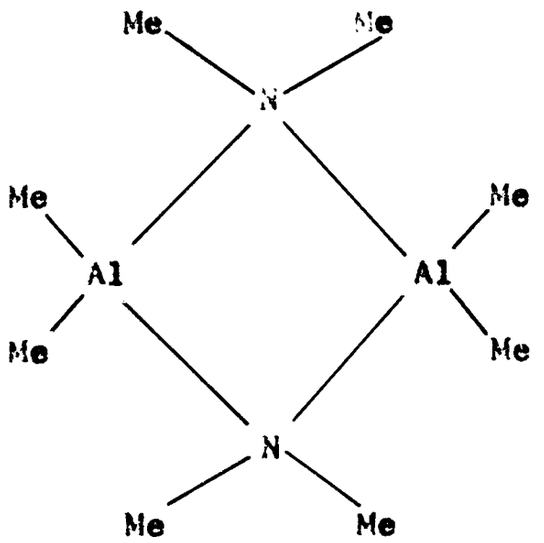

which is only very slowly attacked by water.

On this basis, electron deficient systems are encountered amongst the compounds of Li, Be, Mg, B, Al, Ga, In, Tl formed with hydrogen, organic radicals and possibly halogen. Table 1.3 (p.20) summarizes the structures of some of these compounds containing the representative ligating groups hydrogen, methyl, phenyl and chlorine.

(b) The Bonding in Electron-Deficient Molecules

The structures of electron-deficient hydrides and alkyls remained

Element	Phase	H	Me	Ph	Cl
Li	Fluid	-	T (80)	D (79)	I
	Solid	P	T (81)	-	P
Be	Fluid	-	M⇌O (82)	-	M⇌D (84)
	Solid	LP	LP (83)	-	LP (85)
Mg	Fluid	-	-	-	I
	Solid	LP?	LP (86)	-	P
B	Fluid	D (74)	M (11)	-	M (87)
	Solid	-	-	-	M (88)
Al	Fluid	M⇌D (89)	M⇌D (22)	D (45)	M⇌D (91)
	Solid	P (90)	D (37)	D (47)	P (92)
Ga	Fluid	-	M (50)	M (57)	M⇌D (93)
	Solid	-	-	LP (59)	D (94)
In	Fluid	-	M (61)	M (56)	M⇌D (95)
	Solid	-	T (63)	LP (59)	P (96)
Tl	Fluid	-	M (64)	M (56)	-
	Solid	-	T/P (67)	-	P (96)

M = monomer; D = dimer; O = oligomer; T = tetramer;

LP = linear polymer; P = polymeric network;

I = conductivity of melt implies some ionic character.

[The term 'fluid' phase refers to vapour, pure liquid or solution in a non-ionizing solvent depending upon the availability of results. Key references only are given. All unreferenced information is taken from Cotton and Wilkinson[79]]

Table 1.3: Representative Electron Deficient Compounds.

inexplicable at all but an empirical level until recognition was given to the idea[97,98] that an electron-pair bond need not be localised between a pair of atoms, but can be delocalized over all the low-energy orbitals. In this way, not only can the Lewis noble-gas structure be achieved for each atom in the molecule, but the available structural data can also be explained.

In the case of trimethylaluminium, the bond lengths[37], taken in conjunction with spectroscopic studies[22] indicating the absence of anomalously weak carbon-hydrogen bonds, imply that the only bonds which cannot adequately be described in terms of localized electron-pairs are those between the four bridge atoms. Moreover, the bridge Al-C length of 2.14 Å agrees well with the 2.16 Å calculated for half-bonds using Pauling's rule[99], and the ring angles of 74.7° (M-$\hat{C}$-M) and 105.3° (C-$\hat{M}$-C) suggest a form of bonding requiring relatively close approach of aluminium atoms. This structure is readily explicable in terms of maximal overlap of a carbon sp^3 orbital with two aluminium sp^3 orbitals to yield a three-centre molecular orbital, as shown in Figure 1.5(a) (p.22)[37]. A fuller M.O. consideration[100] involving these orbitals yields the M.O. diagram depicted in Figure 1.5(b). The formally non-bonding degenerate pair of orbitals (of b_{1g} and b_{3u} symmetry) are, in fact, slightly anti-bonding, because of nuclear repulsion between the aluminium nuclei, and so the dimeric structure is likely to be energetically most advantageous when only two electron pairs are to be accommodated, as in Al_2Me_6 or B_2H_6. This simple M.O. description is generally accepted as correct, at least in essence, and can readily be

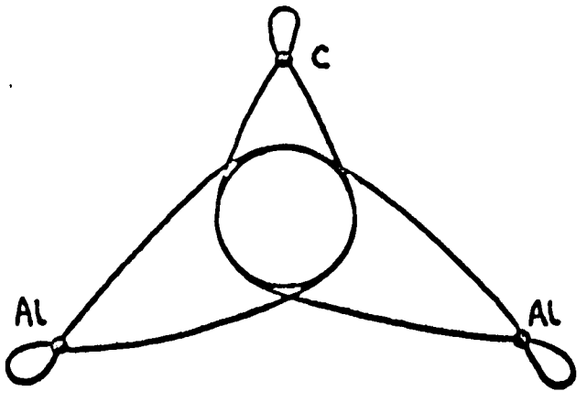

Figure 1.5(a): Pictorial Representation of the Overlap of sp^3 Atomic Orbitals in Al_2Me_6 to yield a 3-centre Molecular Orbital

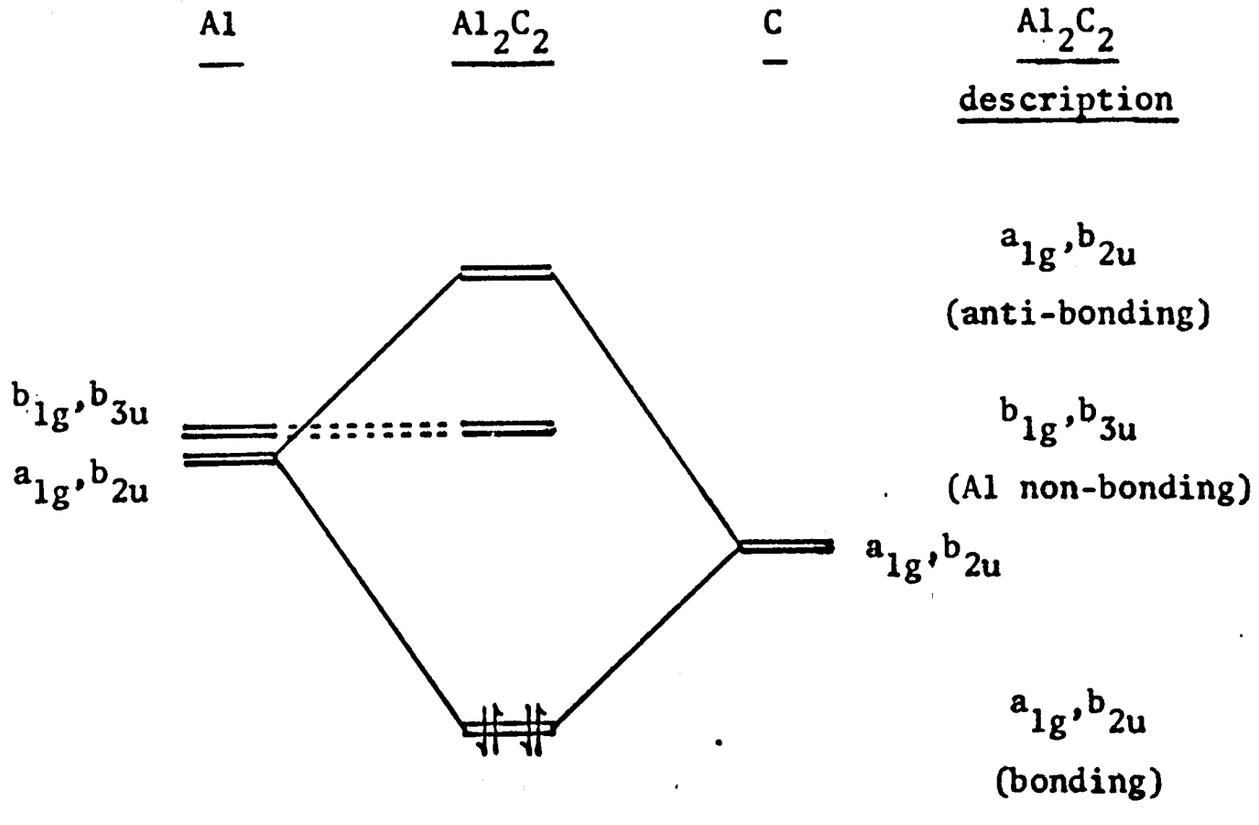

Figure 1.5(b): Molecular Orbital Diagram for the Bridge Bonding in Trimethylaluminium Dimer

extended to rationalise the more complex electron-deficient structures[101].

For Al_2Me_6 the question of the participation or non-participation in the bonding of direct metal-metal interactions, possibly involving the use of aluminium 3d orbitals, remains a vexed one[102,103]. The Al-Al distance (2.60 Å) is almost that calculated from the Pauling covalent radius[104] (2.52 Å) and it is certainly far from inconceivable that metal-metal bonding is a stabilizing factor here. The admixture of other atomic orbitals of the correct symmetry to the above M.O. system can only result in further stabilization of the bonding, and de-stabilization of the anti-bonding molecular orbitals, but the extent of these effects depends on the relative energies of the new atomic orbitals and of those contributing most strongly to the bonding: this remains an inestimable factor.

To conclude, a simple molecular orbital approach has been able adequately to describe the bonding in simple electron-deficient systems and to rationalize the unusual stability of such structures, but the nature and relative importance of the various factors conceivably contributing towards the bonding remains unclear.

(c) The Factors Governing Oligomerization

There have been several attempts to rationalize the irregular variations exhibited by electron-deficient Group III systems in their capacity to undergo oligomerization[37,38,100], but most discussions have been rather inconclusive and unsupported either by calculation or by experiment. The pertinent factor involved in the consideration of any oligomerization is the free energy change ΔG, for the equilibrium:

$$n\ (\text{monomer}) \rightleftharpoons \text{oligomer}$$

where n is the number of monomer units forming one oligomer unit. The ΔG term can be divided into an entropy term, ΔS, which favours the monomer and increases in importance with both n and temperature, and an enthalpy term, ΔH, which is essentially temperature-independent and which is influenced by a number of factors, some of which favour the monomer, some the dimer.

For the particular case of the formation of the Al_2Me_6 type dimer it is possible not only to single out a number of distinct factors contributing towards the enthalpy term, but also, for some of them, to assess their approximate importance by means of simple geometric considerations. These factors are:

(I) M-M Distance

Close M-M approach is required for good overlap of the metal and carbon orbitals, but if the M-M distance falls much below that for a single M-M bond, inner shell repulsions disfavour dimerization. If the M-M distance is between that appropriate to a single bond and that required for van der Waals contact, the possibility of metal-metal bonding, which would favour dimerization, cannot be discounted.

(II) M-C Bond Enthalpies

Since the number of M-C bonds is increased in forming the dimer, a large M-C bond enthalpy will favour this process. In general, a large electronegativity difference between the metal and carbon leads to a high bond enthalpy, and thus a low metal electronegativity should favour dimerization.

(III) s → p Promotion Energy for the Metal

In forming the dimer from the monomer, the hybridization of the metal changes from approximately sp^2 to approximately sp^3. Dimerization will be favoured, therefore, if a small amount of energy is required to promote an electron from an s to a p orbital for the metal in question.

(IV) Van der Waals Repulsion of Non-Bonded Atoms

If dimer formation requires non-bonded atoms to come into closer contact than the sum of their van der Waals radii then repulsive interactions will occur and dimerization will be impeded.

(V) Special Stabilization of the Monomer

If there is any factor, such as partial M-C multiple bond character, stabilizing the monomer, dimer formation will be disfavoured.

In assessing the importance of factors I and IV above it is useful to have some indication of the M-M and non-bonded C-C distances, respectively, for a hypothetical M_2Me_6 dimer model for boron, gallium, indium and thallium. In order to calculate such distances it is necessary to estimate the $\hat{MCM}$ angle in the four-membered ring and the M-C 'half-bond' length. Table 1.4 (p.26) summarizes the data available for the $\hat{MCM}$ angle in M_2C_2 rings. Unfortunately figures are available only for rings involving beryllium, magnesium or aluminium; with the exception of beryllium, the $\hat{MCM}$ angle is approximately 75°. For Al_2Me_6 the length of the M-C bridge bonds (2.14 Å) corresponds well with the 2.16 Å calculated from the single bond using Pauling's rule for partial bond lengths[99]:

COMPOUND	M $\hat{C}$ M (°)	Reference
$[BeMe_2]_n$	66.0	83
$[MgMe_2]_n$	75.0	86
$[AlMe_3]_2$	74.7	38
$MgAl_2Me_8$	75.6	105
$[MgEt_2]_n$	72.0	106
$[LiAlEt_4]_n$	77.2	107
$[AlPh_3]_2$	76.5	47

Table 1.4: M $\hat{C}$ M Angles in Compounds with M_2C_2 Rings

$$D(n) = D(1) - 0.60 \log_{10} n$$

where:

D(n) = bond length for a bond of order n

D(1) = bond length for a bond of order 1

(The numerical term is approximately 0.19 for n = 0.5).

Table 1.5(a) (p.28) lists the values for M-M and non-bonded C-C for each of the Group III trimethyls, calculated on the basis of a 75° $\hat{MCM}$ angle and a half-bond length calculated from the experimental single-bond length (Table 1.2, p.15) on the basis of Pauling's rule. These M-M and C-C distances are intended only to provide rough data on which to base a qualitative discussion: no precise numerical significance is to be placed on them. Also included in Table 1.5(a), for comparison, is the M-M distance given by doubling the Pauling tetrahedral covalent radius. In Table 1.5(b) the experimental data are given for trimethylaluminium, dimethylberyllium and dimethylmagnesium.

Table 1.6 (p.29) lists salient data for use in conjunction with Table 1.5 in assessing the feasibility of dimer formation for the Group III trimethyls. The Van der Waals radii have been obtained either by adding approximately 0.8 to the covalent radii, or from Pauling[104].

It is now possible to consider the effect of factors I - V on dimer formation for each of the Group III trimethyls. Comparison is made throughout to aluminium, the only element for which a dimeric trimethyl has been obtained to date.

(i) Boron

(I) The M-M distance for the hypothetical dimer (2.16 Å) is much

	M-C Single		M-C	M-M		C-C
Element	Exptl.[i]	∑Cov.Rad.[ii]	Bridge (calc)	Calc.	2xCov.Rad.[ii]	non-bond. (calc)
B	1.58	1.65	1.77	2.16	1.76	2.68
Al	1.96 1.97	2.03	2.16	2.63	2.52	3.30
Ga	-	2.03	2.16	2.63	2.52	3.60
In	2.16	2.21	2.35	2.86	2.88	3.60
Tl	2.30	2.23	2.49	3.03	2.92	3.83

(All dimensions in Å)

(i) see Table 1.2 (p. 15)

(ii) see Table 1.6 (p. 29)

(a) Calculated Results

Element	M-C Single	M-C Bridge		M-M		C-C
	∑Cov.Rad.	Exptl.	Calc.	Exptl.	2xCov.Rad.	Non-bond. (exptl.)
Al[38]	2.03	2.14	2.22	2.60	2.52	3.30
Be[83]	1.83	1.93	2.02	2.09	2.12	3.11
Mg[86]	2.17	2.24	2.36	2.72	2.80	3.74

(b) Experimental & Calculated Results

Table 1.5: M-M and Non-bonded C-C for M_2Me_6 and $(MMe_2)_n$

Element	Tetrahedral Cov.Rad.[i] Å	Van der Waals Radius[ii] Å	Electronegativity		$s \rightarrow p$[110] promotion E x 10^3 cm^{-1}
			Pauling[108]	Allred/ Rochow[109]	
B	0.88	1.65	2.04	2.01	46.4
Al	1.26	2.05	1.61	1.47	43.1
Ga	1.26	2.05	1.81	1.82	53.9
In	1.44	2.20	1.78	1.49	49.2
Tl	1.46	2.25	2.04	1.44	61.9
C	0.77		2.55	2.50	33.9
CH_3		2.0			

(i) Ref. 104 p.246 (ii) Ref. 104 p.263

Table 1.6: Data Relating to M_2Me_6 Formation for Group III

greater than that for a single B-B bond (1.76 Å). A very considerable reduction in bond angle and length would be required to produce a B-B distance compatible with any substantial degree of metal-metal bond stabilization for the dimer.

(II) The high electronegativity of boron would disfavour dimerization.

(III) The s → p promotion energy is greater than for aluminium, militating against dimerization.

(IV) The non-bonded C-C distance required for the dimer is very short (2.68 Å vs. 3.30 Å for aluminium), and any decrease in the B-B distance, as required by Factor I, would lead to even closer contact between the non-bonded carbon atoms. In $(BeMe_2)_n$ and $(MgMe_2)_n$, because all the M-C bonds are partial in character, the non-bonded C-C distances are much greater (3.11 Å and 3.74 Å respectively).

(V) Recent bond length investigations[11] do not support the idea of hyperconjugative stabilization for the monomer.

In view of the high stability of the dimer B_2H_6 with respect to the monomer BH_3 ($\Delta H = \sim 35$ k.cal./mole [11]), it seems probable that factors I and IV are most important in preventing the dimerization of trimethylboron. For B_2H_6 factor IV is not applicable and the B-B distance of 1.77 Å[76] corresponds almost exactly to twice the tetrahedral covalent radius for boron (1.76 Å). In $(BeMe_2)_n$ and $(MgMe_2)_n$ the M-M bond lengths are 2.09 Å and 2.72 Å respectively, compared with 2.12 Å and 2.80 Å for twice the respective tetrahedral covalent radii. These

data, taken with the values for trimethylaluminium, tend to support the hypothesis that metal-metal interactions are of paramount importance in stabilizing electron-deficient four-membered rings.

(ii) Aluminium

(I) The Al-Al distance in the dimer is only slightly larger than that required for a single Al-Al bond, eliminating the possibility of inner-shell repulsions and suggesting some metal-metal bonding interaction.

(II) Aluminium has the lowest electronegativity of the Group III elements.

(III) Aluminium has the lowest s → p promotion energy in Group III.

(IV) The non-bonded C-C distance is 3.30 Å compared to 4.0 Å for twice the Pauling Van der Waals radius for a methyl group. However, the methyl group is not spherical and a distance of 3.30 Å probably need not require that individual atoms approach more closely than the sum of their Van der Waals radii (e.g. 2 x Van der Waals radius for carbon = 3.14 Å approximately).

(V) Trimethylaluminium monomer does not appear, from bond length considerations, to have any special stabilization energy[41].

For aluminium, therefore, each of the factors I - V favours dimerization, with the possible exception of factor IV, which is still non-prohibitive.

(iii) Gallium

(I) The M-M distance for the hypothetical dimer corresponds exactly

to that for aluminium.

(II) The high gallium electronegativity disfavours dimerization.

(III) Because of the greater penetration of s over p orbitals within the inner electron shells, the s → p promotion energy is much greater than for aluminium, operating against dimer formation for gallium relative to aluminium.

(IV) The C-C non-bonded distance is the same as for aluminium.

(V) As far as is known, $GaMe_3$ monomer has no special stabilization.

Thus for trimethylgallium the factor most strongly opposing dimerization appears to be III. The importance of this factor is difficult to assess, however, and it is possible, in view of the dimeric nature of Ga_2Cl_6 and of the favourable dimensional calculations (factors I and IV), that dimerization of trimethylgallium can occur at low temperatures.

(iv) Indium

(I) The M-M distance for the hypothetical dimer is almost ideal - neither too short, thereby invoking inner shell repulsions, nor too long, thereby eliminating the possibility of metal-metal bonding.

(II) The electronegativity of indium is slightly higher than that of aluminium, slightly disfavouring dimerization.

(III) The s → p promotion energy is greater than that of aluminium but not as high as that of gallium.

(IV) The non-bonded C-C distance is greater than that for the aluminium compound, favouring dimerization.

(V) Trimethylindium monomer has not been reported to have any special stabilization.

From the above factors it seems that dimerization should be more feasible for trimethylindium than for trimethylgallium, but probably, because of factors II and III, not as favourable as for aluminium.

(v) Thallium

(I) The M-M distance for the hypothetical dimer is a little larger than that for a single thallium-thallium bond.

(II) The electronegativity of thallium is probably comparable to that of aluminium.

(III) The s → p promotion energy is higher than that for any other Group III element, opposing dimerization.

(IV) The non-bonded C-C distance is greater than that for aluminium, favouring dimerization.

(V) No special stabilization has been reported for trimethylthallium monomer.

From the above data trimethylthallium would be expected to be roughly comparable with trimethylgallium in its tendency to dimerize.

To summarize: in the Group III trimethyl series dimerization would be expected to be energetically most favourable for the aluminium compound with the other elements falling in the order indium > gallium ≈ thallium > boron. In the cases of gallium, indium and thallium none of the five

factors appears to be so unfavourable that dimerization can be rejected out of hand as energetically unfavourable.

It is less easy to formulate the factors affecting the formation of higher oligomers from the monomer. It is probable, however, that the factors I - V are still important and the conclusions reached regarding dimer formation can probably be extrapolated to give a broad guide to the general feasibility of oligomer-formation. Any discussion of oligomer/oligomer equilibria, such as that between the dimer and tetramer for indium, requires more accurate estimation of the effect of each of the factors I - V for each oligomer than is at present possible, and such equilibria will not be discussed further here.

In concluding this section it is interesting to note that the melting and boiling points of the Group III trimethyls do not increase regularly with increasing molecular weight of the monomer. These melting and boiling points[1] are listed in Table 1.7 (p.35) and presented graphically in Figure 1.6 (p.36). Trimethylaluminium lies very much above a median line for both melting and boiling points. The same is true of the melting point of trimethylindium. By contrast, trimethylboron has a very low melting point and boiling point - amongst the lowest of all organometallic compounds.

Thus, in as much that melting point and boiling point can be correlated with molecular complexity, the tendency of the Group III trimethyls to form oligomers agrees with the series predicted from theoretical considerations:

aluminium > indium > gallium ≈ thallium >> boron

Element	M.W.	M.Pt. (°C)	B.Pt. (°C)
B	55.92	-159.9	-21.8
Al	72.09	15.0	126
Ga	114.83	-15.7	56
In	159.93	88.4	136
Tl	249.48	38.5	147 (extrap.)

Table 1.7: Melting Points and Boiling Points for the Group III Trimethyl Compounds

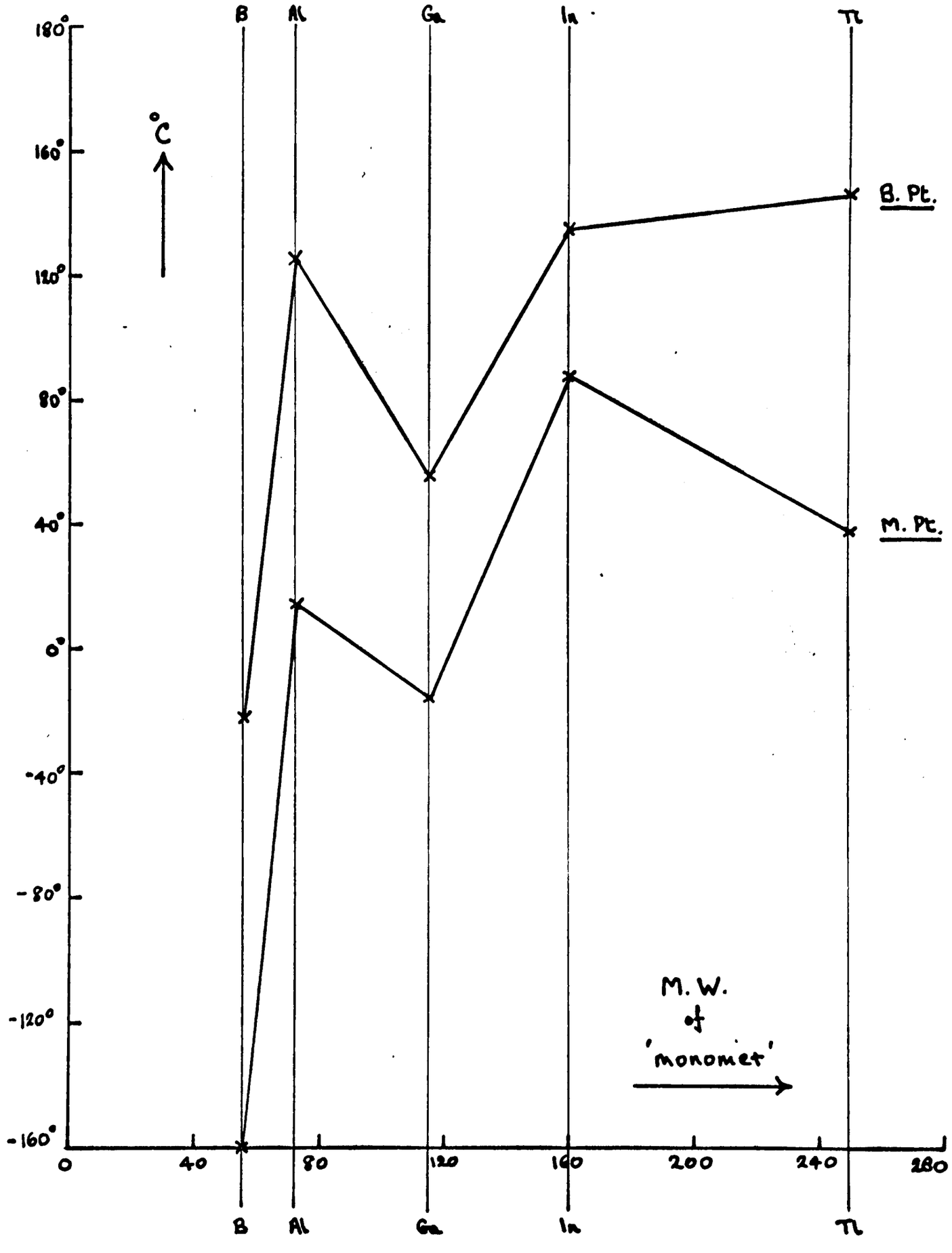

Figure 1.6: Melting and Boiling Points for the Group III Trimethyl Compounds

1.4. Lines of Attack

From the preceding discussion it is clear not only that oligomerization is of widespread occurrence amongst Group III compounds in general and within the trimethyl series in particular, but also that oligomerization is feasible for the trimethyls of all four heavier elements. The series of compounds was, therefore, considered worthy of systematic investigation with the aims of elucidating the structures of all the trimethyls in all three phases and of producing and examining 'anomalous' species, such as monomeric trimethylaluminium or dimeric trimethylgallium. In this way it was hoped that it might be possible to shed further light on the factors governing oligomerization.

In order to undertake such an investigation in this series of compounds it is necessary to use an unusually flexible technique for structural investigation. Such a method must fulfil the following requirements:

(i) it must be possible to examine each compound in all three phases;

(ii) it must be applicable over a very wide temperature range;

(iii) it must be possible to examine samples which react vigorously with air, moisture, grease and many sealing compounds;

(iv) it must be adaptable to the examination of trapped unstable species (i.e. matrix-isolation).

Of the various diffraction and spectroscopic techniques available for structural investigation, only vibrational spectroscopy meets all

these requirements. Moreover, by use of this technique it is possible not only to examine structures on an a priori basis, but also to correlate structural characteristics determined, for example, using one of the diffraction techniques, with those of the compound in other phases. Differences between the spectra of different phases can be interpreted either, in the case of radical changes, in terms of difference in structure, or, in the case of relatively minor changes, in terms of modified intermolecular interactions.

Vibrational spectroscopy can be used over a wide range of temperatures, both above and below ambient. By the use of specially constructed variable temperature probes surrounded by vacuum jackets (Chapter 3) it is possible to undertake the detailed examination of each compound in the solid, liquid and gaseous phase, as well as in an individual phase (e.g. liquid) over a wide range of temperatures.

It is also possible to use vibrational spectroscopic techniques (in particular that of infrared absorption) to examine unstable species trapped in inert matrices. Moreover, by the use of nitrogen and noble-gas matrices at liquid hydrogen temperatures (20-35°K), the reactions of unstable species can be studied by allowing the matrix to warm to its diffusion temperature. The course of reactions, in particular of oligomerization, can then be followed in a novel and informative way. The validity and experimental application of the matrix-isolation technique, together with its drawbacks, are discussed more fully in Chapter 5.

The main drawback of vibrational spectroscopy as a tool for structural investigation is its inherently relatively low sensitivity. In

general, unless a species gives rise to features in an entirely new part of the spectrum it must be present in roughly 5% proportion in a mixture before it can be characterized.

With the exception, therefore, of the sensitivity problem, vibrational spectroscopy is an almost ideal tool for the investigation of oligomerization problems of the type presented by the Group III trimethyls and the lines of attack employed in this investigation can be summarized as:

(i) Examination of the spectra (infrared, Raman or both) of each compound in all three phases.

(ii) Examination of solution spectra (Raman) over wide temperature ranges, both above and below ambient.

(iii) Examination of species produced by thermolysis and trapped in inert gas matrices at 20°K (infrared).

(iv) Examination of the reactions of monomers induced at very low temperatures by allowing the inert gas matrices to diffuse.

Trimethylgallium has also been examined in the solid state by X-ray powder photography and in solution by proton magnetic resonance spectroscopy. Figure 1.7 (p. 40) gives a summary of the researches undertaken in this thesis. The shaded areas indicate where previous work, not necessarily conclusive or complete, has taken place.

With the exception of the next chapter, which summarizes the interpretation of the vibrational spectra, the remainder of the thesis is divided into three sections: Chapters 3, 4 and 5 describe the experimental work carried out; the results of the investigations are described

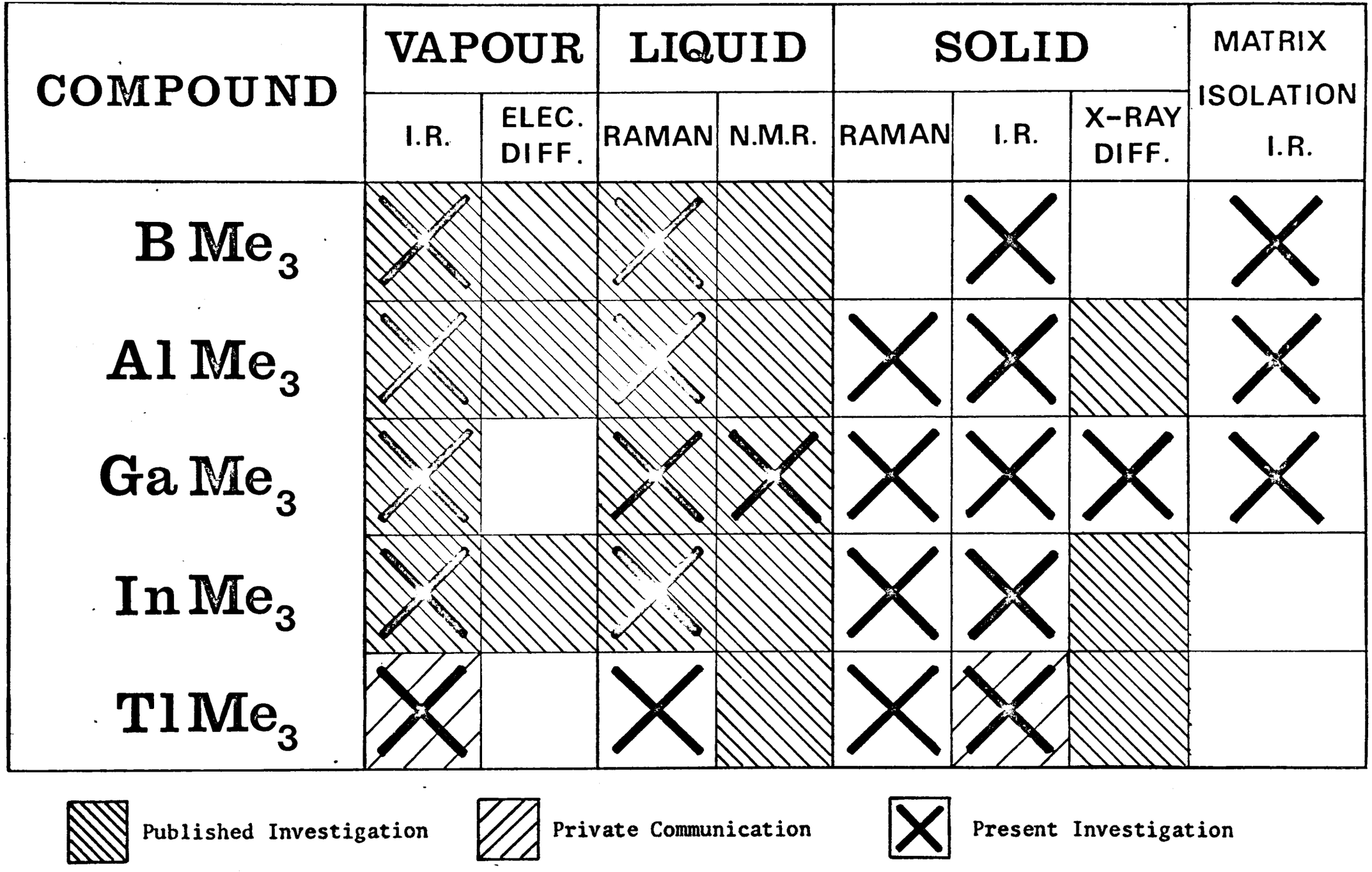

Figure 1.7: Summary of Research Undertaken in this Investigation

in Chapters 6, 7 and 8 and these results are discussed and interpreted in Chapter 9.

Chapter 2

The Interpretation of Vibrational Spectra

The vibrational motions of molecules manifest themselves experimentally as infrared and Raman spectra, and the purpose of this chapter is to show the way in which information on molecular structure can be obtained from such spectra. The treatment presented here is intended only to give the basic principles behind the interpretation of vibrational spectra since details of the methods are well documented elsewhere.[112,113,114,115]

The first section of the chapter discusses the origins of infrared and Raman spectra and the following three sections describe the derivation of the number and nature of vibrational features expected for an isolated molecule. The XY_3 planar unit, of which the MC_3 skeleton of the Group III trimethyls in the fluid phases is an example, is used throughout for exemplification purposes. In the final section of the chapter the spectroscopic effects of including a molecule in a crystal lattice are considered. For this section the trimethylindium crystal structure[63], which consists essentially of distorted XY_3 molecules, is used to exemplify the methods.

2.1. The Origins of Infrared and Raman Spectra

The physical origins of infrared and Raman spectra are fundamentally different and, in consequence, the results obtained are complementary in many respects. Both types of spectra arise from transitions

between vibrational energy levels of a molecule, normally in the electronic ground state. However, whilst infrared absorption originates in the interaction of oscillating dipoles within the molecule with electromagnetic radiation in the infrared region of the spectrum, Raman scattering originates in the electronic polarization of a molecule induced by electromagnetic radiation of any appropriate frequency (in practice, visible light). Vibrational frequencies are given directly by the frequencies of the infrared absorptions, but are measured as displacements from the frequency of the polarizing radiation in Raman scattering. Thus, whilst infrared spectra arise from a straightforward absorption phenomenon, Raman spectra are less easily explained and it is worthwhile to discuss briefly the origin of such spectra.

When a beam of monochromatic light is passed through a homogeneous medium which does not absorb light of this frequency, the spectrum of the emergent light consists of a strong component of the same frequency as the incident radiation (Rayliegh scattering) plus a number of very much weaker components symmetrically positioned relative to the Rayleigh feature. These satellites are the Raman lines first observed by Raman[116] in 1928, but predicted theoretically by Smekal[117] in 1923. For liquids the intensities of the Rayleigh and Raman scattering are respectively, ca. 10^{-5} and 10^{-8} of the intensity of the incident light. The lines at lower frequency than the exciting radiation are called the Stokes lines; those at higher frequency are the anti-Stokes lines.

The frequency shifts from the exciting line are independent of the frequency of that line and correspond to transitions between the

vibrational energy levels of the molecule. Such Raman lines are caused by the interaction of photons of the incident radiation with the vibrational motion of the scattering molecules, and by means of such interactions the photon may gain or lose energy. For a vibrational transition from the vibrational ground state (v = 0) to the first excited state (v = 1) of a molecule, occurring with the absorption of energy $h\nu_{vib}$ and induced by photons of energy $h\nu_o$, scattered photons have an energy of $h(\nu_o - \nu_{vib})$ and a line appears on the Stokes side of the exciting line, from which it is displaced by a frequency of ν_{vib}. The transition v = 1 to v = 0 gives rise to the corresponding anti-Stokes line. The relative intensities of these lines depend on the populations of the initial levels. Since the vibrational levels are populated according to a Boltzman distribution, the ratio of the number of molecules with v = 1 to those with v = 0 is small for all but low frequency transitions (kT = 200 cm^{-1}), so that the anti-Stokes lines are normally considerably weaker than the corresponding Stokes lines. The disparity in intensity is enhanced as ν_{vib} increases and the anti-Stokes lines are of limited value in practice.

As in the case of infrared absorption, the vibrational selection rule is $\Delta v = \pm 1$ for simple harmonic vibrations, and the shifts observed correspond to the fundamental vibrational frequencies of the scattering molecule.

By the use of polarized incident light it is possible to find the degree of depolarization of each Raman line. This factor, which is discussed in section 2.4, is a valuable index to vibrational assignments

and, at least for investigations of comparatively small molecules, tends to make Raman spectra inherently more informative than their infrared counterparts.

2.2. Molecular Vibrations: Normal Modes

For a simple diatomic molecule, the vibrational motion is approximately described by a simple harmonic motion of the nuclei along their line of centres. The motions of the nuclei are in phase and of identical frequency and can be specified by a single time-dependent variable, q, the normal coordinate of the vibration. The motion of the molecule along this normal coordinate is said to constitute the normal mode of vibration of the molecule.

The complex and seemingly aperiodic internal motions of a vibrating polyatomic molecule can be resolved into a relatively small number of normal modes, each of which can be described by a normal coordinate, q_i. In each normal mode the nuclei execute in-phase simple harmonic motions with the same frequency, though, in general, with differing amplitudes. Each normal mode is separately quantised thus giving rise to a number of sets of vibrational energy levels for the molecule between which transitions may be induced by electromagnetic radiation. The infrared and Raman spectra of a molecule therefore give information about the normal modes of vibration of the molecule.

The number of normal modes possessed by a molecule depends on the number of atoms in the molecule. Each atom has three degrees of freedom and this is an invariant property with respect to the state of chemical combination of the atom. Thus an n-atomic molecule has 3n degrees of

freedom. Of these, however, three describe translations and three more describe rotations (for a non-linear molecule), leaving 3n-6 internal or vibrational degrees of freedom. In the case of a linear molecule, only two degrees of freedom are needed to specify rotation and hence there are 3n-5 vibrational degrees of freedom. There are, then, 3n-6 and 3n-5 normal modes of vibration for non-linear and linear molecules, respectively.

Two fundamental points concerning normal modes are to be noted:

(i) not all normal modes give rise to spectral features;

(ii) in some cases two or more normal modes have the same frequency (degenerate modes).

Both of these details depend on the symmetry of the molecule, and this is discussed in the next section.

2.3. Molecular Symmetry

Most molecules possess some degree of symmetry and by the application of simple group theoretical methods[112,114] it is possible to examine rigorously all the likely models for the system under consideration. For a particular model it is possible to determine:

(i) The total number of distinct fundamental vibrations (allowing, that is, for degeneracies).

(ii) The infrared and Raman activity of these fundamentals.

(iii) The polarization properties of the Raman-active modes.

(iv) The activity of various secondary effects, such as overtone and combination transitions.

It is worth noting here that symmetry considerations alone are unable to give any indication of the frequency of a given vibration. This cannot be calculated a priori. It is also possible only to consider model systems and to compare experimental with predicted spectra. It is rarely possible to deduce anything more explicitly from the experimental spectra. Vibrational spectroscopy cannot therefore be considered a definitive technique for structural investigation.

(a) The Symmetry Elements: Assignment to a Point Group

The molecule in its equilibrium position possesses a number of symmetry elements, each of which has an associated symmetry operation. When each operation is performed on the molecule, it is transformed into a configuration indistinguishable from the original. The symmetry operations occur in sets (classes), each of which constitutes a mathematical group. The classes themselves constitute a larger group which describes the geometry of the molecule. The determination of the symmetry operations characteristic of the molecule enables it to be assigned to one of the Schoenflies point groups.[114a] Figure 2.1 (p. 48) shows the symmetry elements of the XY_3 molecule, which, in the planar configuration, belongs to the point group D_{3h}.[115a]

(b) The Character Table

The character table for the D_{3h} point group is illustrated in Table 2.1 (p. 49). Basically this gives a group-theoretical representation of the transformation properties of any directional or spatial function (in this case internal vibrations) of the molecule.

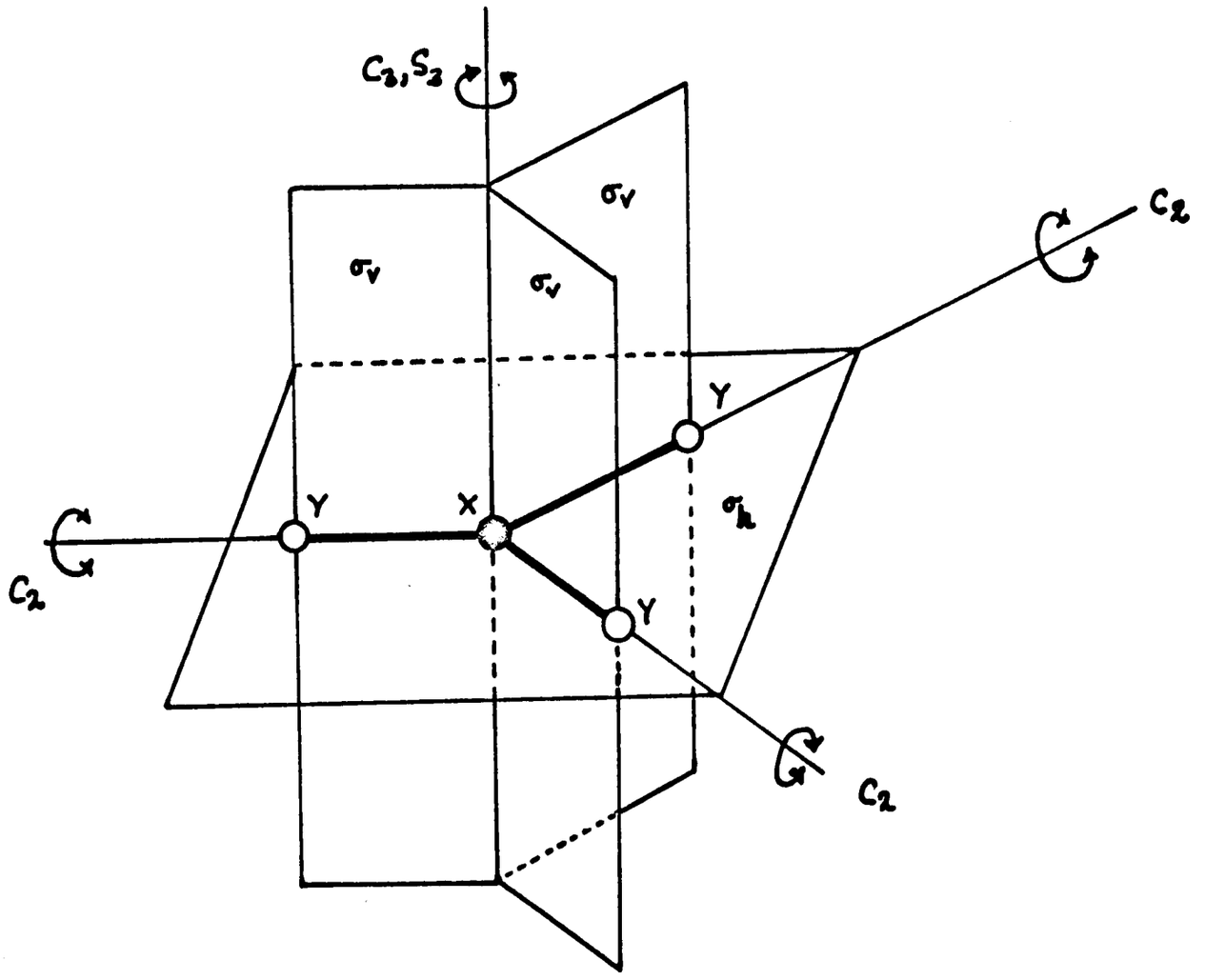

Symmetry Elements:

E = identity

C_3 = threefold proper axis of rotation

C_2 = twofold proper axis of rotation

σ_h = horizontal plane of symmetry

S_3 = threefold improper axis of rotation

σ_v = vertical plane of symmetry

Figure 2.1: Symmetry Elements of the D_{3h} Point Group

D_{3h}	E	$2C_3$	$3C_2$	σ_h	$2S_3$	$3\sigma_v$		
A_1'	1	1	1	1	1	1		$(\alpha_{xx}+\alpha_{yy})$, α_{zz}
A_2'	1	1	-1	1	1	-1	R_z	
E'	2	-1	0	2	-1	0	(T_x,T_y)	$(\alpha_{xx}-\alpha_{yy}, \alpha_{xy})$
A_1''	1	1	1	-1	-1	-1		
A_2''	1	1	-1	-1	-1	1	T_z	
E''	2	-1	0	-2	1	0	(R_x,R_y)	$(\alpha_{xz}, \alpha_{yz})$
(i)			(ii)				(iii)	(iv)

Table 2.1 Character Table for the D_{3h} Point Group

The following features of the table are relevant to the classification of normal modes of vibration:

(i) In area (i) the symmetry classes to which the normal modes belong are given. These symbols, which are the generally accepted Mulliken symbols, represent the various irreducible representations of the group and are labelled with reference to certain symmetry elements and in accordance with certain rules.[114b] A represents a non-degenerate vibration, E a doubly degenerate one.

(ii) In area (ii) are the characters of the irreducible representations of the group describing the behaviour with respect to the symmetry elements of the point group.

(iii) Area (iii) gives the symmetry classes of the non-genuine vibrations: the rotations (R_x, R_y, R_z) and the translations (T_x, T_y, T_z). These are to be subtracted from the number of normal modes calculated for each symmetry class in order to arrive at the number of genuine (or internal) vibrations for that class.

(iv) The components of the polarizability elipsoid of the molecule are assigned to symmetry classes here. This column provides a simple index to the Raman activity of modes (see section 2.4b).

(c) The Normal Modes

From the character table the number and type of the normal modes are calculated. It is first necessary to find the character, χ_j, of the transformation matrix of the atomic coordinates for each symmetry operation; these characters together constitute the "reducible

representation" of the molecule. The character of a matrix is the sum of the leading diagonal elements. It can be obtained by constructing the matrix from consideration of a model,[114c] or more simply as follows.[112a] For atoms which are only interchanged during the symmetry operation the diagonal elements are zero. Hence only unshifted atoms contribute to χ_j and the contributions per unshifted atom, χ_j^{atom}, have been tabulated for each symmetry operation.[112b] The results for the XY_3 (D_{3h}) molecule are given in Table 2.2a (p. 52)

The number of vibrations (both genuine and non-genuine) per symmetry class r is calculated by means of the expression:

$$n_r = \frac{1}{g} \sum_j g_j \chi_j^r \chi_j$$

where:

g_j = number of symmetry operations in class j

g = total number of symmetry operations.

χ_j^r = character (from character table) for the symmetry class r and symmetry element j.

The values of the various terms in the summation are also collected together in Table 2.2a. The number of vibrations per symmetry class is now readily calculable:

$$n_{A_1'} = \frac{1}{12}(1.12 + 1.0 + 1(-6) + 1.4 + 1(-4) + 1.6) = 1$$

$$n_{A_2'} = \frac{1}{12}(1.12 + 1.0 + (-1)(-6) + 1.4 + 1(-4) + (-1)\,6) = 1$$

$$n_{E'} = \frac{1}{12}(2.12 + (-1)0 + 0(-6) + 2.4 + (-1)(-4) + 0.6) = 3$$

Symmetry Operation	E	C_3	C_2	σ_h	S_3	σ_v
No. of Unshifted Atoms	4	1	2	4	1	2
χ_j^{atom}	3	0	-1	1	-2	1
χ_j	12	0	-2	4	-2	2
n_j	1	2	3	1	2	3
$n_j\chi_j$	12	0	-6	4	-4	6

Table 2.2a: Reducible Representation for XY_3 (D_{3h})

Class	n_j	Trans.ns	Rot.ns	Vib.ns
A_1'	1	-	-	1
A_2'	1	-	1	0
E'	3	1	-	2
A_1''	0	-	-	0
A_2''	2	1	-	1
E''	1	-	1	0

Table 2.2b: Number of Genuine Vibrations for XY_3 (D_{3h})

$$n_{A_1''} = \frac{1}{12}(1.12 + 1.0 + 1(-6) + (-1)4 + (-1)(-4) + (-1)6) = 0$$

$$n_{A_2''} = \frac{1}{12}(1.12 + 1.0 + (-1)(-6) + (-1)4 + (-1)(-4) + 1.6) = 2$$

$$n_{E''} = \frac{1}{12}(2.12 + (-1)0 + 0(-6) + (-2)4 + 1(-4) + 0.6) = 1$$

Finally, the number of genuine vibrations is found by subtraction of the contributions to the symmetry classes from translations and rotations, as shown in Table 2.2b.

The representation then has the form:

$$\Gamma_{gen} = A_1' + 2E' + A_2''$$

where the subscript gen indicates the reducible representation for genuine vibrations only.

From this expression it is evident that a maximum of four distinct fundamentals can give rise to spectral features for the $XY_3(D_{3h})$ molecule.

(d) The Representation of Normal Modes: Symmetry Coordinates

By using linear combinations of the internal coordinates of the molecule (bond lengths and interbond angles) it is possible to obtain a set of symmetry coordinates corresponding to each of the symmetry classes of the molecule.[114d] The normal coordinate for a given mode can be expressed as a linear combination of the symmetry coordinates of the class to which that mode belongs. If there is only one mode to a class (as in the A_1' for $XY_3(D_{3h})$), then the symmetry coordinates give an exact description of the nuclear displacements. However, when there

are several modes of a particular class the exact description of the nuclear displacements for a given mode depends upon the symmetry coordinates of all the modes in the class. Thus each such normal mode consists of a mixture of all the symmetry coordinates of its class.

From considerations of symmetry coordinates it is possible to obtain pictorial representations of the different modes showing approximate relative displacements. Figure 2.2 (p. 55) shows such pictorial representations for the XY_3 (D_{3h}) molecule[115b].

2.4. The Selection Rules

In the previous section the distinct vibrational frequencies have been enumerated and their symmetry classes assigned. It is now necessary to find whether vibrations of a given symmetry class will absorb infrared radiation or give rise to Raman scattering.

(a) Infrared Activity

The absorption of electromagnetic radiation by a molecule, with simultaneous excitation from a state with wave function ψ to a state of higher energy with wave function ψ', involves normally the interaction of the oscillating electric vector of the radiation with an oscillating dipole in the molecule. The intensity of the absorption, I, determined by the incidence of such dipolar interaction, is shown from quantum mechanics to be:

$$I \alpha \left[\int \psi' \mu \psi \, d\tau \right]^2 \qquad 2.4.1$$

where μ is an operator corresponding to the vector sum of the three classical components of an electric dipole:

$$\mu = \sum_i e_i x_i + \sum_i e_i y_i + \sum_i e_i z_i \qquad 2.4.2$$

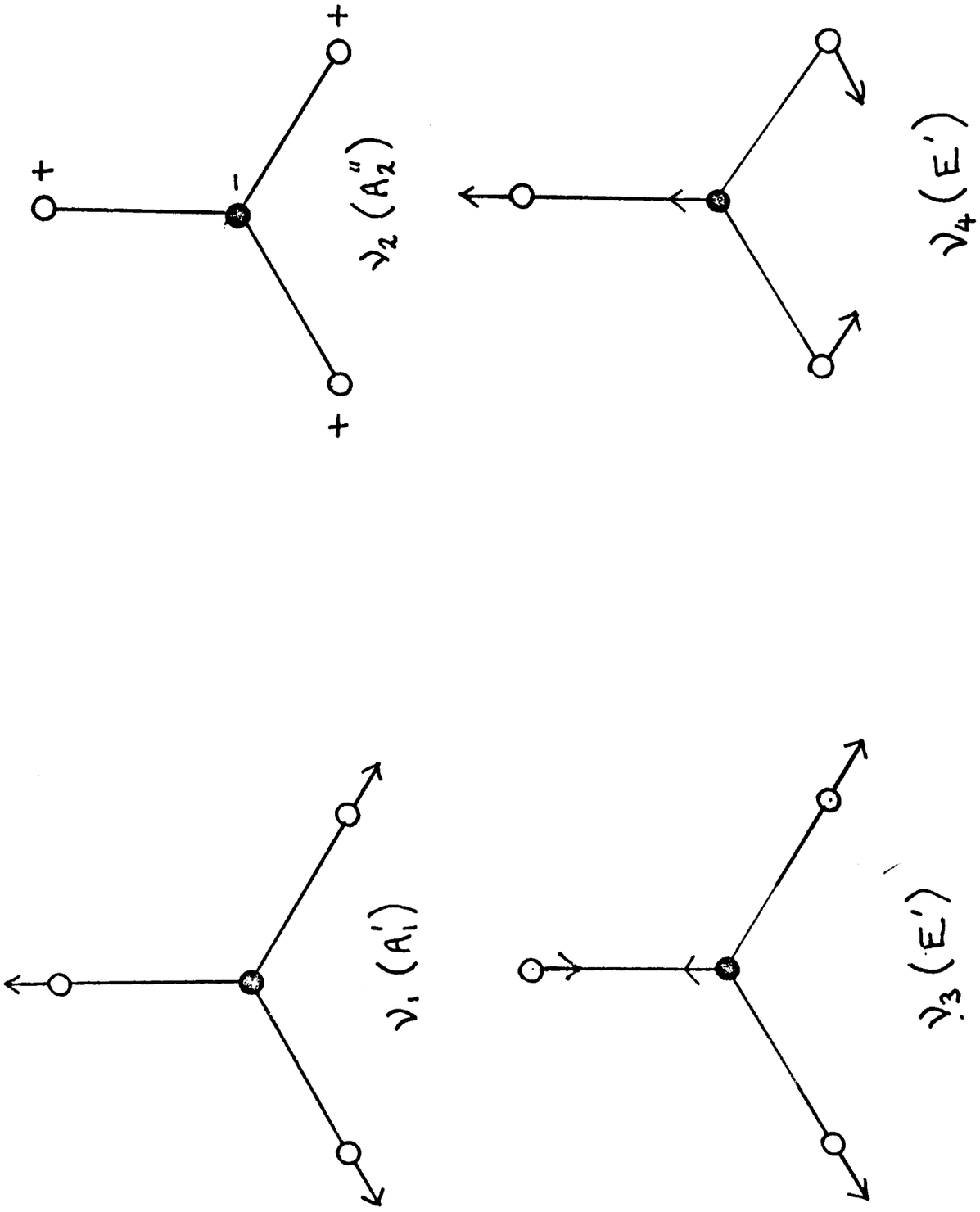

Figure 2.2: The Normal Modes of Vibration of the XY_3 (D_{3h}) Unit

where e_i is the charge on the ith particle and x_i, y_i, z_i represent its coordinates. The e_i terms are scalars and can be absorbed into the proportionality constants so that equation 2.4.1. becomes:

$$I_x \alpha [\int \psi' x \psi d\tau]^2$$

$$I_y \alpha [\int \psi' y \psi d\tau]^2$$

$$I_z \alpha [\int \psi' z \psi d\tau]^2$$

Thus for a vibrational transition to occur by absorption of infrared radiation it is necessary that one of the above integrals be non-zero. For an integral to be non-zero it must be totally symmetric with respect to all the symmetry operations characteristic of the point group to which the molecule belongs (i.e. the integrand is invariant under these operations). For a given transition, ψ, the wave function of the molecule in the ground state, is totally symmetric. It follows that ψ', where one mode is singly excited, and the coordinate, x, for example, must belong to the same representation in order that the representation of the direct product should contain the totally symmetric representation. Since ψ' belongs to the same representation as the normal mode which is excited the rule for infrared activity is:

RULE A fundamental is infrared active if the normal mode involved belongs to the same representation as any one or several of the Cartesian coordinates.

The Cartesian coordinates belong, of course, to the same representation as the translations of the molecule, T_x, T_y, T_z, and the infrared-active modes are, therefore, readily found by inspection of the group

character table.

For the XY_3 (D_{3h}) molecule, Tables 2.1 and 2.2b show that the infrared active modes are:

$$(\Gamma_{gen})_{IR\ active} = 2E' + A_2''$$

i.e. three features are expected in infrared absorption arising from fundamental vibrations.

Overtone and combination bands are commonly observed even though they are strictly forbidden for a simple harmonic oscillator. Their existence can be ascribed to the anharmonicity of the molecular vibrations. An overtone corresponds to multiple excitation of one mode and a combination to simultaneous excitation of more than one mode. Again not all combinations are active and there are symmetry-based selection rules analogous to those governing fundamental transitions. Occasionally, examination of overtone and/or combination features permits the location of fundamentals which are inactive in both the infrared and Raman spectra. This is so for several of the fundamental vibrations of the benzene molecule.

(b) Raman Activity

In the Raman effect the oscillating electric vector, E, associated with the exciting radiation induces an electric dipole μ_{ind}, in the molecule:

$$\mu_{ind} = \alpha E$$

where α is the electronic polarizability of the molecule. For isotropic molecules it is a scalar quantity, but most molecules are anisotropic

and the polarizability is then a tensor with appropriate directional properties.

If a vibration causes no change in α, the frequency of the induced dipole moment is the same as that of the incident radiation and Rayleigh scattering occurs. However, if a vibration causes periodic changes in α and thus in μ, the frequency of the scattered radiation is modulated by the frequency of the vibration, thereby giving rise to Raman lines. Raman shifts result, therefore, from changes in polarizability during the vibration of a molecule.

The intensity, I, of a Raman feature is given by the expression:

$$I \alpha [\int \psi' (\mu_{ind}) \psi \, d\tau]^2 \qquad 2.4.3$$

which is exactly analogous to expression 2.4.1 for infrared absorption. When the molecule is anisotropic:

$$[\mu_{ind}] = [\alpha][E]$$

where the square brackets indicate that the quantities enclosed are matrices. Nine components of α are defined by these matrices:

$$\mu_x = \alpha_{xx}e_x + \alpha_{xy}e_y + \alpha_{xz}e_z$$

$$\mu_y = \alpha_{yx}e_x + \alpha_{yy}e_y + \alpha_{yz}e_z$$

$$\mu_z = \alpha_{zx}e_x + \alpha_{zy}e_y + \alpha_{zz}e_z$$

Thus equation 1.4.3 with the above results yields nine integrals of the type:

$$I \alpha [e_g \int \psi' \alpha_{gg'} \psi \, d\tau]^2$$

where g and g' equal x, y or z.

From these nine integrals the Raman activity of the various modes can be deduced. For I to be non-zero $\psi' \alpha_{gg'} \psi$ must be totally symmetric with respect to all the symmetry operations characteristic of the point group to which the molecule belongs. As before, ψ is totally symmetric and hence ψ' and $\alpha_{gg'}$ must belong to the same representation for their direct product to be totally symmetric. ψ' belongs to the same representation as the normal mode excited, and hence the rule for Raman activity is:

RULE A fundamental transition is Raman-active if the normal mode involved belongs to the same representation as one or more of the components of the polarizability tensor of the molecule.

The components of the polarizability tensor, which transform as the products x^2, y^2, xy, yz, etc., are listed in the group character table and the Raman-active modes are readily found.

For the XY_3 (D_{3h}) molecule, Tables 2.1 and 2.2b show that the Raman-active modes are:

$$(\Gamma_{gen})_{R \text{ active}} = A_1' + 2E'$$

i.e. three features due to fundamental vibrations are expected in the Raman spectrum.

Overtone and combination features are also possible in the Raman effect.

Raman scattering shows interesting variations in polarization properties which are a valuable aid to spectral analysis. In a

conventional Raman spectrometer the scattered light is viewed at right angles to the incident radiation, thereby achieving the maximum discrimination against exciting light at the monochromator. The polarization properties of the scattered light are most easily assessed in terms of the depolarization ratio, ρ, defined by:

$$\rho = \frac{\text{Scattered intensity polarized perpendicular to direction of E}}{\text{Scattered intensity polarized parallel to direction of E}}$$

where E is the electric vector of the incident radiation.

If a fluid phase sample is considered, where the molecules are randomly orientated, for unpolarized incident light the depolarization ratio, ρ_n, of the scattered light viewed at 90° to the incident light, lies between 0 and $\frac{6}{7}$ for a totally symmetric vibration, but has the value $\frac{6}{7}$ for all modes that are not totally symmetric. Thus, by the measurement of depolarization ratios it should be possible to identify the totally symmetric modes of vibration (i.e. the A_1' mode for the XY_3 (D_{3h}) molecule). ρ_n may not, however, be measurably less than $\frac{6}{7}$ for a totally symmetric vibration and polarization measurements are of positive value in vibrational assignment only when they yield values significantly less than $\frac{6}{7}$.

In concluding this section on selection rules the following limitations of the method are to be emphasised:

(i) Symmetry considerations are able only to predict the activity of vibrational modes and cannot give any indication of the intensity of the spectral features associated with them. Failure to observe a

spectral feature is, therefore, a negative result, in that the failure to see a feature may be caused by the inherent weakness of the absorption or scattering, rather than by the operation of selection rules.

(ii) Strict adherence to the formal selection rules may not be found as a result of such factors as anharmonicity of vibrations or intermolecular interactions. In the Raman spectrum of liquid CS_2, for example, the formally "forbidden" bending mode, ν_2, is observed at 390 cm^{-1}. Investigation of the variation of relative intensity of this band with the concentration of CS_2 in an inert solvent[118] shows that the breakdown of selection rules is here caused by intermolecular interactions.

(iii) If a change of configuration of the molecule occurs in a time comparable to, or shorter than, the time of a vibration, which is typically of the order of 10^{-13} sec., then only the time-averaged configuration of the molecule may be observed by vibrational spectroscopy. For example, $(SiH_3)_2O$ was shown by electron diffraction studies, which have a time-scale of ca. 10^{-20} sec., to have a bent form.[119] When studied by vibrational spectroscopy, however, the rapid change of configuration by means of the skeletal deformation, involving a low-frequency vibration of relatively large amplitude, appears to give rise to selection rules for the molecule which are analogous to those of a linear molecule.[119, 120]

Table 2.3 (p. 62) gives the predicted vibrational spectrum for the XY_3 (D_{3h}) molecule. Apart from the above complications this type of molecule is one of the few for which all the classes of normal modes

Symmetry Class	Number of Frequencies	Infrared	Raman	Polarization
A_1'	1	Inactive	Active	Polarized
A_2'	0	-	-	-
E'	2	Active	Active	Depolarized
A_1''	0	-	-	-
A_2''	1	Active	Inactive	-
E''	0	-	-	-

Table 2.3: Predicted Spectral Features for $XY_3(D_{3h})$ Molecules

can be distinguished unambiguously by simple considerations of the spectroscopic selection rules.

2.5. Effects of the Solid State[114e]

The treatment outlined above refers essentially to a molecule which is isolated from all other molecules. In liquids and crystals, however, molecules are in close proximity and intermolecular interactions may have a significant effect on the vibrational modes and vibrational transitions of individual molecules. For liquids the effects, commonly quite small, are usually neglected, but in crystals the fixed and well-defined configuration of the molecules or polyatomic ions within the lattice can have a substantial effect on the spectrum of the molecules or ions.

The level of sophistication required in interpreting the vibrational spectra of solids depends on the nature and degree of interaction. In the case of relatively weak interactions it is usually sufficient to consider the effect of altering the symmetry of the molecule by inclusion in a crystal lattice. If interactions in the solid state are such as to produce relatively tightly bound aggregates with relatively weak inter-aggregate interactions then it may be appropriate to consider the vibrations of the aggregate unit. If, on the other hand, relatively strong interactions exist throughout the lattice, then the only satisfactory approach is that of factor group analysis, which deduces the vibrations of the whole lattice by consideration of the symmetry elements of the crystallographic unit cell. To exemplify the three approaches the effect of inclusion in a crystal lattice on the M-C stretching modes

for the MC_3 unit of either trimethylindium or trimethylthallium is considered. The spectroscopic features arising from the M-C stretching vibrations occur in a highly characteristic region of the spectrum, well removed from other spectroscopic features and their position is little affected by variation of the alkyl group or by deuteration. The vibrational modes are therefore almost 'pure' and it is possible to assign a single internal displacement coordinate to stretching of the M-C bonds.[121] It is then particularly easy to visualise the effect of including the MC_3 unit in the crystal lattice and it is also possible to deduce the number and spectroscopic activity of the modes very much as described above using space-fixed cartesian coordinates for an isolated molecule.

The solid-state structures are illustrated in Figures 1.2 and 1.3 (p. 10 and p. 13, respectively). Four MC_3 units, originally of D_{3h} symmetry, form a tetrameric unit of S_4 symmetry and there are two of these tetrameric units to a unit cell of the crystal. The symmetry of the crystal is C_{4h}^4.

(a) Site Symmetry Approach[122]

In this treatment the molecules surrounding a given molecule are considered to provide an environment of fixed symmetry in which the molecule vibrates. The form of the vibrational modes then depends both on the intrinsic symmetry of the molecule itself and on the symmetry of the environment, that is on the site symmetry. The collection of symmetry elements possessed by the environment constitutes a point group which can be used to specify the site symmetry of a molecule whose

centre of mass lies at this point. The site symmetry can never be such as to contain symmetry elements not possessed by the free molecule, and, in general, the site symmetry is lower than the molecular symmetry.

Incorporation of a molecule into a lattice of lower symmetry has two principal effects on the vibrational spectrum of the molecule:

(i) The degeneracy of certain modes may be lifted causing splitting of spectral features. The degree of splitting has been empirically correlated with the degree of interaction in some cases.[123]

(ii) There may be changes in the selection rules such that some modes which are inactive for the isolated molecule now become active with respect to infrared absorption or to Raman scattering or to both effects.

For the MC_3 unit of trimethylindium or trimethylthallium the symmetry of the molecule is lowered from D_{3h} to C_S by inclusion in the crystal lattice. It is useful to consider the lowering of the symmetry as taking place in two stages. Firstly one of the M-C bonds becomes non-equivalent to the other two and the symmetry is lowered from D_{3h} to C_{2v} and then the approach of two further carbon atoms, one above and one below the metal atom, but not both normally to the MC_3 plane, lowers the symmetry to C_S, the MC_3 plane no longer being a symmetry element. Figure 2.3 (p. 66) shows the effect on the vibrational stretching modes. It is evident that the effects of (i) and (ii) above are both to be expected for trimethylindium and trimethylthallium. The

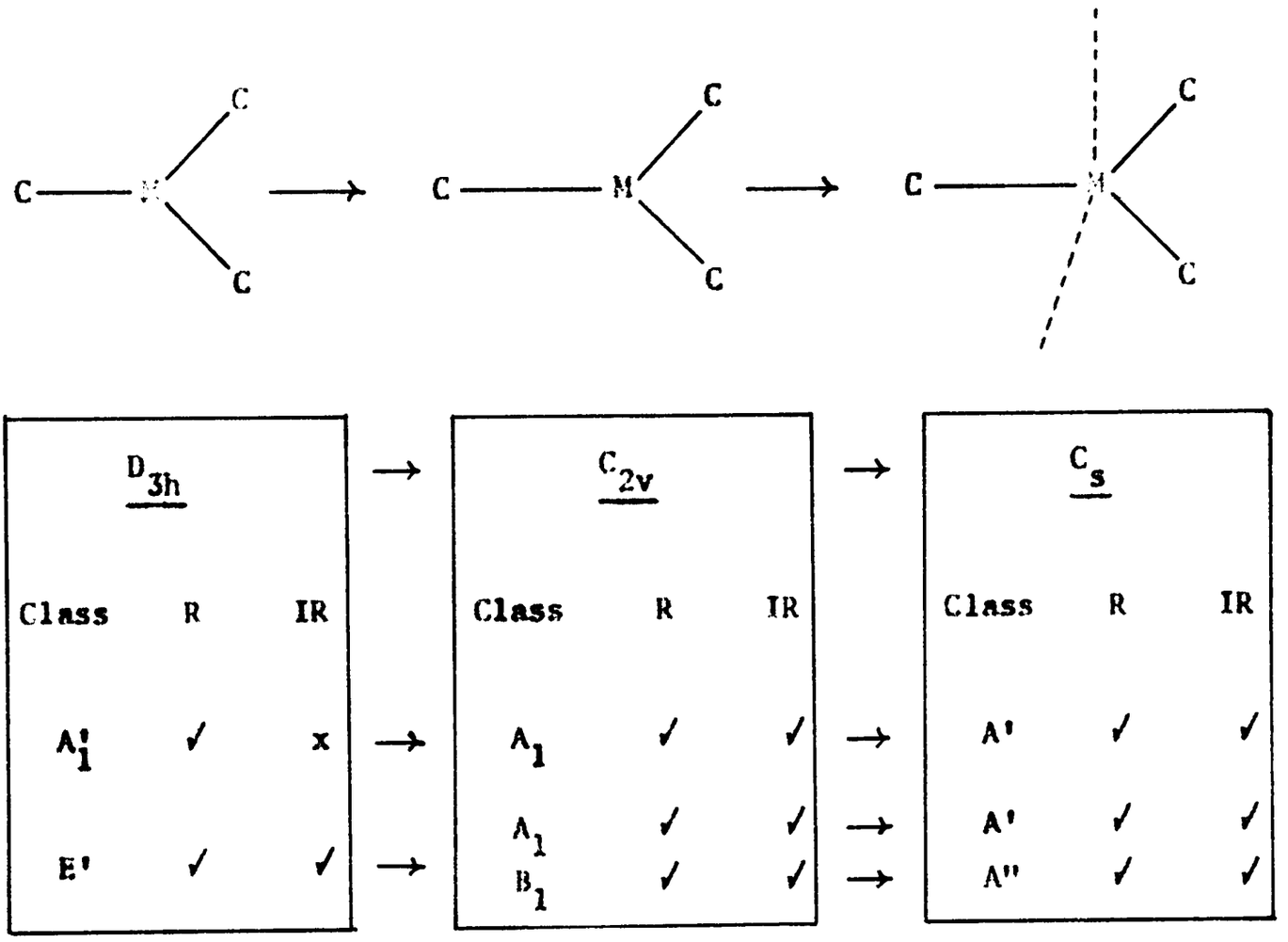

Figure 2.3: The M-C Stretching Modes for the MC_3 Unit in Different Site Symmetries

degeneracy of the e' stretching mode for the D_{3h} unit is lifted and the a_1' mode becomes infrared active.

It is to be noted that the total number of vibrational modes (allowing, that is, for degeneracies) remains invariant using the site symmetry approach. Thus, for the M-C stretching region of the spectrum the number of vibrational modes is three, changes occurring merely in the degree of degeneracy and selection rules. The observation of extra features in a particular region of the spectrum is an indication that a more sophisticated approach to the problem is required.

(b) Aggregate Unit Approach

In solid trimethylindium discrete tetrameric units of S_4 symmetry can be distinguished. For the M-C stretching region of the spectrum the reducible representation is deduced exactly as for an isolated molecule:

$$(\Gamma_{gen})_{\text{M-C stretching}} = 4A + 4B + 4E$$

Raman activity: R R R

Infrared activity: IR IR

Of these modes, however, one of each symmetry class is associated with vibrations of the long and relatively weak inter-MC_3 bonds and the spectroscopic features associated with these transitions would be expected to lie at frequencies much lower than those characteristic of the stretching of 'normal' M-C bonds. Thus consideration of the aggregate unit implies no less than nine features in the M-C stretching region of the Raman spectrum, six of which are coincident with features in the

infrared spectrum.

(c) Factor Group Approach[124,125]

In order to undertake a factor group analysis of the vibrational modes of a compound in the solid state the crystal structure of the compound must be known. For trimethylindium and trimethylthallium the appropriate factor group is C_{4h}^4, which is isomorphous with the corresponding point group C_{4h}. The difference between the factor group and the point group is essentially that the extended elements of symmetry of the former, such as glide planes or screw axes, become more restricted elements in the latter - mirror planes or rotation axes. Otherwise a factor group analysis of the vibrational modes of a crystal follows much the same pattern as that of a point group analysis for an individual molecule.

In the case of trimethylindium or trimethylthallium the unit cell contains eight MC_3 units (i.e. two S_4 tetrameric units). None of the atoms lies on the symmetry elements of the crystal and the calculation of the number of M-C stretching modes is particularly simple. The reducible representation is found to be:

$(\Gamma_{gen})_{M\text{-}C\ stretching}$	=	4Ag +	4Bg +	4Eg +	4Au +	4Bu + 4Eu
Raman activity		R	R	R		
Infrared activity					IR	IR

As in the treatment of the aggregate unit, one mode in each class is associated with the stretching of long M...C bonds and is thus unlikely to be observed in the spectroscopic region usually associated with M-C

stretching. This region is hence expected to contain nine Raman and six infrared features attributable to fundamental vibrations; because of the centre of symmetry of the factor group there should be no coincidences between the Raman and infrared frequencies.

For the vibrational spectra of the crystalline solids, therefore, the two more sophisticated approaches, based on the symmetry properties of the oligomer unit or of the factor group, are in agreement in predicting many more features in the M-C stretching region than does the simple analysis in terms of site symmetry. However, the more elaborate treatments differ fundamentally in the number of coincidences between Raman and infrared features that they predict.

Table 2.4 (p.70) summarizes the spectroscopic selection rules appropriate to the three approaches.

Feature	Site Symmetry			Aggregate Unit	Factor Group
	D_{3h}	C_{2v}	C_S	S_4	C_{4h}^4
Raman	2	3	3	9	9
Infrared	1	3	3	6	6
Number of Coincidences	1	3	3	6	0

Table 2.4: M-C Stretching Features for Solid Trimethylindium and Trimethylthallium

SECTION II

SWEAT

Chapter 3

Instruments and Apparatus

By way of introduction to the experimental section of this thesis it is useful to give some indication of the fundamental problems involved in studying the Group III alkyls. Technically they are difficult to handle and instrumentally it is difficult to obtain complete spectra. In section 3.1, therefore, the general problems involved in examining these compounds are briefly discussed. In the remaining sections of the chapter the instruments used and the new apparatus constructed in the course of the investigation are described.

3.1 Problems Encountered in the Study of the Group III Trimethyl Compounds

(a) General

All the Group III trimethyls react vigorously and spontaneously with air and all except trimethylboron, which is only slowly hydrolysed, react violently with water. In the liquid phase the compounds, which are almost non-polar, readily dissolve hydrocarbon greases and such sealants as 'Apiezon W' wax. Neoprene is also slowly attacked, but the fluorocarbon rubbers commonly used in greaseless tap diaphragms and washers, fortunately are not.

These properties mean that the trimethyls of Group III can be stored safely only in break-seal ampoules and that they should be

handled, ideally, only in a carefully flamed, all-glass, evacuated system. In practice, this is excessively tedious and the compounds can be handled on a conventional greased vacuum line successfully if care is taken to keep the compounds frozen down except when actually carrying out manipulative operations, and even then to keep the pressure as low as possible. It is also desirable to evacuate the system for several days, 'flaming out' wherever possible, prior to transferring the alkyl compound to the line.

Because of the range of melting and boiling points (Table 1.7 p.35) each compound poses a number of problems peculiar to itself. Trimethylboron is a gas at room temperature and special precautions are required for its storage on the line. It also has a finite vapour pressure at liquid nitrogen temperatures and cannot, therefore be examined in the solid state using a liquid nitrogen probe. Trimethylaluminium and trimethylgallium are easier to manipulate and store, but react vigorously with any traces of oxygen or moisture to yield a variety of partially oxidized or hydrolyzed alkyl species, some of which are volatile and can give rise to spurious features in the spectra. For this reason it is necessary to examine each spectrum repeatedly using a number of different samples in order to confirm the authenticity of spectral features. Trimethylindium is barely volatile at room temperature and requires the application of gentle heat (commonly a hot-air blower) in its manipulation. In consequence it is necessary to use a vacuum line lubricated with a high-temperature grease, such as 'Apiezon H'. Trimethylthallium is similarly rather involatile, but decomposes

readily at temperatures above 40°C (it is reported to detonate above 90°C) and it is also photosensitive, characteristics which make its manipulation and examination particularly exacting.

(b) Sampling

The trimethyls of the four heavier elements show startling volume changes in passing from the solid to the liquid phase, the density of the former being greater than that of the latter. As a result, great care has to be taken in sealing up samples for examination in the liquid phase. At no time can a thin layer or column of liquid alkyl safely be frozen in an enclosed space, since hydrostatic forces are liable to cause the vessel to shatter on warming. It is therefore necessary to attach relatively spacious reservoirs when preparing, for example, capillary cells for use in the examination of liquid-phase Raman spectra.

The examination of the infrared spectra of vapours is made difficult by the avidity of the alkyls for moisture and the readiness with which window sealants are dissolved. Cells with polythene windows for far-infrared work require continuous evacuation for a number of days prior to use, in an attempt to remove adsorbed moisture from the polythene, and cells involving alkali halide windows require frequent dismantling and replacement of the sealant.

(c) Spectroscopic

A number of general problems make difficult the production of complete spectra and their interpretation. In the Raman spectra the features ascribable to fundamental vibrations may differ in relative

intensity by two orders of magnitude; in the vapour-phase infrared spectra some features are still unobservable (with 10 cm. cells) even at the saturation vapour pressure of the compound at elevated temperatures. Trimethylboron is a particularly poor Raman scatterer and absorber of infrared radiation.

Especially when weakly linked, the monomer and the oligomer frequently have bands in very close proximity (often within 5 cm^{-1}). This not only makes their existence difficult to verify, but also renders impossible the measurement of meaningful relative intensities. This problem is particularly troublesome where oligomer-formation occurs for less than 20% of the monomer molecules, as is commonly the case in matrix-isolation work.

The investigation of the Group III trimethyls is, therefore, a far from straightforward undertaking in technical terms and much of the work described in this thesis has required the construction of new apparatus and the repetition of experiments to achieve consistency of results.

3.2. Instrumentation

(a) Raman Spectroscopy: (i) Cary 81 Spectrometer

In all the studies described here, use was made of a Cary 81 spectrometer equipped with laser excitation. This instrument incorporates a number of features designed to give optimum light-gathering power with maximal discrimination against scattered radiation of the exciting frequency:

(1) Image slicers are located between the sample and the entrance slits of the monochromator to convert the circular image of the sample into slit-shaped images without the usual wastage of light.

(2) The monochromator is a two-grating double monochromator with triple slits. This affords high discrimination against Tyndall and Rayleigh scattered radiation from the sample. As a result, the Raman spectra of crystalline samples can be obtained, even though the crystal faces may be rough and irregular and effective light scatterers.

(3) Use of the Shurcliff double slit system, in which the slits are arranged in parallel pairs, gives, effectively, the light-gathering power of two monochromators in parallel, with no mutual interference except when close to the exciting line. For this reason, one set of slits is masked when recording spectra below about 200 cm^{-1}.

(4) The largest available gratings of 1200 lines/mm., 4500 Å blaze, are coupled to a suitably large optical system to provide the maximum light-collecting efficiency.

(ii) Lasers and Polarization Measurements

The monochromatic radiation required for sample excitation was supplied by continuous gas lasers of two types. For the majority of the spectra, a Spectra-Physics Model 125 helium-neon laser, providing approximately 70 mW of radiation of wavelength 6328Å, was used, but for the

solid-phase spectra of the four heavier trimethyls a Coherent Radiation Laboratories Model 54 argon ion laser was employed. Of the several spectral lines emitted by the CRL 54, those of wavelength 4880 Å and 5145 Å were of sufficient intensity (approximately 250 mW) to be valuable as exciting radiations. Because of the dependence of the intensity of Raman scattering on the frequency of the exciting radiation ($I \alpha \nu^4$), the response of the detector and the blaze of the gratings, an approximately forty-fold increase in sensitivity is obtained by using the argon ion laser.

Lasers provide plane-polarized radiation and for the purpose of determining the depolarization properties of Raman features, use is made of a half-wave plate and a polaroid element. The half-wave plate, which is used to rotate the polarization plane of the incident radiation through 90°, permits measurements to be made in 'parallel' and 'perpendicular' excitation modes. The polaroid element analyses the scattered radiation, passing only light polarized in one plane.

(iii) Viewing Techniques

With the Cary 81 spectrometer equipped for laser excitation it is possible to use two modes of sample examination. The coaxial viewing technique shown in Figure 3.1 (a) (p.77) requires the use of a patented lens-prism assembly[126] to direct the laser beam axially through the glass capillary sample cell. Raman radiation, contained within the cell by internal reflection at the air-to-glass interface, emerges at 180° to the incident radiation, is collected by the lens of the lens-prism

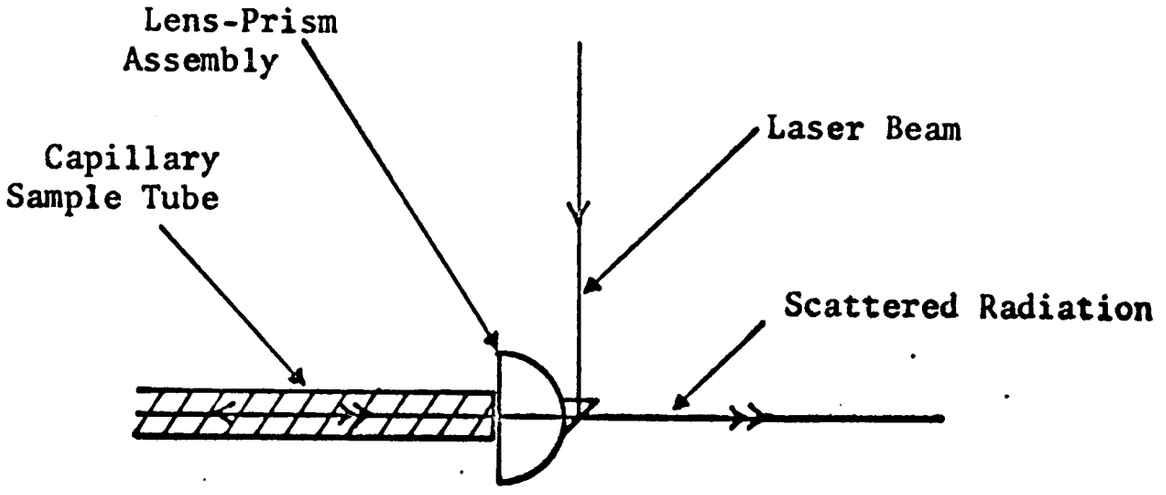

(a)

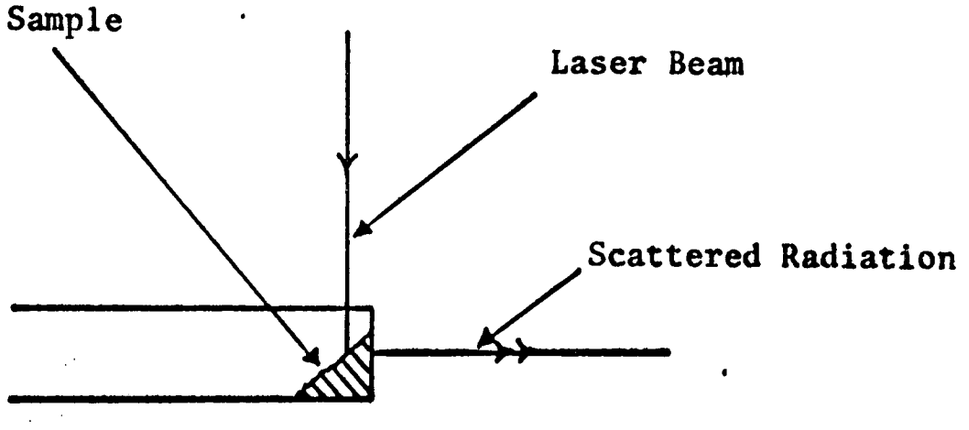

(b)

Figure 3.1: The Coaxial (a) and Right-Angle (b) Viewing Techniques

assembly and thence passes into the monochromator. To obtain good spectra it is necessary to ensure optical contact between the cell and the lens-prism assembly by the interspersion of a little glycerol and to optimize carefully the alignment of the cell. The coaxial viewing technique is particularly advantageous for small liquid samples, where considerable signal amplification is observed with respect to alternative methods of viewing.

The conventional method of right-angle viewing (Figure 3.1 (b)) has the advantage that a lens-prism assembly, together with the necessity of optical contact, is not required and samples can be more easily studied at low temperatures. Moreover, the right-angle viewing technique yields considerably lower levels of background light and hence, for a shot-noise-limited system, a higher signal to noise ratio.

(b) Infrared Spectroscopy

Two infrared spectrometers were used in the investigation:

(i) a Perkin-Elmer 225 spectrometer
(covering the range 5000-200 cm^{-1})

(ii) a Beckman I.R.11 far-infrared spectrometer
(covering the range 800-33 cm^{-1})

(i) Perkin-Elmer 225 Spectrometer

This instrument was used to record the bulk of the infrared data presented in this study. It is of the double-beam, optical null type, with an Ebert grating monochromator, an electrically heated silicon carbide rod ('Globar') as the source of infrared radiation, and a

thermocouple as the detector. A pre-dispersion system, or fore-monochromator, uses a KBr prism in the range 5000-400 cm^{-1}, and two scatter plates (which act as one low pass filter) and a transmittance filter to cover the range 450-200 cm^{-1}. The double pass monochromator employs two gratings, each used in two orders, to cover the whole spectral range in four stages:

Grating 1	150 lines/mm	2nd Order	5,000-2,000 cm^{-1}
		1st Order	2,500-1,000 cm^{-1}
Grating 2	30 lines/mm	2nd Order	1,000-400 cm^{-1}
		1st Order	450-200 cm^{-1}

The pre-dispersion system ensures that the spectrum contains no undesired orders and discriminates against stray radiation.

To reduce the energy loss caused by water vapour absorption, particularly in the region of the spectrum below 450 cm^{-1}, a purging system, which recirculates air through a column of molecular sieve is connected to the instrument.

(ii) Beckman I.R.11 Spectrometer

The Beckman instrument was used to obtain vapour phase spectra of the Group III trimethyl compounds in the region from 200-50 cm^{-1}. In essence it is a conventional double-beam spectrometer with optical null and incorporating a filter pre-dispersion system to obtain high resolution.

The source of radiation is a mercury lamp enclosed in a quartz envelope and the detector takes the form of a sensitive diamond-windowed

Golay. The pre-dispersion system consists of eight turret-mounted transmission filters together with an extra gate-mounted transmission filter. The dispersion system proper consists of four turret-mounted gratings, each used in the first order only:

Grating 1	3 lines/mm	33-80 cm^{-1}
Grating 2	8 lines/mm	70-150 cm^{-1}
Grating 3	20 lines/mm	140-350 cm^{-1}
Grating 4	50 lines/mm	340-800 cm^{-1}

Grating and filter changes are manually effected by means of a slave system. With a standard slit programme a resolution of ca. 1 cm^{-1} over virtually the entire spectral range is possible.

The instrument is continuously purged with oil-free, compressed air via an 'Electrodryer' twin-tower dryer containing molecular sieve. In this way the strong absorptions at low frequency (< 200 cm^{-1}) due to water vapour are greatly reduced in intensity.

3.3 Special Sampling Devices

This section relates to the special apparatus developed during the course of the investigation to enable the compounds to be studied at temperatures other than ambient.

(a) Raman: (i) Variable Temperature Assembly for Liquid Samples

In order to study the effect of temperature on oligomer formation in the liquid phase it was necessary to develop a sampling device capable of covering the temperature range -160°C to +150°C. To obtain

sufficient signal intensity it was necessary to employ the coaxial viewing technique and this, in turn, implies direct contact between the end of the sample tube and the lens-prism assembly of the instrument. Simple heating or cooling of the sample in a standard tube was impracticable because heat transfer to or from the lens-prism assembly would not only make difficult the attainment of the desired temperature but would also result in the following effects:

(1) a temperature gradient along the sample leading to thermal currents in the liquid and, in consequence, unsatisfactory spectra;

(2) in the case of cooled samples, ice formation on the lens-prism assembly with concomitant interference with the light-path;

(3) in the case of heated samples, possible damage to the cemented lens-prism assembly.

In order to overcome these difficulties it was decided to use a sample remotely mounted in a Dewar vessel and to achieve optical contact between the sample cell and the lens-prism assembly by means of a light-pipe. Heating or cooling could then be achieved in the usual way[127, 128, 129] by passage of air or nitrogen at a suitable temperature around the Raman cell mounted within the Dewar vessel.

In the first prototype a 2 cm. light-pipe was sealed at its mid-point through the base of a Dewar-jacketed vessel. To support the sample tube in contact with the lens-prism assembly a small section of glass

tubing was 'tacked' on to the inner end of the light-pipe. This prototype arrangement yielded poor spectra essentially for the following reasons:

(1) alignment of the components relative to each other and to the instrument was extremely difficult;

(2) light losses at the light-pipe to Dewar seal were large;

(3) a suitably involatile low temperature lubricant for the interface between the sample cell and light-pipe could not be found;

(4) severe icing of the end of the Dewar and light-pipe precluded prolonged or very low temperature work.

In the second design of apparatus, depicted in Figure 3.2 (a) (p. 83), an all-glass sample cell with an integral light-pipe (Figure 3.2 (b)) was utilized. A plastic collar lubricated with high-vacuum silicone grease was employed to form a gas-tight seal of low thermal conductivity between the hole in a Dewar vessel and the light-pipe, which protruded beyond the base of the vessel to make contact with the lens-prism assembly. A polythene collar was found to be suitable for experiments over the temperature range -160° to +70°C and a 'Teflon' collar over the range 0 to +150°C.

For temperatures below ambient the liquid nitrogen boiler depicted in Figure 3.2 (a) was employed to supply a stream of cold, dry nitrogen. For temperatures above ambient a small electric fire element was

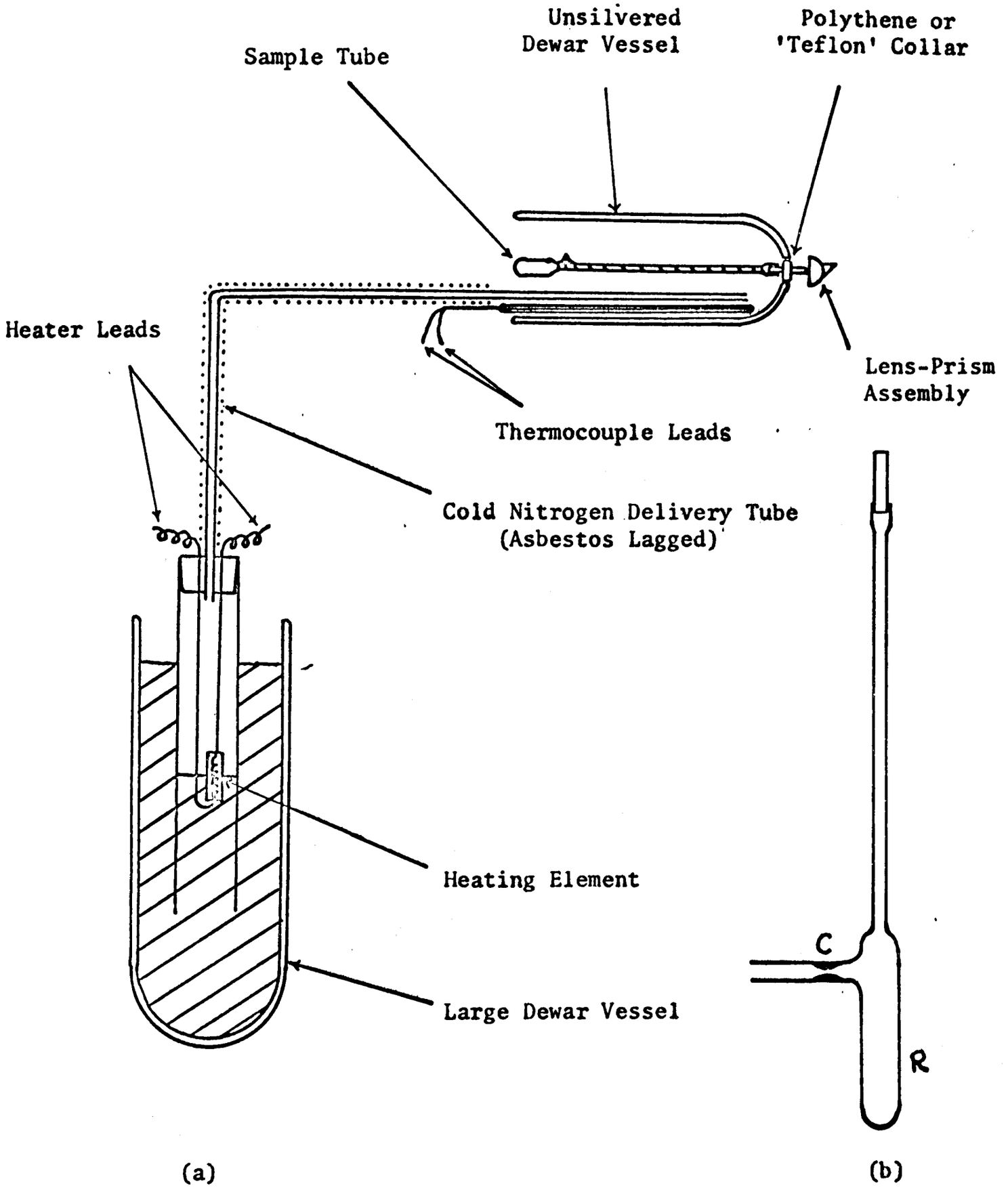

Figure 3.2: Raman Variable Temperature Assembly for Liquid Samples

suspended in the air flow provided by a hair dryer, the hot air being delivered to the Dewar by means of silicone rubber tubing. In both cases efficient lagging of the delivery system was essential to attain a high or low temperature reasonably quickly and to maintain a stable temperature. The temperature in the region of the sample was measured by means of a single junction copper-constantan thermocouple and temperature regulation was by means of a 'Variac' auto-transformer: temperatures stable to ±5°C could be maintained for a period of hours.

A special kinematic mounting device for the whole Dewar assembly was constructed in order that the accurate alignment of the cell required to obtain good spectra could be achieved. The light-pipe and Dewar showed a slight tendency to ice-up at very low temperatures but this problem could be cured by the administration of a little acetone.

The sample cell was filled by freezing the sample into the reservoir (R in Figure 3.2 (b)) and then sealing the constriction at C. Direct freezing of a sample into the light-pipe tube was also possible if great care was taken to melt the sample progressively from the end of the column remote from the light-pipe.

The light-pipes, of 2.5 mm. diameter and 2 cm. length, had optically squared and polished faces and were prepared to special order by T.W. Wingent Ltd. The sample cells were prepared in the Department by opening out 1.5 mm. i.d., 3.5 mm. ex.d. tubing and sealing it, using minimal heat, to the light-pipe on a glass-blower's lathe. Axial symmetry of the cell was found to be essential if good spectra were to be obtained.

Using the variable temperature assembly described above, liquid trimethylboron was examined at temperatures down to -160°C and solutions of trimethylgallium, trimethylindium and trimethylthallium in dichloromethane were likewise studied at temperatures down to -100°C. Trimethylaluminium was examined in benzene solution at temperatures up to 120°C.

(ii) Low Temperature Solid Sampling Assembly

In order to examine the spectra of the Group III trimethyl compounds in the solid state under similar conditions it was decided to develop a solid-sample cell capable of functioning at liquid nitrogen temperatures. It was hoped that such a cell would also be useful in the development of a Raman matrix-isolation assembly, enabling samples trapped in matrices of solid carbon tetrachloride, carbon dioxide or even xenon to be examined.

The first design to be tested, based on a cell developed by Carlson[130], is illustrated in Figure 3.3 (p. 86). Carlson's original design involved the use of a mechanical rack-and-pinion device operating at liquid nitrogen temperatures to move a solid sample into contact with a light-pipe initially at ambient temperature and it was decided to eliminate this potentially troublesome component by spraying the sample directly on to the cooled end of a light-pipe. The whole assembly, including spray arm, was designed to fit inside the sample chamber of the Cary 81 spectrometer and, in consequence, the sample spray arm had to be located at 90° to the light-pipe. The cell proved inviable for a number of reasons:

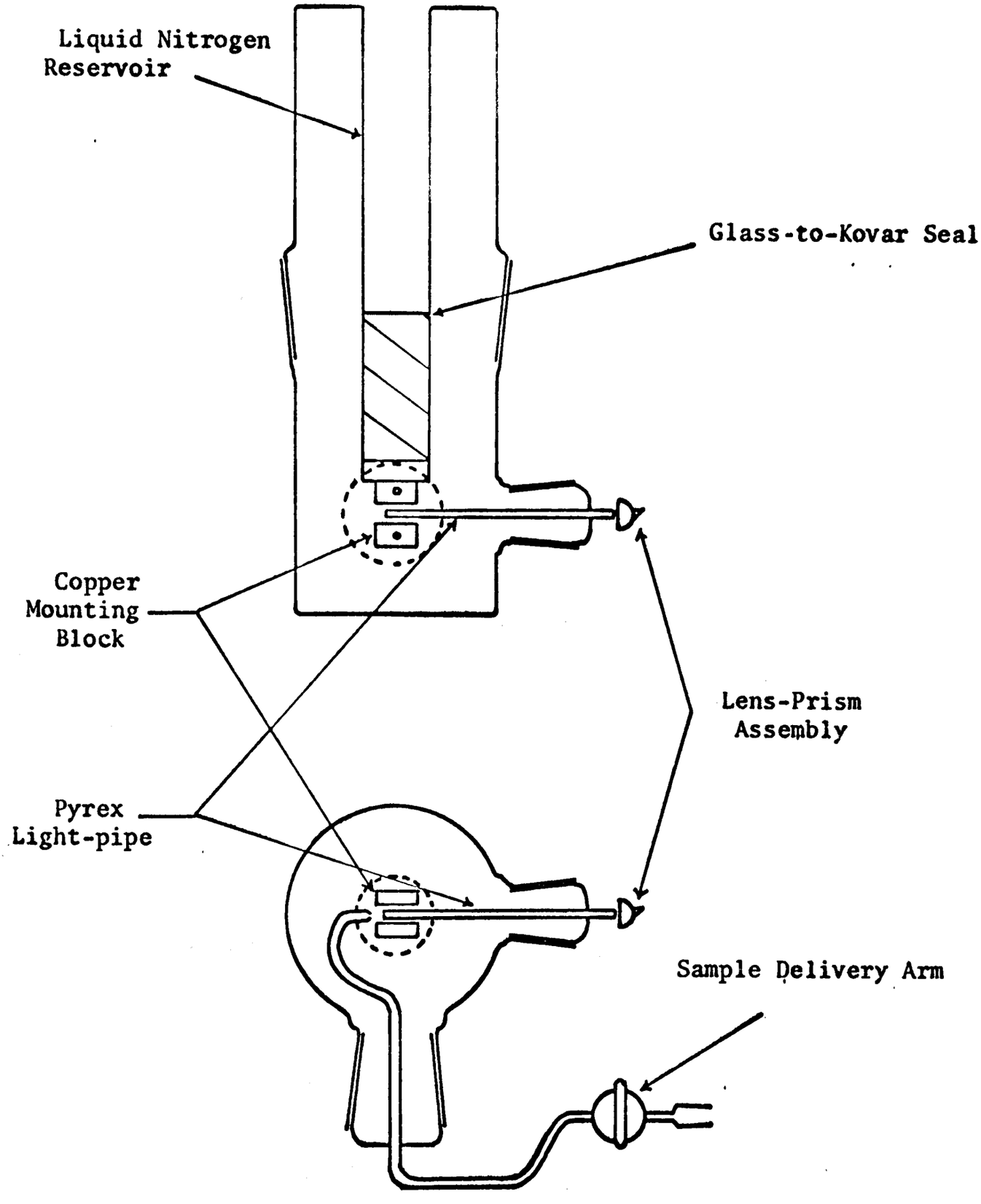

Figure 3.3: Raman Low-Temperature Solid-Sampling Assembly (Coaxial Viewing)

(1) optical losses along the 7 cm. light-pipe were excessive,

(2) the 'Pyrex' glass of the light-pipe yielded broad spectral bands on which the relatively feeble sample spectrum was superimposed;

(3) the external part of the light-pipe and the surrounding part of the cell were prone to severe ice-formation;

(4) condensed water droplets in the air currents around the Dewar vessel led to fluctuations in the intensity of the laser beam and hence fluctuations in the intensity of the spectra.

In order to overcome these problems it was clear that the coaxial viewing technique would have to be abandoned, since the optical contact between the sample and the lens-prism, with or without the interspersion of a light-pipe, required by this technique in order to obtain spectra of reasonable quality, could not be achieved without excessive problems caused by heat transference. The right-angle viewing technique, on the other hand, requires no such contact and initial experiments were carried out to compare the two modes of viewing using a variety of solid samples, including both good and poor scatterers, at room temperature. It was found that, whilst the intensity of the features was roughly five times greater using the coaxial viewing technique, the background level was also significantly greater, and, in consequence, the signal to noise ratio for the two techniques was comparable.

Using the right-angle viewing technique throughout, several designs of sample mounting were tested, including metal blocks cut to angles of 30, 45 and 60°, but the best results were obtained using the arrangement depicted in Figure 3.4 (p. 89). The sample is tamped against a glass cover-slide located at right angles to a groove in a metal block. The tamping tool is shaped so that the sample presents an angle of approximately 45° to the laser beam, which illuminates the sample immediately behind the glass slide. In this way direct reflection of radiation into the monochromator is minimised and very low levels of background radiation are attainable. It was found that alignment of the sample was extremely critical and depended not only on the size of the sample, but also on its nature: careful optimization of the cell and laser beam alignment for each sample was essential. This sampling arrangement is based on an idea originally examined by the Cary Instrument Company.(131)

The cold cell developed using the right-angle viewing technique is illustrated in Figure 3.5 (p. 90). It consists essentially of a copper block of the design described above located by means of a Kovar seal at the base of a glass liquid nitrogen reservoir. The whole assembly is surrounded by a sectionalized glass jacket; the laser beam is admitted, and the scattered radiation examined, through optical flats sealed on to the section of the jacket surrounding the tip of the copper block. Facility is provided for continuous evacuation of the cell and samples are admitted by a separate spray arm directed at an angle of 45° into the niche formed between the groove in the metal block

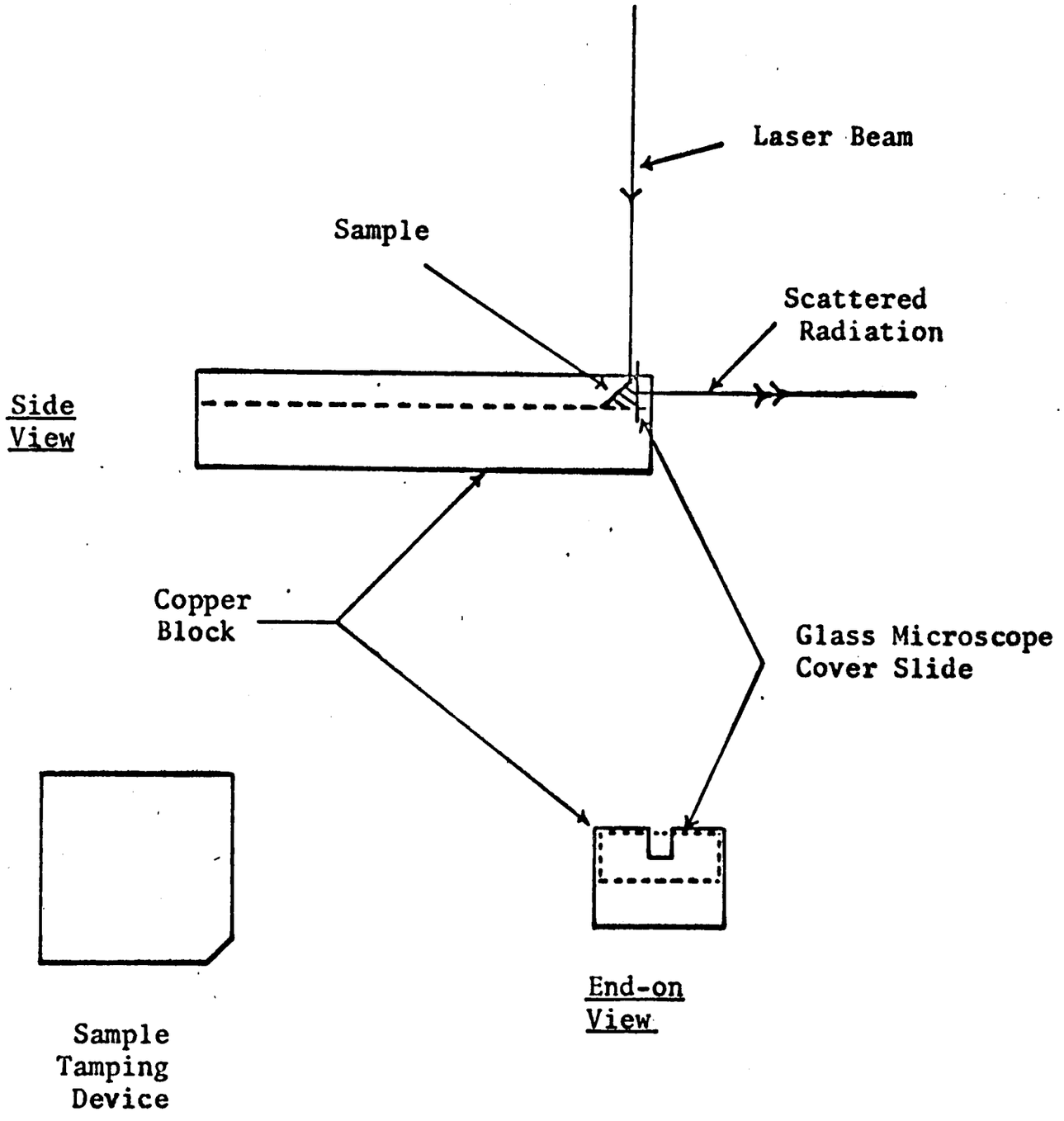

Figure 3.4: Right-Angle Viewing Arrangement for Solid Samples

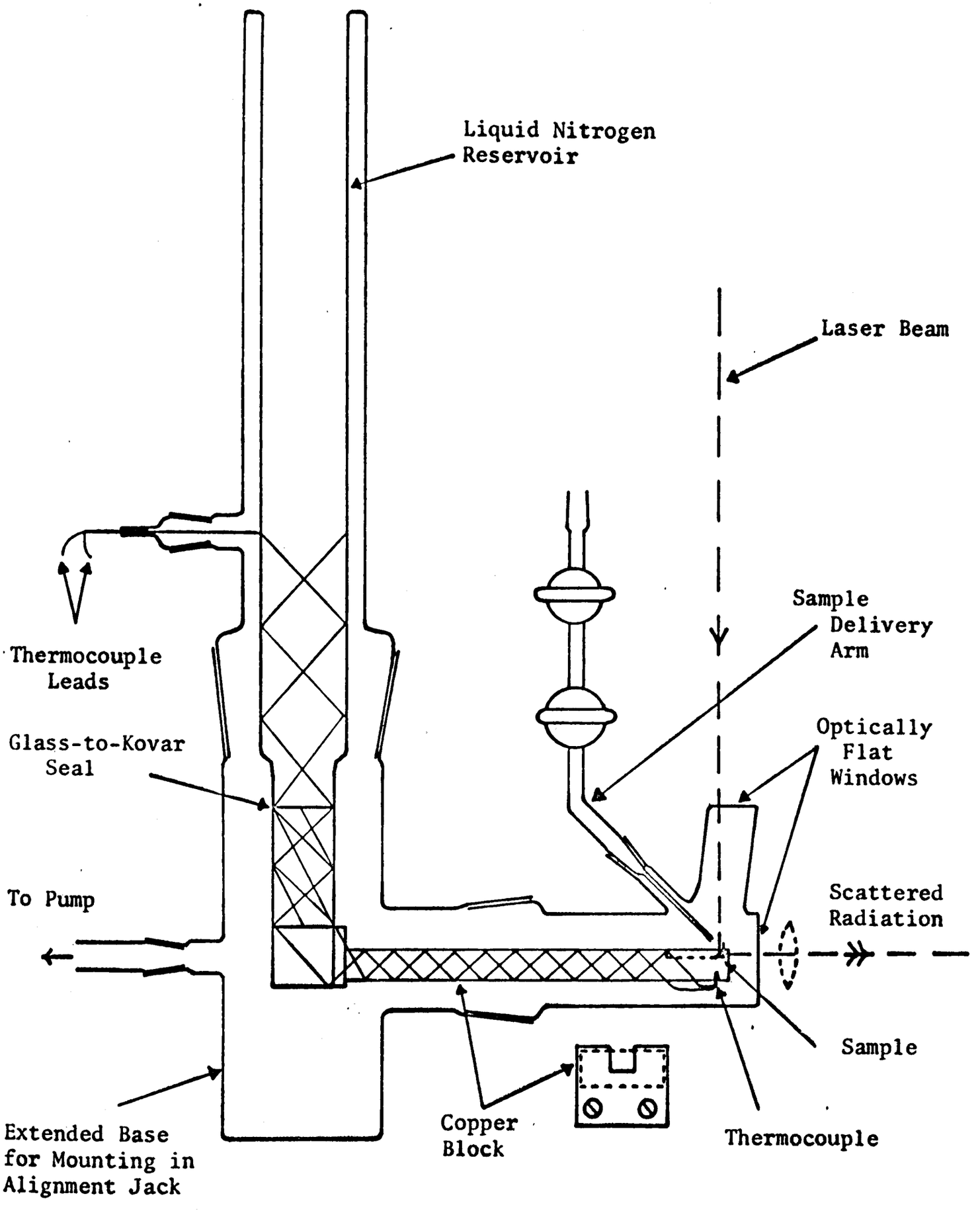

Figure 3.5: Raman Low-Temperature Solid-Sampling Assembly (Right-Angle Viewing)

and the glass cover-slide. In order to facilitate replenishment of the liquid nitrogen reservoir and to eliminate water droplet formation in the laser beam the Dewar vessel was located outside the sample chamber and for this purpose it was necessary to remove a large section from the side panel of the sample chamber. A robust jack with fine adjustment in all three dimensions was also constructed to hold the cell: this clamped directly on to the optical bench of the Cary 81 spectrometer. The temperature in the region of the sample was measured by means of a copper-constantan thermocouple held in good thermal contact with the block by gallium metal. The cell was continuously evacuated during operation using an N.G.N. combined rotary and oil diffusion pump capable of maintaining a vacuum of 10^{-6} mm. Hg.

In examining a sample, the block was cooled to the temperature of liquid nitrogen and the vapour of the compound sprayed on to the copper block so that solid built up against the face of the cover-slide remote from the monochromator. The sample was approximately aligned in the laser beam and the spectrum examined until a strong feature was found: the alignment of the cell and laser beam was then optimized by maximization of the peak height of this feature. In order to anneal the sample, the liquid nitrogen was blown out of the Dewar and the sample allowed to warm to approximately -100°C. During the annealing process the molecular aggregates initially frozen on to the block and slide become sufficiently mobile to orientate themselves into the long range order characteristic of the crystal. As a result, the spectral features become better resolved and usually appear more intense; the progress of

the annealing could usually be followed by repetitive examination of a suitable region of the spectrum until no further change occurred. After re-cooling and re-optimization of the alignment (the slight density changes in the crystal during annealing were sufficient to affect the alignment) the spectrum could be examined in detail.

The temperature in the region of the sample was found to be approximately 5°C higher than that of liquid nitrogen, the laser beam having no measurable effect on this temperature. Replenishment of the liquid nitrogen reservoir was required at approximately fifteen minute intervals to avoid slightly affecting the critical alignment and the cell was capable of running continuously for periods of hours.

Using the apparatus detailed in this section it was possible to examine the Raman spectra of the solid trimethyl compounds of the four heavier Group III elements and also to carry out a number of studies on trimethylaluminium and trimethylgallium in such matrices as dichloromethane, carbon tetrachloride and xenon. The design proved sufficiently successful to warrant proceeding with the construction of an essentially similar system capable of functioning at liquid hydrogen temperatures for the examination of the Raman spectra of unstable species trapped in inert matrices (see Chapter 5).

(b) Infrared: Low Temperature Solid Sampling Assembly

Simple Dewar-type cells for obtaining the infrared spectra of solids at low temperature have been widely used for several years;[132,133] the apparatus of this type used in the present investigation is depicted

in Figure 3.6 (p. 94). The central caesium iodide window was maintained in good thermal contact with the copper mounting plates by the interspersion of thin lead gaskets. One of the copper plates was hard soldered to a Kovar seal and in this way the caesium iodide window could be maintained at -196°C by the use of liquid nitrogen. The inner window and liquid nitrogen reservoir were surrounded by a glass outer jacket fitted with polished caesium iodide windows; these were sealed in place using Apiezon 'W' wax. The cell was continuously evacuated using an N.G.N. combined rotary and oil diffusion pump.

Samples were sprayed on to the cooled central window via the rotatable spray arm. Annealing of the samples was carried out in the infrared beam until no further change in a particular region of the spectrum could be observed. The liquid nitrogen reservoir required replenishment at roughly fifteen minute intervals and it was possible to examine spectra over a period of hours.

Using this apparatus the infrared spectra of the solid trimethyl compounds of the four heavier elements of Group III were obtained. Trimethylboron, which has a finite vapour pressure at -196°C, was examined at 20°K using the basically similar assembly built for matrix-isolation investigations and described in Chapter 5.

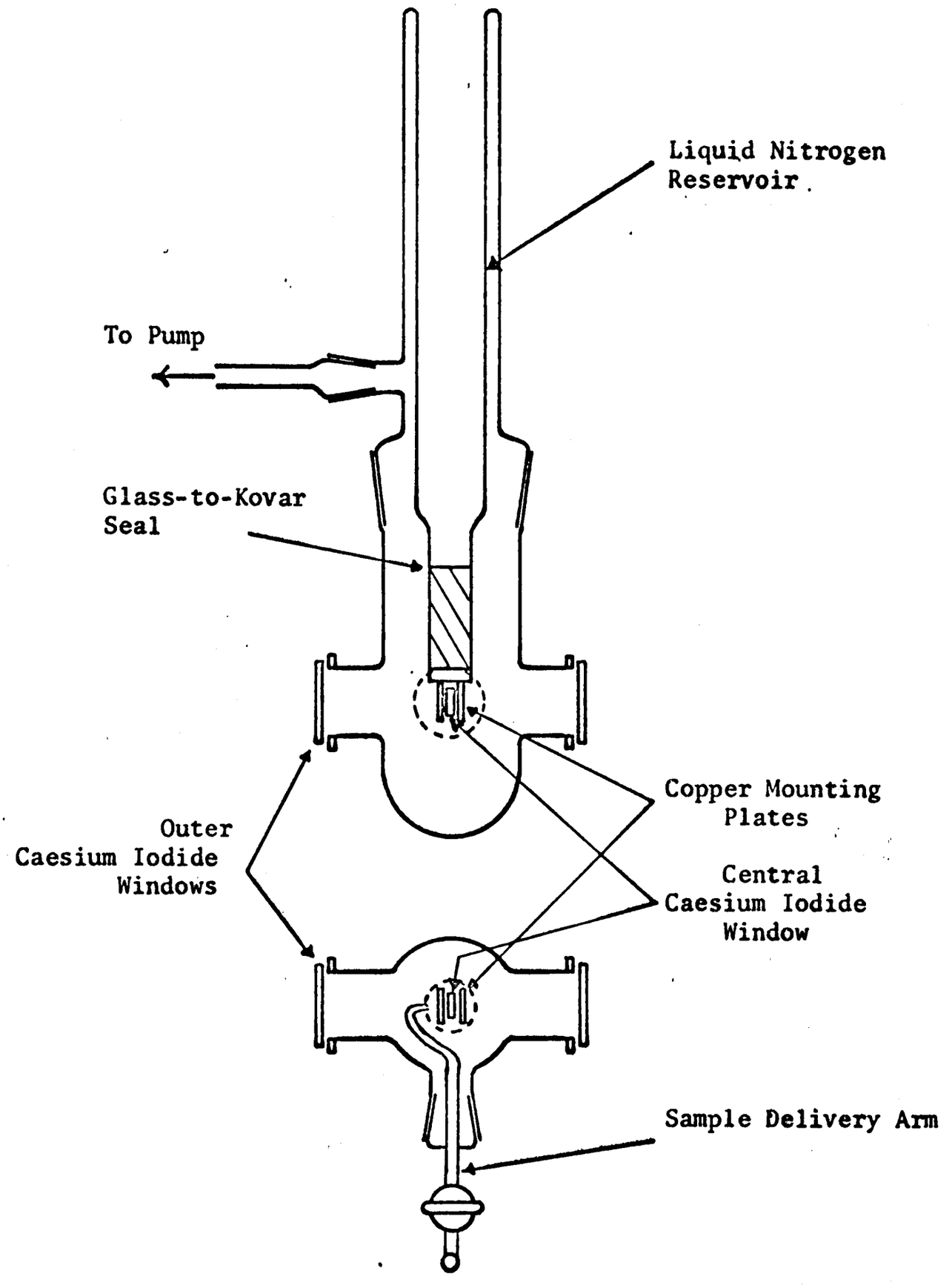

Figure 3.6: Infrared Low-Temperature Solid-Sampling Assembly

Chapter 4

Sample Preparation and Manipulation

4.1. The Vacuum Line

Because of the sensitivity to oxygen and moisture of the compounds studied in this investigation all manipulative operations were carried out in vacuo using a greased vacuum line.[134, 135, 136, 137] The vacuum line designed and constructed for the present work is depicted diagramatically in Figure 4.1 (p.96) and illustrated in Photograph 1 (p.97); a number of special features were incorporated into its construction to adapt it to the stringent requirements of the investigation, as detailed below.

The line was continuously evacuated by two pumping units comprising glass mercury diffusion pumps of large capacity backed by "Genevac" single-stage rotary pumps. Such units were capable of producing and maintaining a vacuum of 10^{-5} to 10^{-6} mm. Hg. The system was constructed with a number of by-pass routes so that, in the event of the failure of one pumping unit, any particular section of the main line could be evacuated using the second unit.

The use of two distillation trains (A and B in Figure 4.1) enabled a solvent and a solute species to be simultaneously purified by trap-to-trap fractionation prior to sample preparation. The traps were made especially long to allow species with a high affinity for grease to be stored safely frozen down in liquid nitrogen for a period of days.

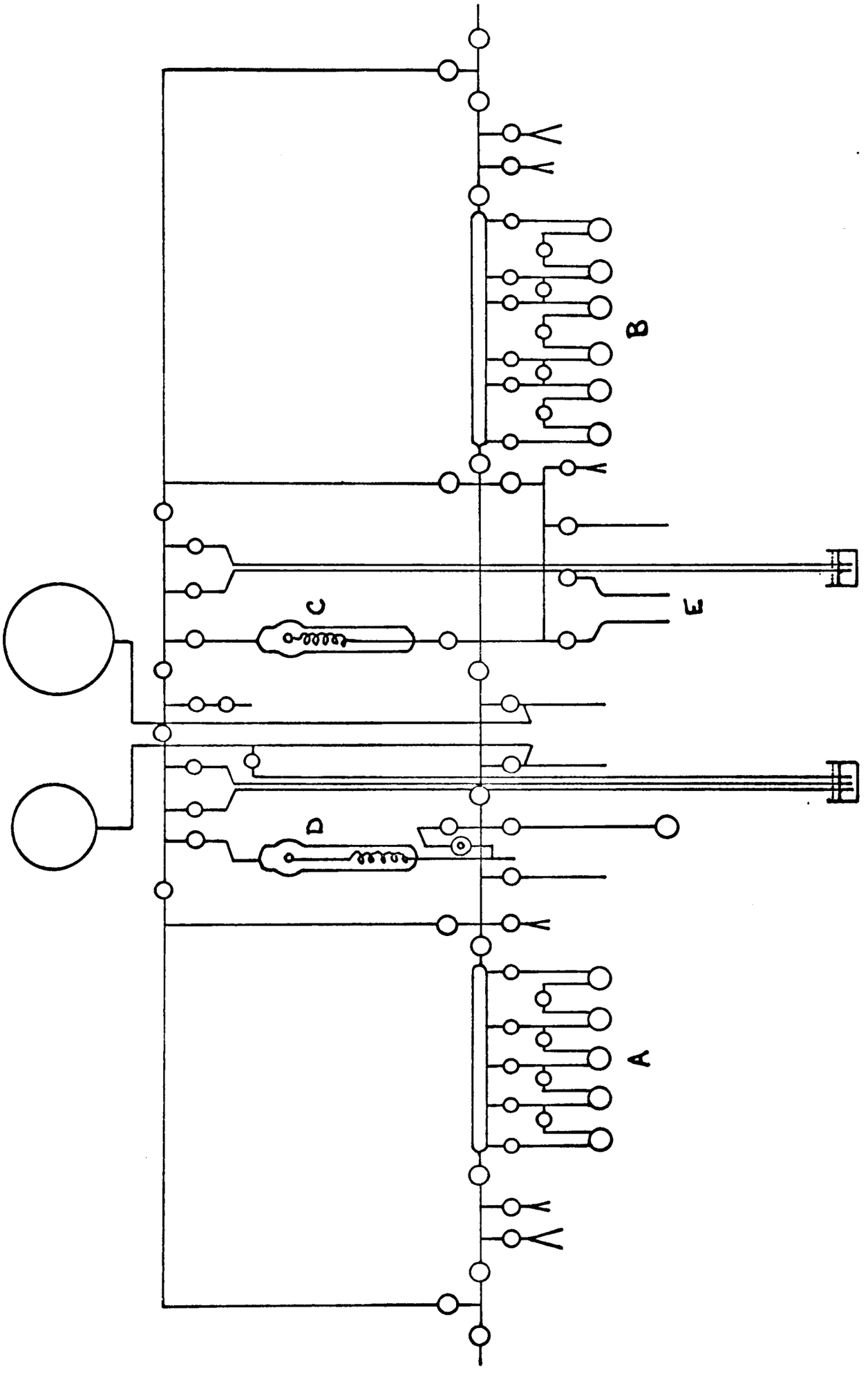

Figure 4.1: The General Purpose Vacuum Line

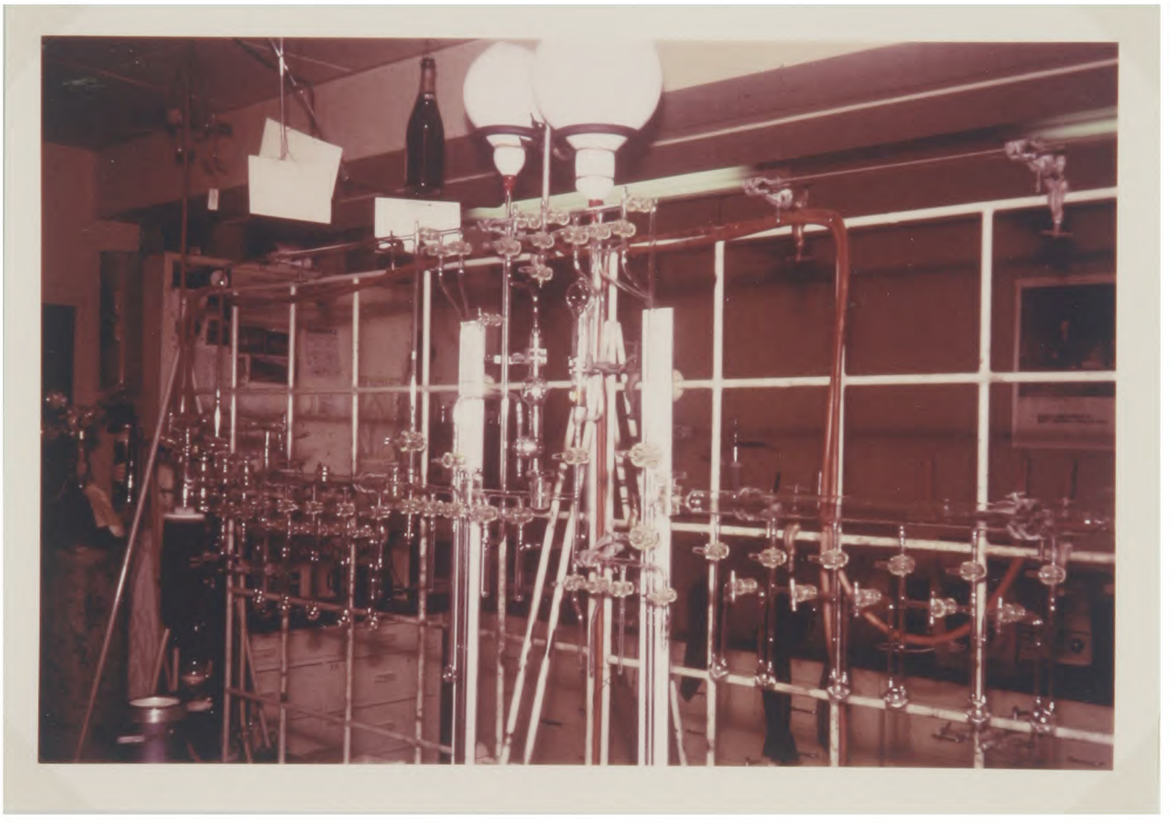

Photograph 1: The General Purpose Vacuum Line

Ground-glass attachment points enabled sample cells, gas bulbs, etc., to be attached to the line in close proximity to the samples. Two gas bulbs, one of 2 and one of 5 litre capacity, were provided for the storage of such compounds as trimethylboron. The former bulb was constructed with an integral manometer so that gas amounts could be measured directly.

Pressures were measured out of contact with mercury by the use of glass spiral gauges (C and D) as null-deflection instruments. Gauge D was specially constructed with a reservoir and greaseless diaphragm tap so that vapour pressures could be measured at elevated temperatures by immersion of the lower part of the gauge in an oil bath. The two cold fingers located in close proximity to each other (at E) enabled tensimetric tests to be made of the homogeneity of successive samples from trap-to-trap fractionation.

Apeizon 'L', a pure hydrocarbon grease with a vapour pressure of 10^{-10} to 10^{-11} mm. Hg. at 20°C, was used as a tap and joint lubricant for all operations carried out at room temperature. When the operating temperature was above 25°C, Apiezon 'H', a polymer containing, hydrocarbon grease of low vapour pressure, was used; this grease retains its lubricating properties at temperatures up to 250°C.

In the absence of an ionization gauge, evacuated glass systems were tested for leaks with a 'Tesla' high tension leak detector. This produced a violet discharge, the exact colour of which depended on the quality of the vacuum present in the system. The absence of a discharge was used as the working criterion of satisfactory conditions.

4.2. Preparation

(a) Trimethylboron

Since trimethylaluminium was available trimethylboron was conveniently prepared by the direct metathesis between trimethylaluminium and tri-n-butyl borate:[138, 139]

$$B(OBu^n)_3 + Me_3Al \rightarrow Me_3B + Al(OBu^n)_3$$

The reaction occurs spontaneously in the liquid phase and as trimethylboron (b.p. - 21.8°C) is much more volatile than any other component of the reaction mixture it can readily be removed in a relatively pure state.

The reaction vessel used in the preparation consisted of a one litre bulb carrying, at the bottom, a cold finger of relatively wide bore. The bulb was attached to the vacuum line via a constricted limb bearing a ground-glass joint; a side arm containing a break-seal was located immediately below the constriction. Prior to use the vessel was purged with a stream of dry nitrogen (delivered to the base of the vessel) and repeatedly flamed out.

In an attempt to reduce the formation of partially methylated species, stoichiometric proportions of the reagents were employed. Quantities were calculated such that the vessel would contain a trimethylboron pressure of approximately 40 cm. Hg. at room temperature (assuming complete reaction).

The tri-n-butyl borate (Schuchardt) was dried over 'Drierite' and fractionated at atmospheric pressure, the fraction boiling at 231°C

being retained. 7.5 ml. of the borate [6.5g.; ρ = 0.857] was introduced into the reaction vessel by means of a long glass spill. The vessel was attached to the vacuum line, the ester frozen down in liquid nitrogen and the vessel evacuated. To remove entrained gases the ester was melted and re-frozen, and the vessel re-evacuated, three times. 2.02g. of trimethylaluminium was then distilled into the reaction vessel (to form a ring of material above the ester in the cold finger) and the vessel was sealed at the constriction. The contents were allowed to warm slowly and as soon as the reaction commenced the vessel was carefully cooled to prevent the reaction becoming too violent. After one hour, the vessel was re-attached to the line via the break-seal side arm, and, after evacuation of the line as far as the seal, the seal was broken in the usual way by means of a glass-sheathed iron breaker. The volatile contents of the reaction vessel (essentially trimethylboron) were then transferred to a vacuum-line trap immersed in liquid nitrogen. The product was purified by trap-to-trap distillation as described in Section 4.3.

The final yield of pure material was 0.46g. (29% theoretical).

(b) Trimethylaluminium, trimethylgallium, trimethylindium

Trimethylaluminium,[140] trimethylgallium,[141, 142] and trimethylindium[143] are all readily prepared by the interaction of the pure metal (M) with dimethylmercury:

$$2M + 3Me_2Hg \rightarrow 2Me_3M + 3Hg$$

The all-glass condenser flask depicted in Figure 4.2 (p.101) was

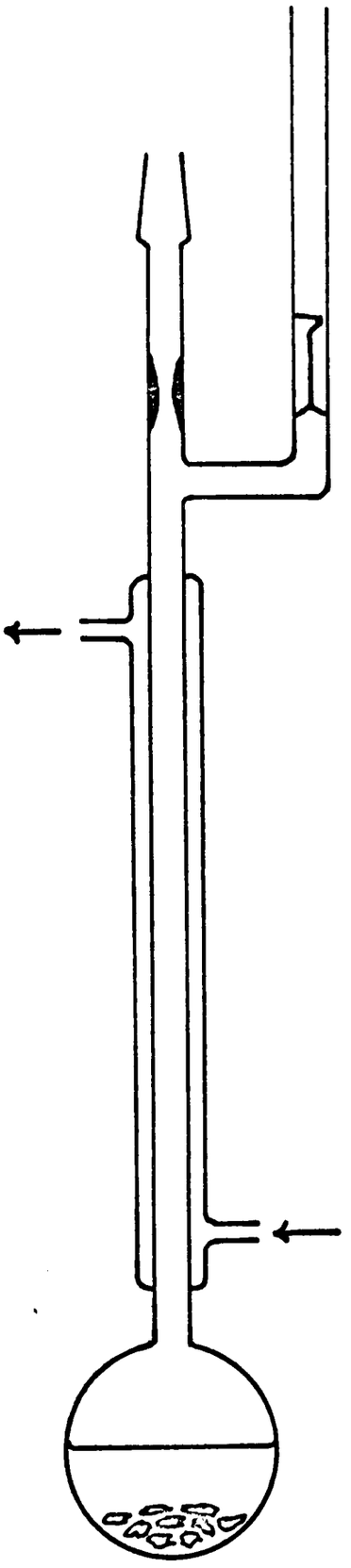

Figure 4.2: The Preparation of Trimethylaluminium, Trimethylgallium and Trimethylindium

found to be a satisfactory reaction vessel for the preparation of all three alkyls. In each case an excess of the metal was introduced into the flask and the apparatus was purged with dry nitrogen for one hour, moisture being eliminated as far as possible by repeated flaming. The dry dimethylmercury was then added, the system attached to the vacuum line and, after cooling in liquid nitrogen, the flask evacuated. After three freeze/thaw cycles the vessel was sealed off at the constriction.

(i) Aluminium

In the aluminium preparation 6g. of 'Analar' aluminium wire (99.9% purity), cut into short lengths, was used with 10 ml. of dimethylmercury (ca. 31g., corresponding to a 25% excess of aluminium). The reaction mixture was left at room temperature for 48 hours, during which time the aluminium was seen to amalgamate and eventually form a liquid pool at the bottom of the reaction vessel. The flask was then warmed to 90°C with water passing through the condenser jacket for 24 hours, to complete the reaction. At the end of this period the trimethylaluminium was transferred to the line and purified by trap-to-trap fractionation (see Section 4.3). About 6g. of trimethylaluminium was ultimately isolated corresponding to virtually quantitative conversion based on the amount of dimethylmercury taken.

(ii) Gallium

7g. of gallium metal (Johnson, Matthey; total metallic impurities < 10 ppm.), cut into small pieces, was heated with 10 ml. of dimethylmercury (corresponding to a 10% excess of gallium), a little mercury(II)

chloride being included as a catalyst. The flask was heated in a small air furnace to ca. 130°C for four days, cooling water being passed continuously through the outer jacket. During this time the liquid metal pool became more mobile and decreased in volume; the volume of the clear liquid increased. At the end of the heating period the volatile contents of the reaction vessel were transferred to the vacuum line for purification. About 10 g. of trimethylgallium (65% yield) was fully isolated.

(iii) Indium

In the trimethylindium preparation, 12 g. of indium metal (B.D.H., 99.9% purity) and 10 ml. of dimethylmercury (indium in 20% excess) were used, catalytic quantities of iodine, mercury(II) chloride and metallic magnesium also being included in the reaction mixture. Heating at 130°C was carried out for six days, at the end of which time the contents of the flask solidified to a white crystalline mass on cooling. After transference to the main line and purification the yield of trimethylindium was approximately 12 g. (60%).

The dimethylmercury used in these preparations was prepared by the reaction of mercury(II) chloride and methyl magnesium iodide:[144]

$$HgCl_2 + 2MeMgI \rightarrow Me_2Hg + MgI_2 + MgCl_2$$

The mercury(II) chloride was held in a Soxhlet extractor thimble and was slowly eluted by refluxing ether into the Grignard reagent. The dimethylmercury was purified by fractional distillation at atmospheric pressure, the fraction boiling over the range 92-93°C being retained.

(c) Trimethylthallium

Trimethylthallium cannot be prepared by the reaction of thallium metal with dimethylmercury for two reasons:

(i) Dimethylmercury and trimethylthallium are of comparable thermodynamic stability and an equilibrium mixture of the two compounds results; in fact dimethylmercury predominates in such a mixture.

(ii) For a reasonable rate of reaction, the temperature would need to be above the explosive decomposition temperature (ca. 90°C) of trimethylthallium.

The trimethylthallium samples used to provide the data reported in this thesis were kindly supplied by Mr. A.G. Lee of the Inorganic Chemistry Department, University of Cambridge, and by Mr. J.H. Darling of this Department. Both of these samples were prepared by the reaction of an ethereal solution of lithium methyl with thallium(I) iodide in the presence of methyl iodide.[145]

$$2MeLi + MeI + TlI \rightarrow Me_3Tl + 2LiI$$

4.3. Purification

All the compounds were purified by trap-to-trap fractionation using the vacuum line of Figure 4.1. The products from the preparation were subjected to three freeze/thaw cycles to remove volatile impurities and were then divided, under static vacuum, into three fractions by maintaining three inter-connected traps at suitable temperatures:

a fraction containing the high boiling impurities (I), a fraction containing the purified compound (II) and a fraction containing the volatile impurities (III). The temperatures of the baths surrounding these traps were chosen to provide an effective separation at a reasonable rate; their values are listed in Table 4.1 (p.106), together with the constituents of the baths. In all cases the product in trap (II) was either a colourless liquid or a completely white solid. In the case of trimethylboron, the vapour pressure at -64.5°C was found to be 7.95 cm.Hg., corresponding to the literature value.[15] The vapour pressure of trimethylgallium at 0°C (6.4 cm. Hg.) was also identical with that previously reported.[146]

Samples for spectroscopic examination were re-purified using the above procedure immediately prior to removal from the line.

4.4 Sample Cells

(a) Raman Liquid Cell

The cell used for the investigation of the liquid-phase Raman spectra at, or slightly above, room temperature is depicted in Figure 4.3 (p.107). The cell was attached to the line by the ground-glass joint and, after repeated flaming, the sample was frozen into the reservoir (A) and the constriction (B) sealed. The cell was then tilted through 90° (to the position shown) and the spectrum of the sample in the tube C examined. It was found that the tube C could be constructed of reasonably thick glass (1.5 mm. i.d., 3.5 mm. ex.d.) and that a tube with a carefully rounded end would yield spectra of good quality

Compound	Trap I °C	Trap II °C	Trap III °C
BMe_3	-112	-129	-196
$AlMe_3$	0	-46	-196
$GaMe_3$	0	-64	-196
$InMe_3$	Ambient	0	-78
$TlMe_3$	Ambient	-23	-196

(a) Fraction Temperatures

Temperature °C	Bath Constituents
-23	Carbon tetrachloride slush
-46	Chlorobenzene slush
-64	Chloroform slush
-78	Acetone/solid CO_2
-112	Carbon disulphide slush
-129	Pentane slush
-196	Liquid nitrogen

(b) Bath Constituents

Table 4.1: Fractionation Temperatures for the Purification of the Group IIIB Trimethyls.

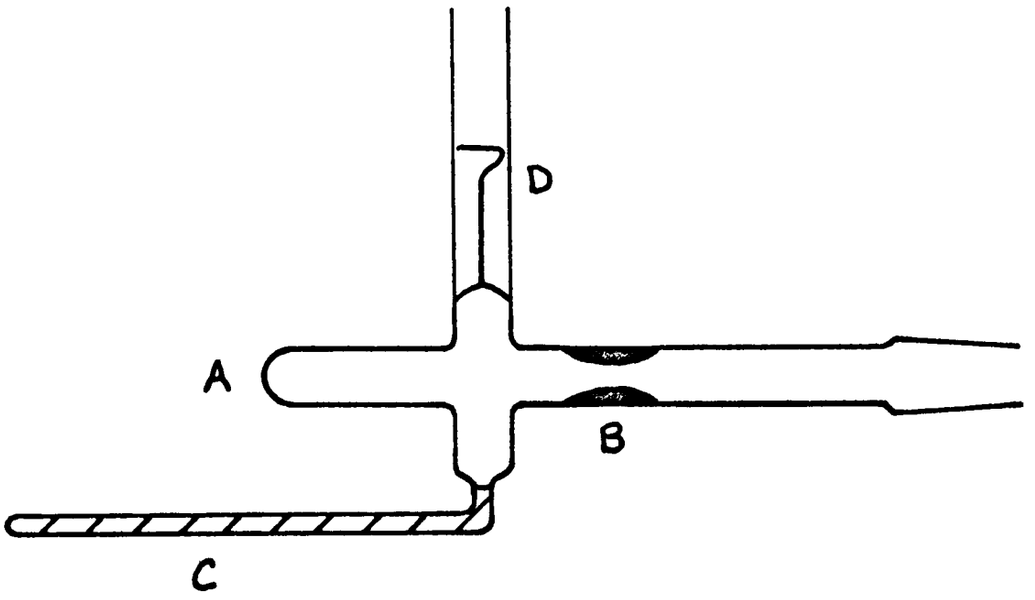

Figure 4.3: Liquid Cell for Raman Spectroscopy

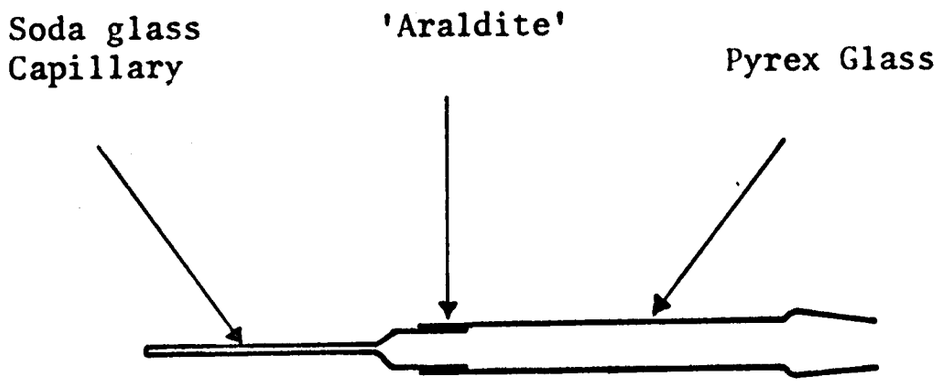

Figure 4.4: X-ray Diffraction Cell

provided that optical contact with the lens-prism assembly was maintained using a little glycerol. After examination the sample could be recovered via the break-seal D.

(b) Infrared Gas Cells

In the near-infrared region (5000-200 cm^{-1}), a pair of conventional 10 cm. glass gas cells, fitted with Edwards greaseless taps (having Viton 'A' diaphragms) and cold fingers, were used. Polished caesium iodide windows, of 3.5 cm. diameter, were held in place using Apiezon 'W' wax. A suitable quantity of the sample was introduced into one evacuated cell and, with the second cell in the reference beam, the infrared spectrum of the material was examined.

For the far-infrared region (600-50 cm^{-1}), cells of essentially similar design were employed, but with 5 cm. diameter windows of high-density polythene 1 mm. in thickness. These windows were held in place between two Viton 'A' 'O' rings by metal clamping rings; the 'O' rings were lightly greased with Apiezon 'H' grease to ensure a vacuum-tight seal. Polythene, while exhibiting only a few feeble absorption peaks at frequencies below 600 cm^{-1}, does attenuate appreciably the infrared radiation and it is therefore important to use the minimum thickness consistent with mechanical requirements. It was found that the windows bowed appreciably under vacuum but did eventually reach an equilibrium position. Since polythene also absorbs moisture, it was necessary continuously to evacuate the cells for several days prior to use.

(c) X-ray Diffraction Cell

0.5 mm. i.d. soda-glass capillaries were used in obtaining the X-ray diffraction data. In order to attach these to the vacuum line they were sealed using 'Araldite' inside Pyrex tubing of suitable diameter, as shown in Figure 4.4 (p.107). The compound was frozen into the capillary using an acetone/solid CO_2 bath and the capillary sealed off using a tiny, oxygen-free, coal-gas flame. A pair of tweezers, the jaws of which were lined with Apiezon 'Q' sealing compound, were used to hold the tube; after sealing the Apiezon 'Q' was used as a mounting material for the cell. In one attempt to combat the porosity of the thin soda glass, a coating of polyurethane varnish was used as a sealant; however, this caught fire during the sealing off process, destroying the sample, and this refinement had to be abandoned.

X-ray diffraction photographs of microcrystalline samples of trimethylgallium and trimethylindium were obtained using a Weissenberg camera with copper Kα radiation. To maintain the samples at the low temperature required for the investigation (down to -60°C), a liquid nitrogen boiler, similar in design to that used in the low-temperature, liquid-phase Raman studies (Fig. 3.2, p. 83) was employed.[147] The apparatus was developed by, and the samples examined in conjunction with, Mr. I.J. Tickle of the Department of Chemical Crystallography, University of Oxford.

Chapter 5

Matrix-Isolation Methods

5.1. The Nature of the Technique

The technique of matrix isolation consists of trapping a species in a rigid, inert matrix at such a dilution that intermolecular interaction is minimized, it is then possible spectroscopically to examine the species at leisure. The idea was introduced by Lewis[148] and developed by Becker and Pimentel[149] for the study of free radicals, characterization initially being by electron spin resonance spectroscopy.

Infrared spectroscopy was first used in conjunction with the matrix isolation method by Pimentel,[150] and its application has proved one of the most direct means of elucidating the structures of reactive species. It was found that the noble gases and nitrogen are almost ideal matrix materials for infrared investigations on account of their weak intermolecular forces, low chemical reactivity and low absorption of infrared radiation, but for many years the low temperatures required to produce rigid matrices (liquid hydrogen, $\sim 20^{\circ}K$, or liquid helium, $\sim 4^{\circ}K$) precluded the extensive use of the technique. In 1963, however, the miniature Joule-Thomson cryostat was introduced,[151] and with the commercial availability of such units in 1965,[152] the technique became one of general applicability. The range of species examinable has also been broadened considerably in recent years; a noteworthy advance in this respect was the development of techniques for the isolation of high-temperature species issuing directly from a furnace in the form of a

molecular beam.[153]

A number of general reviews of infrared studies involving matrix isolation have appeared: the early work has been described by Pimentel[154, 155, 156] and the more recent developments have been reviewed by Hallam.[157, 158] The free-radical[159] and high temperature[160] aspects of the subject have also been reviewed.

In the following sections of this chapter the scope and validity of the technique are considered and a description is given of the experimental arrangement employed in the present investigations. The particular problems associated with the systems investigated are then discussed and, in conclusion, there is an account of some development work aimed at producing Raman spectra of matrix-isolated species.

5.2. The Scope of the Technique

Although the matrix-isolation technique was originally developed for the investigation of reactive transient species, the method is also valuable in the examination of stable, long-lived species and, increasingly, in the study of novel types of reaction. The following aspects of the technique are now exploited:

(a) Unstable Species

Free radical species were originally produced exclusively by photolysis in situ of stable precursors entrapped in the matrix, but by the use of diffusion methods (see (c) below) it has also proved possible to produce by chemical reaction novel species which are unstable under conventional conditions. The methyl radical, for example, has been

produced by the reaction of lithium atoms with methyl halide molecules, both initially trapped in a matrix.[161, 162] Species stable at high temperatures may be produced thermolytically and it is sometimes possible to correlate the spectra of the matrix-isolated species with those obtained directly at high temperatures, although the latter are usually much more complicated (see (b) below).

(b) Vibrational Analysis

At 20°K vibrational transitions originate from the lowest vibrational and rotational levels of the electronic ground state for the vast majority of molecules. In consequence, the spectra of matrix-isolated molecules approximate to pure vibrational spectra of single molecules; the following complications are absent:

(i) rotational fine structure;

(ii) 'hot' bands arising from transitions from higher vibrational levels;

(iii) band-broadening associated with intermolecular interactions,

(iv) splittings and new modes ascribable to crystal environment effects.

Simple spectra are therefore observed often with very sharp features (under favourable conditions, half peak widths as small as 1 cm^{-1} are found) and it is often possible to measure isotopic splittings which are unresolvable under ordinary conditions (e.g. $^{35}Cl/^{37}Cl$ in $Al_2Cl_6/AlCl_3$[163]).

Accordingly it is sometimes highly advantageous to use this approach to examine species which are stable at room temperature or which are readily examined at elevated temperatures, as an aid to vibrational assignment.

(c) Diffusion Experiments

In order to obtain true isolation it is essential to use a rigid matrix. To achieve this it is necessary, in general, to operate at a temperature of less than half the melting point of the matrix material measured in degrees Kelvin:[164]

$$(T \text{ rigid})^{\circ}K < \left(\frac{T \text{ melt}}{2}\right)^{\circ}K$$

At temperatures above this the matrix becomes progressively less rigid and it is possible for molecules of the solute to diffuse through the matrix and thereby to come into contact with other solute molecules, of either the same or different species. For processes with low free energies of activation it is then possible for reaction to occur. Moreover, because the temperature-dependence of the free energy of activation varies from reaction to reaction, it is possible that reactions which are unfavourable at room temperature relative to alternative reactions may become the preferred reactions at the temperature of the matrix. In principle, therefore, it is possible to carry out in matrices reactions which are not feasible at room temperature. At the same time, however, this represents a drawback to diffusion experiments: conclusions drawn from such experiments cannot necessarily be extrapolated to room temperature situations.

Diffusion experiments are normally carried out by increasing the back pressure on the liquid hydrogen reservoir adjoining the sample window, thereby increasing the boiling point of the hydrogen to a practical maximum of 34°K. An increase or decrease of spectral features is commonly observed during the course of the warming-up procedure. Such diffusion experiments are particularly valuable in the study of molecular association since, under favourable conditions, it is possible to control oligomerization in such a way as to allow the identification of individual steps in that process. By varying the matrix ratio (see below) it is possible ultimately to produce bands characteristic of the pure, solid solute. Hydrogen-bonding studies of methanol[165], water[166] and ammonia[167] have been made in this way.

In concluding this section it is worth mentioning two aids to spectral elucidation commonly utilized in matrix isolation work:

(i) Diffusion Experiments

Diffusion experiments of the type described above are frequently used when a number of different species are present in a matrix. Peaks with intensities which increase or decrease simultaneously and proportionately can usually be confidently ascribed to the same species and in this way it may be possible to assign features of otherwise doubtful origin to the correct species.

(ii) Matrix Ratio

During condensation of a matrix gas and reactive species some aggregation normally takes place. The extent of this 'quenching' depends on the mole ratio of the reactive species to matrix gas. Little

quenching takes place during the condensation of a very dilute matrix (1:5000), while in a more concentrated matrix (1:800) considerable quenching is likely. Study of the changes in relative peak intensity with change in matrix ratio usually makes it possible to distinguish the spectra of the different species present.

5.3. The Validity of the Technique: Matrix Environment Effects[157]

Whilst it is tempting to consider that the matrix merely provides a convenient low temperature support for isolated gas molecules and that the vapour phase parameters are not significantly perturbed by the presence of the matrix, it is clear that there must be some sort of matrix-solute interactions and it is important to be able to assess the nature and degree of such interactions. To date, theoretical considerations have not been well developed and the most informative approach to the problem of matrix effects is to compare spectral features where both vapour-phase and matrix-isolated spectra are available. Matrix environment effects are most conveniently considered under two headings:

(a) the matrix shift, $\Delta\nu$, where

$$\Delta\nu = \nu_{matrix} - \nu_{gas}$$

(b) matrix splittings (of vapour-phase singlet features)

(a) The Matrix Shift

The direct interaction of a matrix-isolated molecule with the matrix causes a shift in the gas phase vibrational frequency. Such shifts have been tabulated for a number of small molecules (e.g. water, methane,

nitric oxide, ammonia):[156] these results are presented in Table 5.1 (p.117). From such data and similar results for other molecules the following generalizations can be deduced:

(i) The magnitude of the shift is greater for bending than for stretching modes, and is greater the lower the vibrational frequency.

(ii) The magnitude of the shift falls along the series:[168]

nitrogen > argon > krypton > xenon

(iii) Compact molecules have comparatively small matrix shifts.[169]

(iv) Molecules with large dipole moments have comparatively large matrix shifts.[153]

There have been a number of attempts to interpret these observations theoretically and the most successful have been based on a perturbation approach originally proposed by Buckingham[170] in the consideration of solvent effects. Charles and Lee[169] estimated the interaction energy of dispersion, induction and repulsion forces for carbon monoxide molecules trapped in a number of matrices and were able to calculate matrix shifts. The agreement between the observed and calculated shifts was reasonable and the change in $\Delta\nu$ between matrices was accurately predicted.

Thus, in general, the interaction of a trapped species with the surrounding matrix will result in a perturbation of the vapour phase parameters and a shift in the observed vibrational frequencies. In this

Mode	Matrix Gas	No. of Examples	av. $\Delta\nu$	Range
Stretching Modes	Nitrogen	16	-3	+21 to -32
	Argon	8	-5	+5 to -12
Bending Modes	Nitrogen	12	+10	+40 to -6
	Argon	2	+3	+11 to -6

(All matrix shifts in cm^{-1})

Table 5.1.: Matrix Shifts for Small Molecules[156]

investigation, the molecules considered, the trimethyls of Group III, are all relatively large, compact and non-polar and, according to the above generalizations, matrix shifts would be expected to be small.[171] Comparisons between the spectra of matrix-isolated and gaseous molecules have confirmed this expectation.

(b) Matrix Splittings

The interpretation of matrix-isolation spectra may be complicated by the observation of multiplet features arising in regions of the spectrum associated with a single feature of the vapour-phase spectrum. Such splittings can be caused by several matrix environment effects: aggregation, molecular rotation and multiple trapping sites.

(i) Aggregation

The matrix shift resulting from interaction of a solute molecule with the matrix depends upon the exact nature of the matrix cage. If this cage itself includes a second or third solute molecule (of either the same or a different species) then the matrix shift is likely to be significantly different from, and probably greater than, the shift resulting from a cage comprising only matrix species, and over the whole matrix this effect may give rise to a number of distinct infrared absorptions. The statistical probability of this 'aggregation' depends upon the matrix ratio, and is quite appreciable for matrix ratios below 1:600.[168] Splittings attributable to this cause are of fairly common occurrence (e.g. water[166] and ammonia[167] in N_2) and decrease in intensity with increasing dilution of the matrix.

(It is to be emphasised that aggregation in the matrix is not to be confused with oligomerization, in which a new molecular species is formed: the splitting patterns given by molecular aggregates on isotopic substitution resemble those of the parent molecule, whereas different patterns are found for monomer and oligomer species).

(ii) Molecular Rotation

The rotation of small molecules (e.g. water[172]) in noble-gas matrices can give rise to multiplet splittings in the vibrational spectra. However, such splittings are found neither when using nitrogen matrices nor with molecules larger than, for example, methane. Accordingly this effect can probably be discounted in considering such molecules as those of the Group III trimethyl compounds.

(iii) Multiple Trapping Sites

Nitrogen (below 35°K) and the noble gases crystallise in face-centred-cubic lattices and there are several possible sites which can conceivably accommodate solute molecules:

(1) substitutional sites, surrounded by 12 matrix molecules;

(2) interstitial sites, surrounded by either 3 or 6 matrix molecules;

(3) dislocation sites.

The intermolecular forces between the matrix and absorber are different for each type of site and the resulting vibrational energy levels of the solute molecules are perturbed to different degrees. In consequence, it is often possible to observe a number of distinct spectral features all

originating from the same vibrational transition in the solute molecule. All the above sites are relatively small, however, and when the solute molecules involved are large, as in this investigation, the matrix molecules provide a uniform environment about each solute molecule, which formally occupies a number of substitutional sites. Under such circumstances multiplet splittings ascribable to site differences are not observed.

Thus, whilst it is important to bear in mind the various possible environmental effects that can complicate matrix-isolation spectra, for the most part the effects are small when dealing with large, compact, non-polar molecules. The spectra of such molecules can usually be interpreted in terms of the properties of unperturbed single molecules.

5.4. The Experimental Arrangement

The experimental assembly employed in this investigation was constructed in the department by Dr. J.S. Ogden and Dr. M.J. Ricks for the investigation of high-temperature metal/oxygen systems. The equipment being described in detail elsewhere,[173] only the salient features of the apparatus will be mentioned here.

The all-metal vacuum system, depicted in Figure 5.1 (p.121), is built into the sampling area of a Perkin-Elmer 225 infrared spectrometer (see Section 3.2(b), p.78). The system comprises a cryotip section and a furnace section; the two sections are separated by a vacuum-tight shutter and are independently evacuable by two N.G.N. combined rotary and diffusion pumps. The various components are connected together by 'Viton A' O rings, bolted between flanges to effect good vacuum seals.

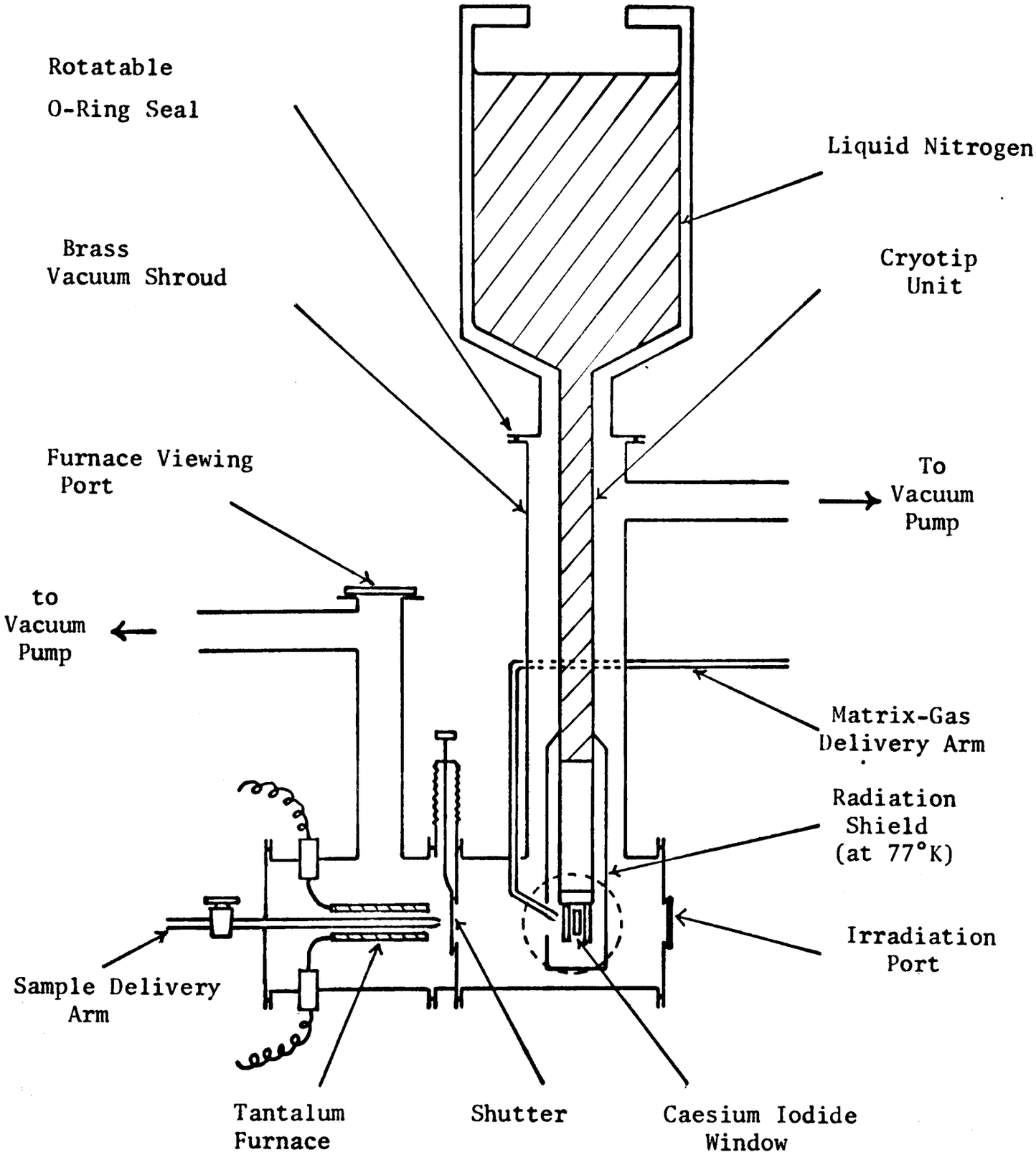

Figure 5.1: The Infrared Matrix-Isolation Assembly

(a) The Furnace Section

To provide the relatively low thermolysis temperatures (< 200°C) required in this investigation samples were passed through a Pyrex-glass tube surrounded by a spiral heating element of tantalum. Radiation shields were incorporated to prevent heat transference from the furnace directly to the cold window. Temperatures were measured on the outside of the Pyrex tube using a Pt vs Pt/13% Rh thermocouple.

(b) The Cryotip Section

The cryotip unit (see section (c)) bearing the cold caesium iodide window was mounted inside a copper vacuum shroud on an 'O' ring mounting enabling the unit to be rotated through 90°. The caesium iodide window was held in good thermal contact with the copper mounting by the interspersion of indium washers and leaf springs to take up any differential contraction effects. A Chromel vs Gold/0.03 atomic % Fe thermocouple was sealed into a small hole in the window with Wood's metal and a similar thermocouple affixed to the cold tip. The inner window was surrounded, as far as possible, by a silvered copper radiation shield attached to the section of the cryotip held at liquid nitrogen temperatures (77°K).

The vacuum shroud was fitted with two outer CsI windows which were carefully positioned in the sample beam of the spectrometer; a spray arm for the delivery of matrix gas was located so that it was opposite the inner window when this was in the 'spray-on' position. The spray arm was connected to an external vacuum system via an Edwards High Vacuum needle valve, the flow being monitored using a U-tube manometer

filled with silicone oil.

(c) The Cryotip

The Air Products AC-3L-110 three stage Cryo-Tip was capable of operating at either liquid hydrogen or liquid helium temperatures, but since liquid hydrogen temperatures were adequate for this investigation the two colder stages were both operated using hydrogen. The liquid hydrogen was produced by open-cycle Joule-Thomson expansion of hydrogen gas originally at pressures available from commercial cylinders, initial cooling of the gas below its inversion temperature being achieved by passage through a liquid nitrogen reservoir.

Figure 5.2 (p.124) gives a schematic representation of the Cryo-Tip flow system; for simplicity only one hydrogen circuit is shown. This circuit consists of a pair of very fine capillary tubes wound round a mandrel, one connected to the high pressure gas inlet and the other to an outlet vent. After initial cooling, the high-pressure hydrogen is expanded by a throttling process, producing, ultimately, a small pool of liquid hydrogen at the base of the unit. The exact low temperature achieved at the pool is a function of the gas pressure above it (i.e. the hydrogen back-pressure); with the outlet vent open to the atmosphere the temperature of the pool is 20.3°K. By pumping on the outlet system, however, it is possible to maintain a temperature of approximately 16°K and, conversely, by applying a back-pressure to the system, the temperature can be raised above 20°K. The control system of the cryotip permits a continuous variation of the back pressure to a maximum of 200 p.s.i., and in this way it is possible to vary the temperature between 20 and 34°K

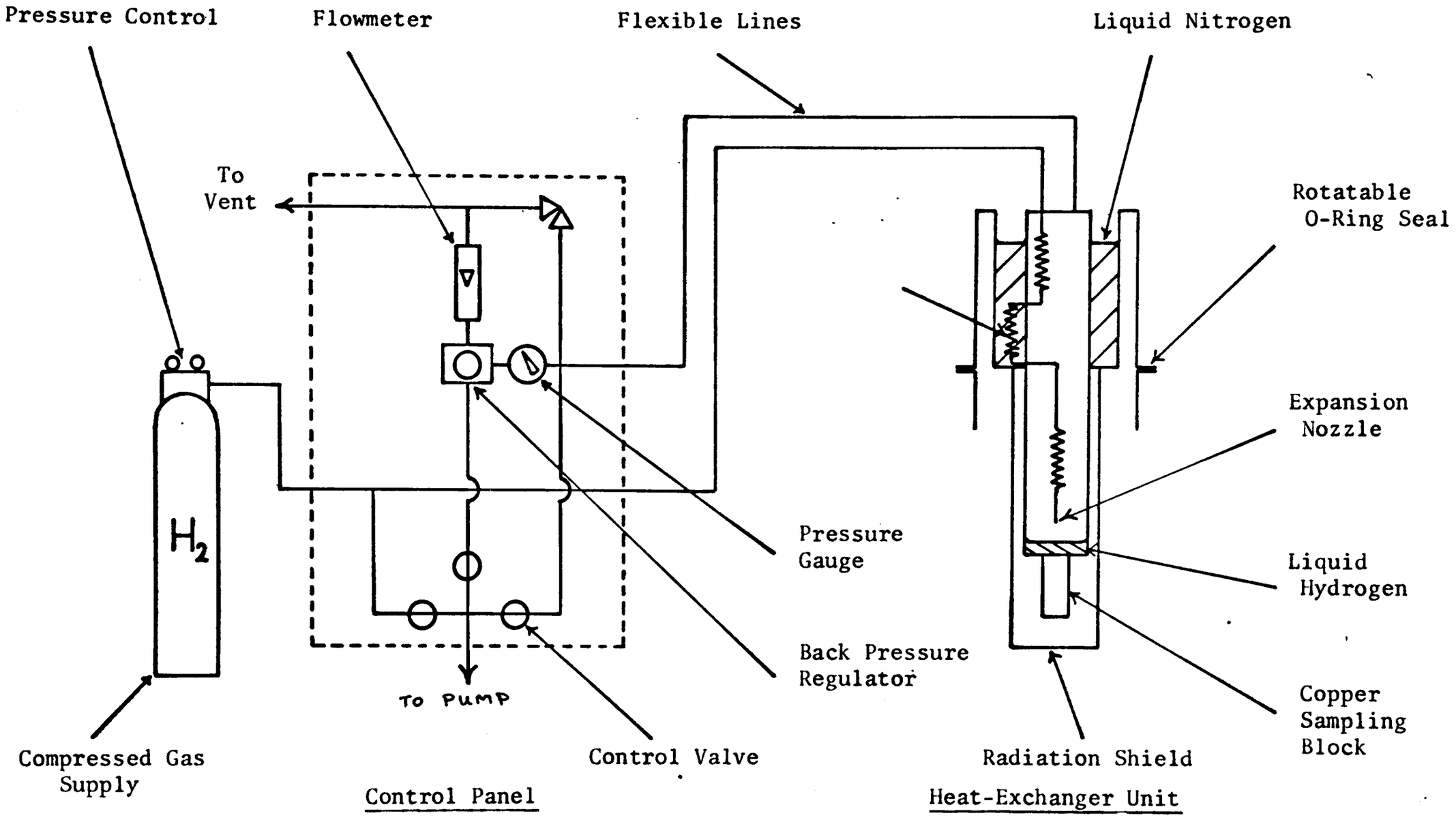

Figure 5.2: The AC-3L-110 Cryo-Tip Flow System

with a control of ± 0.5°K. Higher temperatures can be produced and maintained by simultaneous variation of the hydrogen inlet and outlet pressures ('dense gas' operation).

The Cryo-Tip is capable only of a relatively limited heat dissipation (a maximum of 2.5 watts at 20°K) and great care was necessary to minimise heat leakage to the tip itself. For this reason the tip was surrounded by the radiation shield and the thermocouple leads were repeatedly wound round the tip itself and the shield to minimise conductive gains.

(d) Operation

Prior to 'cooldown', the whole system, including the lines to the matrix and sample, were evacuated until a vacuum of 10^{-4} mm. Hg or better was achieved. Then, with sufficient hydrogen passing through the liquefaction circuits to prevent blockage of the tubes by ice, liquid nitrogen was poured into the Dewar of the cryotip. A small siphon was used to convey liquid nitrogen to the base of the cryotip to expedite cooling. When the tip was at 77°K the hydrogen flow was increased until the tip reached 20°K and a small pool of liquid hydrogen had collected; the flow was then stabilized at a suitable maintenance pressure.

With the cold window in the correct position the matrix was sprayed on to the window, either entirely from the matrix tube or partly from the tube and partly from the furnace. Matrix thickness was checked at intervals spectroscopically; a typical total spray-on time would be one hour. If recombination of unstable species were possible, it was sometimes advantageous to spray on at 16°K, using a high-capacity vacuum pump to reduce the hydrogen back-pressure. It was essential to deposit

matrices slowly to ensure a rapid freezing of high-temperature equilibria and to produce matrices of acceptable infrared transparency.

With the cold window aligned in the spectral path of the instrument, the spectrum was examined. Diffusion experiments were carried out by increasing the hydrogen inlet pressure and regulating the outlet pressure, the temperature being followed on a slave recorder. Spectral changes were observed during the warm-up procedure using a slave recorder coupled to the repetitive scan feature of the spectrometer. On completion of the diffusion experiment the cryotip was re-cooled by releasing the hydrogen back-pressure.

At the end of the matrix-isolation experiment the system was allowed to warm, in vacuo, to room temperature, the process requiring about four hours. Liquid nitrogen consumption at 20°K was approximately two litres per hour and a 250 cu.ft. hydrogen cylinder lasted approximately four hours, depending upon the exact operating conditions.

5.5. Problems Encountered

(i) Moisture

Metallic surfaces attract a layer of moisture and such adsorbed water molecules cannot readily be removed by evacuation for short periods of time. When experiments requiring the rigorous exclusion of moisture are to be undertaken, it is important either to ensure that such metallic surfaces are maintained at low temperatures (as in the cold cell developed for the solid-state Raman investigations, Fig. 3.5, p.90) or that the system is continually evacuated for a period of several days prior to use, preferably at an elevated temperature.

Since the matrix-isolation equipment was available for periods of, at most, only two or three days at a time, such precautions were not possible in the present investigation and features attributable to traces of moisture were invariably present in the spectra of the matrix-isolated systems. For this reason, especial care was needed in the interpretation of the results of the diffusion experiments, particularly since partially hydroxylated methyl species give rise to features in the same region of the spectrum as the various oligomers of the trimethyl compounds themselves. It was important, therefore, to ensure that features ascribable to water were included in the recorded diffusion spectra in order that their intensities could be monitored.

(ii) Matrix Opacity

Although nitrogen exhibits no true infrared absorptions in the 200-4000 cm^{-1} region of the spectrum (apart from a very weak one at approximately 210 cm^{-1}), it was found that the level of background absorption was quite appreciable and this factor limited the thickness and, in consequence, the minimum concentration of the matrix. Moreover, as the nitrogen lattice became less disordered on diffusion, the level of background absorption altered appreciably, further complicating the interpretation of diffusion experiments.

(iii) Non-specificity

The distances between pairs of solute molecules have, in general, a completely random distribution and, on diffusion, some solute molecules will readily come into contact with similar molecules, whilst others will remain isolated. Moreover, it is quite possible for some solute

molecules to remain in a state of isolation whilst others are able to associate with perhaps as many as three other similar species. It is also possible for association to occur during the condensation process and diffusion experiments usually lead to changes in the relative intensities of the features present rather than to the production of new features. Such intensity changes frequently amount to no more than 10% of the original intensity of a feature, particularly when a decrease in intensity is involved.

The best method of combatting the above difficulties was found to be the repetition of experiments and the variance of matrix concentration and spray-on conditions until consistent and rational results had been obtained.

5.6. Matrix-Isolation Raman Spectroscopy

In the examination of relatively simple, symmetrical species, infrared spectroscopy alone is often able to provide less than half the information potentially derivable from vibrational considerations. In particular, the number of coincidences between infrared and Raman features may provide an important means of distinguishing between a number of structural models for a particular species; again, it is often the case that the features ascribable to totally symmetric vibrations, which are frequently active only in Raman scattering, are more readily correlated with bond strengths than are their less symmetric counterparts.

The monomer of trimethylaluminium provides a good example of a

problem of the above type. Of the four AlC_3 skeletal vibrations only one lies within the range of the Perkin-Elmer 225 infrared spectrometer, the antisymmetric stretching mode of E' symmetry, and this mode cannot be correlated directly with the strength of the aluminium-carbon bond. Moreover, a further mode of E' symmetry (ascribable to a rocking motion of the methyl groups) is expected to occur in a similar region of the spectrum, and the frequency of the feature formally attributable to the Al-C antisymmetric stretching vibration is unlikely to be even a reasonable approximation to the true frequency of this vibration. By contrast the symmetric stretching mode, of A_1' symmetry is a direct function of the aluminium-carbon stretching force constant and would be expected to occur in a spectral region at least 500 cm^{-1} removed from any other vibrations of the same symmetry class. It is, however, active only in Raman scattering and remains, therefore, inaccessible using the existing matrix-isolation equipment.

In view of the severe limitation that the restriction of the matrix-isolation technique to infrared spectroscopy places on the value of the method, it was considered highly desirable to develop a matrix-isolation assembly for use in conjunction with the Raman spectrometer. Previous work in the field of Raman spectroscopy as applied to matrix isolation has been restricted to one early[174] and two more recent studies,[175, 176] all of a preliminary nature.

(a) Development Work

(i) At 77°K

Initial experiments were carried out using the Raman liquid-nitrogen

assembly developed for solid-state spectroscopy (Figure 3.5, p.90). Carbon tetrachloride, dichloromethane and xenon were used as matrix materials and trimethylgallium as the solute species; matrices ranging in concentration from 1 in 25 to 1 in 100 were investigated. The spectra were obtained using the helium/neon laser for excitation with the following results:

(1) With 1 in 100 matrices in dichloromethane and carbon tetrachloride the inherently intense bands due to the symmetric and antisymmetric stretching modes of the GaC_3 unit were just within the sensitivity range of the spectrometer; they occured in the same positions as in the liquid-phase spectrum. As the concentration of the matrix was increased the spectrum changed to that characteristic of solid trimethylgallium. The spectral features associated with the matrix materials were relatively very intense and precluded a full investigation of the solute spectrum.

(2) With the xenon matrices (1 in 100, 1 in 10) the background scattering was both low and constant in intensity, but the trimethylgallium features were those appropriate to the solid state, presumably because of the appreciable mobility of a xenon matrix at 77°K. The matrix also evaporated slowly during the course of the investigation.

(ii) At 20°K

The experiments at 77°K were sufficiently successful to warrant

the production of an assembly employing the same viewing principle, but constructed of metal and capable of operation at 20°K. The assembly, which was developed in conjunction with Mr. A.J. Hinchcliffe of this Department, is depicted in Figure 5.3 (p.132).

An Air Products AC-2-109 Cryo-Tip unit was used to cool the sample block. This model is essentially similar to the AC-3L-110 used for the infrared work, both in design and in operation, but only two stages are used, both consisting of gas liquefaction circuits. The first of these produces liquid nitrogen by Joule-Thomson expansion of gaseous nitrogen (the inversion temperature of nitrogen is higher than ambient) and this is used to cool the incoming gaseous hydrogen prior to expansion. Because there is no liquid nitrogen reservoir the unit is capable of operating in a horizontal position. The heat dissipation capacity is 4 watts and diffusion experiments can be carried out in the usual way.

The block containing the sampling groove and slide was located, within radiation shields, at the base of the cryotip. The laser beam entered through an optically flat window and the scattered radiation emerged through a similar window located immediately in front of the collecting lens of the instrument. Furnace, thermocouple and spray-arm facilities were essentially similar to those described in Section 5.4.

A number of different solutes, including both trimethylaluminium and trimethylgallium, in nitrogen and argon matrices, were examined using the above apparatus. Excitation of the spectra was provided by either the helium/neon or argon laser, but even with the latter spectra of relatively poor quality were obtained. The results did, however, tend

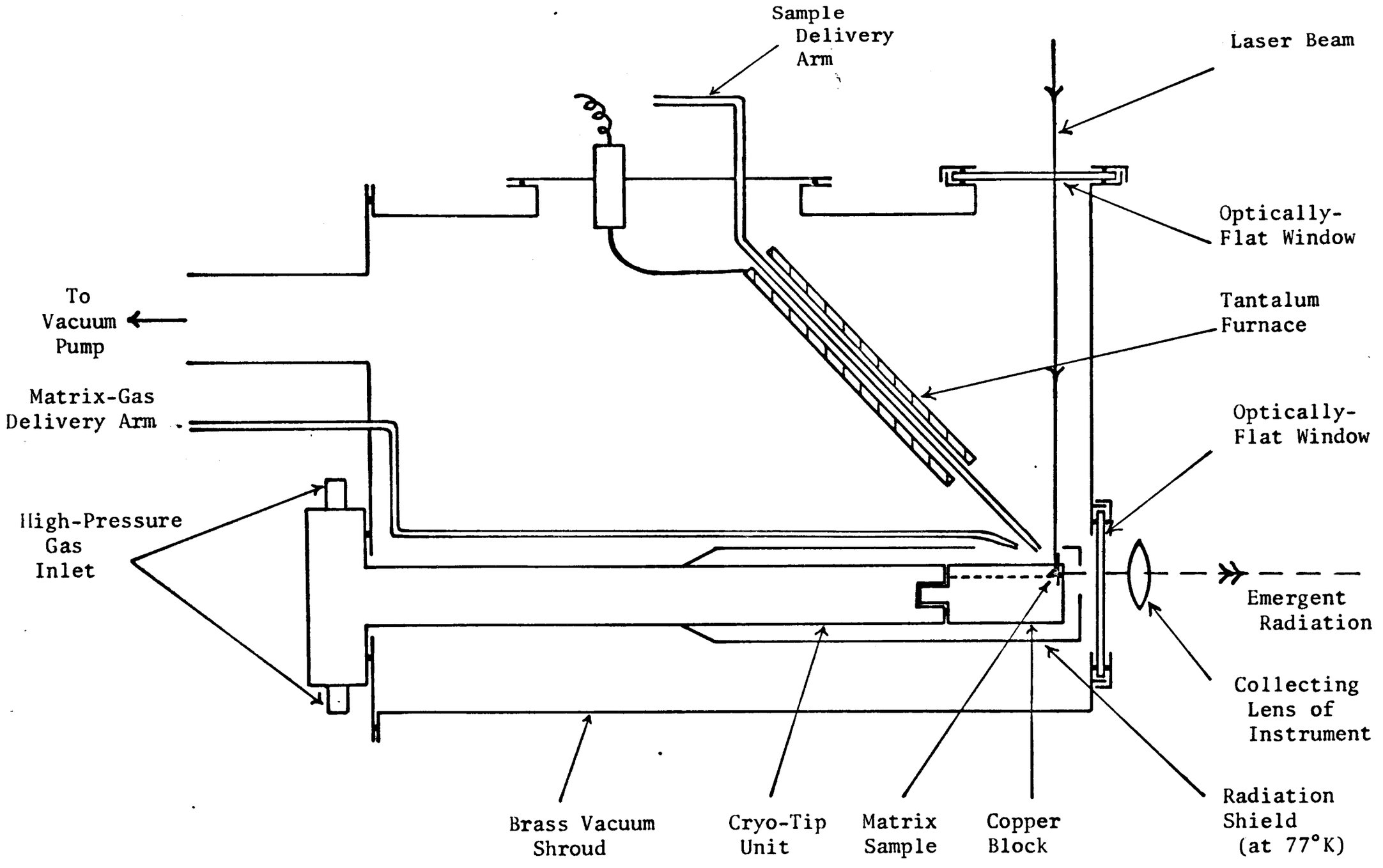

Figure 5.3: The Raman Matrix-Isolation Assembly

to confirm the feasibility of the technique, and to furnish a basis for the continued development of such apparatus. The main problems encountered are discussed in the following section.

(b) The Problems Encountered

(i) Intensity

The amount of Raman scattering detectable from a sample depends on the number of scattering molecules lying both in the laser beam and in the field of view of the collecting lens of the instrument and on the intensity and frequency of the laser beam. Since, to achieve a realistic degree of isolation, it is important to use matrices no more concentrated than 1 in 100, the fundamental problem involved in the production of Raman spectra of matrix-isolated molecules is to produce a signal of sufficient intensity. There are a number of lines of attack on this problem:

(1) Laser The Spectra-Physics 125 laser gave an output of only 70 mW. at 6328 Å and the CRL 54 250 mW. at 4880 Å. Argon-ion lasers capable of producing 3 watts of light at 4880 Å are now commercially available and, other things being equal, the use of such a laser should yield at least a ten-fold increase of signal intensity.

(2) Alignment Because of the weight of the matrix-isolation assembly the kinematic jack designed for the alignment of the Raman cold cell could not be used. With the mounting substituted it was not possible to achieve the highly critical alignment required by the optical characteristics of the spectrometer. The

construction of a more robust jack should eliminate this problem.

(3) Sample Size and Light Collection The size of the present sample, dictated by the instrument optics, is of the order of 1 cubic millimetre, and it is necessary to use a narrow laser beam to achieve maximum spectral intensity. A greater total signal intensity would probably be obtained by the use of a larger sample in conjunction with a wider laser beam and a wider field of view for the collecting system of the instrument (see also below).

(ii) Diffusion

During the experiments it was observed that the matrix sample tended to migrate away from the area of impingement of the laser beam. It was not possible during the initial experiments, however, to assess whether the matrix was appreciably mobile under the conditions of operation (i.e. whether diffusion of solute molecules was occurring spontaneously during the experiment). Were a larger laser to be employed, the use of a wider optical system (as suggested above) might prove obligatory in order to avoid excessive mobility of the matrix.

Thus the potentially exciting possibility of examining the Raman spectra of matrix-trapped molecules is still at a relatively early stage of development.

SECTION III

TOIL

Chapter 6

The Vapour and Liquid Phase Spectra

In the three chapters of this section the results obtained from the various facets of the investigation are presented: the present chapter deals with the spectra given by the molecules in the fluid phases, whilst the solid-state and matrix-isolation data are contained in Chapters 7 and 8 respectively. Some of the results presented for trimethylindium, and most of the results for trimethylthallium, were obtained in collaboration with Mr. J.H. Darling of this Department.[177]

As the fluid-phase vibrational spectra of the Group III trimethyl compounds have already been the subject of considerable study, it was considered pointless to repeat the work of previous investigators on a general basis and all the results described here were obtained from experiments undertaken because of deficiencies in the literature data. Some of the room temperature investigations were carried out in order to provide precise data for direct comparison with results obtained at higher or lower temperatures, whilst others were undertaken because of the availability of more sophisticated instrumentation. Thus, most of the vapour-phase infrared results reported here extend at least 200 cm^{-1} further into the far-infrared than do previous data.

6.1. The Presentation of Results

For the most part, the spectral details are reported in tabular form; pictorial representations of the actual instrument traces are

included only where these serve to illustrate specific points. The results for the various compounds are presented individually in this section; the various correlations with the nature of the phase and of the Group III atom are discussed and illustrated (in the form of line diagrams) in Section IV.

(a) The Tables

The contents of the tables of results given in this section are divided vertically into three areas. The columns to the left of each table are devoted to the details of the spectra obtained in this investigation. The central column gives the vibrational assignment, based either on the literature or on arguments presented in the final section. In the case of the solid-phase and matrix-isolation data the assignment column refers to the fluid phases and is included for comparison purposes only. Such vibrational assignments are made on the basis of a D_{3h} model in the cases of trimethylboron, -gallium, -indium and -thallium and on the basis of a D_{2h} model in the case of dimeric trimethylaluminium. The columns on the right of each table contain the spectral data listed in the literature, the appropriate references being included.

The frequencies of features originating from the same vibrational transition are coupled by brackets in the tables. In the case of the vapour-phase infrared results the letters P, Q and R are used to denote the maxima of the branches of the vibrational envelope where these can be distinguished.

Various spurious factors, such as laser lines in the Raman spectra

and the inverted carbon dioxide features in the infrared spectra, have been eliminated from the results and in the case of solution spectra only the solute features are listed. Where a solute feature is obscured by a solvent band an asterisk is included at the appropriate position in the column relating to the solution data. Assignments of a speculative nature are preceded by a question mark and any features suspected of being spurious are marked '?sp'. Overtone and combination features have been separately assigned wherever possible and where the spectral range of an investigation is less than that included in the table the limits of the investigation are marked by dotted lines in the appropriate columns.

(b) Intensities

(i) Raman

Numerical relative intensities are reported for the Raman spectra, the strongest feature being arbitrarily given an intensity of 100. In estimating these intensities allowance has been made on a simple, linear basis for the sensitivity settings, slit widths and number of slits in use under the conditions of operation. Features with a relative intensity of less than one are described simply as weak or very weak (w or vw respectively).

In the case of liquid samples, wherever qualitative polarization measurements proved possible, the results of such measurements are included in the tables.

(ii) Infrared

In the case of the infrared spectra, a qualitative estimate of

intensities is given, the following arbitrary scale being employed:

vs	=	very strong	w	=	weak
s	=	strong	vw	=	very weak
m	=	medium	vvw	=	very very weak

(Each step on the scale corresponds to an approximately two-fold change in intensity).

(iii) Broad Features and Unresolved Features

In both the Raman and infrared spectra the abbreviation 'bd' signifies a broad feature; the exact frequencies of such features are very difficult to assess and the precise numerical values of such frequencies are to be treated with some latitude. The abbreviation 'sh' is used to indicate a feature incompletely resolved from a stronger feature; the distinctness of such features ranges from a slight asymmetry of the main feature to a definite 'shoulder'. Whenever such a feature occurred in association with a spectroscopically important feature every effort was made to resolve the shoulder or, if instrumental resolution proved impossible, to assess its frequency by simple curve-fitting methods. Frequencies obtained in the latter way are annotated in the tables. The intensities of such features are, of course, difficult to assess.

6.2. Calibration

(a) Raman Spectra

The Raman spectra were calibrated in three distinct ways:

(i) All the spectra were calibrated with reference to the exciting line; the peak due to Rayleigh scattering (0 cm^{-1}) was recorded both before and after the experiment to check for any alignment drift.

(ii) When the sampling assembly could readily be removed from the instrument, each spectrum was directly calibrated with reference to the Raman frequencies of benzene, carbon tetrachloride and chloroform.[113]

(iii) When the sampling assembly could not readily be removed from the instrument, it was possible only to check the calibration of the instrument before and after the series of experiments.

Discrepancies between the read-out from the instrument and the calibration values were within one wavenumber in all cases.

(b) Infrared Spectra

In the near-infrared region (4000-200 cm^{-1}) the spectra were calibrated using the fine structure of bands of ammonia or of water.[178, 179] For calibration with ammonia a sealed cell containing the gas at 7 cm. pressure was used in the reference beam of the instrument, the sample beam being blocked; for calibration with water a little moist air was admitted to the instrument, which was again operated with the sample beam blocked. The far-infrared spectra (400-50 cm^{-1}) were also calibrated with reference to water vapour features.[180]

6.3. Trimethylboron

(a) Room Temperature Spectra

Both the Raman spectrum of the pure liquid and the infrared spectrum of the vapour were re-investigated. The Raman spectrum was obtained using the helium-neon laser with the sample contained either in a sealed, round-ended tube or in a cell fitted with a light-pipe (the investigation being carried out just prior to the low temperature investigations). The infrared spectrum was examined from 4000-200 cm^{-1} using conventional gas cells of 10 cm. path-length equipped with caesium iodide windows. Trimethylboron pressures ranging between 0.5 and 50 cm. Hg were employed.

The results which were obtained are presented in Table 6.1 (p.141), together with the results of previous Raman[9] and infrared[7] investigations. Although trimethylboron is both a poor Raman scatterer and a poor absorber of infrared radiation, the agreement between the two sets of results is, for the most part, remarkably good. However, no trace of the previously reported[9] Raman feature at 397 cm^{-1} could be found at room temperature and it was decided to carry out an investigation at low temperature (see below). The Raman feature found at approximately 495 cm^{-1} in this investigation has not previously been reported.

The assignments included in Table 6.1 are those given in reference 9, with the exception of the E' modes ν_{15} & ν_{16}. These have been transposed to maintain consistency with the assignments reported for trimethylgallium and trimethylindium.[52]

(b) Low Temperature Raman Spectrum

A sample of trimethylboron sealed in a light-pipe cell was examined

Table 6.1

PRESENT INVESTIGATION					Assignment[9]	PREVIOUS INVESTIGATIONS				
Raman (Liquid)			Infrared (Vapour)			Infrared (Vapour)[7]		Raman (Liquid)[9] (-100°C)		
ν (cm^{-1})	int.	pol.	ν (cm^{-1})	int.		ν (cm^{-1})	int.	ν (cm^{-1})	int.	pol.
			308	vw sh	P					
322	31	dp	321	vw	Q } ^{11}B e' ν_{17}	320	m	321	m	dp
			335	vw	R } ^{10}B a_2'' ν_{10}	336	m			
			351	vvw sh		345	sh			
					? sp			397	vw	-
~495	vw bd	-			? e'' ν_{20}					
			651	vvw	2x321 = 642 ($A_1'+E'$)					
679	100	p			a_1' ν_3			680	s	p
862	5	-	857	w	e' ν_{15}	855	m	862	mw	-
			967	m	^{11}B a_2'' ν_9	968	s			
			983	m	^{10}B	983	m			
1151	30	dp	1147	s	P ^{11}B	1149	vs	1149	s	dp
			1160	s	R } ^{10}B e' ν_{16}	1162	vs			
1178	4	-	1185	m		1189	m	1177	m	dp
1287	7	dp	1299	vs	P } ^{11}B e' ν_{14}	1300	sh	1297	m	dp
			1308	vs	R } & ^{10}B & $a_1''\nu_2$	1309	vs			
1422	15	dp			e' ν_{19}			1422	s	dp
			1451	w	a_2'' ν_8 & e' ν_{13}	1459	m			
			1714	vvw	2x857 = 1714 ($A_1'+E'$)	1721	vw			
			1822	vvw	1151+679 = 1830 (E')	1828	vw			
			1974	vw	1304+679 = 1983 (E')	1976	w			
			2162	vw	1304+857 = 2161 ($A_1'+E'$)	2167	w			
			2255	vvw	1287+967 = 2254 (A_2'')	2255	vw			
			2348	vw sh	1287+1154= 2441 (E')	2444	w			
			2451	vw	1304+1154= 2458 ($A_1'+E'$)	2456	w			
			2470	vw sh	1287+1185=2472 (E_1' ^{11}B ^{10}B)	2472	vw			
						2591	vw			
2888	80	p			a_1' ν_1			2880	vs	p
			2915	s	e' ν_{12}	2921	s			
2972	4	-			e'' ν_{18}			2974	s	dp
			2980	s	a_2'' ν_7 & e' ν_{11}	2986	s			
			3291	vw	2972+321 = 3293 ($A_1''+A_2''+E''$)	3300	w			
			3545	vw	2888+2x321 = 3530 ($A_1'+E'$)	3522	w			
			3750	vvw	2888+857 = 3745 (E')	3729	w			
			3845	vw	2888+967 = 3855 (A_2'')	3853	w			

Table 6.1: The Vibrational Spectra of the Fluid Phases of Trimethylboron

using the apparatus depicted in Figure 3.2 (p.83) over the temperature range +20 - -150°C, the spectral range 200 - 1500 cm^{-1} being scanned repeatedly during the cool-down period. As the density of the liquid column increased the overall intensity of the spectrum also increased, but no significant changes occurred in either the frequencies or relative intensities of the features. The spectrum was carefully examined at -150°C and only the most intense feature showed a measurable frequency shift - from 679 cm^{-1} at 20°C to 687 cm^{-1} at -150°C. No trace of any feature could be found at 397 cm^{-1} and the rather weak feature at approximately 490 cm^{-1} retained, within the accuracy of measurement, the same relative intensity throughout the cool-down procedure.

6.4. Trimethylaluminium

(a) Room Temperature Spectra

The Raman spectra of solutions of trimethylaluminium in dichloromethane and benzene (1:10 molar proportions) were examined in light-pipe cells as preliminaries to the high-temperature studies described below. The benzene and dichloromethane used for this purpose were carefully dried over phosphoric oxide prior to transference to the vacuum line and were subsequently purified by trap-to-trap fractionation. Two different dichloromethane samples and one benzene sample were examined using the helium neon laser for excitation throughout. The results of the investigation are listed in Table 6.2 (p.143), together with the results of the most recent previous investigation of the pure liquid[30] and the most recent spectral assignment.[181] Some of the features

Table 6.2

PRESENT INVESTIGATION										(181) Assignment	PREVIOUS INVESTIGATION LIQUID (30)		
SOLUTION				SATURATED VAPOUR									
CHLOROFORM		BENZENE		SPEX (∿150°C)		CODERG DIMER (∿130°C)		CODERG MONOMER (∿170°C)					
$\nu(cm^{-1})$	int.	$\nu(cm^{-1})$	int.	$\nu(cm^{-1})$	int.	$\nu(cm^{-1})$	int.	$\nu(cm^{-1})$	int.		$\nu(cm^{-1})$	int.	pol.
156	32			145	95	141	s			$b_{2g}\ \nu_{12}$	153	40	0.8
				160	sh					$b_{3g}\ \nu_{15}$	185	sh	0.7
				220	17					? Laser			
315	71	316	70	305	74	305	78			$a_{1g}\ \nu_3$	313	39	0.52
				349	13					? Laser			
459	100	458	100	441	87	441	100			$a_{1g}\ \nu_2$	453	53	0.13
∿495	bd 13	∿495	20	489	bd 34	491	45			?	495	14	0.06
				527	42			527	vs	$a_1'\ \nu_3$ Monomer			
595	64	592	sh	588	100	594	81			$a_{1g}\ \nu_1$	592	56	0.21
										b CH_3 rock	632	2	p
								∿685	sh w	? e' ν_{16} Monomer			
*		*		682	22	687	sh			t CH_3 rock	683	19	0.80
*				735	17					? Laser & b CH_3 rock	725	3	dp
1157(+)	25												
1200	22					1210	32			t CH_3 sym. bend	1200	29	0.33
										t CH_3 sym. bend	1255	2	dp
										?	1315	1	p
										t & b CH_3 asym.bend	1436	4	0.80

t = terminal; b = bridging; + = feature probably attributable to solvent.

Table 6.2: The Raman Spectra of the Fluid Phases of Trimethylaluminium

found in the spectrum of the pure liquid were obscured by solvent bands in the solution spectra; the frequencies of the remaining features were in reasonably good agreement with those reported for the pure liquid.

The infrared spectrum of the saturated vapour of trimethylaluminium was examined in the region 500-50 cm^{-1}, the remainder of the spectrum already being well documented.[26, 28] A cell of 10 cm. path-length fitted with polythene windows was employed with the results listed in Table 6.3 (p.145). The data are in reasonable agreement with the results reported (i) for thin films of liquid[26] and (ii) for the vapour phase at frequencies above 300 cm^{-1} [28], but a new feature of low intensity was found at 298 cm^{-1}. Such a feature is readily accommodated within the existing vibrational assignment for the molecule[181].

(b) High Temperature Solution Spectra

Since gaseous trimethylaluminium exhibits a temperature-dependent monomer/dimer equilibrium[19, 20] it was decided to examine Raman spectra of solutions at elevated temperatures using the apparatus depicted in Figure 3.2 (p.83). Such investigations were not successful, probably because of the very high reactivity of the monomer species. It was calculated that, at the concentrations used, appreciable dissociation should begin only at temperatures above 100°C. Not surprisingly, then, the spectrum showed no detectable alteration over the temperature range 20 - 80°C. Above 80°C, however, the samples started to 'bump' violently with the formation of a white deposit and concomitant loss of spectral quality; further experiments were not undertaken.

PRESENT		Assignment[180]	PREVIOUS INVESTIGATIONS		
Vapour Phase (Saturated)			Vapour Phase[28]		Thin Film[26]
ν (cm^{-1})	int.		ν (cm^{-1})	int.	ν (cm^{-1})
476	vs	b_{2u} ν_{13}	480	m	480
366	s	b_{3u} ν_{17}	369	s	366
298	w	? b_{14} ν_{9}			
170	s	b_{2u} ν_{14} & b_{3u} ν_{18}			175

Table 6.3: The Low Frequency Infrared Spectra of the Fluid Phases of Trimethylaluminium

(c) High Temperature Vapour-Phase Spectra

In the closing stages of this investigation it proved possible to examine the Raman spectra of gaseous trimethylaluminium at elevated temperatures. The first examination was made using a Spex 'Ramalog' spectrometer equipped with a CRL 52 argon-ion laser capable of producing 750 mW of radiation at 4880Å: later studies were made using a Coderg PHl spectrometer excited by a Spectra-Physics 125 helium-neon laser producing 74 mW of 6328Å radiation. Small glass ampoules, about 1 cm. in diameter and 5 - 10 cm^3 in capacity, were filled with sufficient trimethylaluminium to maintain a saturated vapour and the ampoules were heated using a small furnace to temperatures as high as 170°C, the whole assembly being contained within the sample compartment of the spectrometer.

Partly because of mounting and alignment difficulties, but also because of photolytic decomposition it was possible to obtain only a preliminary spectrum using the Spex instrument; the frequencies of the observed bands are included in Table 6.2 (p.143). The spectrum was recorded at approximately 150°C and it was noted at the end of the experiment that the walls of the sample ampoule were coated with a metallic deposit at the point of impingement of the laser beam. Most of the features recorded for the vapour agree well, both in position and relative intensity, with those obtained for the dimer in the liquid phase, but three completely new features were observed at 220, 349 and 527 cm^{-1}. The feature at 527 cm^{-1} was of an intensity comparable with that of the dimer features, but those occurring at 220 and 349 cm^{-1} were both rather feeble. In the solid-state experiments it was noted that the argon-ion

laser gave rise to primary lines at 231 (w), 352 (m), 528 (s) and 736 (m) cm^{-1} relative to the Rayleigh line at 4880Å: hence the new features at 220 and 349 cm^{-1}, plus that at 735 cm^{-1}, are probably best considered to be spurious. The feature at 527 cm^{-1} is, however, almost certainly genuine, at least in part (see below).

Using the Coderg instrument and 6328Å excitation, it proved possible to obtain the spectrum of the saturated vapour at 130 and 170°C without decomposition; the results are illustrated in Figure 6.1 (p.148). To improve the signal intensity it was necessary to remove the incident-light filters and the spurious laser features thereby introduced are noted in the figure. The spectrum at 130°C closely resembled that obtained using the Spex instrument except that the features at 220, 349 and 735 cm^{-1} were not present and that at 527 cm^{-1} was very weak. At 170°C the 527 cm^{-1} feature was extremely strong, however, and the weak feature at 685 cm^{-1} seemed to be of greater intensity relative to the other dimer features than at 130°C. The frequencies of all the features are reported in Table 6.2; the features at 527 and 685 cm^{-1} have been assigned respectively to the symmetric and antisymmetric stretching modes of the AlC_3 unit in the $Al(CH_3)_3$ monomer.

6.5. Trimethylgallium

(a) Room Temperature

Although the Raman and infrared spectra of trimethylgallium are well documented,[52, 53] it was decided to re-examine the spectra at room temperature using the more sophisticated equipment presently

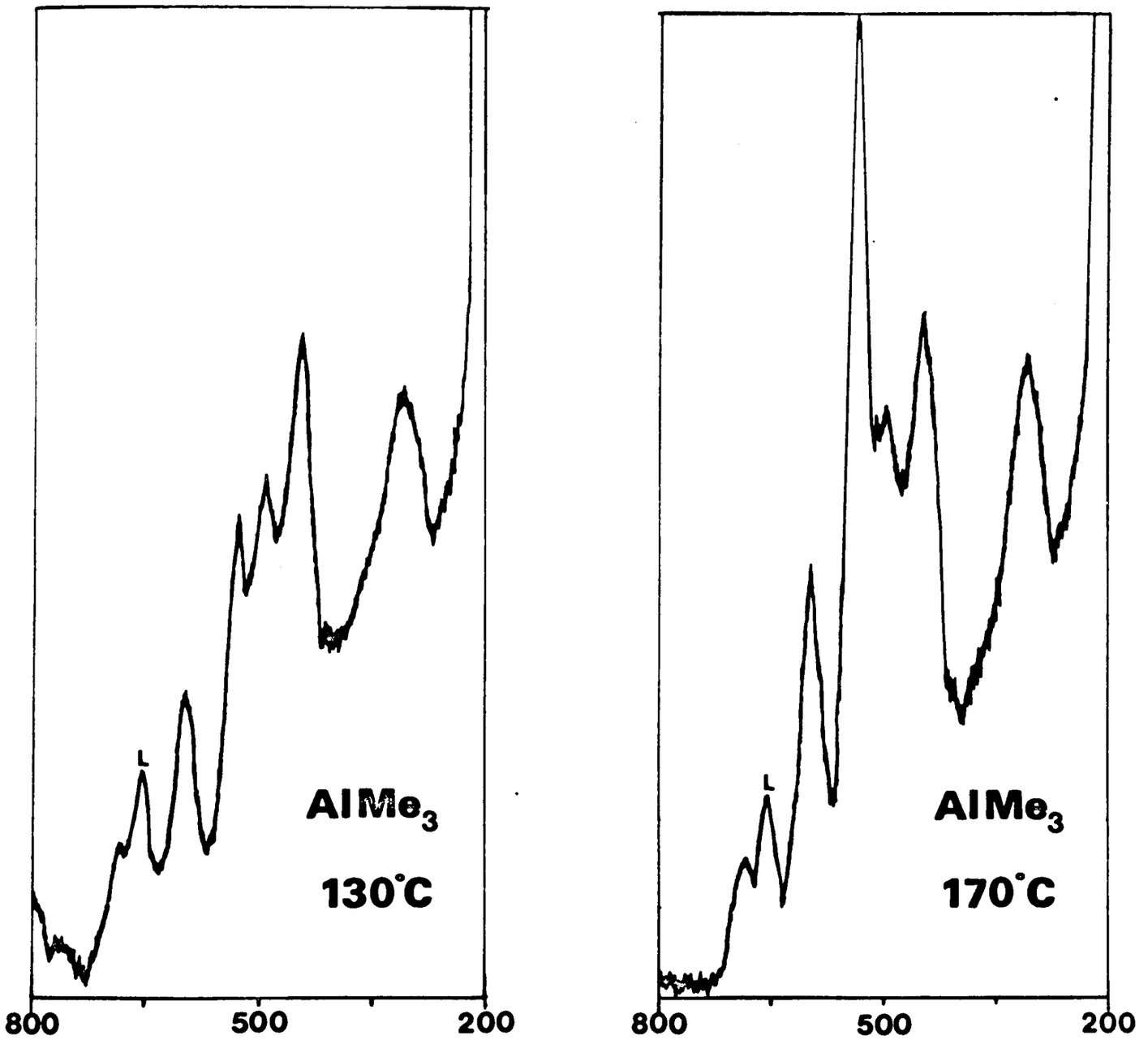

(L = spurious laser feature)

Figure 6.1: The Vapour-Phase Raman Spectrum of Trimethylaluminium

available in the hope of observing previously undetected weak features and, in the case of the infrared spectrum, of observing the GaC_3 deformation modes, expected to lie below 300 cm^{-1}. The results obtained are listed in Table 6.4 (p.150) together with those from a previous investigation[53] and the accepted vibrational assignment.[52]

The Raman spectrum of the pure liquid was obtained using a break-seal cell of the type depicted in Figure 4.3 (p.107). The spectrum was examined at frequencies up to 3200 cm^{-1} using the helium-neon laser for excitation, qualitative polarization measurements being made wherever possible. A solution in dichloromethane ($Ga(CH_3)_3$:CH_2Cl_2, 1:10) was also examined at frequencies up to 1500 cm^{-1} as a preliminary to the low temperature work. All the spectral frequencies were found to agree well with the literature results and only one new feature, of dubious authenticity, was found, namely at 410 cm^{-1}. The weak features previously reported (using mercury-arc excitation) at 465 and 1328 cm^{-1} were not observed.

The vapour-phase infrared spectrum was examined from 4000 to 50 cm^{-1} using cells with caesium iodide or polythene windows and pressures ranging between 0.5 and 50 cm. Hg. The results were again entirely consistent with the data previously reported for the pure liquid. One new feature, an intense band at 156 cm^{-1}, corresponding to the scattering found at 163 cm^{-1} in the Raman spectrum of the liquid, was beyond the range of the previous investigations (lower limit 400 cm^{-1}), and a number of weak features, all probably ascribable to overtones or combinations of the fundamentals, were also found.

Table 6.4

PRESENT INVESTIGATION							Assignment[52]	PREVIOUS INVESTIGATION[53]				
Raman (CH_2Cl_2 soln)		Raman (Liquid)			Infrared (Vapour)			Infrared (Vapour)		Raman (Liquid)		
$\nu(cm^{-1})$	int.	$\nu(cm^{-1})$	int.	pol.	$\nu(cm^{-1})$	int.		$\nu(cm^{-1})$	int.	$\nu(cm^{-1})$	int.	pol.
168	23	163	56	dp	156	s	e' ν_{17}			162.5	s	dp
		410	bd vw	-			? sp			465	w	-
523	100	520	100	p			a_1' ν_3			521.5	vs	p
					571		P	571				
572	11	570	14	dp	577	vs	Q e' ν_{16}	577	vs	570	s	dp
					584		R	587				
622	1	617	sh vw	-			e" ν_{20}			612	w sh	-
					680	vw	520+163 = 683 (E)					
					723	s	a_2'' ν_9	727	ms			
*		769	1	dp	771	vs	e' ν_{15}	769	s	769	w	dp?
		1046	w	p?			2 x 520 = 1040 (A_1')			1038	vw	-
					1055	w	? sp					
							2 x 570 = 1140 (A_1'+E')			1139	w sh	-
					1198		P	1198				
*		1185	sh m	dp	1205	s	Q e' ν_{14}	1205	s	1186	w sh	-
					1213		R	1211				
1199	s	1198	9	p			a_1' ν_2			1198	s	p
							? sp			1328	vw	-
					1359	w	1198+156 = 1354(E')					
							1205+156 = 1361(A_1'+A_2'+E')	1356	vw			
					1411	vw	a_2'' ν_8 & e' ν_{13}	(1405)[52]	vw			
*		1433	2	dp			e" ν_{19}			1428	vw	-
					1732	w	1205+520 = 1725(E')	1730	vw			
					1785	w	1205+577 = 1782(A_1'+A_2'+E')	1786	vw			
		2370	w	-			2 x 1185 = 2370(A_1'+A_2'+E')			(2369)[52]	vw	-
					2391	w	1198+1205= 2403(E')	(2390)[52]	vw			
					2860	bd w	2 x 1433 = 2866(A_1'+E')	2865	sh m	(2865)[52]	w	-
		2905	5	p			a_1' ν_1			2903	vs	p
					2919	s	e' ν_{12}	2914	br s			
		2960	sh w	-			e" ν_{18}			2961	br s	dp
					3001	s	a_2'' ν_7 & e' ν_{11}	2999	s			
					3055	vw	2905+156 = 3061(E')	3046	m sh			
					3152	vw	3001+156 = 3157(A_1'+A_2'E')					
					3510	vw	3001+520 = 3521(A_2''or E')					
					3571	vw	3001+577 = 3578(A_1'+A_2'+E')					
					3637	vw	2905+723 = 3628(A_2'')					

Table 6.4: The Vibrational Spectra of the Fluid Phases of Trimethylgallium

(b) Low Temperature

Excited with the helium-neon laser, the Raman spectrum of the solution of trimethylgallium in dichloromethane was examined over the temperature range +20 to -100°C using the assembly depicted in Figure 3.2 (p.83). The sample was cooled very gradually and the spectrum carefully examined at 20°C intervals. No new features could be detected nor were there observed any significant changes in the frequencies or relative intensities of any of the original features. The largest shifts over the 120°C temperature-decrease occurred in the features originally at 168, 523 and 576 cm^{-1}; these increased in frequency by 6,3 and 3 cm^{-1} respectively. Because of the increased density of the solution at low temperature a general increase in spectral intensity was also observed.

(c) Nuclear Magnetic Resonance Spectrum

The n.m.r. spectrum of trimethylgallium was investigated using an A.E.I. R.S.2 spectrometer operating at 60 Mc/sec. The neat liquid was examined at room temperature and at -15°C, while a 10 mole % solution in dichloromethane was examined at temperatures down to -80°C. No splitting or appreciable broadening was observed in the ^1H resonance due to trimethylgallium, and the chemical shift likewise showed very little change. For liquid trimethylgallium over the temperature range +20 to -15°C the chemical shift was found to be +0.232 ± 0.007 p.p.m. relative to tetramethylsilane (used as an internal standard).

6.6. Trimethylindium

(a) Room Temperature

Although previous results[53] are not completely satisfactory, trimethylindium was not fully investigated in the fluid phases, mainly because of technical difficulties. The Raman spectrum of a solution of trimethylindium in dichloromethane ($(CH_3)_3In:CH_2Cl_2$, 1:10) was examined in a light-pipe cell using the helium-neon laser with the results tabulated in Table 6.5 (p.153), together with the previously reported data obtained for the pure liquid at 95°C. Although no new features were observed, shifts of up to 8 cm^{-1} were noted between the results for the solution at room temperature and those for the high-temperature melt.

The infrared spectrum of the saturated vapour was also examined in the frequency range 4000-50 cm^{-1}, using cells fitted with caesium iodide or polythene windows. Because of the low vapour pressure of the solid at the operating temperature of the instruments (approximately 40°C) it was possible to detect only the stronger features of the spectrum. The results obtained, which are listed in Table 6.5, include a new strong feature located at 118 cm^{-1} and a broad, weak feature, of dubious authenticity, at 590 cm^{-1}.

(b) Low Temperature

Using the assembly depicted in Figure 3.2 (p.83) attempts were made to obtain a Raman spectrum of the dichloromethane solution of trimethylindium at low temperatures. The sample started to deposit crystals at approximately -20°C, no change in the spectrum being detectable

Table 6.5

PRESENT INVESTIGATION					Assignment[52]	PREVIOUS INVESTIGATION[52]				
Raman (CH_2Cl_2 Sol^n.)			Infrared (Vapour)			Infrared (Vapour)		Raman (Liquid, 95°C)		
ν(cm^{-1})	int.	pol.	ν(cm^{-1})	int.		ν(cm^{-1})	int.	ν(cm^{-1})	int.	pol.
125	w	dp	118	s	e' ν_{17}	-----	----	132	s	dp
475	100	p			a_1' ν_3			467	vs	p
493	29	dp	493 509	vs vs	P, R } e' ν_{16}	500	s	495	s	dp
			590	bd w	475+118 = 593(E')					
626	1	dp			e' ν_{20}			635	br w	dp
			~690	bd s	a_2'' ν_9	687	ms			
			729	vs	e' ν_{15}	725	s			
			1128	vw	501+626 = 1127 ($A_1''+A_2''+E''$)					
					e' ν_{14}	~1155	vw	1116	br m	dp
1157	21	p			a_1' ν_2			1157	s	p
			1650	vw	1157+501 = 1658 (E')					
			2250	vw	2 x 1128 = 2256 ($A_1'+E'$)					
			2320	vw	2 x 1160 = 2320 ($A_1'+E'$) 1160+1157= 2317 (E')					
			2850	w	2 x 1425 = 2860	2860	m	2861	sh w	-
2912	5	p			a_1' ν_1			2910	ms	dp
			2910	m	e' ν_{12}	2920	s			
*			2960	vw	e'' ν_{18}			2974	mw	dp
			3002	m	a_2'' ν_7 & e' ν_{11}	3000	s			

Table 6.5: The Vibrational Spectra of the Fluid Phases of Trimethylindium

prior to this; the crystals re-dissolved as the sample warmed to room temperature.

6.7. Trimethylthallium

No previous investigations of the vibrational spectra of trimethylthallium have been published, although the infrared spectrum has been examined,[182] as have the two most intense features of the Raman spectrum of the liquid.[183] The latter study was undertaken using mercury-arc excitation, which caused the sample to undergo very rapid photolytic decomposition.

The Raman spectrum of the pure liquid was obtained with the sample contained in a break-seal ampoule of the type depicted in Figure 4.3 (p.107). The spectrum was excited using the helium-neon laser, the sample being maintained above its melting point with the aid of a hot-air blower; polarization measurements were made wherever possible. No decomposition could be detected during the course of the examination. The results are listed in Table 6.6 (p.155) together with the vibrational assignment originally proposed on the basis of an investigation of solid trimethylthallium.[183]

The infrared spectrum of the saturated vapour was examined over the frequency range 4000 - 50 cm^{-1} using cells fitted with caesium iodide or polythene windows. The results obtained are in accordance with, but of better quality than, those obtained in the previous investigation.[182] A strong absorption was found at 96 cm^{-1}, corresponding to the scattering found in the Raman spectrum of the liquid at 99 cm^{-1}, and a very much weaker band was found at 620 cm^{-1}.

Table 6.6

PRESENT INVESTIGATION					Assignment[177,183]	PREVIOUS INVESTIGATIONS			
Raman (Liquid, ~40°C)			Infrared (Vapour)			Infrared (Vapour)[182]		Raman (C_6H_6 Sol^n)[183]	
ν(cm^{-1})	int.	pol.	ν(cm^{-1})	int.		ν(cm^{-1})	int.	ν(cm^{-1})	int.
96	w	dp	99	s	e' ν_{17}				
445	100	p			a_1' ν_3			450	vs
			456	vs	P } e' ν_{16}	465	vs		
			468	vs	R }				
			620	bd vw	? sp				
656	1	dp			e'' ν_{20}				
			697(†)	sh w	a_2'' ν_9	710	sh		
747	w	dp	754	vs	e' ν_{15}	753	vs		
895	w	p			2 x 445 = 890 (A_1')				
1115	12	p			?				
1141	23	p			a_1' ν_2			1146	s
			1143	m	P } e' ν_{14}	1148	m		
			1158	m	R }				
1325	w	-			3 x 445 = 1335 (A_1')				
			1395	bd w	? a_2'' ν_8				
1429	bd w	-			e' ν_{13} & e'' ν_{19}				
1585	w				1141+445 = 1586 (A_1')				
			1604	m	1141+462 = 1603 (E')				
			2280	m	1151+1141= 2292 (E')	2276			
			2877	s	2 x 1430 = 2860(many)				
2917	4	p			a_1' ν_1				
			2930	vs	e' ν_{12}	2931	m		
2984	w	dp			e'' ν_{18}				
			3020	s	a_2'' ν_7 & e' ν_{11}	3023	s		

† = Frequency obtained by curve fitting

Table 6.6: The Vibrational Spectra of the Fluid Phases of Trimethylthallium

No low temperature measurements were made for trimethylthallium. A solution of trimethylthallium in dichloromethane ($(CH_3)_3Tl:CH_2Cl_2$, 1:10) was prepared but this decomposed rapidly on irradiation, only the features at 450 and 1140 cm^{-1} being observable. During the course of the decomposition a white solid appeared within the sample tube.

Chapter 7

The Solid-State Results

7.1. Introductory

None of the Group III trimethyl compounds has previously been examined in the solid state using vibrational spectroscopy and it was decided to undertake such an examination, with the following objectives:

(i) To elucidate the solid-state structures of trimethylboron, trimethylgallium and trimethylthallium and to examine the validity of recent suggestions regarding the structure of trimethylaluminium in the solid state.[38,39] The published X-ray crystal structures of trimethylindium[63] and, to a lesser extent, trimethylaluminium[37] are valuable in this connection in providing 'fixed points' on which to base comparisons.

(ii) To produce, in the case of the infrared investigations, thick layers of the compounds, thereby facilitating the examination of weak features. In this way it was hoped that it might be possible to extend the assignments made for the fluid phases (particularly for trimethylindium and trimethylthallium).

(iii) To eliminate the rotational envelopes of spectroscopic features given in the vapour phase, thereby revealing such

details as isotope splittings and near-degeneracies.

(iv) To place the molecules in different environments and thereby to test the hypothesis of accidental degeneracy postulated for certain modes in the assignments for the fluid phases. Such degeneracies are, in general, unlikely to be retained with change of state.

The spectra given by solid samples customarily differ quite radically from their fluid-phase counterparts: the features are often much sharper and many of the fluid-phase singlets are split into multiplets as a result of crystal environment effects. Figure 7.1 (p.159) illustrates this point for the infrared spectrum of trimethylgallium in the 1200 cm^{-1} region. The upper trace shows the vapour-phase spectrum, which comprises one simple vibrational/rotational envelope. By contrast, the solid-state spectrum contains six features, and the whole multiplet is shifted appreciably to lower frequency.

7.2. The Results

(a) The Experiments

The infrared spectra of all five Group III trimethyl compounds and the Raman spectra of all but the boron compound are reported in this chapter. In the case of the compounds of the four heavier elements the spectra were examined at the boiling point of liquid nitrogen (77°K), but the infrared spectrum of trimethylboron, which still retains a significant volatility at this temperature, was examined, with the sample

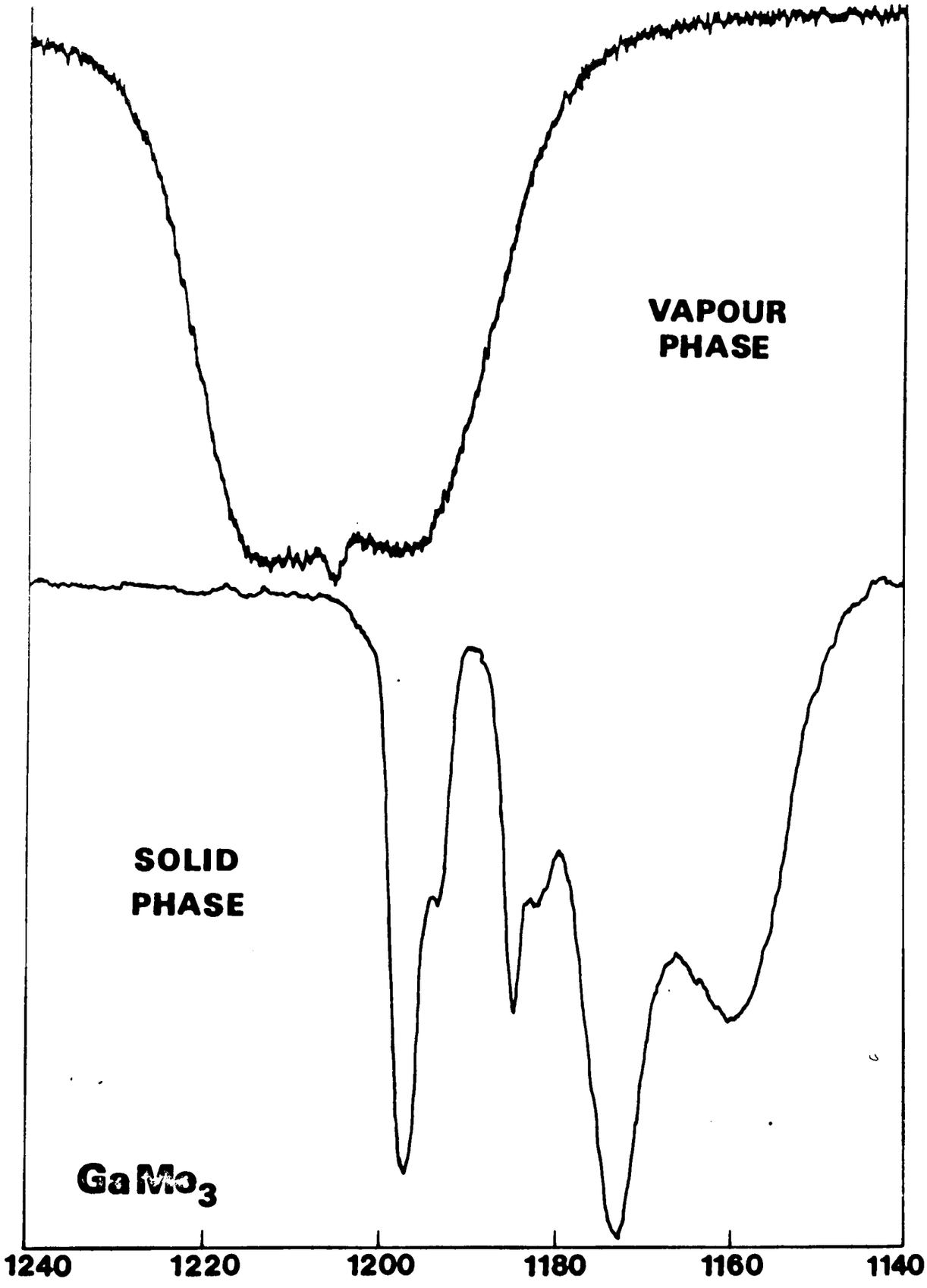

Figure 7.1: The Vapour-Phase and Solid-Phase Infrared Spectra of Trimethylgallium in the 1200 cm^{-1} Region

at 20°K, the matrix-isolation assembly (Section 5.4, p. 120) being used for the purpose. The corresponding Raman spectrum was not measured.

The infrared spectra of the other four compounds in the solid state were measured over the range 4000-200 cm^{-1} using the cell described in Section 3.3(b) (p. 92). In order to eliminate spurious features three distinct samples of successively greater thickness were examined for each compound. The Raman spectra were obtained using the right-angle viewing cell described in Section 3.3(a) (p. 80). All four compounds were examined using the argon-ion laser. Trimethylgallium and trimethylthallium were also examined using the helium-neon laser; for both of these compounds the results obtained with the different lasers were in complete agreement. In order to eliminate spurious instrumental features, the spectra of trimethylaluminium, trimethylgallium and trimethylindium were excited using both the blue (4880Å) and green (5145Å) lines of the argon-ion laser, but this precaution was not possible in the case of trimethylthallium since the blue line induced photolytic decomposition.

All the samples were carefully annealed prior to detailed examination, the progress of the process being followed spectroscopically. In general, the spectral features became more intense and better resolved during the process, but this was not the case for trimethylboron (see Section 7.3).

(b) The Tables

Since none of the solid-state spectra has previously been investigated and since it is impossible to assign all the features of such

spectra, the frequencies reported in the tables of results are listed opposite the fluid-phase features from which they arise. Thus, whilst the columns to the left of the tables contain the new, solid-state results, the central assignment column refers to the data listed to the right of the table for the fluid phases (except for the overtone and combination features). Wherever possible the fluid phase data are taken from Chapter 6; only the results for trimethylaluminium and for the Raman spectrum of liquid trimethylindium are taken from the literature. It is to be noted that the juxtaposition of solid-state infrared and Raman frequencies does not necessarily imply coincidence as in the fluid-phase results.

In the following sections of this chapter the results for trimethylboron and trimethylaluminium are considered separately, but the remaining three compounds are considered as a group. The final section contains the results of the X-ray powder investigations for trimethylgallium and trimethylindium.

7.3. Trimethylboron

The details of the infrared spectrum of solid trimethylboron are listed in Table 7.1 (p.162). In many respects these results were the least satisfactory of those obtained for any of the compounds in the solid state. The spectrum given just after the sample had been frozen on to the window at 20°K was very similar to that given in the vapour phase, but during the annealing process a number of changes occurred. The features at 350 cm^{-1} broadened and altered in relative intensity,

Table 7.1

SOLID (20°K)		Assignment[9]	TABLE 6.1 VAPOUR
ν (cm^{-1})	int.		ν (cm^{-1})
~ 317	sh		308
323	vw	e' ν_{17}	321
351	vw	a_2'' ν_{10} ^{11}B	335
354	vw	a_2'' ν_{10} ^{10}B	351
358	vw	a_2'' ν_{10} ^{10}B	
		o/c	651
852	w	e' ν_{15}	857
958	m	^{11}B a_2'' ν_9	967
982	sh	^{10}B a_2'' ν_9	983
1144	s	^{11}B e' ν_{16}	1154
1174	m	^{10}B e' ν_{16}	1185
1277	vs	^{11}B e' ν_{14}	1299
1296	vs	^{11}B e' ν_{14}	
1310	m	^{10}B e' ν_{14}	1308
1428	w	a_2'' ν_8 & e' ν_{13}	1451
1440	w	a_2'' ν_8 & e' ν_{13}	
1490	vvw		
1555	vvw		
			1714
			1822
1924	vvw		
1984	vvw	o/c	1974
		o/c	2162
		o/c	2255
2325	vvw		
2420			2438
			2451
			2470
2923	m	e' ν_{12}	2915
2945	m	a_2'' ν_7 & e' ν_{11}	2980

Table 7.1: The Infrared Spectrum of Solid Trimethylboron

whilst those at 950 cm^{-1} similarly broadened, but also shifted to lower frequency. At 1300 cm^{-1} the original single feature split into a partially resolved multiplet. Additionally it was noted that the temperature vs. time curve for the annealing process showed a distinct temperature plateau at approximately 50°K, an observation consistent with the occurrence of an endothermic ordering process or phase change. The final spectrum showed, however, no radical differences from the vapour-phase spectrum, in either nature or degree. In particular, the vibrationally-degenerate features in the 1150 cm^{-1} region of the spectrum, associated with the antisymmetric stretching of the BC_3 unit, remained as single features and no new bands appeared in the region of the spectrum associated with the symmetric stretching of the BC_3 unit (approximately 680 cm^{-1}). Such behaviour indicates that the monomer unit is probably little perturbed in the solid state.

7.4. Trimethylaluminium

Since all the postulated structures for the trimethylaluminium dimer in the solid state[37,38,39] feature a centre of symmetry no coincidences between the infrared and Raman spectra are to be expected. This proved to be the case and, for convenience of presentation, the results of the two investigations are tabulated separately - the Raman data in Table 7.2 (p.164) and the infrared in Table 7.3 (p.165). The results of the previous investigations of the liquid-phase Raman[29,30] and vapour-phase infrared[26,28] spectra are also included in the tables, together with the assignments appropriate to the fluid phases.[30,181]

Table 7.2

PRESENT INVESTIGATION		Assignment[30,181]	PREVIOUS (29,30) INVESTIGATIONS
SOLID (-196°C)			LIQUID (20°C)
ν (cm^{-1})	int.		ν (cm^{-1})
80	bd 1	?	
148	8	a_{1g} ν_4 & b_{2g} ν_{12}	153
159	8		
188	3	b_{3g} ν_{15}	185
211	sh 2	? b_{1g} ν_7	
324	34	a_{1g} ν_3 & b_{1g} ν_6	313
334	55		
477	100	a_{1g} ν_2	453
520	6	? 334+188 = 522 or sp.	495
~575	sh vw	348+230 = 578	
590	88	a_{1g} ν_1	592
~610	sh vw	? b_{2g} ν_{11}	
		? b CH_3 rock	632
680	27	t CH_3 rock	683
720	5	t CH_3 rock	725
734	4		
1120	vw	? CH_3 sym. bend	1125
1184	sh 3	t CH_3 sym. bend	1200
1193	19		
~1205	w		
1272	1	b CH_3 sym. bend	1255
		o/c	1315
1431	7	t & b CH_3 asym. bend	1436
2357	1	2 x 1184 = 2368	
2820	13	2 x 1410 = 2820	2824
2879	8	CH_3 stretches (t & b)	2892
2887	92		
2929	110		2932
2960	9		

t = terminal b = bridging

Table 7.2: The Raman Spectrum of Solid Trimethylaluminium

Table 7.3

PRESENT INVESTIGATION		Assignment[30,181]	PREVIOUS (26,28) INVESTIGATIONS
SOLID (-196°C)			VAPOUR PHASE (20°C)
ν (cm^{-1})	int.		ν (cm^{-1})
		b_{2u} ν_{14} & b_{3u} ν_{18}	175
230	bd w	b_{1u} ν_9	
348	sh vw	? b CH_3 torsion	
378.5	s	b_{3u} ν_{17}	369
489	s	b_{2u} ν_{13}	480
559	vs	b_{3u} ν_{16}	572
563	sh s		
596	sh w		
614	bd s	b CH_3 rock	616
644	m	? b_{1u} ν_8	652
696	vs	t CH_3 rock	700
713	s		
764.5	vs	t CH_3 rock	772
820	w	477(g) + 348(u) = 825	
848	w	477(g) + 379(u) = 856	
883	w	559(u) + 324(g) = 883	
962	w	489(u) + 477(g) = 966	
1070	vw	596(u) + 477(g) = 1073 or 590(g) + 489(u) = 1079	1055
1191	vs	t CH_3 sym. bend	1208
1235	sh w	b CH_3 sym. bend	1255
1248	s		
1325	w	734(g) + 596(u) = 1330 or 713(u) + 610(g) = 1323 or 680(g) + 644(u) = 1324	
1380	sh vw	t & b CH_3 asym. bend	1445
1434	w		
1741	vw	1184(g) + 559(u) = 1743	
1778	vw	1191(u) + 590(g) = 1781	
1835	vw	1248(u) + 590(g) = 1838	
1872	vw	1191(u) + 680(g) = 1871 or 1184(g) + 696(u) = 1880	
2335	vw	1191(u) + 1120(g) = 2311	
2495	vw	1380(u) + 1120(g) = 2500	
2610	vw	1434(u) + 1184(g) = 2618	
2828	vw	1431(g) + 1380(u) = 2811	2837
2891	m	CH_3 stretches (t & b)	2899
2930	vs		2941
3060	vw	2887(g) + 175(u) = 3062	
3110	vw	2887(g) + 230(u) = 3117	
3255	vw	2930(u) + 324(g) = 3254	
3435	vw	2879(g) + 559(u) = 3438	
3495	vw	2929(g) + 559(u) = 3488	
3525	vw	2930(u) + 590(g) = 3520	

t = terminal

b = bridging

Table 7.3: The Infrared Spectrum of Solid Trimethylaluminium

The solid-state spectra obtained corresponded closely to the fluid-phase results for the most part. No sizeable new features were observed and the only features to show appreciable shifts in position relative to the corresponding bands of the fluid phases were those lying at 477 cm^{-1} in the Raman spectrum of the solid (453 cm^{-1} for the liquid) and 559 cm^{-1} in the infrared spectrum of the solid (572 cm^{-1} for the vapour). A number of the transitions predicted by force constant calculations[24,181] to underly more intense features were revealed in the solid-state spectra and these have been assigned in the tables, as far as possible, in accordance, with the calculated frequencies.

The bands observed at 520 and 1184 cm^{-1} in the solid-phase Raman spectrum are of questionable authenticity since dimethylmercury, which exhibits, as a liquid, very strong features at 515 and 1181 cm^{-1} in its Raman spectrum, could have been present in trace quantities. Thus the single fractionation process employed for purification (Section 4.3, p.104) would not have been able to separate a constant boiling mixture of trimethylaluminium and dimethylmercury. The 520 cm^{-1} feature could also, however, be ascribed to a combination mode.

The spectra of solid trimethylaluminium bore virtually no resemblance to the spectra of the other four compounds of the Group III elements either in the number of features or in their overall pattern.

7.5. Trimethylgallium, Trimethylindium and Trimethylthallium

The vibrational spectra of solid trimethylgallium, trimethylindium and trimethylthallium are presented in Tables 7.4(p's 167 and 168)

Table 7.4

SOLID				Assignment[52]	TABLE 6.4	
Raman (-196°C)		Infrared (-196°C)			Infrared (vap.)	Raman (liq.)
ν (cm^{-1})	int.	ν (cm^{-1})	int.		ν (cm^{-1})	ν (cm^{-1})
92	vw					
118	w					
169	3					
186	4			e' ν_{17}	156	163
				?sp		410
515	100					
~530	sh vw	525	m	a_1' ν_3		520
535	7					
564	16	563	vs			
573	13	573.5	s	e' ν_{16}	577	570
		~578	sh			
~645	sh vw	644	sh	e" ν_{20}		617
662	2	666	vvw	or		
~670	sh vw			o/c o/c	680	
745	bd sh	748	s	a_2'' ν_9	723	
778	1	771 (†)	sh	e' ν_{15}	771	769
		785 (†)	sh			
1033	vw			2 x 515 = 1030		
1047	w			535 + 515 = 1050 o/c	1055	1046
~1080	bd vw			564 + 515 = 1079		
1124	w			2 x 564 = 1128		
1156	4					
1161	9	1160.5	m			
1170	14					
1178	1	1173.5	m			
1183	2	1182.5	sh			
		1185.5	m	e' ν_{14}	1205	1185
		1194	sh			
1195	6	1198	m	a_1' ν_2		1198
1310	vw			748 + 563 = 1311		
				o/c	1359	
1426	w	1419	vw	a_2'' ν_8 & e' ν_{13}	1411	
1443	sh			E" ν_{19}		1433

(†) = Frequency obtained by curve fitting

Table 7.4: The Vibrational Spectra of Solid Trimethylgallium

Table 7.4
(continued)

SOLID				Assignment[52]		TABLE 6.4	
Raman (-196°C)		Infrared (-196°C)				Infrared (vap.)	Raman (liq.)
ν (cm^{-1})	int.	ν (cm^{-1})	int.			ν (cm^{-1})	ν(cm^{-1})
1690	bd vw			1170 + 515 = 1685			
		1702	vw	1186 + 515 = 1701			
		1720	vw	1186 + 535 = 1721			
					o/c	1732	
		1737	vw	1174 + 563 = 1737			
		1740	vw	1178 + 563 = 1741			
		1758	vw	1198 + 563 = 1761			
		1771	vw	1198 + 574 = 1772			
					o/c	1785	
1840	bd vw	1840	vvw	1174 + 662 = 1836			
		1930	vvw	1186 + 748 = 1934			
		1963	vvw	1186 + 778 = 1964			
2275	vw			1156 + 1124 = 2280			
		2292	vw	1170 + 1129 = 2299			
2300	vw			2 x 1156 = 2312			
2321	w	2322	vw	2 x 1161 = 2322			
2327	w			1174 + 1156 = 2330			
		2340	vw	2 x 1170 = 2340			
2346				1174 + 1170 = 2344			
2364				1186 + 1174 = 2360			
					o/c		2369
		2378	vw	2 x 1186 = 2372			
					o/c	2391	
		2850	sh	2 x 1426 = 2852			
					o/c	2860	2865
2892	11			a_1' ν_1			2903
		2895	w				
2908	sh vw			e' ν_{12}		2919	
2945	sh vw						
2956	10			e'' ν_{18}			2961
		2959	m				
2966	sh w			a_2'' ν_7 & e' ν_{11}		3001	
					o/c	3055	
		3140	vw	2956 + 186 = 3142			
					o/c	3152	
					o/c	3510	
		3550	vw	2892 + 662 = 3559			
					o/c	3571	
		3650	vw	2959 + 662 = 3621			
					o/c	3637	

Table 7.4 (continued): The Vibrational Spectra of Solid Trimethylgallium

Table 7.5

SOLID				Assignment[52]	TABLE 6.5	REF. 52
Raman (-196°C)		Infrared (-196°C)			Infrared (vap.)	Raman (liq.95°C)
ν (cm^{-1})	int.	ν (cm^{-1})	int.		ν (cm^{-1})	ν (cm^{-1})
89	w					
130	1			e' ν_{17}	118	132
170	w					
264	w			2 x 130 = 260		
450	sh					
462	100	~465	sh	a_1' ν_3		467
470	1	476	vs			
478	5					
482	4	~484	sh			
		489	vs			
493	32	~492	sh	e' ν_{16}	501	495
506	22	505	s			
		~508	sh			
		536	w	476 + (60) = 536		
		543	sh vw	484 + (60) = 544		
		549	sh vw	489 + (60) = 549		
				o/c	590	
662	bd w			e' ν_{20}		635
680	1	666	w	a_2'' ν_9	690	
727	1	727	s	e' ν_{15}	729	
744	w	771	m			
		887	vvw	666 + 130 + 89 = 885		
		912	vvw	460 + 450 = 910		
930	vw			2 x 462 = 924		
951	w			2 x 476 = 952		
978	vw			2 x 489 = 978		
		1035	sh vw	2 x 476 + 89 = 1041		
		1058	sh vw	2 x 484 + 89 = 1057		
		1084	s			
1087	23	1087	sh			
1121	19	1114	s	e' ν_{14}	(1155)	1116
1151	20	1153	m			
		1156	m	a_1' ν_2		1157
1255	bd vw	1254	vvw	771 + 489 = 1260		
1320	vw			2 x 662 = 1334		
		1392	w	a_2'' ν_8		
~1415	sh vw	1430	vw	e' ν_{13}		
1445	w	1463	vw	e'' ν_{19}		

( ) = result from Ref. 52

Table 7.5: The Vibrational Spectra of Solid Trimethylindium

Table 7.5
(continued)

SOLID				Assignment[52]	TABLE 6.5	REF.52
Raman (-196°C)		Infrared (-196°C)			Infrared (vap.)	Raman (liq.95°C)
ν (cm^{-1})	int.	ν (cm^{-1})	int.		ν (cm^{-1})	ν (cm^{-1})
1508	vw			1415 + 89 = 1504		
1554	vw			1087 + 462 = 1549		
1591	vw	1586	vw	1121 + 462 = 1583		
		1605	vw	1114 + 489 = 1603		
		1628	vw	1153 + 476 = 1629		
				o/c	1650	
1657	vw	1657	vw	1156 + 505 = 1661		
		1704	vw	1445 + 264 = 1709		
1786	vw			1121 + 666 = 1787		
1846	vw	1850	vvw	1121 + 727 = 1848		
		1865	vvw	1121 + 744 = 1865		
		2136	vw	1392 + 744 = 2136		
2145	w			1415 + 727 = 2142		
		2194	vw	1114 + 1084 = 2198		
2210	w			1121 + 1087 = 2208		
				o/c	2250	
2284	w	2281	sh w	1156 + 1121 = 2277		
		2287	w			
				o/c	2320	
2328	vw			2 x 1156 = 2312		
		2780	bd w	2 x 1392 = 2784		
				o/c	2850	2861
		2889	m			
2906	7			a_1' ν_1		2910
2916	7	2911	m	e' ν_{12}	2910	
~2965	sh vw			e'' ν_{18}		2974
		2967	s		2960	
2976	s			a_2'' ν_7 & e' ν_{11}	3002	
		3120	vw	2965 + 170 = 3135		
		3578	vw	2911 + 666 = 3577		
		3640	vw	2911 + 727 = 3638		
		3968	vw	2889 + 1084 = 3973		

Table 7.5 (continued): The Vibrational Spectra of Solid Trimethylindium

Table 7.6

SOLID				Assignment[177,183]	TABLE 6.6	
Raman (-196°C)		Infrared (-196°C)			Infrared (vap.)	Raman (liq.)
ν (cm^{-1})	int.	ν (cm^{-1})	int.		ν (cm^{-1})	ν (cm^{-1})
65	sh w					
73	l					
82	sh w					
106	l			e' ν_{17}	99	96
154	w					
444	100	444.5	vs	a_1' ν_3		445
		454	s			
457	32	~458	sh			
468	16	472	s	e' ν_{16}	462	
		~476	sh			
		488	sh vw	446 + (42) = 488		
		496	sh vw	454 + (42) = 496		
				e'' ν_{20}		656
				a_2'' ν_9	697	
689	w					
748	sh vw	746	s	e' ν_{15}	754	747
759	w					
893	w			2 x 444 = 888		
903	w			457 + 444 = 901		895
		940	vvw	2 x 472 = 944		
		1057	sh vw	2 x 472 + 106 = 1050		
		1078	sh vw	2 x 457 + 154 = 1068		
1100	23	1099	m			
1106	vw	1108	m	e' ν_{14}	1150	1115
1110	18	1110	m			
		1135	sh vw			
1138	12	1140	m	a_1' ν_2		1141
		1395	sh vw	a_2'' ν_8	1395	
		1433	vw	e' ν_{13}		1429

Table 7.6: The Vibrational Spectra of Solid Trimethylthallium

Table 7.6
(continued)

SOLID				Assignment[177,183]	TABLE 6.6	
Raman (-196°C)		Infrared (-196°C)			Infrared (vap.)	Raman (liq.)
ν (cm^{-1})	int.	ν (cm^{-1})	int.		ν (cm^{-1})	ν (cm^{-1})
∿1545	sh			1100 + 444 = 1544		
1550	w	1550	vvw	1108 + 444 = 1552		
		1557	sh	1100 + 457 = 1557		
		1585	vvw	1140 + 444 = 1584		
				o/c		1585
		1595	vvw	1140 + 454 = 1594		
				o/c	1604	
		1608	vw	1140 + 468 = 1608		
		1855	vvw	1108 + 746 = 1854		
2171	vw	2172	w	1433 + 746 = 2179		
2184	vw	2185	w	1433 + 759 = 2192		
2208	vw			1108 + 1100 = 2208		
2240	vw	2329	vw	1140 + 1100 = 2240		
2255	vw	2261	w	1140 + 1110 = 2250		
2274	vw			2 x 1138 = 2276		
				o/c	2280	
2327	vw			1433 + 2 x 446 = 2385		
		2805	bd w			
2907	2	2907	m	a_1' ν_1		2917
∿2920	sh vw	∿2915	sh	e' ν_{12}	2930	
2975	sh vw	2980	m	e'' ν_{18}		2984
2992	1	2991	m	a_2'' ν_7 & e' ν_{11}	3020	
		3590	vvw	2907 + 689 = 3596		
		3660	vvw	2980 + 689 = 3669 or 2907 + 746 = 3653		

Table 7.6 (continued): The Vibrational Spectra of Solid Trimethylthallium

7.5 (p.'s 169 and 170) and 7.6 (p.'s 171 and 172) respectively.

Although the spectra were considerably more complicated than their fluid-phase counterparts, most of the solid-state features occurred in regions of the spectrum associated with fluid-phase bands. For all three compounds two spectral regions exhibited changes of particular interest as a result of change of phase - the region at approximately 500 cm^{-1} (associated with metal-carbon stretching vibrations) and the region at approximately 1200 cm^{-1} (associated with the symmetric deformations of the methyl groups). For the fluids two features only are observed in both spectral regions, one ascribable to a mode of A_1' symmetry and the other to a mode of E' symmetry. For the solids, however, not only were three intense features observed in each case (ascribable to the A_1' and E' modes of the free molecule), but a number of new features, some of considerable intensity, were also noted. The exact significance of the data obtained in these regions is discussed in Chapter 9, but the overall similarity of the spectra for the three compounds suggests immediately that the compounds are probably isostructural in the solid state, a conclusion later confirmed by X-ray crystallography (see Section 7.6, below).

A number of strong features were observed in the region below 200 cm^{-1} in the Raman spectrum of all three solid compounds and these too are further discussed in Chapter 9. For trimethylindium and trimethylthallium a number of weak features were also observed in the infrared spectrum at approximately 500 cm^{-1}. These features can most readily be rationalised as combination features involving unobserved features at 60

and 42 cm^{-1} for trimethylindium and trimethylthallium rospectively and they have been assigned on this basis in the tables. A number of features were also observed in the corresponding region of the spectrum of solid trimethylgallium, but because of the expected occurrence of features ascribable to other modes in this region it did not prove possible to assign the features on the above basis.

In the case of the infrared spectrum of solid trimethylindium it proved possible to observe a number of features too weak to be distinguished in the vapour-phase spectrum and to assign these by analogy with the results for trimethylgallium and trimethylthallium.

7.6. X-ray Diffraction Results for Trimethylgallium and Trimethylindium

The X-ray diffraction data for a single crystal of trimethylindium[63] have shown that the crystals are tetragonal and belong to the $P4_2/n$ space group with 8 molecules per unit cell. Tetrameric units can be distinguished, each indium atom being roughly penta-coordinated by carbon atoms. The solid-state vibrational spectra of trimethylgallium and trimethylthallium were found to be very similar in basic pattern to that given by trimethylindium and a recent X-ray diffraction study of a single crystal of trimethylthallium,[67] undertaken in cognisance of the preliminary Raman results for the solid, confirmed that trimethylthallium and trimethylindium are formally isostructural. It was decided, therefore, to examine the X-ray diffraction pattern of trimethylgallium in order to test whether this compound is isostructural with the other two.

Three distinct microcrystalline samples of trimethylgallium were

were examined at 200°K and it proved possible to index 13 strong reflections on the zero layer. These were found to correspond with the strong reflections reported for trimethylindium and trimethylthallium. A microcrystalline sample of trimethylindium was also examined, both at room temperature and at 200°K. Apart from a slight sharpening of the diffraction rings, no detectable change occurred on cooling the sample and the overall pattern of intensities was exactly similar to that given by the trimethylgallium samples. The cell dimensions determined for trimethylgallium are listed in Table 7.7 (p.176) together with the literature values of the cell dimensions for trimethylindium[63] and trimethylthallium.[67]

As a result of these investigations it was concluded that trimethylgallium is isostructural with trimethylindium and trimethylthallium and the vibrational spectra of the solids are discussed in the light of this conclusion in Chapter 9. Single-crystal data for trimethylgallium would be required to elucidate any further details of the structure, such as interatomic distances.

Compound	a = b (Å)		c (Å)		Reference
	Value	Error	Value	Error	
$GaMe_3$	13.00_5	±0.02	6.3	±0.1	this investigation
$InMe_3$	13.24	±0.01	6.44	±0.01	63
$TlMe_3$	13.464	±0.010	6.379	±0.009	67

Table 7.7: Unit Cell Dimensions for Trimethylgallium Trimethylindium and Trimethylthallium

Chapter 8

The Matrix-Isolation Spectra

8.1. Introductory

None of the Group III trimethyl compounds has previously been examined using the matrix-isolation technique and it was decided to examine trimethylboron, trimethylaluminium and trimethylgallium in this way in order to explore the value of the technique in relation not only to the present project but also to the investigation of organometallic systems in general. The general problems encountered in the experiments have been discussed in Section 5.5 and the results reported in this chapter differ from those described in Chapters 6 and 7 in that some of the experiments (particularly those involving diffusion processes) yielded results which were not entirely complete or conclusive.

Since the experimental techniques employed and the results obtained varied considerably among the three compounds, the experiments carried out on each compound are described separately in the following three sections. In accordance with the chronological order of the investigations the results for trimethylgallium are considered first, followed by those for trimethylaluminium and finally those for trimethylboron. Each section commences with a brief statement of the objectives of the experiments.

Spectroscopically pure nitrogen (British Oxygen Company 'X' grade) was used as a matrix material throughout the experiments described here and it was found that, for all three compounds, relatively concentrated

matrices were required to produce a sufficient degree of sample absorption without too low a level of transmittance for the matrix. Matrices ranging in concentration from 1 in 25 to 1 in 250 (molar proportions) were employed.

Wherever possible, fruitful experiments were repeated until consistent results had been obtained. On this basis a number of features of dubious authenticity have been omitted from the tables presented in this chapter.

8.2. Trimethylgallium

The first series of matrix-isolation experiments was made on trimethylgallium, with two prime objectives:

(1) To test the validity of the matrix-isolation technique in the examination of the Group III trimethyl compounds, the vapour-phase infrared spectrum of trimethylgallium being particularly well documented.[51,52,53]

(2) To examine the oligomerization properties of the Me_3Ga monomer at the temperature of the matrix.

All the trimethylgallium gaseous mixtures were prepared on the standard vacuum line and were sprayed on to the cold window via the matrix-gas spray arm. Diffusion experiments were carried out at temperatures up to 40°K, at which temperature the nitrogen matrix became volatile and started to evaporate from the cold window.

The results obtained are listed in Table 8.1 (p. 179) and

Table 8.1

MATRIX ISOLATION INVESTIGATION				MONOMER ASSIGNMENT[52]	TABLE 6.4
MONOMER		DIFFUSION SPECIES A	DIFFUSION SPECIES B		Vapour
ν (cm^{-1})	int.	ν (cm^{-1})	ν (cm^{-1})		ν (cm^{-1})
		520	521		
572.5	vs	575	574	e' ν_{16}	577
651	vw			? sp	
				o/c	680
729	s	739	743	a_2'' ν_9	723
761	s	761 (?)	762	e' ν_{15}	771
		783	785		
		1178	1174	? sp	1055
1201	s	1205	1199	e' ν_{14}	1201
				o/c	1359
1395	vw			a_2'' ν_8 & e' ν_{13}	
1445	vw				
1722	vw			1201 + (520) = 1721 (E')	1732
1771	vw			1201 + 573 = 1773 ($A_1' + A_2' + E'$)	1785
				o/c	2391
				o/c	2860
2914	w			e' ν_{12}	2919
2960	m	2960	2959	a_2'' ν_7 & e' ν_{11}	3001
2974	m				

Table 8.1: The Infrared Spectrum of Matrix-Isolated Trimethylgallium

illustrated, for the 1500-450 cm^{-1} region of the spectrum, in Figures 8.1 and 8.2 (p.'s 181 and 182 respectively). In figure 8.1 the spectra of gaseous and matrix-isolated trimethylgallium are compared. The extremely sharp features of the matrix-isolated spectrum are typical of the absorptions obtained by this technique. Figure 8.2 compares the infrared spectrum of the same matrix before and after diffusion at 35°K. The nature and extent of the changes is typical of a successful diffusion experiment. The most noteworthy changes are to be seen in the features at 1178 and 520 cm^{-1}, which both grow very appreciably in intensity on diffusion, and in those at 729 and 1201 cm^{-1}, which both fall in intensity, though to a less marked extent. The feature at 1301 cm^{-1} in both traces, attributable to a very intense absorption of methane, presumably arises from the reaction of trimethylgallium with surface moisture in a remote part of the apparatus. The intensity of this feature before and after diffusion is the same: if it were to grow appreciably in intensity on diffusion, this would invalidate the results of the diffusion experiment. (Both Figure 8.1 and 8.2 were obtained photographically from instrument tracings and have not been re-drawn).

The frequencies attributable to the matrix-isolated monomer are listed in the extreme left-hand column of Table 8.1, and the vapour-phase results (Table 6.4, p. 150) and assignments[52] are included on the right of the table. Agreement between the two sets of frequencies is very good, differences being less than 5 cm^{-1} for most features.

On diffusion at 35°K a distinct new set of sharp bands appeared, together with definite shoulders on some of the original monomer features.

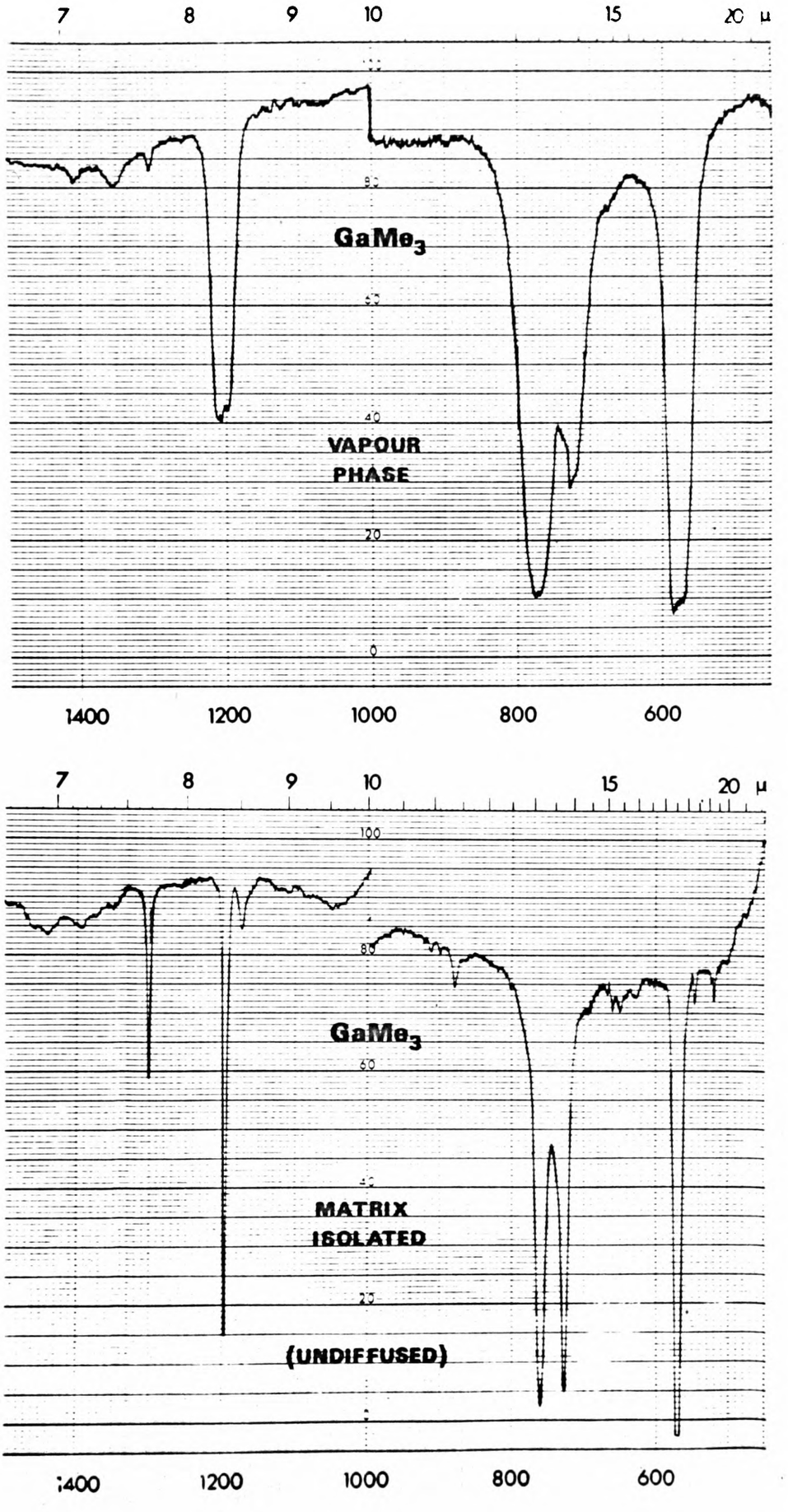

Figure 8.1: The Infrared Spectra of Vapour-Phase and Matrix-Isolated Trimethylgallium

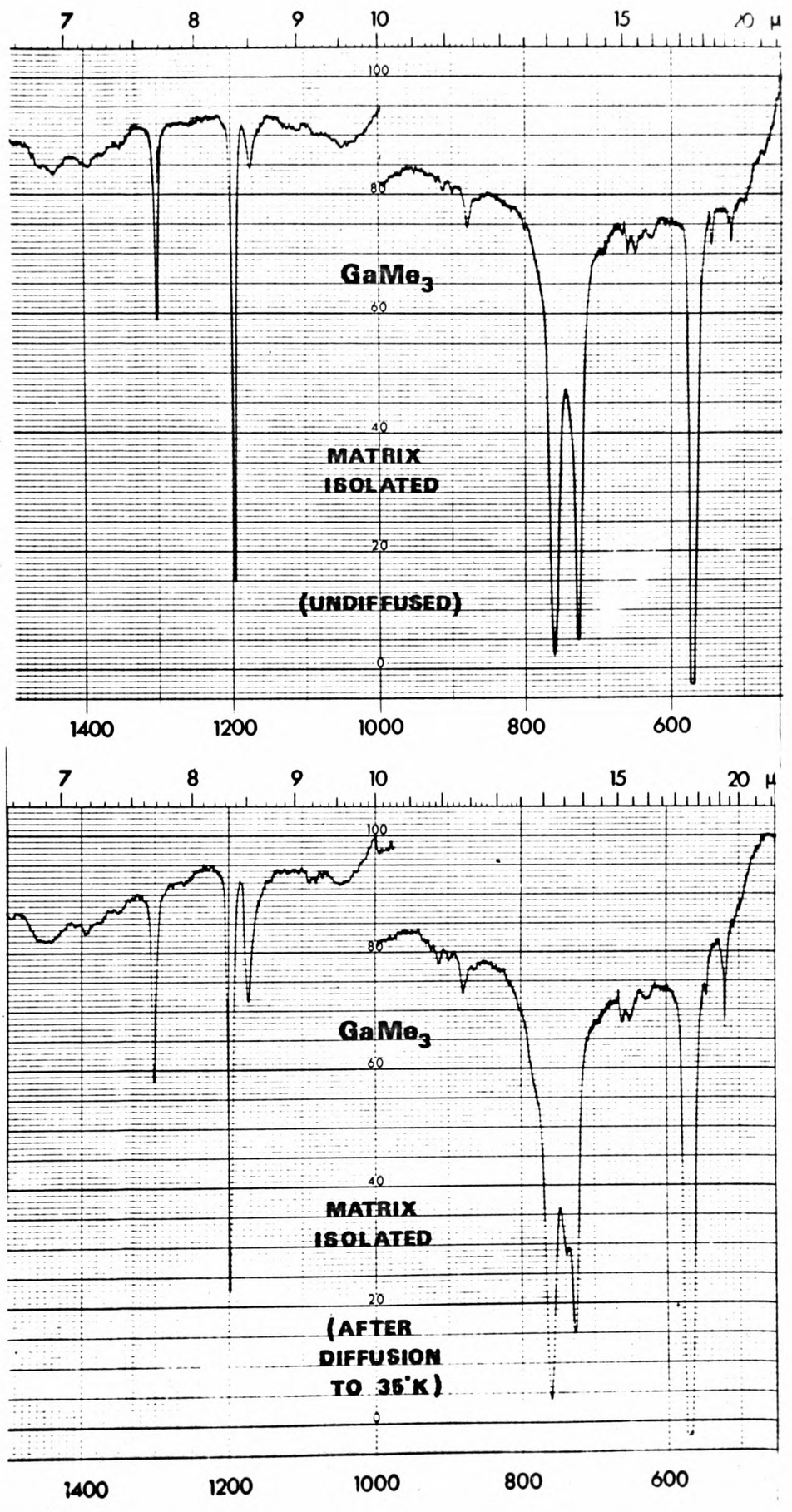

Figure 8.2: The Infrared Spectrum of Matrix-Isolated Trimethylgallium Before and After Diffusion

At the same time the monomer features showed slight decreases in intensity. The new features are listed in the column headed 'Diffusion Species A' in Table 8.1. The two most interesting of these new features are those occurring at 520 and 1178 cm^{-1} since their positions almost coincide with those of the lines observed at 523 and 1186 cm^{-1} in the Raman spectrum of the liquid and ascribed to totally symmetric vibrations of the monomer unit. The significance of these results is discussed in Chapter 9. Warming the matrix to higher temperatures caused several of the most intense features to broaden appreciably, yielding ultimately a spectrum characteristic of the monomer with underlying broad features in all the spectral regions populated by bands characteristic of the pure solid. The frequencies of this second set of new features are tabulated in the column of Table 8.1 headed 'Diffusion Species B'. It is noteworthy that, even when very thick layers of concentrated matrix were allowed to diffuse over prolonged periods of time, no new features were observed in the region of the spectrum between 500 and 200 cm^{-1}.

Attempts were also made to measure the Raman spectrum of matrix-isolated trimethylgallium, but only the scattering at 520 and 570 cm^{-1} could reliably be distinguished. On diffusion the band at 570 cm^{-1} broadened, ultimately yielding two features, whilst that at 520 cm^{-1} showed no detectable change.

8.3. Trimethylaluminium

The spectra of matrix-isolated trimethylaluminium were investigated with the following aims:

(1) To simplify the rather complex vapour-phase spectrum of the dimer in order to clarify the vibrational assignment, and to produce a layer of absorbing species sufficiently thick for the detection of any hitherto unobserved weak features.

(2) To obtain for the first time the infrared spectrum of the monomer.

(3) To examine the oligomerization properties of the monomer and dimer at matrix temperatures.

In the infrared investigation matrices were prepared both from premixed gaseous samples and by mixing trimethylaluminium vapour issuing from a furnace with matrix gas just prior to condensation. The spectrum obtained using matrices prepared by the first method corresponded closely with that reported for the dimer in the vapour phase, whilst the spectrum obtained from matrices prepared by the second method was completely different, being much simpler in the region below 1000 cm^{-1}. The latter spectrum also corresponded in overall pattern to those given by the monomeric trimethyls in the vapour phase and was therefore attributed to the monomer of trimethylaluminium. With the furnace set at approximately 200°C it was possible to obtain virtually pure monomer, but even with the furnace at room temperature, it was found that the matrices so produced still contained appreciable quantities of monomer, presumably because of the low partial pressure of trimethylaluminium vapour used in these experiments, coupled with the pressure-dependence of the monomer/dimer equilibrium.[19,20] It was found that a suitable pressure of

trimethylaluminium could be produced by surrounding the sample reservoir with a Dewar vessel containing an ice-salt bath at -10°C.

Diffusion experiments were carried out at temperatures up to 34°K both with matrices containing the dimer and with matrices containing the monomer. In the former case no change was detectable, but in the latter case not only did absorptions attributable to the dimer appear or grow but a distinct, new set of absorptions also appeared. This new set of features usually showed a greater degree of growth on diffusion than did those of the dimer, although it was difficult to assess the exact nature and degree of all the changes taking place. It did not, unfortunately, prove possible to investigate the system completely and the results reported below for this new species are neither complete nor entirely authenticated.

The data obtained in the investigation of trimethylaluminium are presented in Table 8.2 (p. 186); Figure 8.3 (p. 187) compares the spectra of the monomer and dimer in the region of the spectrum 1300 - 200 cm^{-1}. In Table 8.3 the results for the matrix-isolated dimer are listed on the right of the table, together with the vapour-phase frequencies[26,28] and assignments.[30,181] The monomer results are reported on the left of the table, together with tentative assignments, while the column headed 'Diffusion Species' contains the data obtained for the new species described above.

Agreement between the vapour-phase and matrix-isolation results is reasonably good and the resolution of the vapour-phase absorption at 700 cm^{-1} into four new features is entirely in accordance with the results

Table 8.2

MONOMER ASSIGNMENT (D_{3h})	MATRIX ISOLATION INVESTIGATION: MONOMER $\nu(cm^{-1})$	MONOMER int.	DIFFUSION SPECIES $\nu(cm^{-1})$	DIFFUSION SPECIES int.	DIMER $\nu(cm^{-1})$	DIMER int.	DIMER ASSIGNMENT (D_{2h})[30,181]	PREVIOUS INVESTIGATION DIMER 26,28 (VAPOUR) $\nu(cm^{-1})$
							$b_{2u}\ \nu_{14}$ & $b_{3u}\ \nu_{18}$	175
					371	m	$b_{3u}\ \nu_{17}$	369
					489	m	$b_{2u}\ \nu_{13}$	480
			531	s				
					564	vs	$b_{3u}\ \nu_{16}$	572
			597	vs				
					612	s	? b CH_3 rock	616
? $a_2''\ \nu_9$	638	w						
					646	s	$b_{1u}\ \nu_8$	652
			656	m				
					686	s		
$e'\ \nu_{16}$	694	s			698	vs	t CH_3 rock	700
			703	vs	703	sh		
					724	w		
$e'\ \nu_{15}$	735	vs						
					770	s	b CH_3 rock	772
							? sp	1055
$e'\ \nu_{14}$	1195	s	1192	sh	1197	s	t CH_3 sym.bend	1208
					1254	m	b CH_3 sym.bend	1255
$a_2''\ \nu_8$ & $e'\ \nu_{13}$	1432	vw			1440	vw	t & b CH_3 asym. bend	1445
1195+520 = 1715(E')	1719	vw						
(~1170+638 = 1808(E')	1811	vw						
2 x ~1410 = ~2820 (many)	2820	vw			2821	vw	CH_3 stretching vibrations (t & b)	2837
$e'\ \nu_{12}$	2901	w			2901	w		2899
$a_2''\ \nu_7$ & $e'\ \nu_{11}$	2940	m	2935	sh	2943	m		2943
	2950	m						

t = terminal b = bridging

Table 8.2: The Infrared Spectrum of Matrix-Isolated Trimethylaluminium

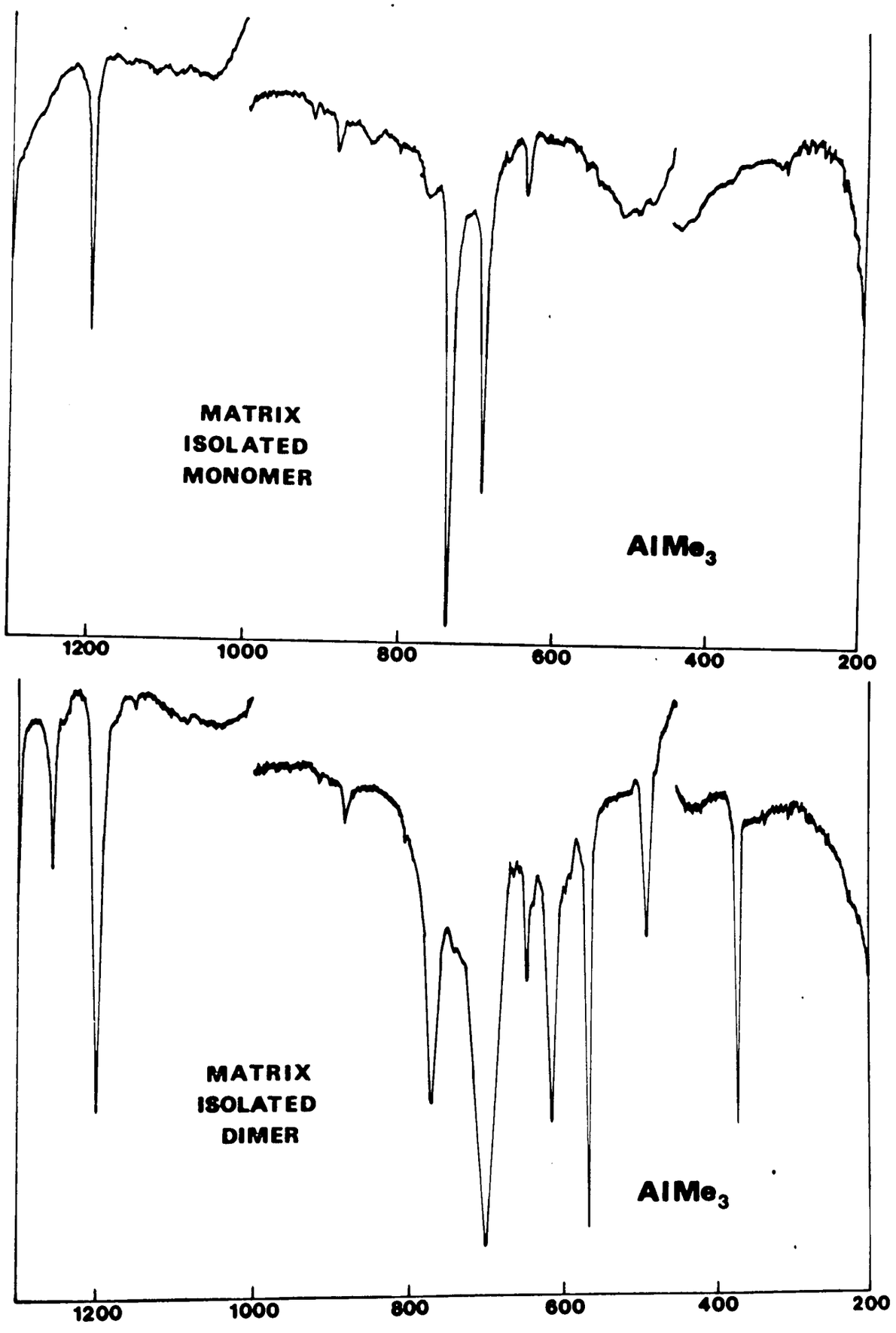

Figure 8.3: The Matrix-Isolation Infrared Spectra of Trimethylaluminium Monomer and Dimer

of force constant calculations.[181] The observation of two, rather than three, distinct strong features in the spectrum of the monomer at frequencies below 1000 cm^{-1} is discussed in Chapter 9.

The Raman spectrum of trimethylaluminium matrix-isolated in nitrogen was also partially investigated. All the samples were prepared by mixing the matrix gas and the trimethylaluminium vapour just prior to freezing; by the use of a heated inlet system it proved possible to prepare matrices containing different proportions of dimeric and monomeric molecules. Only the strongest features in the 200-800 cm^{-1} region of the spectrum could be observed with the results listed in Table 8.3 (p. 189), together with the liquid-phase frequencies[30] and assignments.[30,181] The agreement between the matrix-isolation and liquid-phase results is reasonably good for the dimer features. The scattering at 520 cm^{-1}, which was of variable intensity relative to the dimer features, decreased in intensity on diffusion. This feature can therefore be ascribed to the symmetric stretching mode of the AlC_3 unit of the monomer Me_3Al.

8.4. Trimethylboron

Trimethylboron was studied last of the three trimethyl compounds, the investigation having the following objectives:

(1) To eliminate the rotational fine structure present in the vapour-phase spectrum, thereby revealing more clearly the underlying vibrational features.

(2) To reveal the splittings of the features caused by the natural

MATRIX ISOLATION INVESTIGATION		Assignment[30,181]	PREVIOUS INVESTIGATION	
MONOMER/DIMER			DIMER (liq.)[30]	
ν (cm^{-1})	int.		ν (cm^{-1})	int.
321	m	a_{1g} ν_3	313	39
465	vs	a_{1g} ν_2	453	53
		?	495	14
520	m	A_1' ν_3 MONOMER & laser		
591	vs	a_{1g} ν_1	592	56
		b CH_3 rock	632	2
681	s	t CH_3 rock	683	19
730	w	b CH_3 rock	725	3

Table 8.3: The Raman Spectrum of Matrix-Isolated Trimethylaluminium in the range 200-800 cm^{-1}

existence of the two boron isotopes, $^{10}B(18.8\%)$ and $^{11}B(81.2\%)$. In this way it was hoped to clarify the vibrational assignment for trimethylboron monomer[9] and to shed some light on the problem of 'mixing' between vibrational energy levels of the same symmetry in the series of trimethyl compounds.

(3) To yield information regarding the nature of new features found in the spectra of matrix-isolated trimethylgallium and trimethylaluminium.

When the investigation of matrix-trapped trimethylboron was undertaken, it was already clear that, as predicted theoretically, this compound showed no tendency to associate. It was therefore hoped that the production or non-production of new features on diffusion of trimethylboron matrices would show whether the new features found on diffusion of the trimethylaluminium and trimethylgallium matrices were caused by aggregation effects rather than by the formation of genuine oligomers.

Gaseous mixtures containing trimethylboron, prepared using the standard vacuum line, were sprayed on to the cold window exclusively from the matrix-gas spray arm. Diffusion experiments were carried out at temperatures up to 40°K in the usual way.

The results of the experiments are presented in Table 8.4 (p. 191) together with the frequencies[7] and assignments[9] from previous vapour-phase investigations. The results are in complete agreement. The isotopic components of certain bands were clearly visible as two distinct peaks in the spectrum of the matrix-trapped molecule. The region of the

Table 8.4

MATRIX ISOLATION INVESTIGATION (20°K)		Assignment[9]	TABLE 6.1 Vapour
ν (cm^{-1})	int.		ν (cm^{-1})
			308
320	vw	e' ν_{17}	321
339	vvw	^{11}B } a''$_2$ ν_{10}	335
350	vvw	^{10}B }	351
638	vw	2 x 320 = 640 (A_1' + E')	651
857	w	e' ν_{15}	857
962	m	^{11}B } a''$_2$ ν_9	967
980	w	^{10}B }	983
1148	vs	^{11}B } e' ν_{16}	1154
1177	m	^{10}B }	1185
1298	vs	^{11}B } e' ν_{14}	1299
1304	m	^{10}B }	1308
1437	w	a''$_2$ ν_8 & e' ν_{13}	1451
1495	vvw	1177 + 320 = 1497 (A_1' + E')	
1555	vvw	857 + ∿680 = ∿1537 (E')	
		o/c	1714
		o/c	1822
1925	vvw	1298 + 2 x 320 = 1938 (A_1' + A_2' + E')	
1993	vvw	1298 + ∿680 = ∿1978 (E')	1974
		o/c	2162
		o/c	2255
2435	vw	1298 + 1148 = 2446 (A_1' + A_2' + E')	2448
		o/c	2451
		o/c	2470
2873	vw	2 x 1437 = 2874 (A_1' + E')	
2930	m	e' ν_{12}	2915
2963	m	a''$_2$ ν_7 & e' ν_{11}	2980

Table 8.4: The Infrared Spectrum of Matrix-Isolated Trimethylboron

matrix-spectrum between 380 and 260 cm^{-1} is compared with its vapour-phase counterpart in Figure 8.4 (p. 193). The simple, broad envelope of the vapour-phase spectrum in this region could well be interpreted as a simple rotational envelope possessing P-, Q- and R- branches, but the matrix spectrum exhibits three clearly resolved peaks, confirming the correctness of the original vibrational assignment.

No new features were observed on diffusion, even at 40°K, but some of the original peaks broadened slightly and showed small frequency shifts. In the 350 cm^{-1} region of the spectrum, the relative intensities of the absorptions altered appreciably and the final spectrum appeared to be a blend of that appropriate to the matrix-isolated monomer and that appropriate to the solid state (see p. 162).

The Raman spectrum of matrix-isolated trimethylboron was not investigated.

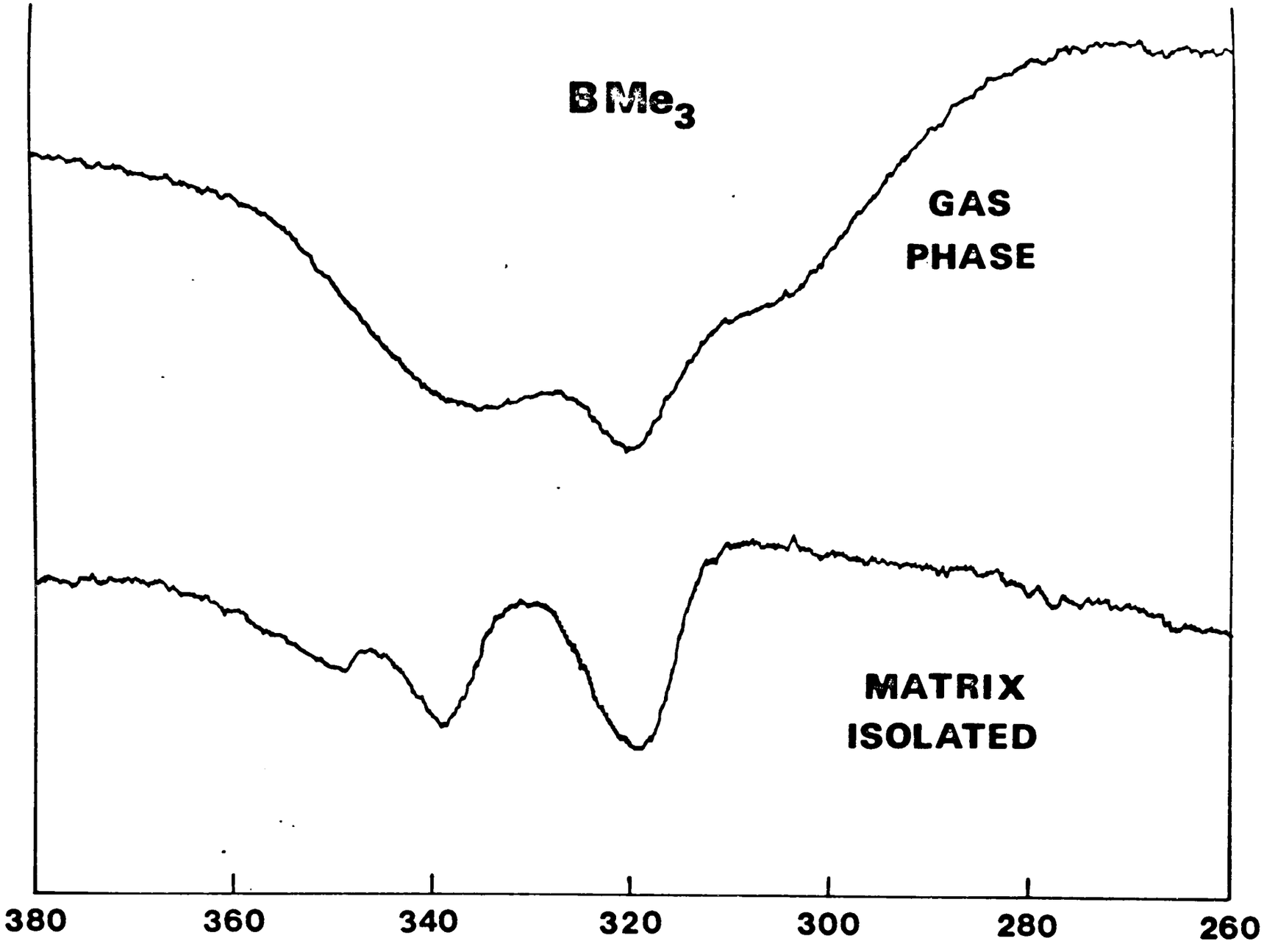

Figure 8.4: The Infrared Spectra of Vapour-Phase and Matrix-Isolated Trimethylboron in the 260 - 380 cm^{-1} Region

SECTION IV

TEARS

Chapter 9

Discussion

In the previous section of this thesis the spectra of the individual Group III trimethyl compounds have been described for a variety of conditions and it is the purpose of this final chapter to show the manner in which these results can be correlated and to extract whatever chemical information they contain.

In order to compare the results and to indicate the basis of the assignments the elements are considered together, the chapter being rationalised in accordance with the state of aggregation of the molecules. Thus sections 9.1 and 9.2 consider the monomeric and dimeric species, respectively, whilst the new species produced in the matrices and the larger aggregates of the solid state are discussed in sections 9.3 and 9.4. The last section of the chapter enumerates the conclusions reached regarding the oligomerization properties of each of the compounds and the reasons for these conclusions.

9.1. Monomeric Species

(a) The Table

The fundamental frequencies for the five monomers are assigned in Table 9.1 (p. 195). In accordance with the conclusions of entropy calculations[9] and electron diffraction studies,[11] the results have been interpreted in terms of a model of D_{3h} symmetry in which the MC_3 skeleton is planar and the methyl groups are freely rotating: if these

Table 9.1

XY_3 planar mode	Mode		Description	Activity	$^{10}BMe_3$	$^{11}BMe_3$	$AlMe_3$	$GaMe_3$	$InMe_3$	$TlMe_3$
		ν_1	C-H sym. stretch		2888	2888		2905	2912	2917
	A_1'	ν_2	CH_3 sym. deformation	R	1287	1287		1198	1157	1141
ν_1		ν_3	M-C sym. stretch		679	679	527	520	467	445
		ν_4	C-H asym. stretch							
	A_2'	ν_5	CH_3 asym. deformation	IA						
		ν_6	CH_3 rock							
		ν_7	C-H asym. stretch		2980	2980	2940	3001	3002	3020
		ν_8	CH_3 asym. deformation		1451	1451	1432	1411	1392	1395
	A_2''	ν_9	CH_3 rock	IR	983	967	638	723	690	697
ν_2		ν_{10}	MC_3 deformation (out-of-plane)		351	335				
		ν_{11}	C-H asym. stretch		2980	2980	2950	3001	3002	3020
		ν_{12}	C-H sym. stretch		2915	2915	2901	2919	2910	2930
		ν_{13}	CH_3 asym. deformation		1451	1451	1432	1411	1392	1395
	E'	ν_{14}	CH_3 sym. deformation	B	1308	1299	1195	1205	(1155)	1150
		ν_{15}	CH_3 rock		857	857	735	771	729	754
ν_3		ν_{16}	M-C asym. stretch		1185	1155	694	577	501	462
ν_4		ν_{17}	MC_3 deformation (in plane)		321	321		156	118	99
		ν_{18}	C-H asym. stretch		2972	2972		2960	2960	2984
	E''	ν_{19}	CH_3 asym. deformation	R	1422	1422		1433	1445	1429
		ν_{20}	CH_3 rock		495	495		612	635	656

Table 9.1: Vibrational Assignments for the Group III Trimethyls

groups are taken to be in fixed positions the highest symmetry attainable is C_{3h}. The number, symmetry and spectroscopic activity of the normal modes of vibration for the D_{3h} model are tabulated to the left of Table 9.1 and, in the column on the extreme left of the table are indicated the corresponding modes of the simple XY_3 planar unit, as discussed in Chapter 2. It is not possible to illustrate all the normal modes of the D_{3h} model for $M(CH_3)_3$, but approximate descriptions are included in the table and the four normal modes of the MC_3 planar skeleton are depicted in Figure 2.2 (p. 55).

The frequencies listed in Table 9.1 are, in most cases, those obtained in the fluid-phase investigations. The results for the infrared-active modes of trimethylaluminium refer, however, to the matrix-isolated molecule and some of the frequencies reported for the weaker features of trimethylindium are from the solid-phase spectra. In particular, the frequency of the CH_3 symmetric deformation of E' symmetry, ν_{14}, which could not be reliably characterized in the vapour-phase spectrum, has been obtained by analogy with the relationship between the solid-phase and vapour-phase spectra for trimethylgallium and trimethylthallium. In the case of the gallium compound, the feature ascribable to this mode, which is active with respect both to infrared absorption and Raman scattering, showed an appreciable frequency shift between the vapour and liquid phases (1205 to 1185 cm^{-1}). The CH_3 deformation modes would be expected to show a high sensitivity to intermolecular interactions involving the methyl groups and this frequency shift probably indicates some degree of interaction in the liquid phase.

For trimethylindium and trimethylthallium the E' mode ν_{17} has not been observed with certainty in the liquid phase, but the spectral indications are that a similar frequency shift occurs in the corresponding modes of these compounds as well.

For all the compounds the intensities of the features ascribable to the fundamental vibrations vary by as much as two orders of magnitude and, in consequence, the reliability of the data included in Table 9.1 depends very much upon the mode in question. For example, the frequencies of the weak, broad features in the 1400 cm^{-1} region of the spectrum may be as much as 20 cm^{-1} in error.

Whilst most of the assignments in the table are reasonably certain, those made for the CH_3 rocking mode, ν_{20}, of E' symmetry, are speculative. A feature of reasonable intensity was observed in the Raman spectra of all four stable monomers in the positions indicated and, although this feature could be explained in terms of combinations and overtones of the low-frequency modes, a more plausible explanation seems to be that invoked here.

The mode involving MC_3 out-of-plane deformation (A_2'', ν_{10}) requires special mention in that it was not possible to find a feature ascribable to this infrared-active vibration for any of the compounds except trimethylboron, even at very low frequencies. The nature of this mode makes it almost impossible to forecast the effect on the frequency of changing the central atom, and the literature contains no data on which to base meaningful comparisons. It seems probable, however, that this mode moves appreciably to lower frequency with increasing mass of the

central atom, and, because of experimental difficulties in observing infrared spectra below 200 cm^{-1}, it would need to be only an order of magnitude less intense than its in-plane counterpart (ν_{17}, E') to remain completely undetected.

The results for monomeric trimethylaluminium are, of course, incomplete and, in consequence, difficult to assign with any degree of certainty. In the 500-800 cm^{-1} region of the infrared spectrum, instead of the three distinct features expected by analogy with the spectra of the other monomers, only two strong features were observed (at 735 and 694 cm^{-1}) plus a third of rather lower intensity (at 638 cm^{-1}). In the Raman spectrum only one feature was observed above 600 cm^{-1}, at 685 cm^{-1}, and the most satisfactory explanation of these results seems to be to assign the two strong infrared features to E' modes. The A_2'' mode, which is active only in infrared absorption, must then be assigned the low value of 638 cm^{-1}, but it is also possible that the feature arising from this mode underlies one of the stronger infrared features and that the 638 cm^{-1} feature is an artifact. The frequencies of methyl rocking modes (of which the A_2'' mode, ν_9, is an example) seem to depend markedly on the electronegativity of the central atom; this matter is discussed more fully in section (b) below.

The assignment of the CH_3 rocking mode of E' symmetry (ν_{15}) to the feature occurring at 735 cm^{-1} and the AlC_3 antisymmetric stretching mode (ν_{16}) to the feature occurring at 694 cm^{-1} is a little unrealistic in that both of these features probably arise from vibrational modes involving comparable amounts of CH_3 rocking and Al-C stretching motions.

When two modes belonging to the same symmetry class lie close together Fermi resonance[113a] leads to a perturbation of the original energy levels and the resulting vibrational modes have some of the characteristics of both the original modes. The spectral features resulting from these new modes occur at higher and lower frequencies, respectively, than the features expected for the unperturbed modes and, in consequence, the frequencies for 'pure' Al-C antisymmetric stretching and 'pure' CH_3 rocking (of E' symmetry) probably lie closer to each other than the features at 694 and 735 cm^{-1} would suggest.

In a similar way, the bands occurring at 1185 and 1308 cm^{-1} in the spectrum of ^{10}B-trimethylboron and at 1155 and 1299 cm^{-1} in the spectrum of ^{11}B-trimethylboron are probably best ascribed to vibrational modes involving mixtures of B-C stretching and CH_3 deformation motions (ν_{14} and ν_{16} respectively). Support for this conclusion comes from product rule calculations on the frequencies of $^{10}B(CH_3)_3$ and $^{11}B(CH_3)_3$ and from simple force constant calculations (see below), both of which yield irrational results if the complication of mixing is disregarded.

(b) Correlations

For the region 0-1500 cm^{-1}, the spectra of the five monomeric Group III trimethyl compounds are compared in the form of line diagrams in Figure 9.1 (p. 200). For each compound the infrared spectrum is presented in the upper half of the diagram and the Raman spectrum in the lower half; the approximate relative intensities of the features are indicated while the change in position with change of central atom is denoted by dotted lines.

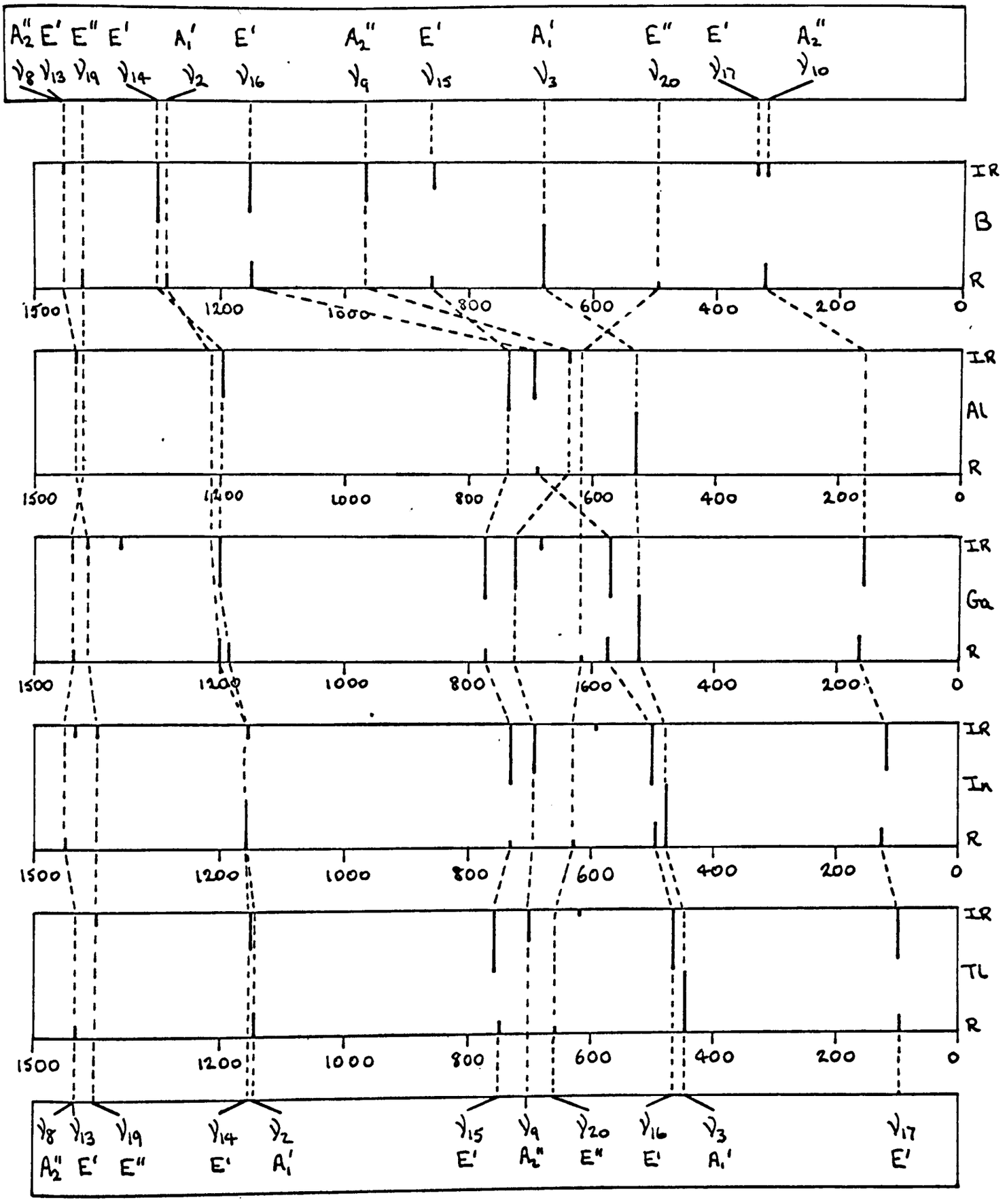

Figure 9.1: Correlation Diagram for the Monomeric Group III Trimethyl Compounds

Most of the vibrational frequencies behave consistently with increasing mass of the central atom. Thus the three observable modes of the MC_3 skeleton (ν_3, ν_{16} and ν_{17}) yield features of decreasing frequency with increasing mass of the Group III element, whilst the modes at approximately 1400 cm^{-1} remain little affected. By contrast the frequencies of the intense bands due to CH_3 rocking modes (A_2'', ν_9 and E', ν_{15}) and to the CH_3 symmetric deformation modes (A_1', ν_2 and E', ν_{14}) do not decrease regularly down the series, both the aluminium and, to a lesser extent, the indium compounds exhibiting frequencies lower than would be expected on the basis of the results for the boron, gallium and thallium compounds. For the symmetric deformation of CH_3 groups in a variety of methyl compounds several investigators[184, 196, 197] have noted a correlation between the frequency and electronegativity of the substituent. The results for compounds comprising only methyl groups and metal atoms have not, however, been compared. Accordingly attention is now directed to such a comparison with the objective of shedding some light on the anomalous frequencies in the present series. of compounds.

The frequencies of the CH_3 symmetric deformation and rocking modes for the methyl compounds of most Main Group elements are tabulated in Table 9.2 (p. 202). Although the molecules belong to a variety of point groups, it is possible to distinguish either one (in the case of Groups I and VII) or two (in the case of Groups II-VI) CH_3 symmetric deformation modes for each species. The situation for the CH_3 rocking modes for Groups II-VI is less straightforward, up to four distinct features being

Table 9.2

GROUP I (C_{3v})			
Element	EN	CH_3 Def. ν_2 (A_1)	CH_3 Rock ν_6 (E)
$Li^{(184)}$	0.98	1158	408
$Na^{(185)}$	0.93	1090	298

GROUP VII (C_{3v})			
Element	EN	CH_3 Def. ν_2 (A_1)	CH_3 Rock ν_6 (E)
$F^{(113b)}$	3.98	1475	1182
$Cl^{(113b)}$	3.16	1355	1015
$Br^{(113b)}$	2.96	1305	954
$I^{(113b)}$	2.66	1252	881

GROUP II (D'_{3h})					
Element	EN	CH_3 Sym. Def.		CH_3 Rock	
		ν_2 (A_{1g})	ν_6 (A_{2u})	ν_{10} (Eg)	ν_{13} (E_u)
$Be^{(186)}$	1.57	-	1222	-	727
$Zn^{(187)}$	1.65	1158	1185	620	707
$Cd^{(188)}$	1.69	1129	1140	642	705
$Hg^{(189)}$	2.00	1182	1205	700	788

GROUP VI (C_{2v})					
Element	EN	CH_3 Sym. Def.		CH_3 Rock	
		ν_4 (A_1)	ν_{15} (B_1)	ν_5 (A_1)	ν_{16} (B_1)
$O^{(194)}$	3.44	1462	1454	1238	1095
$S^{(195)}$	2.58	1331	1308	1027	906
$Se^{(195)}$	2.55	1284	1263	954	857
$Te^{(195)}$	(2.20)	1228	1208	875	790

GROUP III (D_{3h})					
Element	EN	CH_3 Sym. Def.		CH_3 Rock	
		ν_2(A_1')	ν_{14}(E')	ν_9(A_2'')	ν_{15}(E')
^{11}B	2.04	1287	1299	967	857
Al	1.61	-	1195	638	735
Ga	1.81	1198	1205	723	771
In	1.78	1157	(1155)	690	729
Tl	2.04	1141	1150	697	754

GROUP V (C_{3v})					
Element	EN	CH_3 Sym. Def.		CH_3 Rock	
		ν_4 (A_1)	ν_{17} (E)	ν_5 (A_1)	ν_{19}(E)
$N^{(193)}$	3.04	1404	1404	1184	1104
$P^{(193)}$	2.19	1312	1293	973	948
$As^{(193)}$	2.18	1263	1242	884	884
$Sb^{(193)}$	2.05	1213	1194	813	813
$Bi^{(193)}$	2.02	1165	1147	784	784

GROUP IV (Td)					
Element	EN	CH_3 Sym. Def.		CH_3 Rock	
		ν_2(A_1)	ν_{16}(F_2)	ν_7 (E)	ν_{17}(F_2)
$C^{(190)}$	2.55	1430	1370	-	1257
$Si^{(191)}$	1.90	1253	1257	-	869
$Ge^{(192)}$	2.01	1247	1237	825	828
$Sn^{(192)}$	1.96	1205	1196	772	770
$Pb^{(192)}$	2.33	1170	1151	700	768

(All electronegativity values are based on Pauling's Relationship[79a])

Table 9.2: Frequency Comparisons for the CH_3 Symmetric Deformation and Rocking Modes of the Main Group Methyl Compounds

theoretically possible. In the reported spectra, however, two strong features ascribable to CH_3 rocking modes have been found for each compound and the frequencies of these features are listed in Table 9.2.

For the molecules $(CH_3)_nX$ (n=1-4), the weighted arithmetic means of the CH_3 symmetric deformation frequencies and of the CH_3 rocking frequencies are plotted against the electronegativity of X with the results shown in Figures 9.2 (p. 204) and 9.3 (p. 205) respectively. The frequencies missing from Table 9.2 have been estimated by comparison with those for the other elements in the same periodic group. Electronegativity values based on Pauling's formulation[79a] have been employed, that for tellurium being obtained by comparison with the values for the neighbouring elements.

For the CH_3 symmetric deformation frequency (Figure 9.2) a family of curves is obtained, each curve corresponding to a different period of the periodic table. Across any one period the frequency increases with reasonable regularity and between the periods there is a frequency decrease. Such results, which are in accordance with those of previous investigations, have been interpreted[198] in terms of electrostatic repulsion (1) between the C-H bonding electrons and the C-X bonding electrons (where X is the central atom) and (2) between the C-H bonding electrons and the non-bonding valence electrons on the X atom. As these repulsions increase more resistance is offered to enlarging the H-C-H bond angles and the features ascribable to these modes occur at higher frequencies. With advancing electronegativity of X there is an increase in the electron density in the C-X bond and hence in the interelectronic

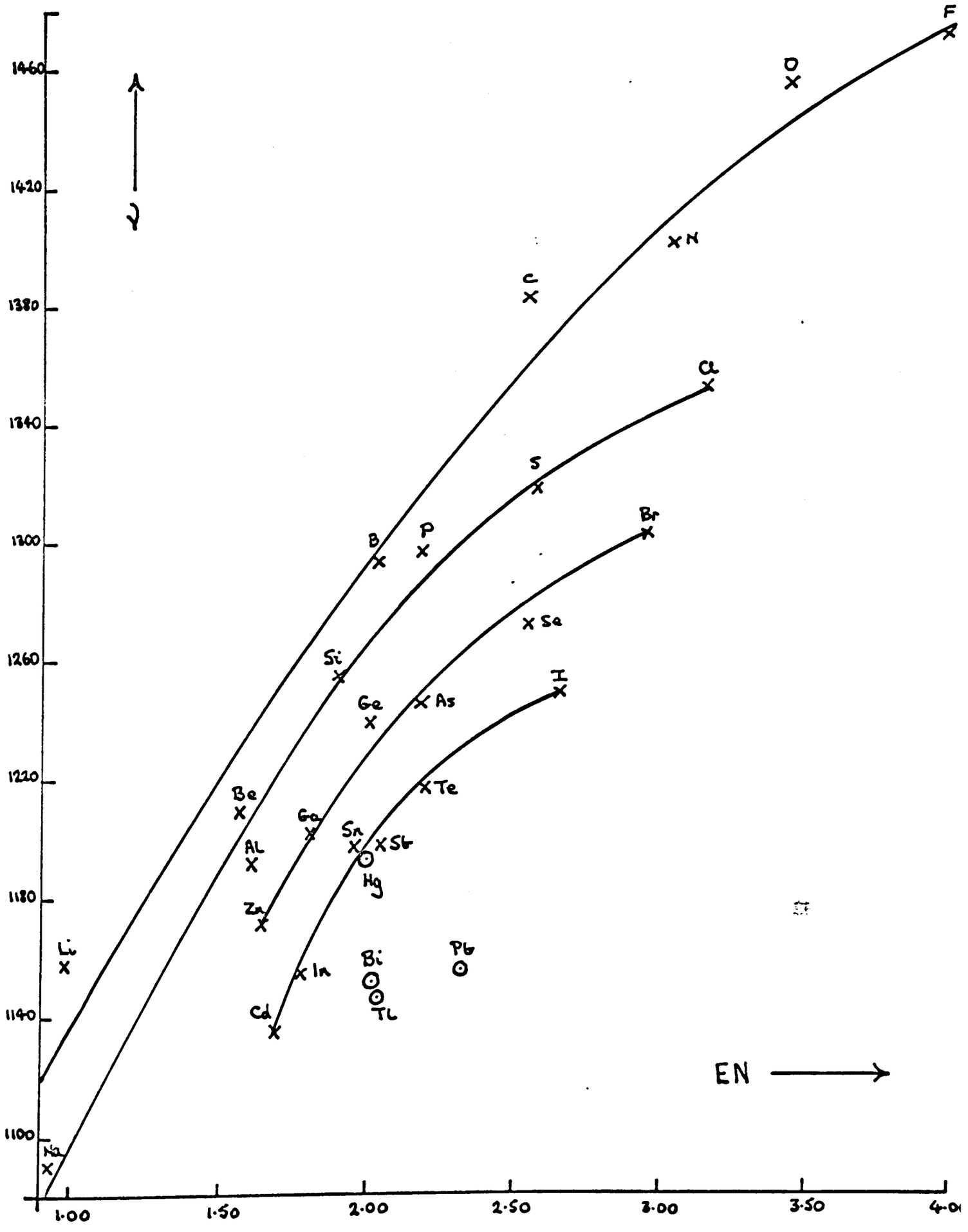

Figure 9.2: CH_3 Symmetric Deformation Frequency vs. Electronegativity for the Main Group Methyl Compounds

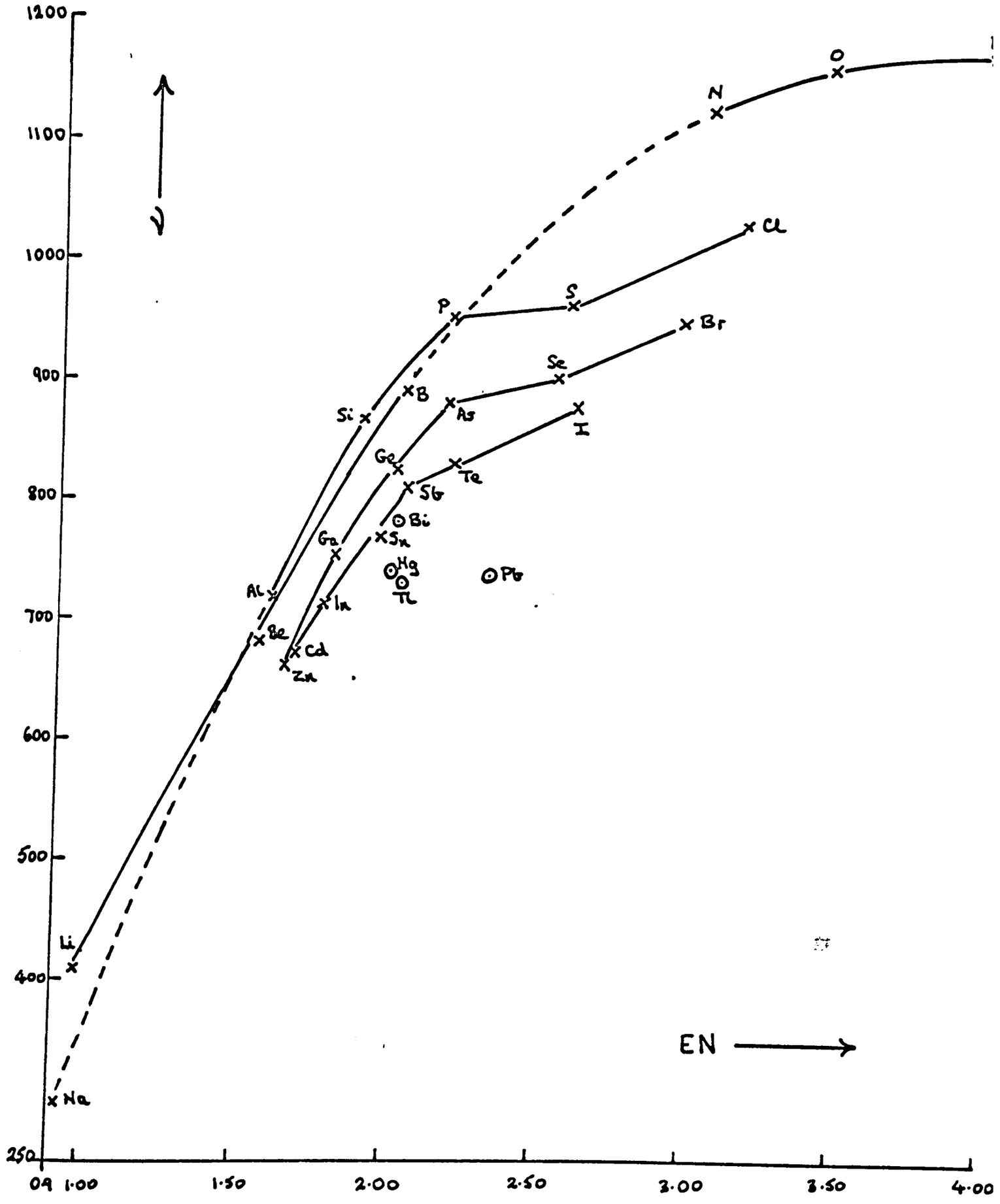

Figure 9.3: CH_3 Rocking Frequency vs. Electronegativity for the Main Group Methyl Compounds

repulsions of type 1 (for Groups I-IV this is, of course, the only type of repulsion that can occur). The differences between the periods can be ascribed to mass effects, though the results for the heaviest elements appear anomalous probably because of the lack of reliable bond energy data on which to base electronegativity calculations.

For the CH_3 rocking frequency (Figure 9.3) the curves given lie much closer together and increase much more steeply with increasing electronegativity than do their counterparts of Figure 9.2. Again the results can probably be interpreted in terms of interelectronic repulsions. The fall in frequency in passing from Group V to Group VI for the second and third periods suggests that the coordination number of the central atom may be a further factor influencing the frequency of such motions. The result for carbon is unreasonably high, probably because of large mixing effects and has not been included in Figure 9.3; the results for the fifth period are again irrational. The mean frequency for aluminium (703 cm^{-1}) seems a little low in comparison with the other frequencies of the same period, but is in reasonable accord with the electronegativity of the element.

The available data for the methyl compounds of Main Group elements tend therefore to confirm that the results for monomeric trimethylaluminium and in particular for trimethylindium are in reasonable concordance with their respective positions in the Periodic Table. In this connection the lack of data for monomeric dimethylmagnesium is regrettable, but the nature of the compound (a pyrophoric, involatile solid) makes spectroscopic investigation particularly difficult.

In concluding this section it is interesting to note that the increasing propensity for oligomerization suggested for the Group III trimethyl compounds on the basis of theoretical considerations (see p.33) closely parallels the decrease of frequency of the CH_3 rocking modes found for these compounds:

Oligomerization: Al > In > Tl ≏ Ga >> B

Mean CH_3 rocking mode frequency: 703 < 716 < 735 < 755 << 897

(c) Calculations

(i) Teller-Redlich Product Rule Calculations[113c]

For two isotopic molecules, a and b, Teller and Redlich showed that the product of the $\frac{\nu(a)}{\nu(b)}$ values for all the vibrations of a given symmetry type should depend only on the masses of the atoms and the geometrical structure of the molecule. For the planar isotopic molecules X^aY_3 and X^bY_3 of D_{3h} symmetry[113d] the mass factor becomes, for all the vibrations involving motion of the X atom:

$$\sqrt{\frac{M_X^{\,b}}{M_X^{\,a}} \cdot \frac{M_X^{\,a} + 3M_Y}{M_X^{\,b} + 3M_Y}}$$

In the case of trimethylboron it is possible to carry out such calculations at two levels of sophistication, either including or excluding the internal motions of the CH_3 groups. The results of such calculations are given in Table 9.3 (p. 208). For the modes of A_2'' symmetry neither calculation yields results in very good agreement with the value calculated for the above expression, but for the E' modes

Symmetry Class	BC_3 ONLY		ALL MODES	
	Modes	Value	Modes	Value
A_2''	ν_{10}	1.0478	$\nu_7 \cdot \nu_8 \cdot \nu_9 \cdot \nu_{10} \equiv \nu_9 \cdot \nu_{10}$	1.065
E'	$\nu_{16} \cdot \nu_{17}$	1.0260	$\nu_{11} \cdot \nu_{12} \cdot \nu_{13} \cdot \nu_{14} \cdot \nu_{15} \cdot \nu_{16} \cdot \nu_{17} \equiv \nu_{14} \cdot \nu_{16}$	1.0331

$$\sqrt{\frac{M_B^{11}}{M_B^{10}} \cdot \frac{M_B^{10} + 3M_{CH_3}}{M_B^{11} + 3M_{CH_3}}} = 1.0389$$

Table 9.3: Product Rule Calculations for Trimethylboron

the calculation including the CH_3 frequencies gives agreement within the experimental error of the spectroscopic results. In the case of the E' modes, therefore, the product rule calculations tend to confirm that there is appreciable mixing between the M-C antisymmetric stretching and CH_3 symmetric deformation modes.

(ii) Force-Constant Calculations

In order to gain some further insight into the strengths of the metal-carbon bonds in the series of trimethyl compounds some simple force-constant calculations have been undertaken with exclusive reference to the vibrations attributable to the MC_3 skeleton. Since most of the MC_3 vibrational features occur in spectral regions well removed from features ascribable to CH_3 vibrations of similar symmetry, this is a reasonable simplification to adopt. Those cases where the purity of the modes is questionable are mentioned in the discussion.

Most of the calculations have been carried out using a Hewlett-Packard Model 9100A programmable calculator, but the results for trimethylaluminium have been calculated by hand using an LME 865 electronic calculator. All the calculations have been carefully checked, both for internal consistency and by re-examining previously reported analyses.

The results of the two simpler sets of calculations are presented in Table 9.4 (p. 210). If the MC_3 skeleton is considered to be held together by three equal and independent bonds (Simple Valence Force Field approach) then the M-C stretching force constant, k_1, can be directly calculated from the M-C symmetric stretching frequency, ν_1, using the relationship[113c]:

COMPOUND	SKELETAL FREQUENCIES (cm^{-1})				FORCE CONSTANTS ($x10^5$ dynes/cm.)				
					SIMPLE [113e]	SELF-CONSISTENT SET [199a]			
	ν_1 (ν_3 A_1')	ν_2 (ν_9 A_2'')	ν_3 (ν_{16} E')	ν_4 (ν_{17} E')	k_1	f	f'	d-d'	d_γ
$^{10}BMe_3$	679	351	1185	321	4.08	3.71	0.188	0.195	0.198
$^{11}BMe_3$	679	335	1155	321	4.08	3.75	0.167	0.197	0.195
$AlMe_3$	527		694		2.46				
$AlMe_3$(calc)		(134)	(693)	(170)		(2.34)	(0.0610)	(0.0596)	(0.0596)
$GaMe_3$	520	(103)	577	156	2.39	2.28	0.0594	0.0580	(0.0580)
$InMe_3$	467	(75)	501	118	1.93	1.88	0.0255	0.0354	(0.0354)
$TlMe_3$	445	(60)	462	99	1.75	1.72	0.0174	0.0263	(0.0263)

All values quoted to 3 significant figures

All estimated values in parentheses.

Table 9.4: Force Constant Calculations for the Group III Trimethyl Compounds

$$4\pi^2C^2M\nu_1^2 = \lambda_1 = \frac{k_1}{M_Y}$$

where: M_Y = mass of a methyl group

and $4\pi^2C^2M$ has the value 5.8894×10^{-2} if all the masses are taken in atomic weight units.

Values of k_1 are given in the central column of Table 9.4. The value of 2.46×10^5 dyne cm^{-1} for aluminium is surprisingly low, being only marginally higher than that for gallium, namely 2.39×10^5 dyne cm^{-1}. This result indicates that the bonding in trimethylaluminium is anomalously weak, a suggestion which is followed up at the end of this section.

It is found that the Simple Valence Force Field does not yield satisfactory values when the A_1' and E' modes are considered together. Accordingly the remaining constants in Table 9.4 have been calculated on the basis of a model in which it is recognised that the stretching or deformation of one bond must have some effect on the other two. A new set of equations can then be defined:

$$\lambda_1 = \frac{(f + 2f')}{M_Y}$$

$$\lambda_2 = \left(\frac{1}{M_Y} + \frac{3}{M_X}\right) d_\gamma$$

$$\lambda_3 + \lambda_4 = \left(\frac{1}{M_Y} + \frac{3}{2M_X}\right) [(f-f') + 3(d-d')]$$

$$\lambda_3 + \lambda_4 = \frac{3}{M_Y}\left(\frac{1}{M_Y} + \frac{3}{M_X}\right) [(f-f')(d-d')]$$

where f = M-C stretching force constant

d_γ = MC_3 out-of-plane deformation force constant

d = MC_3 in-plane deformation force constant

f' = stretch-stretch interaction constant

d' = deformation - deformation interaction constant

M_X = mass of the metal atom

M_Y = mass of a methyl group

Thus, whilst the d_γ constant remains independent of all the other constants (and is therefore the S.V.F.F. constant too), the constants f, d, f' and d' are interdependent. d and d' do not appear independently in the above equations and hence it is possible only to calculate f, f' and d-d'.

The values derived for f, f' and d-d' are presented to the right of Table 9.4; d_γ can be calculated only for trimethylboron. In the series B, Ga, In, Tl, the other three constants all show a fairly consistent decrease with increasing mass of the central atom. The positive stretch-stretch interaction term, f', reflects the fact that if one M-C bond is stretched then it becomes more difficult to stretch the other two bonds. It thus provides some indication of the degree to which the bonds are interdependent with respect to stretching. The interdependence clearly falls off with increasing mass of the central atom, the ratio f' to f decreasing in the series B, Al, Ga, In, Tl.

The feature at 694 cm^{-1} in the spectrum of matrix-isolated trimethylaluminium monomer, tentatively assigned to the E' antisymmetric stretching

mode ν_3, cannot be used alone as a basis for calculations. In order to test the feasibility of this assignment, therefore, a set of frequencies has been computed based on the trimethylgallium force constants, but scaled in accordance with the ratio of the S.V.F.F. stretching force constants (k_1) for the gallium and aluminium compounds. For example the value used for f has been calculated by:

$$f_{Al} = f_{Ga} \cdot \frac{(k_1)_{Al}}{(k_1)_{Ga}} = 2.28 \times \frac{2.46}{2.39} = 2.34$$

The results of these computations are included in parentheses in Table 9.4. The agreement between the postulated and estimated values for ν_3, 694 and 693 cm^{-1}, is remarkably good, and the value for the in-plane deformation frequency, 170 cm^{-1}, whilst probably not in itself accurate, does at least tend to confirm that this feature lies below the limit of the present matrix-isolation investigation (200 cm^{-1}).

It is also to be noted that the constants for the in-plane and out-of-plane deformations, d-d' and d_γ, respectively, are closely similar in the case of trimethylboron. A set of frequencies has therefore been computed for ν_2 for the four heavier elements on the assumption that d_γ and d-d' have the same value. The results of these computations are also included in Table 9.4. Whilst the values are of little precise significance, they do suggest that the out-of-plane deformation feature lies at frequencies below 150 cm^{-1} in all cases other than that of trimethylboron.

The substantial differences between the sets of constants calculated

for ^{10}B-trimethylboron and ^{11}B-trimethylboron indicate that the force field employed in the calculation is imprecise. This could be either because of interactions between the MC_3 skeletal modes and the internal modes of the CH_3 groups or because of the existence of other types of interaction not included in the two simple interaction terms f' and d'. A treatment[199a] more sophisticated than that employed above allows for exchange-interaction binding both between adjacent and non-adjacent angles, the three interdependent equations of page 211 becoming:

$$\lambda_1 = \frac{(f + 2f')}{M_Y}$$

$$\lambda_3 + \lambda_4 = \left(\frac{1}{M_Y} + \frac{3}{2M_X}\right)[(f-f') + 3(d-d')] - \frac{3\ 3}{M_X}(g' - g'')$$

$$\lambda_3\lambda_4 = \frac{3}{M_Y}\left(\frac{1}{M_Y} + \frac{3}{M_X}\right)[(f-f')(d-d') - (g'-g'')^2]$$

where g' and g'' are the interaction constants for exchange-interaction binding between adjacent and non-adjacent angles respectively.

These equations can only be solved explicitly by using the frequencies of more than one isotopic molecule. The results of such calculations are presented in Table 9.5 (p. 215) both for trimethylboron and boron trifluoride. The results for the methyl compound are unsatisfactory, the stretch-stretch interaction constant being both large and negative. Negative values for the stretch-stretch interaction constant have been found before (e.g. for KrF_2[200]), but are not easily explained; in this case the most probable interpretation is that the frequencies for

COMPOUND	SKELETAL FREQUENCIES (cm^{-1})				FORCE CONSTANTS[199a] ($x10^5$ dynes/cm.)				
	ν_1 (A_1')	ν_2 (A_2'')	ν_3 (E')	ν_4 (E')	f	f'	d-d'	g'-g''	d_γ
$^{10}BMe_3$	679	351	1185	321	5.06	-0.488	0.293	0.968	0.198
$^{11}BMe_3$	679	335	1155	321	5.05	-0.485	0.296		0.194
$^{10}BF_3$ (113f)	888	719.5	1497.0	482.0	7.78	0.524	0.498	0.605	0.866
$^{11}BF_3$ (113f)	888	691.3	1445.9	480.4	7.77	0.524	0.500		0.865

Table 9.5: Force Constant Calculations for Trimethylboron and Boron Trifluoride

the MC_3 asymmetric stretching mode are unreliable because of mixing with internal motions of the CH_3 groups.

Since the fluorine atom and the methyl group are of very similar mass the very appreciable difference in the values of the out-of-plane deformation constants (d_δ) for trimethylboron and boron trifluoride must reflect bonding differences. The low Lewis acidity of boron trifluoride (relative to the other boron trihalides) has been attributed to a high degree of boron to fluorine π electron 'back donation'[161,162] and this explanation is supported by the high deformation constant value. The low value of the constant for trimethylboron tends to confirm the postulate that hyperconjugative stabilization for this molecule is insignificantly small.[11]

(iii) Bond Length Calculations

In the past there have been a number of attempts to formulate an expression inter-relating force constants and bond lengths. One of the most successful of the earlier expressions was that originally proposed by Badger:[201]

$$F = 1.86\,(r_e - k_{ij})^{-3}$$

or $$r_e = k_{ij} + 1.23F^{-\frac{1}{3}}$$ (ORIGINAL BADGER'S RULE EXPRESSION)

where F = stretching force constant betweens atoms i and j;

r_e = equilibrium interatomic distance between i and j;

k_{ij} = constant depending upon the respective periods in the Periodic Table of the atoms i and j.

Over the years it has been found that this rule is insufficiently general to cover all cases and a modified form of Badger's Rule involving two constants is found to be of wider applicability:[202]

$$r_e = d_{ij} + (a_{ij} - d_{ij})F^{-\frac{1}{3}} \qquad \text{(GENERAL BADGER'S RULE EXPRESSION)}$$

where both a_{ij} and d_{ij} depend upon the respective periods of the atoms i and j.

More recently still a new expression involving an exponential interdependence of the bond length and force constant has been put forward by Laurie and Herschback:[203]

$$r_e = a_{ij} - b_{ij} \log_{10} F \qquad \text{(LAURIE - HERSCHBACH EXPRESSION)}$$

where the constants a_{ij} and b_{ij} again depend upon the periods of the atoms i and j.

With the force constant data of Table 9.4 interatomic distances have been calculated for each of the Group III trimethyl compounds utilizing all three of the above expressions. In all cases the constants employed are those given in reference (203). The results of the calculations are presented in Table 9.6 (p. 218), together with the experimental bond lengths and the sums of the relevant covalent radii.

For the most part the agreement between the bond lengths calculated by the three different methods is reasonably good. The differences between the values calculated using the S.V.F.F. force constant, k_1 and the more general one, f', are insignificant. On average the calculated

COMPOUND	FORCE CONSTANT[a]		CALCULATED BOND LENGTH						OBSERVED BOND LENGTH[b]		COV. RADII SUM[c]
			from k_1			from f					
	k_1	f	OB	GB	LH	OB	GB	LH	VAP.	SOLID	
BMe_3	4.08	3.73	1.45	1.45	1.44	1.47	1.47	1.46	1.58		1.58
$AlMe_3$	2.46	(2.34)	1.83	1.88	1.81	1.84	1.90	1.82	1.96	1.97	2.03
$GaMe_3$	2.39	2.28	1.94	1.97	1.92	1.95	1.99	1.94	-	-	2.03
$InMe_3$	1.93	1.88	2.10	2.00	2.14	2.12	2.02	2.15	2.16	2.11	2.21
$TlMe_3$	1.75	1.72	2.24	2.24	2.26	2.25	2.25	2.27	-	2.29	2.23

(a) from Table 9.4 (p.210); (b) from Table 1.2 (p.15); (c) from Table 1.6 (p.29)

OB = Original Badger's Rule Calculation
GB = General Badger's Rule Calculation
LH = Laurie-Herschbach Relationship Calculation

} Reference 203

Table 9.6: Bond Length Calculations for the Group III Trimethyl Compounds

values for both the boron and aluminium compounds are approximately 0.1Å too low. On this basis it seems probable that the gallium-carbon distance in trimethylgallium (which has not been measured) is very close to the sum of the tetrahedral covalent radii of gallium and carbon (2.03Å). For indium and thallium the agreement between the calculated and observed values is remarkably good, the only exception being the value calculated for the indium-carbon distance using the General Badger's Rule Expression.

Overall the bond length calculations confirm the trends suggested by spectroscopic and other results, but do not reveal any new information of great significance.

(d) Conclusions

In general terms the spectroscopic results indicate that the bond strengths for the monomers of the Group III trimethyl compounds conform with the positions of the central metal atoms in the Periodic Table. The bonding in trimethylaluminium monomer is considerably weaker than would be predicted on the basis of a direct interpolation of the results for the boron and gallium compounds, but this weakness can be attributed to the marked polarity of the bond. Whilst a small degree of 'ionic character' increases the strength of a bond (this being, of course, the basis of Pauling's electronegativity scale), there must clearly be a polarity maximum beyond which bond strengths, as measured by the stretching force constants, decrease rather than increase to accommodate the very low force constants characteristic of highly polar units such as NaF.

Table 9.7 (p. 221) compares Pauling electronegativity values for the Group III elements and the metal-carbon electronegativity differences with the force constant values for the corresponding trimethyl compounds. The electronegativity difference gives an approximate measure of the bond polarity, which is considerably greater for trimethylaluminium than for the other members of the series. This result suggests that for aluminium the degree of polar character in the bond is greater than that for maximal binding. In general, the values of the force constants suggest that the maximal contribution of 'ionic character' to bond strength occurs for electronegativity differences (using Pauling's scale) of approximately 0.5 units.

Also included in Table 9.7 are some force constant values calculated on the basis of an empirical relationship put forward by Gordy[204] connecting force constant, electronegativity and interatomic distance:

$$F_{AB} = 1.63 \left(\frac{\chi_A \chi_B}{r_e^2} \right)^{\frac{3}{4}} + 0.30$$

where F_{AB} = stretching force constant between atoms A and B

χ_A = Pauling electronegativity of element A

χ_B = Pauling electronegativity of element B

r_e = equilibrium interatomic distance

The force constants calculated using this expression are in no more than fair agreement with the experimental values. However, the most significant feature of the results is that, in keeping with the experimental results, the values calculated for the aluminium and gallium

ELEMENT	ELECTRONEGATIVITY		EXPERIMENTAL FORCE CONSTANTS		GORDY[204] FORCE CONSTANTS	
	VALUE[79a]	Δ for M-C	k_1	f	from r_e vapour	from r_e solid
B	2.04	0.51	4.08	3.73	3.14	
Al	1.61	0.94	2.46	(2.34)	2.00	
Ga	1.81	0.74	2.39	2.28	2.07	
In	1.78	0.77	1.93	1.88	1.96	1.86
Tl	2.04	0.51	1.75	1.72		1.92
C	2.55		x 10^5 dynes/cm			

Table 9.7: Electronegativity Differences and Force Constants for the Group III Trimethyl Compounds

compounds are closely similar. This is a direct result of the low electronegativity of aluminium. Thus the calculated data here support the conclusion previously reached that the large electronegativity difference between aluminium and carbon is the main reason for the relative weakness of the Al-C bond in trimethylaluminium monomer. The high force constant calculated for trimethylthallium probably indicates no more than that the Pauling electronegativity coefficient normally quoted for thallium is incorrect.

9.2. Dimeric Species

The only molecule genuinely falling into this category for the Group III trimethyl compounds is that of trimethylaluminium. In the fluid phases the symmetric, bridged structures of D_{2h} symmetry, is well established, but in the solid state it has recently been shown that the bridged molecule is significantly distorted, the symmetry being lowered to C_{2h} [38]. It has also been suggested that the dimer even adopts a configuration involving a six-membered ring: [39]

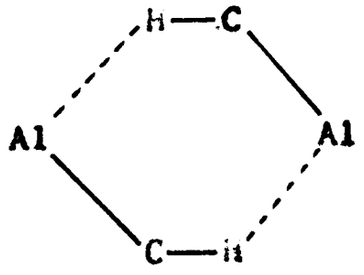

The vibrational modes of the X_2Y_6 unit of D_{2h} symmetry are illustrated in Figure 9.4 (p. 223) and their spectroscopic activities are listed to the left of Table 9.8 (p. 224).

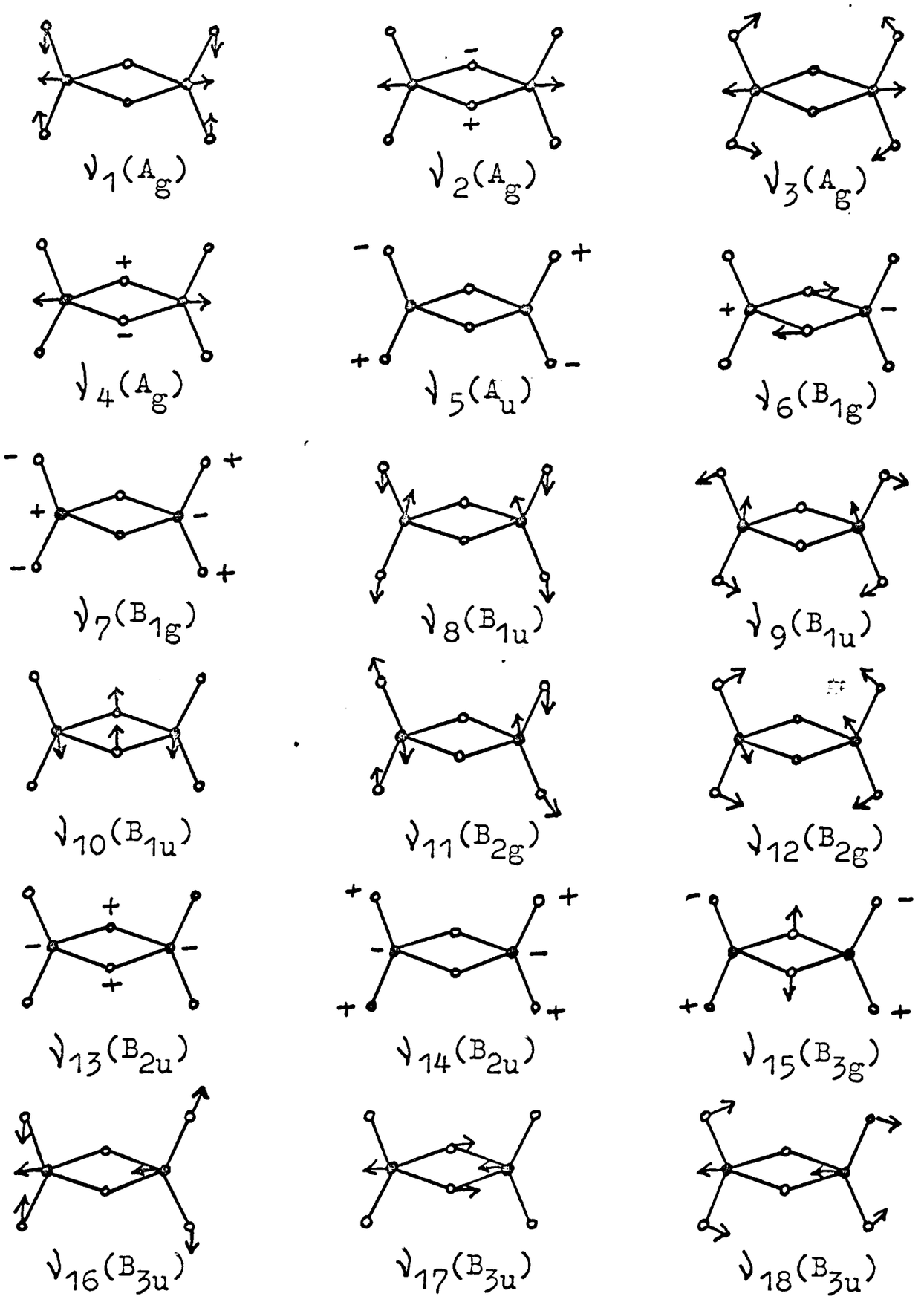

Figure 9.4: The Normal Modes of Vibration for the X_2Y_6 (D_{2h}) Skeleton

Table 9.8

MODE				$Al_2(CD_3)_6$		$Al_2(CH_3)_6$				$Al_2(CH_3)_4Cl_2$		Al_2Cl_6	
Act.	SYMMETRY		t or b	Gray[28]	(180) Ogawa	(30) Hoffmann/ Gray[28]	THIS INV. (SOLID)	(181) Ogawa	(24) Onishi & Shima-nouchi	(30) Hoffmann /Gray[28]	Onishi & Shima-nouchi	(206/ 207)	(24) Onishi & Shima-nouchi
				OBS.	CALC.	OBS.	OBS.	CALC.	CALC.	OBS.	CALC.	OBS.	CALC.
R	A_{1g}	ν_1	t	-	599	592	590	593	599	588	603	506	513
		ν_2	b	-	427	453	477	481	463	330	375	340	339
		ν_3	t	-	290	313	324	312	300	282	255	217	222
		ν_4	b	-	127	153	148	144	145	131	140	112	106
i/a	A_{1u}	ν_5	t	-	156	-	-	156	138	-	116	-	83
R	B_{1g}	ν_6	b	-	368	-	334	336	274	240	295	284	287
		ν_7	t	-	195	-	211	202	192	217	216	-	200
		ν_8	t	579	605	697	644	662	677	720	676	625	616
IR	B_{1u}	ν_9	t	-	191	-	230	219	342	310	296	-	264
		ν_{10}	b	-	34	-	-	40	89	-	88	-	70
R	B_{2g}	ν_{11}	t	-	604	683	610	646	672	713	667	606	598
		ν_{12}	t	-	138	-	159	152	181	170	199	164	157
IR	B_{2u}	ν_{13}	b	435	449	480	489	484	488	440	424	420	425
		ν_{14}	t	-	173	175	(170)*	175	222	-	192	-	155
R	B_{3g}	ν_{15}	t/b	-	172	185	188	185	232	170	163	164	152
IR	B_{3u}	ν_{16}	t	472	486	564	559	556	583	585	599	484	510
		ν_{17}	b	315	305	367	379	345	385	343	386	-	337
		ν_{18}	t	-	162	175	(170)*	183	215	-	220	-	170

* Values in parentheses are vapour phase values

Table 9.8: Vibrational Frequencies for Representative X_2Y_6 Molecules (Skeletal Modes Only)

The change from D_{2h} to the C_{2h} symmetry ascribed to the molecule in the crystalline state in reference (31) should have little effect on the vibrational spectrum. The B_{3g} mode (ν_{15}) becomes a polarised feature and the formerly inactive A_{1u} mode (ν_5) becomes infrared-active:

D_{2h} Modes	C_{2h} Modes
A_{1g} & B_{3g}	A_g
B_{1g} & B_{2g}	B_g
A_{1u} & B_{3u}	A_u
B_{1u} & B_{2u}	B_u

Thus the distortion of the Al_2Me_6 unit reported to accompany the transition from the fluid to the solid phase cannot readily be detected using vibrational spectroscopy.

On the other hand, the formation of a six-membered ring should lead to fundamental changes in the vibrations both of the skeleton and of the methyl groups. The observed vibrational spectra of trimethylaluminium in the solid state show no fundamental differences from their fluid-phase counterparts: in particular, no features attributable to the vibrations of an Al···H - C unit could be detected. Accordingly the suggestion of reference (39) is not substantiated, a failing confirmed by a recent paper,[205] in which such a structure is shown, by simple trigonometry, to be inconsistent with the X-ray crystallographic results.

Because of the sharpness of the solid-state vibrational features and because of the small frequency shifts produced by the phase change,

a number of new features have been revealed in the solid-state spectra in positions close to those already reported for the fluid phases. These new features, in confirming the results of force constant calculations,[24,181] have enabled the vibrational assignment for the dimeric trimethylaluminium molecule to be considerably extended. For the Al_2C_6 skeletal modes the extended assignment is given in Table 9.8, together with the results of previous investigations and of force-constant calculations not only for $Al_2(CH_3)_6$, but also for $Al_2(CD_3)_6$[28], $Al(CH_3)_4Cl_2$[28,30] and Al_2Cl_6[206,207]. The effect on any particular vibration of changing the bridging or terminal groups can thus be examined, and the results confirm that the vibrations have been correctly assigned as between motions of the Al_2X_2 ring and those of the terminal Al-X bonds.

9.3. New Diffusion Species

The results discussed in this section refer to the new features which were observed as a result of diffusion experiments involving matrix-isolated monomeric molecules and which could not be attributed either to a known oligomeric species such as the symmetrical trimethylaluminium dimer, or to the type of aggregation characteristic of the pure solid. Two sets of such features were observed, one for trimethylaluminium and one for trimethylgallium; the frequencies of these sets are presented in Table 9.9 (p. 227).

The most striking facet of the results is that, in both cases, a feature is observed in the infrared spectrum in the spectral position

$GaMe_3$ Table 8.1 (Diff. Species A)	$AlMe_3$ Table 8.3 (Diff. Species B)	Assignment (XY_3 Pyramidal Model: C_{3v})
520	531	A_1 ν_1
575	597	E ν_3
739	656	CH_3 rocking
761 (?)		?
783	703	CH_3 rocking
1178	1192	CH_3 symmetric deformation
1205		
2960		C-H stretching

Table 9.9: Tentative Assignments for the Matrix-Isolation Diffusion Species

normally associated with symmetric stretching of the MC_3 unit. For a D_{3h} (planar) molecule this mode is inactive with respect to infrared absorption, but if a lowering of the symmetry is allowed, it may become active. One change which would bring about this result is the loss of planarity to form an MC_3 pyramidal unit (C_{3v} symmetry). All four skeletal modes would then be active with respect to both infrared absorption and Raman scattering. The corresponding D_{3h} and C_{3v} modes for the MC_3 skeleton are compared in Table 9.10 (p. 229); for both point groups the deformation modes (ν_2 and ν_4) would be expected to lie at frequencies below the lower limit of the matrix-isolation investigations (200 cm^{-1}).

Because no new doublet features were observed, as would be the case if the symmetry of the unit were to be further reduced beyond C_{3v}, it is tempting to interpret the diffusion results on the basis of a C_{3v} model. Such a model would be appropriate to a dimeric species formed by a relatively weak but direct metal-metal interaction:

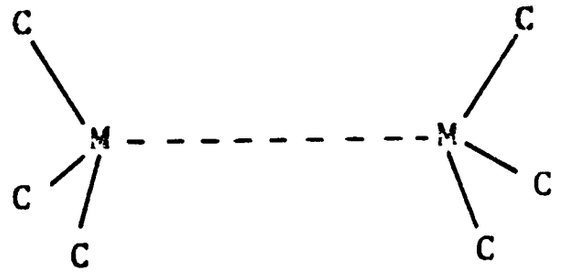

or to one formed by metal carbon interactions of sufficient strength to deform the MC_3 skeleton, but not of sufficient strength to make one M-C bond appreciably different from the other two:

MC_3 PLANAR (D_{3h})					MC_3 PYRAMIDAL (C_{3v})			
MODE		DESCRIPTION	ACTIVITY		MODE	DESCRIPTION	ACTIVITY	
			Raman	I.R.			Raman	I.R.
A_1'	ν_1	M-C symmetric stretch	✓	-	ν_1	M-C symmetric stretch	✓	✓
					A_1			
A_2''	ν_2	MC_3 out-of-plane deformation	-	✓	ν_2	MC_3 symmetric deformation	✓	✓
	ν_3	M-C antisymmetric stretch	✓	✓	ν_3	M-C antisymmetric stretch	✓	✓
					E			
E'	ν_4	MC_3 in-plane deformation	✓	✓	ν_4	MC_3 antisymmetric deformation	✓	✓

Table 9.10: Corresponding Vibrational Modes for the MC_3 Unit with Planar and Pyramidal Configurations

e.g.

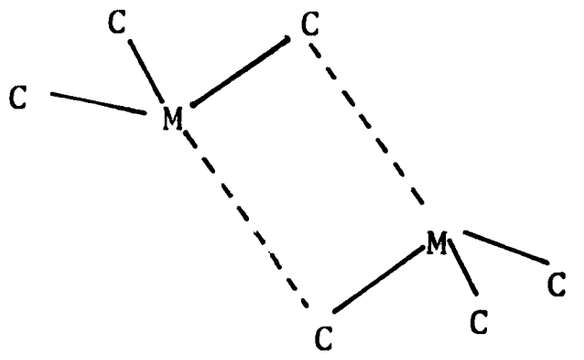

The features characteristic of the new diffusion species have therefore been assigned on the basis of the point group C_{3v} (see Table 9.9). For pyramidal XY_3 species the symmetric and antisymmetric stretching modes frequently lie in much closer proximity than do the corresponding modes of D_{3h} molecules.[115d] Hence the assignment of the feature at 597 cm^{-1} in the spectrum of the trimethylaluminium species to the antisymmetric stretching mode (E,ν_3) is not without justification. It is to be emphasised, however, that the sets of new features are neither complete nor fully substantiated, and the interpretation suggested here must therefore be considered tentative.

9.4. Larger Aggregates

In this section the results of the solid-phase investigations for trimethylgallium, trimethylindium and trimethylthallium are considered. The initial indications of the spectra, namely that trimethylgallium and trimethylthallium are isostructural with trimethylindium[63] in the solid state, have been confirmed by X-ray crystallographic studies of single crystals (for trimethylthallium[67]) or of microcrystalline samples (for

trimethylgallium (section 7.6, p. 174)). The purpose of the present discussion is to determine whether the vibrational spectroscopic results can also shed some light on the relative strengths of the intermolecular interactions involved in the solids. Since all three compounds are monomeric in the liquid phase, it is pertinent in this context to bear in mind the following melting point values (all in °C):

Group III		Group IV	
$GaMe_3$	-15.7	$GeMe_4$	-88
$InMe_3$	88.4	$SnMe_4$	-54.8
$TlMe_3$	38.5	$PbMe_4$	-27.5

In Chapter 2 (p. 63), the structure of crystalline trimethylindium, which comprises weakly-bound tetrameric units of S_4 symmetry more weakly linked together to yield an infinite array of C_{4h}^4 symmetry, was used to exemplify the three approaches to the interpretation of the vibrational spectra of molecules in crystal lattices. In the simplest of these, the site symmetry approach, appropriate to weak intermolecular interactions, the crystal environment is merely considered to alter the symmetry of the isolated molecule. If distinct aggregate units can be distinguished, then a better approach may be to consider the vibrations of such a unit. However, if the intermolecular interactions are appreciable throughout the lattice, a factor group approach, in which the vibrations of the lattice as a whole are considered, provides the only satisfactory model for the interpretation of the vibrational spectra.

For the region of the solid-state spectra characteristic of M-C stretching modes of trimethylgallium, -indium and -thallium, these three approaches yield the following spectroscopic predictions (Table 2.4, p.70).

	Raman-Active Features	Infrared-Active Features	Number of Coincidences
Site Symmetry Approach	3	3	3
Aggregate Unit Approach	9	6	6
Factor Group Approach	9	6	0

These results have been obtained by attributing a single displacement coordinate to the stretching of the metal-carbon bonds in the monomeric unit. A similar internal coordinate can be ascribed to the symmetric deformation of the methyl groups and in consequence the above results apply equally well to the region of the spectrum characteristic of the CH_3 symmetric deformation modes (approximately 1200 cm^{-1}).

The results for these two regions of the solid-state spectra are compared in the form of line diagrams in Figures 9.5 (p. 233) and 9.6 (p. 234) respectively. The number of features observed, in almost all cases more than three, immediately shows that the simple site symmetry approach is inappropriate to the interpretation of the spectra of solid trimethylgallium, -indium and -thallium. In principle, it should be possible to determine which of the two more sophisticated approaches is the more exact on the basis of the number of coincidences observed in the infrared and Raman spectra. Since all the spectra were examined at the same temperature (-196°C) and the accuracy of frequency measurement for

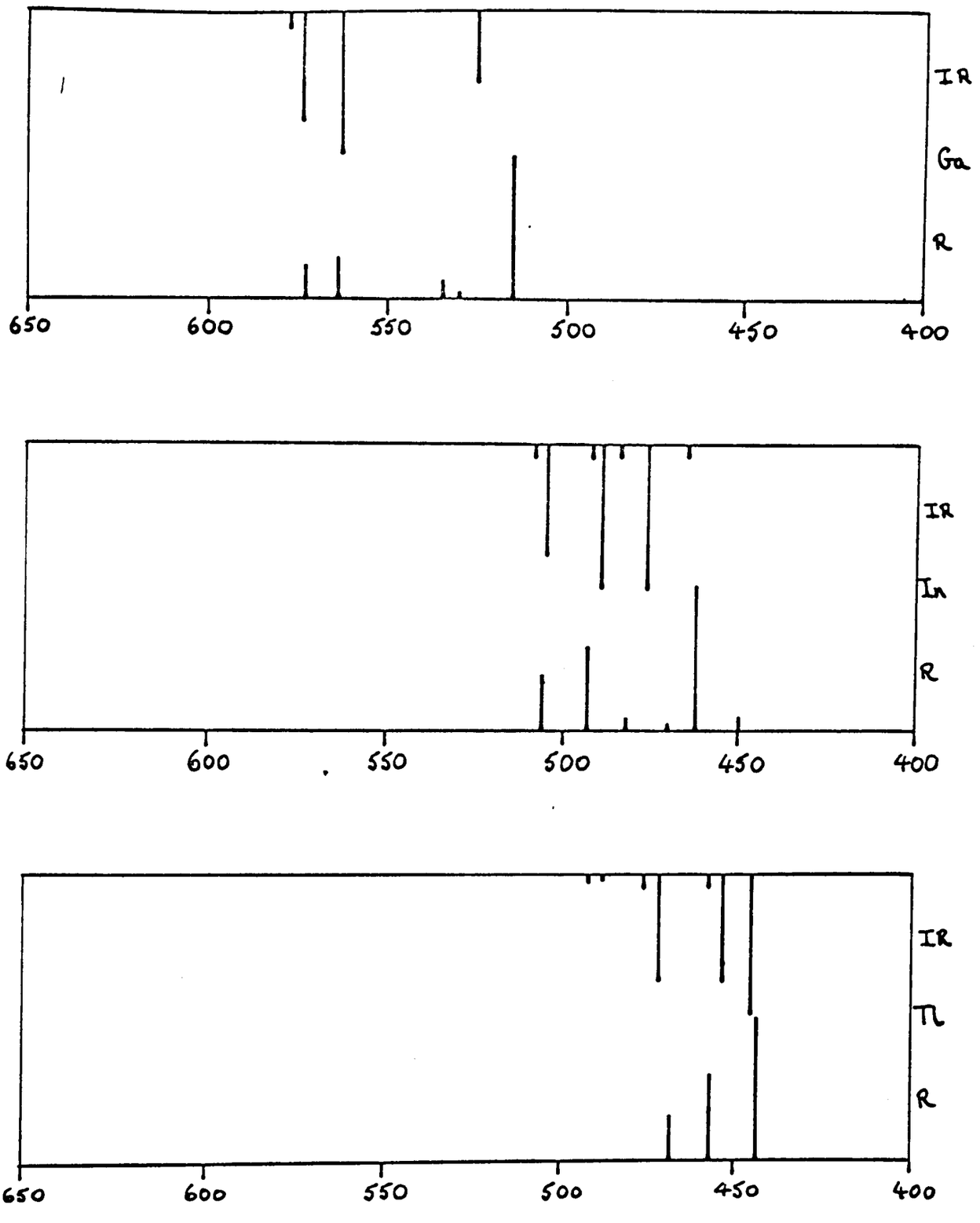

Figure 9.5: Correlation Diagram for the Solid Trimethyl Compounds of the Group III Elements (M-C Stretching Region)

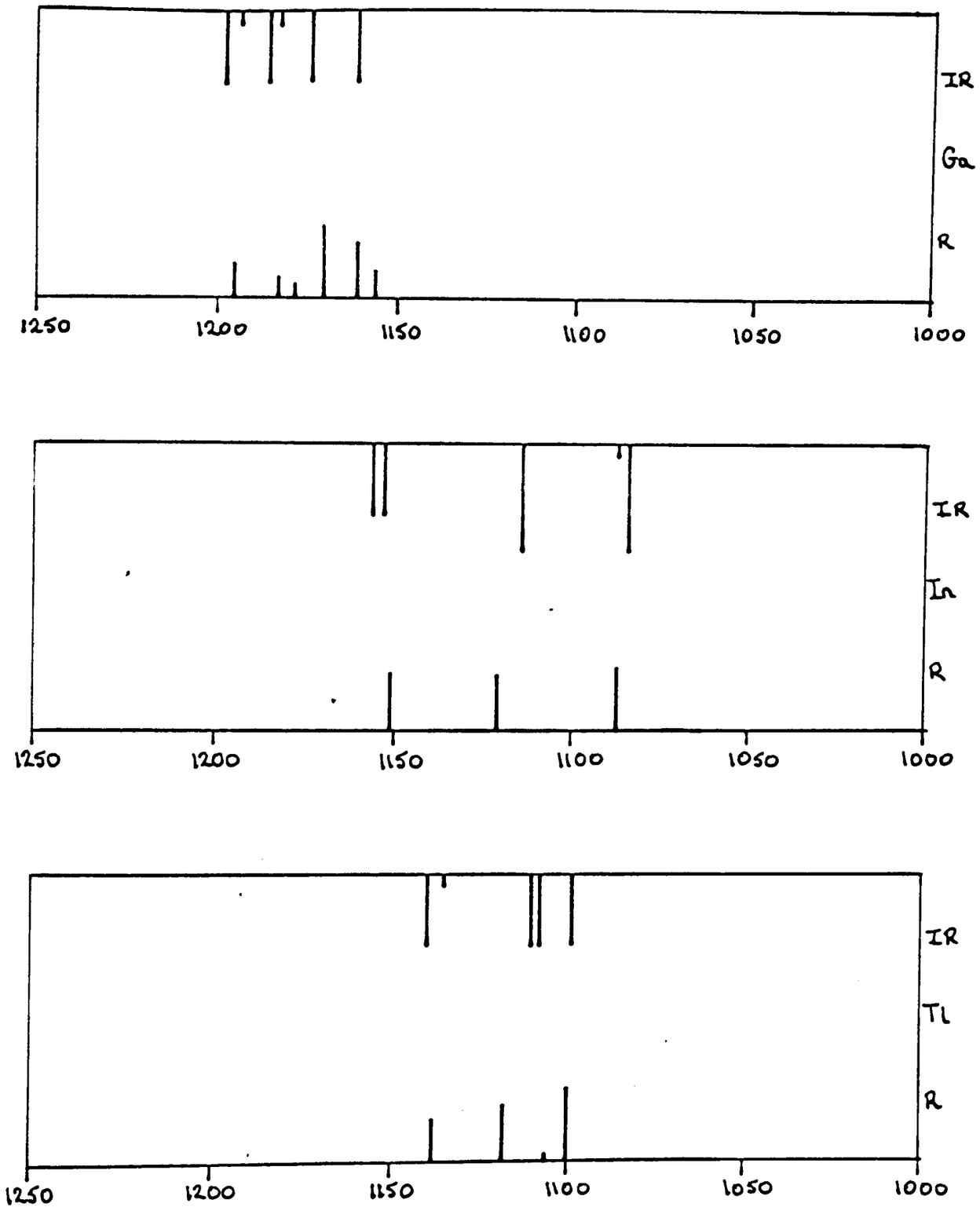

Figure 9.6: Correlation Diagram for the Solid Trimethyl Compounds of the Group III Elements (CH_3 Symmetric Deformation Region)

most features was better than 1 cm^{-1} a reasonable criterion of coincidence would seem to be that an infrared feature and a Raman feature should lie within 2 cm^{-1} of each other. However, for the infrared spectra of solids refractive index effects can lead to small frequency shifts[208] and it is probably more appropriate therefore to consider infrared and Raman features lying within 5 cm^{-1} of each other coincident. On this basis the number of coincidences exhibited by each compound was found to be:

	M-C Stretching	CH_3 Symmetric Deformation
$GaMe_3$	3	4
$InMe_3$	5	2
$TlMe_3$	3	4

The number of coincidences observed thus varies between two and five and since no more than six of the nine possible Raman features were observed in either of the two spectral regions for any of the three compounds it is impossible on the basis of the observed spectra, to decide which of the two extended approaches is the more appropriate. With as many as six features in a spectral region extending over less than 100 cm^{-1} the likelihood of accidental coincidence must necessarily be high.

In considering the overall degree of intermolecular interaction in the solid phase the spectral region associated with the CH_3 symmetric deformation modes is more informative than that associated with the M-C stretching modes. If a carbon atom of one $M(CH_3)_3$ molecule enters into

weak coordination with another $M(CH_3)_3$ molecule then both the reduced mass of the vibrating system and the force constants of the $M(CH_3)_3$ unit will be modified. The effect on the M-C stretching vibrations is likely to be small, but the effect on the symmetric deformation modes of the CH_3 groups may be more drastic. The frequency separations between the outermost strong features due to the CH_3 symmetric deformation modes are as follows:

	Raman	Infrared	Mean
$GaMe_3$	39	38	38
$InMe_3$	64	72	68
$TlMe_3$	28	41	35

These results suggest that the intermolecular binding in trimethylindium is appreciably greater than that in trimethylgallium and trimethylthallium and, if allowance is made for the increasing mass of the molecule, this conclusion is in accordance with the observed melting points of these compounds.

The only other region of interest in the spectra of the solid compounds is that below 200 cm^{-1}, for which it was possible to obtain only Raman data. A line diagram for this region is given in Figure 9.7 (p. 237) and whilst it is not possible to draw too close a parallel between the results for the three compounds, comparison makes it tempting to correlate four of the features (A, B, C & D) in the manner indicated by the dotted lines in the figure. The frequencies of the features are also presented in Table 9.11 (p. 238), together with the frequencies of the feature

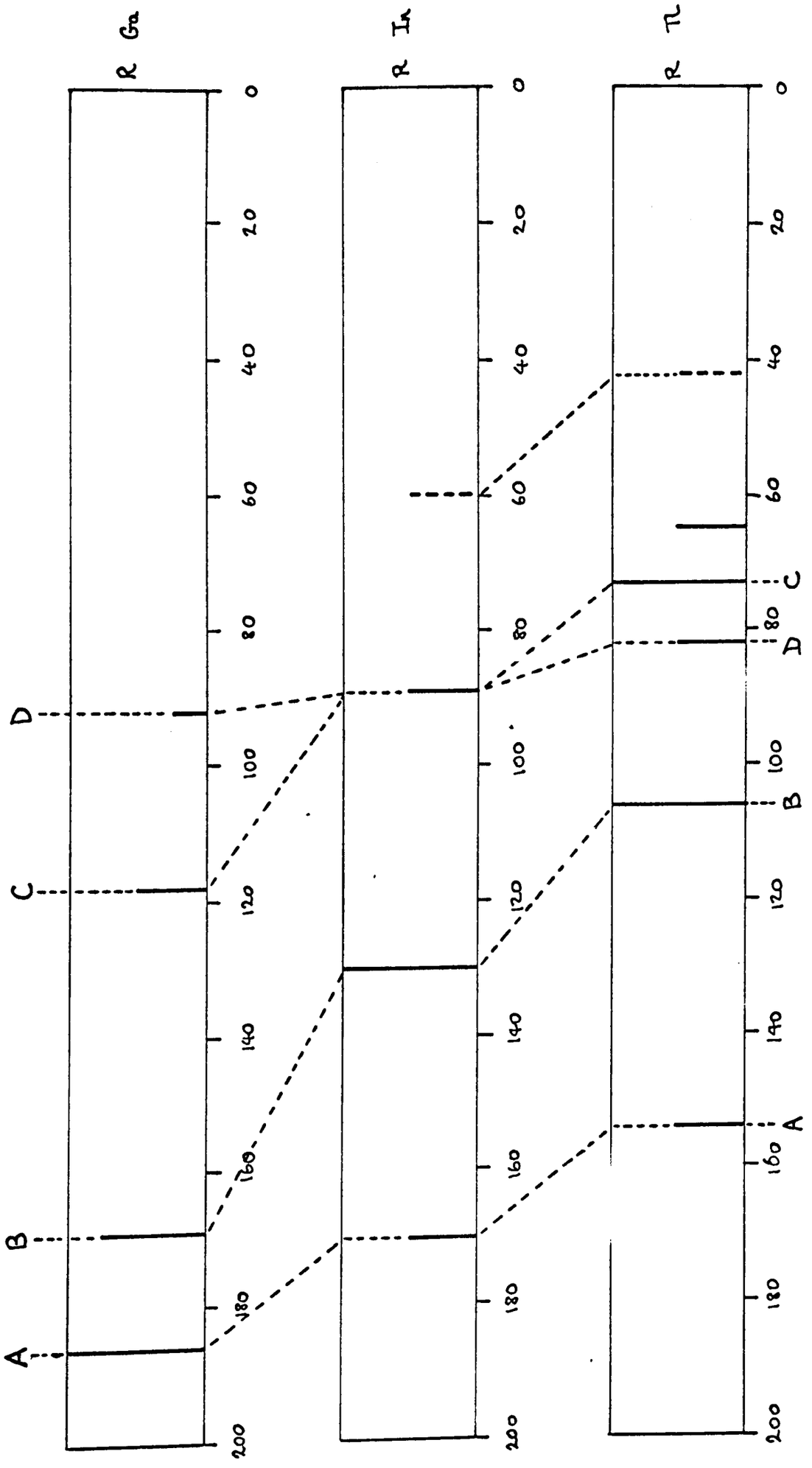

Figure 9.7: Correlation Diagram for the Solid Trimethyl Compounds of the Group III Elements (Low Frequency Region)

FEATURE	$GaMe_3$	$InMe_3$	$TlMe_3$
A	186	170	154
B	169	130	106
C	118	89	73
D	92	89	82
Fluid-Phase e' ν_{17}	156	118	99
Calculated a_2'' ν_{10}	103	75	60
Feature from Combinations	-	60	42

Table 9.11: Low Frequency Features for Solid Trimethylgallium, Trimethylindium and Trimethylthallium

assigned to the in-plane deformation mode (E', ν_{17}) in the fluid-phase results, the frequencies calculated for the out-of-plane deformation mode (A_2'', ν_{10}) and the frequencies suggested by combination features in the infrared spectra of solid trimethylindium and trimethylthallium.

The E' mode ν_{17} can probably be correlated with the feature B with some degree of certainty since a frequency shift of approximately 8% corresponding to the vapour-to-solid phase change is perfectly reasonable. It is also tempting to correlate feature C (or even, conceivably, feature D) with the hitherto unobserved A_2'' mode, ν_{10}. Such a correlation must, however, be considered speculative and the features A, C and D could equally well be explained in terms of at least three other types of vibration:

(i) lattice vibrations (phonons) of the whole crystal;

(ii) vibrations ascribable to weak inter- or intra-tetrameric M-C bonds;

(iii) additional in-plane deformation vibrations of the MC_3 unit produced by incorporation of the molecule into the crystal lattice.

It is possible to test the feasibility of the second of the above possibilities by utilizing the X-ray crystallographic data[63] for the 'long' In-C bonds in solid trimethylindium as a basis for force constant calculations using the Laurie-Herschback formula (c.f. p. 217). If it is then assumed that the modes involved are symmetric stretching modes, approximate frequencies can be calculated. For solid trimethylindium the inter- and intra-tetrameric In-C distances are 3.59 and 3.11Å

respectively and the corresponding frequencies of symmetric stretching modes are approximately 55 and 115 cm^{-1}. These results indicate that any of the features A, B, C or D could realistically be ascribed to vibrations of the weak M-C bonds.

Thus whilst the solid-phase results are unable to provide any explicit information about intermolecular interactions, they do suggest that within the solid compounds the strength of the intermolecular binding decreases in the order:

$$InMe_3 > TlMe_3 > GaMe_3$$

The vibrational spectra do not, unfortunately, provide any clear basis on which to extend to trimethylgallium the conclusions reached in the X-ray crystallographic investigations regarding the relative strengths of the inter- and intra-tetrameric interactions for trimethylindium and trimethylthallium.

9.5. Conclusions

The purpose of this final section of the thesis is to collect together the conclusions reached regarding the structures of each of the Group III trimethyl compounds in the various phases and to discuss the overall tendency towards oligomerization for each element implied by these conclusions.

(a) The Structures

(i) Trimethylboron

For trimethylboron no evidence for oligomeric species has been

obtained in any phase, even, in the case of the liquid, at temperatures as low as -150°C. In the solid phase an ordering process occurs at approximately 50°K, but the effect on the vibrational spectrum is so small that the degree of intermolecular interaction involved in the process must be chemically insignificant. The infrared spectrum of the matrix-isolated monomer of trimethylboron exhibited no new features on diffusion, unlike boron trifluoride which is reported to yield a set of new features ascribable to a dimeric species.[209]

(ii) Trimethylaluminium

For trimethylaluminium the monomeric species and the dimeric species containing symmetrical methyl bridges exist in equilibrium in the vapour phase. Below 100°C the dimer is the predominant form at pressures greater than 1 mm. Hg, and can reasonably be considered the stable form in all three phases. Above 100°C the proportion of monomer becomes appreciable and at 200°C and normal pressures the vapour-phase dissociation is essentially complete. The metal-carbon bonds in the monomer are weaker than would be expected on the basis of the metal-carbon bond strengths for monomeric trimethylboron and trimethylgallium, but the result is in reasonable accord with the high polarity of the aluminium-carbon bond. The low frequency for CH_3 rocking in the monomer is similarly in agreement with the relatively low electronegativity of aluminium and is also in keeping with the results for dimethylberyllium and methyllithium.

The spectrum of the matrix-isolated monomer changes appreciably

on diffusion yielding not only the spectral features appropriate to the matrix-isolated dimer but also a set of entirely new features which it has not been possible to assign with any degree of certainty. However, the initial indications are that these new features might well belong to a species containing an approximately pyramidal MC_3 unit.

(iii) Trimethylgallium

Trimethylgallium is monomeric in both the vapour and the liquid phases even at temperatures as low as -100°C. In the solid phase trimethylgallium adopts the structure characteristic of trimethylindium (see below) in which weakly bound tetrameric units can be distinguished. The spectral data, plus the melting point of the solid, suggest that the intermolecular binding in solid trimethylgallium is not as strong as that found in trimethylindium.

The matrix-isolated monomer yields a new species on diffusion which probably resembles the new species found for trimethylaluminium. As for trimethylaluminium, it has not proved possible to assign the new features with any degree of certainty.

(iv) Trimethylindium

As far as can be ascertained, trimethylindium is monomeric in both the vapour and liquid phases. In the solid phase a curious network of tetrameric units exists in which the intra-tetrameric bonding is appreciably stronger than that between the tetramer units. The spectroscopic data and the melting point suggest that the overall intermolecular interaction in solid trimethylindium is more effective than that in

solid trimethylgallium and trimethylthallium.

(v) Trimethylthallium

In the vapour and liquid phases no evidence has been found for oligomeric species, but in the solid state the structure is analogous to that of trimethylindium. The overall intermolecular bonding in trimethylthallium is less well developed than that in trimethylindium but the strengths of the inter- and intra-tetramer bonds are essentially comparable.

(b) Oligomerization Tendency

The above results enable a tentative sequence of oligomerization tendency to be postulated for the Group III trimethyl compounds:

$$Al > In > Tl \eqsim Ga >> B$$

This order is exactly similar to that proposed on the basis of theoretical considerations in Section 1.3c (p. 23) for the formation of Al_2C_6-like dimer units. It has been tentatively suggested that this order can be extended to oligomer-formation in general; the results of the experimental work tend to support this suggestion.

In the case of dimer-formation the order has been rationalized by examining five factors:

(I) M-M distance in the dimer;

(II) M-C bond enthalpies;

(III) s→p promotion energy;

(IV) van der Waals repulsion between non-bonded atoms in the dimer;

(V) special features tending to stabilize either the monomer or dimer.

The detailed discussion of these factors given in Section 1.3c remains valid, the only additional information now available pertaining to factor (V). The relative weakness and high polarity of the Al-C bond in the monomer amount to special features of destabilization and are thus further factors favouring dimer formation for trimethylaluminium.

References

1. G.E. Coates & K. Wade,
"Organometallic Compounds", 3rd Edn., Vol. 1, Methuen (1967).

2. K. Ziegler,
in "Organometallic Chemistry" (ed. H. Zeiss), Chap. 5, p. 194, Reinhold (1960).

3. R. Köster & P. Binger,
Adv. Inorg. Chem. Radiochem., 7, 263 (1965).

4. K. Yasuda & R. Okawara,
Organometallic Chem. Rev., 2, 255 (1967).

5. A.G. Lee,
Quart. Rev., 24, 310 (1970).

6. J. Goubeau & H.J. Becher,
Z. anorg. Chem., 268, 1 (1952).

7. J.E. Stewart,
J. Res. Nat. Bur. Stand., 56, 337 (1956).

8. W.J. Lehmann, C.O. Wilson & I. Shapiro
J. Chem. Phys., 28, 777 (1958).

9. L.A. Woodward, J.R. Hall, R.N. Dixon & N. Sheppard,
Spectrochim. Acta, 15, 249 (1959).

10. H.A. Lévy & L.O. Brockway,
J. Amer. Chem. Soc., 59, 2085 (1937).

11. L.S. Bartell & B.L. Carroll,
J. Chem. Phys., 42, 3076 (1965).

12. C.D. Good & D.M. Ritter,
J. Amer. Chem. Soc., 84, 1162 (1962).

13. W.D. Phillips, H.C. Miller & E.L. Muetterties,
J. Amer. Chem. Soc., 81, 4496 (1959).

14. H. Nöth & H. Vahrenkamp,
Chem. Ber., 99, 1049 (1966).

15. A. Stock & F. Zeidler,
Chem. Ber., 54, 531 (1929).

16. T.D. Parsons, M.B. Silverman & D.M. Ritter,
J. Amer. Chem. Soc., 79, 5091 (1957).

17. F.E. Brinckman & F.G.A. Stone,
J. Amer. Chem. Soc., 82, 6218 (1960).

18. E.L. Muetterties & W.H. Knoth,
"Polyhedral Boranes", Edward Arnold & Marcel Dekker (1968).

19. A.W. Laubergayer & W.F. Gilliam,
J. Amer. Chem. Soc., 63, 477 (1941).

20. C.H. Henrickson & D.P. Eyman,
Inorg. Chem., 6, 1461 (1967).

21. L.O. Brockway & N.R. Davidson,
J. Amer. Chem. Soc., 63, 3287 (1941).

22. K.S. Pitzer & R.K. Sheline,
J. Chem. Phys., 16, 552 (1948).

23. K.W.F. Kohlrausch & J. Wagner,
J. phys. Chem. (Leipzig), 52B, 185 (1942).

24. T. Onishi & T. Shimanouchi,
Spectrochim. Acta, 20, 325 (1964).

25. T. Ogawa, K. Hirota & K. Fukushima,
Bull. Chem. Soc. Japan, 37, 1243 (1964).

26. T. Ogawa, K. Hirota & T. Miyazawa,
Bull. Chem. Soc. Japan, 38, 1105 (1965).

27. A.P. Gray, A.B. Callear & F.H.C. Edgecombe,
Can. J. Chem., 41, 1502 (1963).

28. A.P. Gray,
Can. J. Chem., 41, 1511 (1963).

29. G.P. van der Kelen & M.A. Herman,
Bull Soc. chim. belges, 65, 362 (1956).

30. E.G. Hoffmann,
Z. Elektrochem., 64, 616 (1960).

31. K.S. Pitzer & H.S. Gutowsky,
J. Amer. Chem. Soc., 68, 2204 (1946).

32. N. Muller & D.E. Pritchard,
J. Amer. Chem. Soc., 82, 248 (1960).

33. M.P. Groenewege, J. Smidt & H. de Vries,
J. Amer. Chem. Soc., 82, 4425 (1960).

34. K.C. Williams & T.L. Brown,
J. Amer. Chem. Soc., 88, 5460 (1966).

35. K.C. Ramey, J.F. O'Brien, I. Hasegawa & A.E. Borchert,
J. Phys. Chem., 69, 3418 (1965).

36. D.E. O'Reilly,
J. Chem. Phys., 32, 1007 (1960).

37. P.H. Lewis & R.E. Rundle,
J. Chem. Phys., 21, 986 (1953).

38. R.G. Vranka & E.L. Amma,
J. Amer. Chem. Soc., 89, 3121 (1967).

39. S.K. Byram, J.K. Fawcett, S.C. Nyburg & R.J. O'Brien,
Chem. Comm., 16 (1970).

40. M.J.S. Dewar & D.B. Patterson,
Chem. Comm., 544 (1970).

41. A. Almenningen, S. Halvorsen & A. Haaland,
Chem. Comm., 644 (1969).

42. E.G. Hoffmann,
Annalen, 629, 104 (1960).

43. K. Ziegler, W. - R. Kroll, W. Larbig & O. - W. Steudel,
Annalen, 629, 53 (1960).

44. J. Smidt, M.P. Groenewege & H. de Vries,
Rec. Trav. chim., 81, 729 (1962).

45. E. Krause & P. Dittmar,
Chem. Ber., 63, 2401 (1930).

46. T. Mole,
Austral. J. Chem., 16, 794 (1963).

47. J.F. Malone & W.S. McDonald,
Chem. Comm., 444 (1967).

48. B. Bartocha, A.J. Bilbo, D.E. Bublitz & M.Y. Gray,
Z. Naturforsch, 16B, 357 (1961).

49. E.A. Jeffrey, T. Mole & J.K. Saunders,
Austral. J. Chem., 21, 137 (1968).

50. C.A. Kraus & F.E. Toonder,
Proc. Nat. Acad. Sci. U.S.A., 19, 292 (1933).

51. G.E. Coates & R.N. Mukherjee,
J. Chem. Soc., 1295 (1964).

52. J.R. Hall, L.A. Woodward & E.A.V. Ebsworth,
Spectrochim. Acta, 20, 1249 (1964).

53. G.E. Coates & A.J. Downs,
J. Chem. Soc., 3353 (1964).

54. N. Muller & A.L. Otermat,
Inorg. Chem., 4, 296 (1965).

55. L.M. Dennis & W. Patnode,
J. Amer. Chem. Soc., 54, 182 (1932).

56. W. Strohmeier, K. Hümpfner, K. Mittenberger & F. Seifert,
Z. Electrochem., 63, 537 (1959).

57. J.P. Oliver & L.G. Stevens,
J. Inorg. Nuclear Chem., 24, 953 (1962).

58. E.A. Jeffrey & T. Mole,
J. Organometallic Chem., 11, 393 (1968).

59. J.F. Malone & W.S. McDonald,
Chem. Comm., 591 (1969).

60. L.M. Dennis, R.W. Work, E.G. Rochow & E.M. Chamot,
J. Amer. Chem. Soc., 56, 1047 (1934).

61. N. Muller & A.L. Otermat,
Inorg. Chem., 2, 1075 (1963).

62. L. Pauling & A.W. Laubengayer,
J. Amer. Chem. Soc., 63, 480 (1941).

63. E.L. Amma & R.E. Rundle,
J. Amer. Chem. Soc., 80, 4141 (1958).

64. H. Gilman & R.G. Jones,
J. Amer. Chem. Soc., 68, 517 (1946).

65. J.P. Maher & D.F. Evans,
Proc. Chem. Soc., 208 (1961).

66. J.P. Maher & D.F. Evans,
J. Chem. Soc., 5534 (1963).

67. G.M. Sheldrick & W.S. Sheldrick,
J. Chem. Soc. (A), 28 (1970).

68. G.N. Lewis,
J. Amer. Chem. Soc., 38, 762 (1916).

69. W. Heisenberg,
Z. Physik, 38, 411 (1926).

70. G.E. Uhlenbeck & S. Goudsmit,
Nature, 117, 264 (1926).

71. A. Stock,
"Hydrides of Boron and Silicon", Cornell University Press (1933).

72. J.S. Kasper, C.M. Lucht & D. Harker,
Acta Cryst., 3, 436 (1950).

73. W.N. Lipscomb,
J. Chem. Phys., 22, 985 (1954).

74. W.C. Price,
J. Chem. Phys., 16, 894 (1948).

75. R.A. Ogg, Jr.,
J. Chem. Phys., 22, 1933 (1954).

76. K. Hedberg & V. Schomaker,
J. Amer. Chem. Soc., 73, 1482 (1951).

77. R.E. Rundle, D.H. Olson, G.D. Stucky & G.R. Engebretson,
International Union of Crystallography, Sixth International Congress, Rome (1963). Abstracts of Communications:
Acta Cryst., 16, A71 (1963).

78. N.R. Davidson & H.C. Brown,
J. Amer. Chem. Soc., 64, 316 (1942).

79. F.A. Cotton & G. Wilkinson,
"Advanced Inorganic Chemistry", 2nd Ed^{n}. Interscience (1966):
(a) p. 103.

80. R. West & R. Waack,
J. Amer. Chem. Soc., 89, 4395 (1967).

81. E. Weiss & E.A.C. Lucken,
J. Organometallic Chem., 2, 197 (1964).

82. G.E. Coates, F. Glockling & N.D. Huck,
J. Chem. Soc., 4496 (1952).

83. A.I. Snow & R.E. Rundle,
Acta Cryst., 4, 348 (1951).

84. O. Rahlfs & W. Fischer,
Z. anorg. Chem., 211, 349 (1933).

85. R.E. Rundle & P.H. Lewis,
J. Chem. Phys., 20, 132 (1952).

86. E. Weiss,
J. Organometallic Chem., 2, 314 (1964).

87. H.A. Lévy & L.O. Brockway,
J. Amer. Chem. Soc., 59, 2085 (1937).

88. M. Atoji & W.N. Lipscomb,
J. Chem. Phys., 27, 195 (1957).
and (amendment) C. Spencer & W.N. Lipscomb,
J. Chem. Phys., 28, 355 (1958).

89. P. Breisacher & B. Siegal,
J. Amer. Chem. Soc., 86, 5053 (1964).

90. J.W. Turley & H.W. Rinn,
Inorg. Chem., 8, 18 (1969).

91. K.J. Palmer & N. Elliot,
J. Amer. Chem. Soc., 60, 1852 (1938).

92. J.A.A. Ketelaar, C.H. MacGillavry & P.A. Renes,
Rec. Trav. Chim., 66, 501 (1947).

93. P.A. Akishin, V.A. Naumov & V.M. Tatevskii,
Kristallografiya, 4, 194 (1959).
(Soviet Physics - Crystallography, 4, 174 (1960).)

94. S.C. Wallwork & I.J. Worral,
J. Chem. Soc., 1816 (1965).

95. I.R. Beattie & J.R. Horder,
J. Chem. Soc. (A), 2655 (1969).

96. D.H. Templeton & G.F. Carter,
J. Phys. Chem., 58, 940 (1954).

97. R.E. Rundle,
J. Amer. Chem. Soc., 69, 1327 (1947).

98. R.E. Rundle,
J. Chem. Phys., 17, 671 (1949).

99. L. Pauling,
J. Amer. Chem. Soc., 69, 542 (1947).

100. R.E. Rundle,
Survey of Progress in Chemistry, 1, 81 (1963).

101. A.H. Cowley & W.D. White,
J. Amer. Chem. Soc., 91, 34 (1969).

102. V. Schomaker,
J. Chim. phys., 46, 262 (1949).

103. K.A. Levison & P.G. Perkins,
Discuss. Faraday Soc., 47, 183 (1969).

104. L. Pauling,
"The Nature of the Chemical Bond", 3rd Ed.^{n},
Cornell University Press (1960).

105. J.L. Atwood & G.D. Stucky,
J. Amer. Chem. Soc., 91, 2538 (1969).

106. E. Weiss,
J. Organometallic Chem., 4, 101 (1965).

107. R.L. Gerteis, R.E. Dickerson & T.L. Brown,
Inorg. Chem., 3, 872 (1964).

108. A.L. Allred,
J. Inorg. Nuclear Chem., 17, 215 (1961).

109. A.L. Allred & E.G. Rochow,
J. Inorg. Nuclear Chem., 5, 264 (1958).

110. C.E. Moore,
"Atomic Energy Levels", Vols. I-III,
National Bureau of Standards Circular 467 (1949).

111. M.E. Garabedian & S.W. Benson,
J. Amer. Chem. Soc., 86, 176 (1964).

112. E.B. Wilson, Jr., J.C. Decius & D.C. Cross,
"Molecular Vibrations", McGraw-Hill (1955):
(a) p. 106; (b) p. 105.

113. G. Herzberg,
"Molecular Spectra and Molecular Structure, Vol. II:
Infrared and Raman Spectra of Polyatomic Molecules",
Van Nostrand (1945): (a) p. 215; (b) p. 315; (c) p. 231;
(d) p. 298; (e) p. 178; (f) p. 279.

114. F.A. Cotton,
"Chemical Applications of Group Theory", Interscience (1963):
(a) p. 38; (b) p. 72; (c) p. 250; (d) p. 257; (e) p. 267.

115. K. Nakamoto,
"Infrared Spectra of Inorganic and Coordination Compounds",
John Wiley (1963):
(a) p. 18; (b) p. 116; (c) p. 120; (d) p. 86.

116. C.V. Raman & K.S. Krishnan,
Nature, 121, 501 (1928).

117. A. Smekal,
Naturwiss., 11, 873 (1923).

118. J.C. Evans & H.J. Bernstein,
Canad. J. Chem., 34, 1127 (1956).

119. A. Almenningen, O. Bastiansen, V. Ewing, K. Hedberg & M. Traetteberg,
Acta Chem. Scand., 17, 2455 (1963).

120. R.C. Lord, D.W. Robinson & W.C. Schumb,
J. Amer. Chem. Soc., 78, 1327 (1956).

121. M.J. Ware,
in "Physical Methods in Advanced Inorganic Chemistry" (eds. H.A.O. Hill & P. Day), Chap. 6, p.214, Interscience (1968).

122. R.S. Halford,
J. Chem. Phys., 14, 8 (1946).

123. C.C. Addison & N. Logan,
Adv. Inorg. Chem. Radiochem., 6, 98 (1964).

124. I.R. Beattie,
in "Essays in Structural Chemistry", (eds. A.J. Downs, D.A. Long & L.A.K. Staveley), Chap. 5, p. 111, Macmillan (1971).

125. I.R. Beattie, M.J. Gall and G.A. Ozin,
J. Chem. Soc. (A), 1001 (1969).

126. R.C. Hawes, K.P. George, D.C. Nelson & R. Beckwith,
Analyt. Chem., 38, 1842 (1966).

127. J.R. Ferraro, J.S. Ziomek & K. Puckett,
Rev. Sci. Instr., 35, 754 (1964).

128. J.E. Griffiths, R.P. Carter, Jr.,& R.P. Holmes,
J. Chem. Phys., 41, 863 (1964).

129. N. Craig & J. Overend,
Spectrochim. Acta, 20, 1561 (1964).

130. G.L. Carlson,
Spectrochim. Acta, 24A, 1519 (1968).

131. H.A. Haber, Private Communication,;
Cary Instrument Company, Monrovia, U.S.A. (1967).

132. R.C. Lord, R.S. McDonald & F.A. Miller,
J. Opt. Soc. Amer., 42, 149 (1952).

133. H.T.J. Chilton,
Spectrochim. Acta, 16, 979 (1960).

134. R.E. Dodd & P.L. Robinson,
"Experimental Inorganic Chemistry", Elsevier (1954).

135. R.T. Sanderson,
"Vacuum Manipulation of Volatile Compounds",
Wiley-Chapman & Hall (1948).

136. A. Farkas & H.W. Melville,
"Experimental Methods in Gas Reactions", Macmillan (1939).

137. D.F. Shriver,
"The Manipulation of Air-Sensitive Compounds",
McGraw-Hill (1969).

138. R. Köster,
Annalen, 618, 31 (1958).

139. E.C. Ashby,
J. Amer. Chem. Soc., 81, 4791 (1959).

140. G.B. Buckton & W. Odling,
Proc. Roy. Soc., 14, 19 (1865).

141. E. Wiberg, T. Johannsen & O. Stecher,
Z. anorg. Chem., 251, 114 (1943).

142. G.E. Coates,
J. Chem. Soc., 2003 (1951).

143. L.M. Davies, R.W. Work, E.G. Rochow & E.M. Chamot,
J. Amer. Chem. Soc., 56, 1047 (1934).

144. H. Gilman & R.E. Brown,
J. Amer. Chem. Soc., 52, 3314 (1930)

145. H. Gilman & R.G. Jones,
J. Amer. Chem. Soc., 68, 517 (1946).

146. C.A. Kraus & F.E. Toonder,
Proc. Nat. Acad. Sci. U.S.A., 19, 292 (1933)

147. C. Altona,
Acta Cryst., 17, 1282 (1964).

148. G.N. Lewis & D. Lipkin,
J. Amer. Chem. Soc., 64, 2801 (1942).

149. E. Whittle, D.A. Dows & G.C. Pimentel,
J. Chem. Phys., 22, 1943 (1954).

150. E.D. Becker & G.C. Pimentel,
J. Chem. Phys., 25, 224 (1956).

151. D. White & D.E. Mann,
Rev. Sci. Instr., 34, 1370 (1963).

152. Air Products and Chemicals Corp.[n],
Allentown, Pennsylvania, U.S.A.

153. M.J. Linevsky,
J. Chem. Phys., 34, 587 (1961).

154. G.C. Pimentel,
Spectrochim. Acta, 12, 94 (1958).

155. G.C. Pimentel,
Pure Appl. Chem., 4, 61 (1962).

156. G.C. Pimentel & S.N. Charles,
Pure Appl. Chem., 7, 111 (1963).

157. H.E. Hallam,
in "Molecular Spectroscopy", Proceedings of the 4th Institute of Petroleum Hydrocarbon Research Group Conference, p. 329, Institute of Petroleum (1968).

158. A.J. Barnes & H.E. Hallam,
Quart. Rev., 23, 392 (1969).

159. G.C. Pimentel,
in "Formation and Trapping of Free Radicals" (eds. A.M. Bass & H.P. Broida), Academic Press (1960).

160. W. Weltner, Jr.,
in "Condensation and Evaporation of Solids", Proceedings of the International Symposium on Condensation and Evaporation of Solids, p. 243, Gordon & Breach (1962).

161. W.L.S. Andrews & G.C. Pimentel,
J. Chem. Phys., 44, 2527 (1966).

162. W.L.S. Andrews & G.C. Pimentel,
J. Chem. Phys., 47, 3637 (1967).

163. A. German,
B.A. Part II Thesis, Oxford (1970).

164. E.D. Becker & G.C. Pimentel,
J. Chem. Phys., 25, 224 (1956).

165. M. van Thiel, E.D. Becker & G.C. Pimentel,
J. Chem. Phys., 27, 95 (1957).

166. M. van Thiel, E.D. Becker & G.C. Pimentel,
J. Chem. Phys., 27, 486 (1957).

167. G.C. Pimentel, M.O. Bulanin & M. van Thiel,
J. Chem. Phys., 36, 500 (1962).

168. K.B. Harvey, H.F. Shurvell & J.R. Henderson,
Canad. J. Chem., 42, 911 (1964).

169. S.W. Charles & K.O. Lee,
Trans. Faraday Soc., 61, 2081 (1965).

170. A.D. Buckingham,
Proc. Roy. Soc., A 248, 169 (1958).

171. J.S. Ogden & J.J. Turner,
J. Chem. Soc. (A), 1483 (1967).

172. E. Catalano & D.E. Milligan,
J. Chem. Phys., 30, 45 (1959).

173. M.J. Ricks,
D. Phil. Thesis, Oxford (1969).

174. A. Cabana, A. Anderson & R. Savoie,
J. Chem. Phys., 42, 1122 (1965).

175. I.R. Beattie & R. Collis,
J. Chem. Soc. (A), 2960 (1969).

176. G.E. Leroi, D. O'Hare & D. Hatzenbuhler,
Paper presented at 2nd International Conference on Raman Spectroscopy, Oxford (1970).

177. J.H. Darling,
B.A. Part II Thesis, Oxford (1970).

178. Tables of Wavenumbers for the Calibration of Infra-Red Spectrometers, I.U.P.A.C. Commission on Molecular Structure and Spectroscopy, Butterworths (1961).

179. E.K. Plyler, A. Danti, L.R. Blaine & E.D. Tidwell,
J. Res. Nat. Bur. Stand., 64A, 29 (1960).

180. K.N. Rao, R.V. de Vore & E.K. Plyler,
J. Res. Nat. Bur. Stand., 67A, 351 (1963).

181. T. Ogawa,
Spectrochim. Acta, 24A, 15 (1968).

182. A.G. Lee,
Ph.D. Thesis, Cambridge (1969).

183. E.M. Johnson,
B.A. Part II Thesis, Oxford (1968).

184. L. Andrews,
J. Chem. Phys., 47, 4834 (1967).

185. K.J. Burczyk, Private Communication,
Oxford (1971).

186. R.A. Kovar & G.L. Morgan,
Inorg. Chem., 8, 1099 (1969)

187. H.S. Gutowsky,
J. Chem. Phys., 17, 128 (1949)

188. H.S. Gutowsky,
J. Amer. Chem. Soc., 71, 3194 (1949)

189. L.A. Woodward,
Spectrochim. Acta, 19, 1963 (1963).

190. C.W. Young, J.S. Köhler & D.S. McKinney,
J. Amer. Chem. Soc., 69, 1410 (1947).

191. I. Simon & H.O. McMahon,
J. Chem. Phys., 20, 905 (1952).

192. E.R. Lippincott & M.C. Tobin,
J. Amer. Chem. Soc., 75, 4141 (1953)

193. H. Siebert,
Z. anorg. Chem., 273, 161 (1953).

194. J.-P. Perchard, M.-T. Forel & M.-L. Josien,
J. Chim. phys., 61, 632 (1964).

195. J.R. Allkins & P.J. Hendra,
Spectrochim. Acta, 22, 2075 (1966).

196. N. Sheppard,
Trans. Faraday Soc., 51, 1465 (1955).

197. L.J. Bellamy & R.L. Williams,
J. Chem. Soc., 2753 (1956).

198. W.L. Jolly,
J. Amer. Chem. Soc., 85, 3083 (1963).

199. H. Siebert,
"Anwendungen der Schwingungsspektroskopie in der Anorgischen Chemie", Springer-Verlag, (1966).

200. H.H. Claassen, G.L. Goodman, J.G. Mahm & F. Schreiner,
J. Chem. Phys., 42, 1229 (1965).

201. R.M. Badger,
Phys. Rev., 48, 284 (1935).

202. D.R. Herschbach & V.W. Laurie,
"Table of Vibrational Force Constants", University of California Radiation Laboratory Publication 9694, Berkeley (1960).

203. D.R. Herschbach & V.W. Laurie,
J. Chem. Phys., 35, 458 (1961).

204. W. Gordy,
J. Chem. Phys., 41, 305 (1946).

205. F.A. Cotton,
Inorg. Chem., 9, 2804 (1970).

206. H. Gerding & E. Smit,
Z. phys. Chem. (Leipzig), B50, 171 (1941).

207. W. Klemperer,
J. Chem. Phys., 24, 353 (1956).

208. I.R. Beattie, Private Communication,
Oxford (1969).

209. J.M. Bassler, P.L. Timms & J.L. Margrave,
J. Chem. Phys., 45, 2704 (1966).

SUMMARY

In this thesis a systematic study of the structures adopted by the trimethyl compounds of the Group III elements under a variety of conditions is described. Oligomerization is a feature of common and apparently irrational occurrence amongst these compounds and the investigation was undertaken with the aim not only of determining the structures themselves but also of elucidating the factors influencing structure within the series. The investigation is presented in four main sections: Introduction (Chapters 1 and 2), Experimental (Chapters 3, 4 and 5), Results (Chapters 6, 7 and 8) and Discussion (Chapter 9).

The background to the problem is discussed in Chapter 1. Previous investigations of the Group III trimethyl compounds have been haphazard and have concentrated, in general, on the elucidation of the structure of one compound in one phase. The fluid phases have received most attention and whilst trimethylboron, trimethylgallium and trimethylindium are all monomeric, the aluminium compound adopts a symmetrical dimeric structure with bridging methyl groups. In the former three compounds the MC_3 skeleton is planar and, since the methyl groups are able to rotate freely, the overall point group of the molecules is D_{3h}; the trimethylaluminium dimer belongs to the D_{2h} point group. The structure of trimethylthallium in the fluid phases has not been reported.

In the solid state trimethylaluminium has been shown by X-ray crystallography to retain the bridged, dimeric structure, whereas trimethylindium adopts an unusual structure with a polymeric network

of tetramer units in which each indium atom is penta-coordinated by methyl groups. The tetrameric unit is held together by unsymmetrical methyl bridges and the tetramers also interact, but more weakly. Within each tetramer nearly trigonal Me_3In 'monomer' units can still be distinguished and the binding within these units is much stronger than the binding between them. Thus the strength of the methyl group to indium bonds in the trimethylindium crystal falls in the order:

Intra-'monomer' >> intra-tetramer > inter-tetramer.

Recently trimethylthallium has been reported to adopt a similar solid state structure, but with more nearly equivalent inter and intra tetrameric bonds. For both trimethylindium and trimethylthallium the point group of the tetrameric unit is S_4 and the overall symmetry of the crystal is C_{4h}^4. The structures of trimethylboron and trimethylgallium in the solid state have not been investigated.

The concept of electron deficiency in the context of the present investigation is briefly discussed and the factors conceivably influencing the equilibrium:

$$n\ (\text{monomer}) \rightleftharpoons \text{oligomer}$$

are considered in some detail. For the specific case of dimer formation five factors are isolated and, as far as possible, their relative importance assessed for each of the Group III elements:

(I) the M-M distance in the dimer;

(II) the M-C bond enthalpy;

(III) the s→p promotion energy;

(IV) The van der Waals repulsion between non-bonded atoms in the dimer;

(V) the stability of the monomer.

In the light of these factors it is concluded that the relative tendency amongst the trimethyl compounds of the Group III elements towards dimer formation in particular, and oligomer formation in general, is given :

$$Al > In > Ga \triangleq Tl >> B$$

The requirements of the technique for structural elucidation are considered:

(i) applicability to all three phases;

(ii) applicability over a very wide temperature range;

(iii) feasibility of examining highly reactive compounds;

(iv) adaptability to special circumstances (e.g. matrix isolation);

and it is concluded that only vibrational spectroscopy is able to meet all these stringent requirements. In consequence the techniques of Raman and infrared spectroscopy were used almost exclusively in the structural investigations described in the thesis. The interpretation of the spectroscopic results is briefly discussed and the value of vibrational spectroscopy as a structural tool critically reviewed in Chapter 2. The solid state is given particular attention and it is concluded that the level of sophistication appropriate to the interpre-

tation of the spectra of solid compounds is dependent upon both the nature and degree of intermolecular interaction involved. The structure of solid trimethylindium is used to exemplify three distinct approaches to the interpretation of solid-phase spectra:

(i) the site symmetry approach;

(ii) the aggregate unit approach;

(iii) the factor group approach.

By way of introduction to the experimental section of the thesis, the general problems involved in the examination of compounds which react avidly with oxygen and moisture are discussed. The salient features of the instruments used in the investigation are then described. A Cary 81 spectrophotometer equipped with either a helium-neon or an argon-ion laser was employed to obtain the bulk of the Raman data. A Perkin-Elmer 225 spectrophotometer and a Beckman I.R.11 spectrophotometer were used to obtain the infrared spectra in the 4000-200 cm^{-1} and 600-50 cm^{-1} regions, respectively. The chapter is concluded by a description of the experimental assemblies developed during the course of the investigation for the examination of the Raman spectra of liquid samples over the temperature range -150 to +150°C and for the examinatinn of the infrared and Raman spectra of solid samples at -196°C. The preparation and manipulation of the five compounds are described in Chapter 4, together with details of the simpler sampling devices developed during the course of the investigation.

In Chapter 5 the nature, scope and validity of the matrix-isolation

method in the context of the present investigation are discussed in some detail. It is concluded not only that the method provides a powerful and valid tool for the investigation of the structures of both stable and unstable species but also that, by allowing the matrix to become mobile, it is possible to use the method to follow oligomerization processes in a novel and potentially highly-informative way. The experimental assembly and technique for the examination of the infrared spectra of species isolated in noble gas or nitrogen matrices at 20°K are described. The assembly comprises in essence a Perkin-Elmer 225 spectrometer coupled to a miniature Joule-Thomson liquid hydrogen cryostat bearing a caesium iodide window and encased within a suitable vacuum system. The potential advantages of obtaining the Raman spectra of matrix-isolated species are discussed and the development of an assembly for use in conjunction with the Cary 81 instrument is described.

The results of the fluid-phase investigations are presented in Chapter 6. The infrared and Raman spectra of pure trimethylboron were fully examined at room temperature and, in the case of the Raman spectrum, at temperatures down to -150°C, no change in the spectrum being detected. Trimethylaluminium was examined both pure and in solution at room temperature and, in the case of the Raman investigation, at elevated temperatures both in solution and in the vapour phase. In particular, it proved possible, by examining the vapour at 170°C, to obtain the major features of the Raman spectrum of monomeric trimethylaluminium for the first time. The infrared and Raman spectra

of pure trimethylgallium were fully investigated and the Raman and proton magnetic resonance spectra of trimethylgallium in dichloromethane solution were examined at temperatures down to -100°C, no change being detectable in either case. Trimethylindium was investigated in the vapour phase by infrared spectroscopy and in solution, both at room temperature and at -23°C, by Raman spectroscopy, again no new features being observed. The vibrational spectra of neat trimethylthallium were fully investigated at 40°C, the compound being monomeric at this temperature.

The spectra of the compounds in the solid phase are described in Chapter 7. The infrared spectrum of solid trimethylboron was examined at 20°K and did not differ appreciably from that of the compound in the vapour phase. The Raman and infrared spectra of the compounds of the four heavier elements were all examined at -196°C, and whilst trimethylaluminium yielded results closely similar to those obtained in the fluid phases, the spectra of trimethylgallium, -indium and -thallium were all very much more complicated than their fluid-phase counterparts. The overall spectral patterns for these latter three compounds were closely similar to one another and the examination of microcrystalline samples of trimethylgallium and trimethylindium by X-ray crystallography confirmed that trimethylgallium is isostructural with trimethylindium in the solid state.

The spectra of matrix-isolated trimethylboron, -aluminium and -gallium are reported in Chapter 8. The infrared results for monomeric trimethylboron and trimethylgallium and for dimeric trimethylaluminium

agreed well with their vapour-phase counterparts and it also proved possible to obtain the infrared spectra of virtually pure monomeric trimethylaluminium for the first time. When the matrices were allowed to diffuse the spectrum of trimethylboron showed no alteration, but a new set of features appeared in that of trimethylgallium and two new sets in that of monomeric trimethylaluminium. One of the two new sets of features for trimethylaluminium belonged to trimethylaluminium dimer, whilst the other set, as far as could be ascertained, corresponded to the set given by trimethylgallium. The major features of the Raman spectra of matrix-isolated trimethylgallium monomer and of matrix-isolated trimethylaluminium monomer and dimer were also recorded.

In the final chapter of the thesis the results are correlated and the chemical information they contain discussed under four headings: monomeric species, dimeric species, diffusion species and larger aggregates. In the first section the results for all five monomers are compared and it is concluded that although the bonding in trimethylaluminium is appreciably weaker than would be expected on the basis of a direct interpolation of the strengths of the bonds in trimethylboron and trimethylgallium, it is in reasonable accord with the high polarity of the aluminium-carbon bond. Comparison is made to the methyl compounds of the other Main Group elements and product rule, force constant and bond length calculations are presented.

The spectra of dimeric trimethylaluminium are compared both with the results of published force constant calculations and with the published results for analogous systems and the assignment for the

skeletal modes of the molecule is considerably extended. The validity of certain ideas recently postulated for the structure of solid trimethylaluminium are also investigated.

The nature of the new species produced by the interaction of trimethylaluminium monomer units and trimethylgallium monomer units in nitrogen matrices at 34°K are considered and it is concluded that the spectroscopic results are best interpreted in terms of species containing pyramidal MC_3 units. It is suggested that direct metal-metal interactions may be involved in the formation of the new diffusion species:

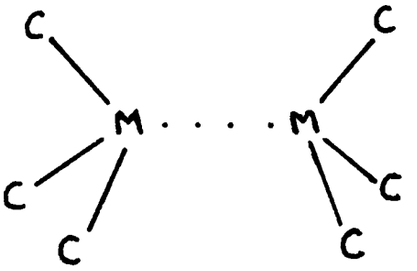

In the discussion of the spectra of the solid compounds of trimethylgallium, -indium and -thallium, it is concluded that whilst a site symmetry approach is definitely inappropriate it is not possible to decide which of the two extended approaches (the aggregate unit or the factor group) is the more suitable. It is further concluded that although the overall degree of intermolecular interaction in solid trimethylgallium is less than that in solid trimethylindium and probably more nearly comparable to that in solid trimethylthallium it is unfortunately not possible to make any definite deductions regarding the relative strengths of inter- and intra-tetrameric bonds in solid

trimethylgallium.

In the concluding section of the thesis the tendency to oligomer formation for each of the Group III trimethyl compounds is discussed in the light both of the theoretical considerations of Chapter 1 and of the experimental results. It is concluded that the tentative sequence of oligomerization tendency suggested on theoretical grounds for the trimethyl compounds of Group III elements is substantiated by experiment:

$$Al > In > Ga \triangleq Tl >> B$$